Assessment of Novel Therapeutics and Development of Monoclonal Antibody Targeting Moieties for Drug Delivery Systems in the Treatment of Osteoarthritis

Bradley Whitehead (MSc)

Thesis submitted for the degree of Doctor of Philosophy

Cardiff University

2019

Abstract

In Part 1 of this work *ex vivo* models of cytokine induced cartilage degradation were developed and extensively characterised for the subsequent assessment of Surfen, a heparan sulphate antagonist as a potential therapeutic for the treatment of osteoarthritis (OA). Cell signalling pathway analysis revealed synergistic activation of the stress-activated protein kinase (SAPK/JNK) pathway mediated by interleukin-1 alpha (IL-1α) + Oncostatin M (OSM) compared to either cytokine alone. Pharmacological inhibition confirmed the role of SAPK/JNK in catabolic gene expression and cartilage matrix degradation. Analysis of cartilage oligomeric matrix degradation (COMP) in cartilage in response to cytokines identified a role for ADAMTS-4 in COMP degradation.

Surfen is a known inhibitor of anthrax lethal factor metalloproteinase. This Thesis identified Surfen as a direct inhibitor of ADAMTS-4 and furin, a pro-protein convertase involved in ADAMTS activation. Surfen inhibited glycosaminoglycan (GAG) loss and aggrecanase activity in IL-1α but not IL-1α+OSM treated cartilage explants. Gene expression studies showed Surfen (7 μM) attenuated IL-1α and IL-1α+OSM mediated increases in catabolic gene expression, however, increased Surfen concentration (15 μM) resulted in increased ADAMTS-4 expression and activity in IL-1α+OSM conditions that likely precludes the use of Surfen as an OA therapy.

Targeting of sustained release drug delivery systems (DDS) to specific tissues within the joint could increase retention whilst reducing off-target effects. In Part 2 lubricin was identified as a candidate cartilage surface target. Conjugation of anti-lubricin mAb to DDS improved binding and retention in *ex vivo* studies. For the targeting of pro-inflammatory M1 subtype macrophages in the synovium, novel mAbs were developed to target human and murine FcγRI/CD64. Assessment of mIgG1 and mIgG2a anti-FcγRI/CD64 binding revealed species and isotype specific differences in non-specific binding to monocyte cell lines, whereas no non-specifc binding of mIgM was observed suggesting in these subtypes are preferential in the specifc targeting of FcγRI/CD64. Combined, this Thesis has assesed the potential of a novel therapeutic and developed novel joint targeting strategies for treatment of OA.

Acknowledgements

I would like to thank my supervisors Professor Clare Hughes and Professor Bruce Caterson for all their guidance and never ending support throughout the project which has been invaluable and also for the productive but extremely fun working environment they have provided. I would also like to thank everybody at Cardiff School of Bioscience that have helped throughout the years, particularly Dr Emma Blain, Dr Shane Wainwright, Dr Polina Prokopovich and also my former supervisor, Associate Professor Ken Howard at Aarhus University, without whom my returning to science would have been impossible.
A very special thank you to my wife who has been extremely patient and supportive throughout and was willing to move country with our son to make this possible. Thank you to everybody in the MSCA-ITN TargetCaRe- it has been great working with you and I will miss the meetings and of course thank you to the European Union for funding this work.

Contents

List of Figures

List of Tables

Abbreviations

ACI - Autologous chondrocyte implantation
ACLT - Anterior cruciate ligament transection
ADAM - A disintegrin and metalloproteinase
ADAMTS - A disintegrin and metalloproteinase with thrombospondin motifs
AGE - Advanced glycation end
AKT - Protein kinase B
AP-1 - Activating protein 1
ASK1 - Apoptosis signal-regulating kinase 1
BCP - Basic calcium phosphate
BMDMs - Bone marrow derived macrophages
BMP - Bone morphogenetic protein
BSA - Bovine serum albumin
CIA - Collagen-induced arthritis
COMP - Cartilage oligomeric matrix protein
COX - Cyclooxygenase
CPPD - Calcium pyrophosphate dihydrate
CREB - cAMP response element-binding protein
CS - Chondroitin sulfate
CYS R - Cysteine Rich
CZ - Calcified zone
DAMP - Damage associated molecular pattern
DMEM - Dulbecco's modified Eagle's medium
DMM- Destabilisation of the medial meniscus
DMMB - Dimethylmethylene blue assay
DMOADs - Disease-modifying osteoarthritis drugs
DS - Dermatan sulfate
DZ - Deep zone
ECM - Extracellular matrix
ERK - Extracellular signal-regulated kinase
EXT1 - Exostosin glycosyltransferase 1
EXT2 - Exostosin glycosyltransferase 2
FACIT - Fibril associated with interrupted helices
FBS - Fetal bovine serum
FGF - Fibroblast growth factor

GAGs - Glycosaminoglycans
GlcA - Glucuronic acid
GlcNAc - N-acetlyglucosamine
GPCR - G-protein coupled receptor
HA - Hyaluronic acid
HAS - Hyaluronic acid synthase
HDAC - Histone deacetylase
HETE - Hydroxyeicosatetraenoic acid
HIF1-α - Hypoxia-inducible factor 1-alpha
HMGB1 - High mobility group box 1
HS- Heparan sulfate
HSPGs- Heparan sulfate proteoglycans
ICE - IL-1 converting enzyme
IGD - Interglobular domain
IL-1 - Interleukin 1
IL-6 - Interleukin 6
JAK - Janus kinase
JNK - Jun N-terminal kinase
KS - Keratan sulphate
LF - Anthrax lethal factor
LIF - Leukaemia inhibitory factor
LPS - Lipopolysaccharide
LRP1 - Low density lipoprotein receptor-related protein 1
mAb - Monoclonal antibody
MAPK - Mitogen-activated protein kinase
MCP-1 - Monocyte chemoattractant protein 1
MED - Multiple epiphyseal dysplasia
MMP - Matrix metalloproteinase
MP - Metalloproteinase
MSU - Monosodium urate crystals
MZ - Middle zone
NFκβ - Nuclear factor κB
NGF - Nerve growth factor
NLRP3 - Nod-like receptor protein 3
NSAIDs - Non-steroidal anti-inflammatory drugs
OA - Osteoarthritis
OSM - Oncostatin M
p38 - P38 mitogen-activated protein kinase
PAMP - Pathogen-associated molecular patterns
PGE2 - Prostaglandin E2
PI3K - Phosphatidylinositol 3-kinases
PLA2 - Phospholipase A2

PLC - Phospholipase C
PLGA- Poly(lactic-co-glycolic acid)
PPARγ - Peroxisome proliferator-activated receptor gamma
PSACH - Pseudoachondroplasia
RA - Rheumatoid arthritis
RAGE - Receptor for advanced glycation end products
RHAMM - Receptor for hyaluronan-mediated motility
ROS - Reactive oxygen species
RT-PCR - Reverse transcription polymerase chain reaction
RUNX2 - Runt-related transcription factor-2
SASP - Secretory associated secretory phenotype
SB - Subchondral bone
sIL-6R - Soluble IL-6 receptor
SLRPs - Small leucine rich proteoglycans
SOX9 - SRY-Box 9
STAT - Signal transducer and activator of transcription
SZ - Superficial zone
TAK1 - Transforming growth factor-beta-activated kinase 1
TGF-β - Transforming growth factor beta
TIMP- Tissue inhibitor of metalloproteinases
TLR - Toll like receptor
TNFα - Tumor necrosis factor alpha
TRPV - Transient Receptor Potential Cation Channel Subfamily V
WOMAC - Western Ontario and McMaster Universities Osteoarthritis Index

Part I

Assessment of Surfen, a Heparan Sulfate Antagonist as a Potential Osteoarthritis Therapeutic

Chapter 1

Introduction

1.1 Cartilage Structure and Composition

1.1.1 Articular Cartilage

Human articular cartilage is a 2-3mm specialised connective tissue coating the long bones which provides resistance to compression, dissipation of mechanical force and a low friction surface to enable smooth and painless articulation of diarthrodial joints (Hunziker *et al.* 2002). Cartilage has an organised, layered structure consisting of superficial (SZ), middle (MZ), deep (DZ) and calcified zones (CZ) above the sub-chondral bone (SB) (Fig 1.1). In addition to the zonal arrangement of cartilage it is also divided into regions based upon matrix composition and distance from the chondrocyte (Fox *et al.* 2009). The area immediately surrounding chondrocytes is the pericellular matrix that is rich in proteoglycans, collagen type VI and small leucine rich proteoglycans (SLRPs) such as decorin (Knudson and Knudson, 2001). Extending beyond the pericellular matrix is the territorial matrix, that comprises the majority of the volume of articular cartilage and concentration of large aggregating proteoglycans.
Collagen fibrils are arranged zonally with superficial zone collagen fibrils being parallel to the cartilage surface whereas in deeper zones the collagen fibrils are larger in diameter and arranged perpendicular to the surface. Cartilage is an avascular tissue that is replenished via nutrients within the synovial fluid that diffuse into the tissue (Ye Ng *et al.* 2017). Water comprises 80% of the wet weight of articular cartilage (Fox *et al.* 2009). The resident cells, chondrocytes, maintain tissue homeostasis and function through the balanced degradation and synthesis of extracellular matrix macromolecules.

1.1.2 Chondrocytes

Chondrocytes, the sole cell type present in cartilage, maintain extracellular matrix (ECM) homeostasis through the balanced synthesis of matrix macromolecules and catabolic factors such as metalloproteinases that mediate articular cartilage ECM turnover. Cartilage has a low cellularity with chondrocytes accounting for 1-5% of the overall volume of articular cartilage (Akkiraju and Nohe, 2015). Chondrocytes have a limited capacity for self-renewal and therefore cartilage regeneration is limited. Chondrocytes display an altered morphology, orientation and metabolic activity dependent upon their location within the articular cartilage. Cells in the superficial zone have a

flattened shape, whereas, those within the deep zone form columnar arrangements perpendicular to the cartilage surface (Fig 1.1). Chondrocytes below the tidemark, within the calcified zone, are larger in size and display a hypertrophic phenotype with increased expression of collagen type X (Akkiraju and Nohe, 2015). The chondron is comprised of the chondrocytes and their pericellular matrix, that is responsible for transmission of mechanical signals to chondrocytes which can then alter gene expression resulting in increased matrix synthesis or degradation (Fox *et al.* 2009). In addition to responding to biomechanical cues, chondrocyte gene expression is sensitive to cytokines and growth factors such as IL-1 and TGF-β which can drive catabolic or anabolic gene expression changes, respectively.

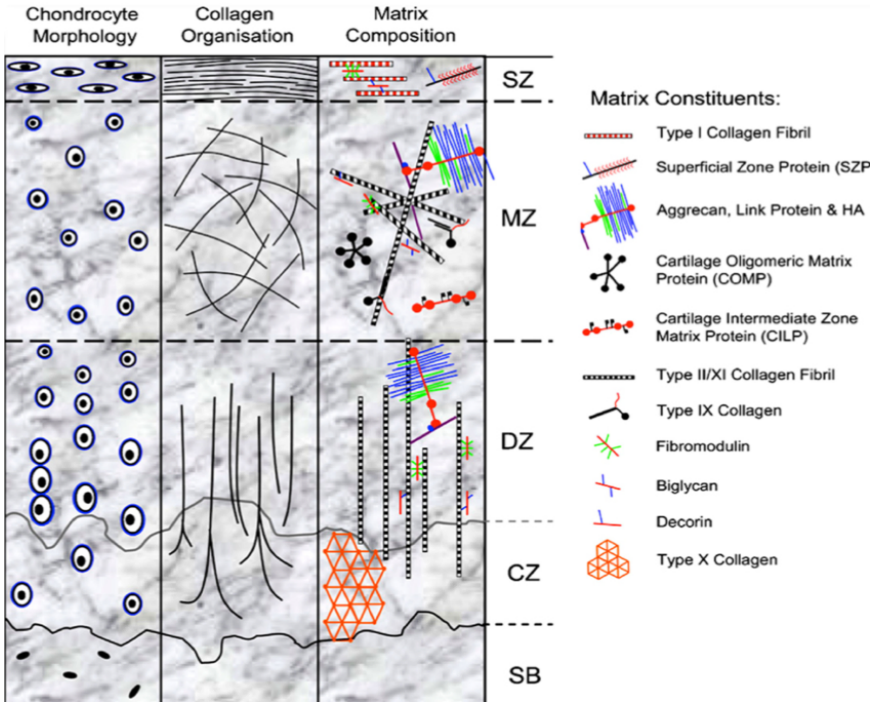

Figure 1.1 – Zonal structure of articular cartilage showing chondrocyte morphology changes dependent upon location, collagen fibril organisation and matrix macromolecule composition. Modified from Hayes *et al* 2007.

1.1.3 Collagens

Collagen is an umbrella term for proteins that form supramolecular structures comprised of α-chains. This family of structural proteins are the most abundant proteins in ECM. Collagens are further classified according to structure, function and location with the most common in cartilage being the fibril forming and fibril associated with interrupted helices (FACIT), although the network forming type VI is present in the pericellular matrix. Collagens comprise around 60% of the dry weight of articular cartilage. Collagens present in cartilage include types I, II, IV, V, VI, IX, and XI (Eyre, 2001) although type II accounts for 95% of all collagen content (Fox *et al.* 2009). Collagen fibrils within the matrix provide the tensile strength and shear stress response of cartilage. The formation of the typical collagen triple helix structure requires a glycine amino acid, due to its small side chain size allowing for tight packing of the triple helix, every three amino acids within the sequence hence the conserved sequence Gly-X-Y throughout collagenous domains. Positions X and Y are often proline or hydroxyproline amino acids which aid fibril formation through hydrogen

bonding with Gly (Shoulders and Raines, 2009). Collagen type II is homo-trimeric, formed from three α-1(II) chains which assemble into fibrils in combination with collagen type XI, which aids in fibrillogenesis (Gelse *et al.* 2003). Collagen type XI is a hetero-trimeric collagen comprised of α- 1, 2 and 3 chains. Collagen type IX, a FACIT type collagen, stabilises the structure via cross-linking to the N-terminal telopeptide enabled by the lysl-oxidases. The predominant form of type II collagen in mature cartilage is a splice variant (IIB) that is lacking the N-terminal globular domain that is present in embryonic collagen type II (IIA). The network collagen type VI is present within most connective tissues but is particularly enriched within the pericellular matrix where it forms a meshwork that protects chondrocytes from mechanical damage whilst also enabling transmission of mechanical signals through the chondron to the chondrocytes which results in gene expression changes in response to such biomechanical cues. Collagen type X is only found within the calcified zone in healthy cartilage and is produced by hypertrophic chondrocytes. Collagen type X has been used extensively as a marker for hypertrophy in chondrocytes (Van der Kraan and Van den Berg, 2012).

1.1.4 Glycosaminoglycans

Glycosaminoglycans (GAGs) are linear unbranched polysaccharides comprised of repeating disaccharide units that are covalently linked to proteins. The disaccharides are composed of a hexosamine, that is often N-acetylated, and a uronic acid. Sulphation of the saccharide monomers lends a negative charge to GAGs with the exception of hyaluronic acid (HA) which is non-sulphated. Although the permutations of GAGs are vast due to variations in length, sulphation position and level of sulphation there are several defined groups of GAGs based upon the disaccharide composition which include HA, chondroitin sulphate (CS), dermatan sulphate (DS), keratan sulphate (KS), heparan sulphate (HS) and heparin (Lindahl *et al*, 2017).

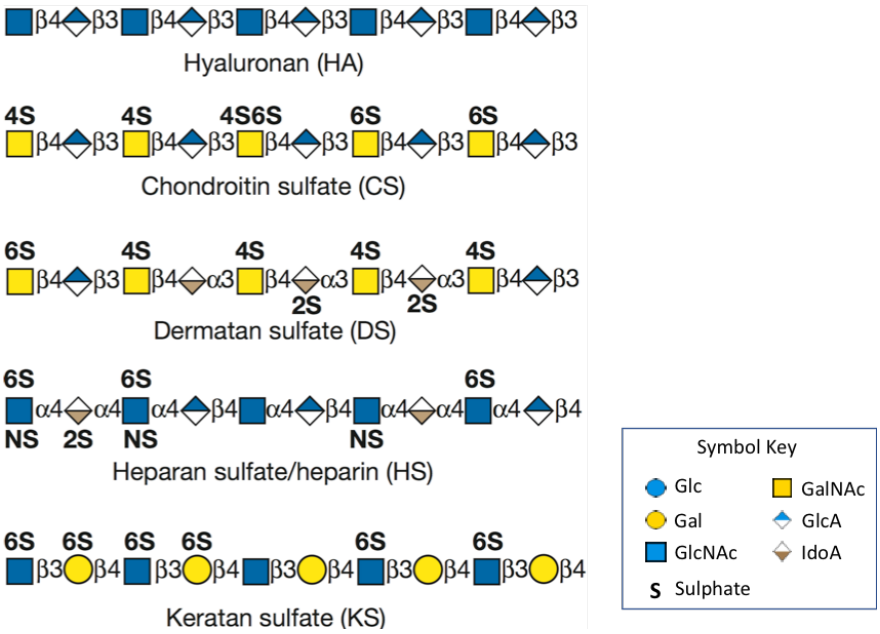

Figure 1.2 – Composition of GAGs subtypes showing disaccharide units, linkage and potential sulphation sites. Modified from Bishop *et al.* 2007.

Hyaluronic Acid

HA is the simplest form of GAG and unlike other members of the group it is not synthesised and covalently linked to proteins in the Golgi. HA is synthesised in the cytoplasm at the cell membrane by hyaluronic acid synthases (HAS) and secreted into the extracellular space as a large polyanionic polymer chain. The disaccharide repeats that comprise HA are N-acetlyglucosamine (GlcNAc) and glucuronic acid (GlcA) that are linked by β1-3 linkages (Necas *et al.* 2008). HA is present throughout the ECM and is shown to act as a template for binding of large aggregating proteoglycans such as aggrecan and versican. This binding is stabilised by link proteins which contain the link module HA binding domain (Kiani *et al.* 2002). HA in the synovial fluid provides lubrication and protection of the joint through its viseoelastic properties (Tamer, 2013). In addition to its structural function HA is implicated in cell signalling through interactions with cell membrane proteins such as CD44 and receptor for hyaluronan-mediated motility (RHAMM).

Chondroitin sulphate

CS is composed of repeating disaccharides of D-glucuronic acid and N-acetylgalactosamine linked by β1-3 and β1-4 linkages. CS N-actylgalactosamine can be sulphated at C4, C6 or be non-sulphated (NS). NS CS is termed chondroitin. More unusual sulphation sites have been identified in some species such as C2S of the glucuronic acid. CS is attached to the serine of proteins as they transit through the Golgi via a tetrasachharide linker. In CS synthesis, xylotransferases covalently attach a xylose residue to a serine amino acid on the protein in the endoplasmic reticulum whereas all subsequent additions occur in the Golgi . Two galactose residues are then added followed by a single glucuronic acid. The tetrasachharide linker is completed by the addition of N-acetylgalactosamine (Ishimaru *et al.* 2013). The majority of all chondroitin sulphate in the body is present within cartilage and intervertebral disc. Differences in sulphation are present dependent upon tissue location and age with foetal cartilage containing predominantly C4S in humans, however, changes in sulphation are evident in ageing with the articular cartilage of aged individuals having an increased C6S/C4S ratio (Plaas *et al.* 1997).

Dermatan Sulphate

Originally designated as CS B, DS shares many similarities with CS with the exception that C5 of D-glucuronic acid is epimerised resulting in L-iduronic acid. DS is found predominantly in the skin and tendon. Iduronic acid residues may be sulphated at the C2 position in addition to potential C4S and C6S sulphation on N-acetylgalactosamine residues (Trowbridge and Gallo, 2002). The SLRPs decorin and biglycan contain DS chains and are the principle source of DS in cartilage.

Keratan Sulphate

KS is comprised of regions of non-sulphated poly-N-acetyllactosamine and repeating disaccharides of D-galactose and N-acetylglucosamine which are joined via β1-4 linkages. Both D-galactose and N-acetylglucosamine can be sulphated at the C6 position. Similar to other GAGs KS is linked to serine and threonine residues but can additionally be N-linked to asparagine residues on proteins. KS was discovered initially in the cornea, although the form of KS in the cornea is of the KSI

type, which is the N-linked asparagine form, whereas the skeletal form of KS, termed KS II, is O-linked to serine or threonine residues. A third form, KSIII, differs from KSI and KSII through its binding to serine or threonine residues on proteins via a 2-O-mannose linkage and is found largely in the brain. KS is present on bovine and human aggrecan (25-50 KS chains) but is not found on murine or rat aggrecan. Additionally, it is present on several SLRPs such as keratocan, lumican and fibromodulin. The association of Ca^{2+} counter-ions with KS may have a functional application as a calcium store with some KS-bearing SLRPs being involved in bone formation (Caterson and Melrose, 2018). The calcium reservoir protein SV2, a KSPG, has a role in synaptic potential generation further suggesting a role for KS in Ca^{2+} storage or transport by KSPGs (Caterson and Melrose, 2018).

Heparan sulphate

HS is produced by almost all cell types whereas heparin is produced exclusively by mast cells. HS is attached to heparan sulphate proteoglycans (HSPGs) through the same tetrasachharide linker as CS although the addition of a GlcNAc by EXTL3 precedes the synthesis of HS as opposed to the addition of GalNAc by CSGALNACT1/2 in the case of CS synthesis. Elongation of the polymer is mediated by a complex of EXT1 and EXT2 adding alternating units of GlcA and GlcNAc (Fig 1.3). HS and heparin are extensively modified, for example by N-deacetylation and N-sulphation, C5 epimirisation of GlcA to IdoA which can be subsequently 2-O sulphated by 2OST. Additionally, HS GlcNAc can be 3 and 6-O sulphated (Lindahl *et al.* 2017). The multitude of potential combinations of these modifications leads to extreme variation amongst HS and therefore potentially its bioactivity, although it has been suggested that the overall level of sulphation, rather than a specific sequence, mediates the binding of receptors and ligands (Bishop *et al.* 2007).

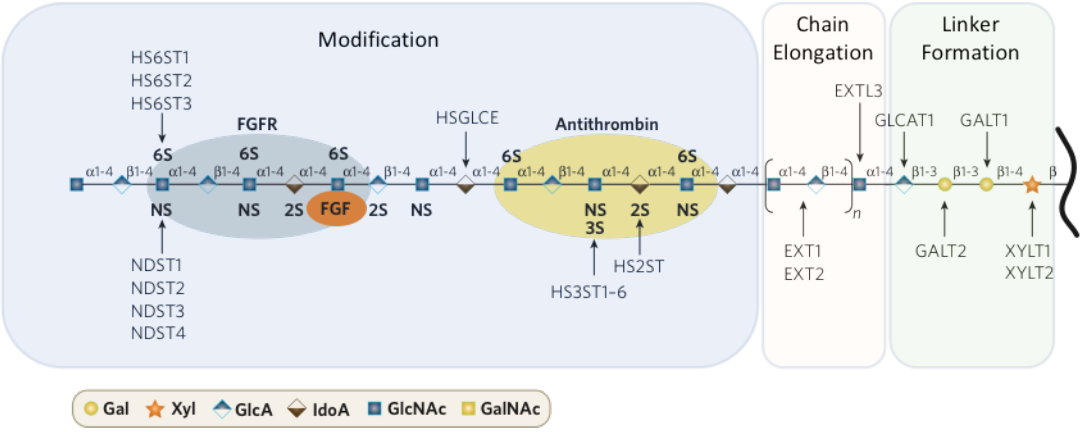

Figure 1.3 – Schematic showing synthesis of HS linker, chain elongation and potential modifications of HS. Modified from Bishop *et al.* 2007.

1.1.5 Proteoglycans

Proteoglycans are comprised of core proteins with one or more glycosaminoglycan side chains of CS, DS, KS or HS but not HA. GAG chains are added to proteins in the Golgi to serine or threonine amino acids via O-linked glycosylation, although in the case of keratan sulphate N-linked

glycosylations on asparagine residues are also possible.

Aggrecan

Aggrecan, the predominant proteoglycan within articular cartilage, is comprised of a core protein with three globular (G) domains and multiple chondroitin sulphate and keratan sulphate side chains, positioned between the G2 and G3 domains, forming a bottle brush like structure. At the N-terminal end of aggrecan is the hyaluronic acid binding domain (G1) that, together with cartilage link protein, bind non-covalently to hyaluronic acid to from large negatively charged aggregates, which largely account for the osmotic potential of cartilage and therefore the resistance to compression through hydration of cartilage in a mechanism described as the Gibbs-Donnan effect (Kiani *et al.* 2002). Human aggrecan contains around 100 chondroitin sulphate side chains which are of roughly 20 kDa in molecular weight (Knudsen and Knudsen, 2001). There are fewer KS chains that are also smaller in molecular weight, around 5-15 kDa. Changes in aggrecan structure throughout development and ageing may contribute to changes in articular cartilage function. The size of CS chains decreases with age whereas KS chains are elongated (Roughley and Mort, 2014). The sulphation pattern of CS also changes upon ageing with a switch to a predominantly 6-sulphated form. The effects of these structural changes upon cartilage function are unknown.

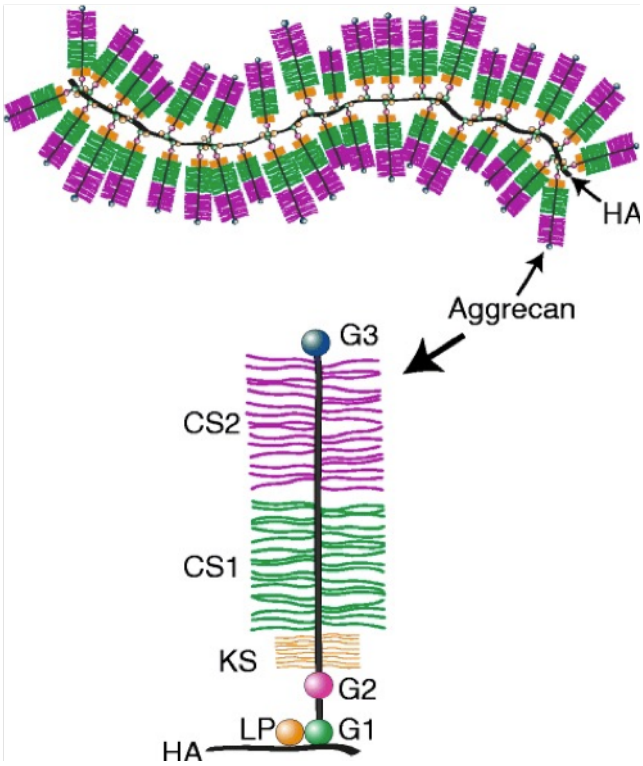

Figure 1.4 – Aggrecan structure showing keratan sulphate (KS), chondroitin sulphate domain 1 (CS1) and chondroitin sulphate domain 2 (CS2). Aggrecan formation of aggregates with HA in conjunction with link protein (LP) shown top (Roughley and Mort, 2014).

1.1.6 Glycoproteins

Lubricin

Lubricin also known as PRG4 or superficial zone protein (SZP) is a large, 345 kDa, mucin-like glycoprotein that serves as a boundary lubricant in articular cartilage. Lubricin is produced by synoviocytes, chondrocytes in the superficial zone and to a lesser extent chondrocytes in deeper zones of cartilage in addition to cells of the meniscus (Schumacher *et al.* 2005). It is bound to the articular cartilage surface and also present in high concentrations in the synovial fluid. The low friction co-efficient of healthy cartilage (<0.01vs 0.04 for Teflon) is in part mediated by lubricin (Jay and Waller, 2014). *In vitro* studies of friction coefficients have revealed that lubricin alone is not sufficient to provide the low friction observed at the surface of articular cartilage. Addition of HA to lubricin lowers the co-efficient but still not to levels observed in native cartilage. Phospholipids have been shown to further contribute to the reduction of friction in combination with lubricin and HA (Schmidt *et al.* 2007). There are varying reports in the literature as to which co-factors are involved in lubrication that may be a result of differences in experimental set-up; for example some groups assess the friction coefficients using cartilage-on-cartilage systems whilst others use cartilage-on-glass or entirely non-biological systems. Lubricin structure comprises of globular domains to the N and C-terminus flanking a central mucin domain with a repeating KEPAPTT motif which is heavily O-linked glycosylated. Binding to surfaces is mediated by the C-terminal domain which presents the mucin domain as a graft polymer brush structure. The N-terminal domain mediates dimerisation (Jones *et al.* 2007). Removal of the glycosyl chains, specifically the penultimate galactose group, significantly reduces the lubricating ability of lubricin (Jay and Waller, 2014). The presence and relative quantities of lubricin present at the surface of cartilage during different stages of OA is debated in the literature, however there is a consensus that immediately post-injury there is an increase in expression. Studies in mid-stage OA point to a decrease although this is not conclusive as a study in horses showed increased lubricin levels at the surface of cartilage in both experimental and naturally-occurring OA (Reesink *et al.* 2017). Furthermore, a study of advanced OA patient cartilage and synovial fluid found increased lubricin levels compared to non-OA controls (Neu *et al.* 2010). *In vitro* cell assays have highlighted an IL-1-mediated reduction of lubricin expression, conversely TGF-β and Oncostatin M (OSM) treatment increased expression (Schmidt *et al.* 2008; Jones and Flannery, 2007) Recombinant human lubricin administered intra-articularly resulted in significant reduction in cartilage degradation compared to animals receiving carrier control in a rat meniscal tear OA model (Flannery *et al.* 2009) and adenoviral expression of PRG4 in mice was protective against both age-related and post-traumatic OA (Ruan *et al.* 2013) suggesting that the increased expression observed in OA studies may be part of a protective response through increased lubrication of articular cartilage that reduces structural damage.

Cartilage Oligomeric Matrix Protein

Cartilage oligomeric matrix protein (COMP) is a 110 kDa glycoprotein of the thrombospondin family that is found within the articular cartilage in homo-pentameric structures. COMP contains a central structure consisting of EGF-like domain repeats and calmodulin-like repeats with a globular C-terminal domain (Fig 1.5A). The cysteine-rich N-terminal forms a coiled coil structure and

mediates the binding between COMP monomers in its pentameric form (Fig 1.5B), which has structural similarities to ion channels (Fig 1.5C). The role of COMP within cartilage is not fully elucidated although numerous binding partners have been identified including collagens, fibronectin, matrillins and aggrecan. Binding of COMP to collagen type I, II, aggrecan and matrillin 1-4 is mediated via the C-terminal domain although some dependence on the calcium-binding domain was evident for aggrecan. The observed binding of retinoic acid, vitamin D and fatty acids suggest COMP may act as a reservoir for such molecules (Acharya *et al.* 2014). The binding of COMP to many structural components of articular cartilage has led to the suggestion that COMP may act as a molecular bridge between matrix macromolecules and therefore may play a role in matrix organisation and stability. In support of this hypothesis it is known that mutations in the COMP gene lead to diseases of the musculoskeletal system. Mutations in the calmodulin and globular C-terminal of COMP result in pseudoachondroplasia (PSACH) and multiple epiphyseal dysplasia (MED) (Fig 1.5A). Interestingly, most pathological mutations are located within the calcium-binding domains of COMP and not in the C-terminal globular domain responsible for binding to ECM (Fig 1.5A). PSACH presents as severely reduced stature and laxity of the ligaments in the joint. In PSACH patients mutated COMP and its binding partners collagen type IX and matrillin accumulate within chondrocytes resulting in cell death and therefore reduced cartilage formation (Hecht *et al.* 2005), although it has also been shown that even in cases where sufficient mutant COMP has been secreted then the structure of cartilage is impaired further implicating COMP in a structural role for healthy cartilage formation (Posey *et al.* 2004). MED is less severe than PSACH and results in short stature and pain in joints (Posey and Hecht, 2008). Interestingly, MED patients have an increased susceptibility for OA with many patients presenting with OA by early adulthood (Treble *et al.* 1990). The observed loss of intact and degraded COMP to the synovial fluid and serum of OA and RA patients presents COMP as a candidate detection or prognostic biomarker for these diseases of the joint. After vigorous exercise, COMP release to the synovial fluid is increased and therefore the use of neo-epitope antibodies targeting pathological cleavage sites of COMP may show more promise as biomarkers of disease compared to traditional ELISA methods detecting total COMP. Using a proteomics approach after protease digestion of COMP, Åhrman *et al.* (2014), identified multiple neo-epitopes and one in particular, Ser^{77}, was also detected in the media of cartilage explants cultured in the presence of TNF-α and IL-6/sIL-6R (Åhrman *et al.* 2014).

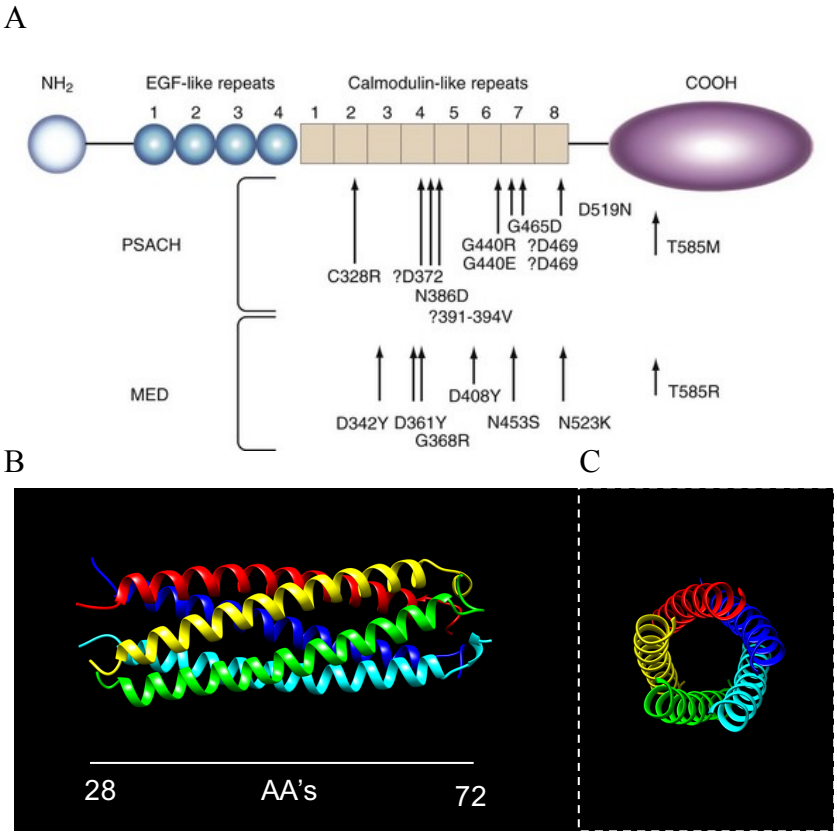

Figure 1.5 – Domain structure of COMP/thrombospondin 5 showing known mutations that result in pseudoachondroplasia (PSACH) and multiple epiphyseal dysplasia (MED) (A). Pentameric association of N-terminal COMP monomers (B) and cross-section showing pore-like structure of the N-terminals of COMP (C). Images produced using USCF-Chimera from rat COMP crystal structure 1VDF (RCSB).

1.2 Osteoarthritis Pathology

Osteoarthritis (OA) is a debilitating joint disease that currently affects over 8 million people in the UK alone and imparts an estimated cost to society of over £5 billion per year (from Arthritis Research UK). The incidence of OA is likely to increase as the population ages. To date, there are no disease-modifying therapeutics and treatments focus upon management of symptoms rather than resolution of pathology. Osteoarthritis is characterised by progressive degradation of articular cartilage, sub-chondral bone re-modelling, and development of osteophytes (Fig 1.6) which combined leads to restricted motility of the affected joint and pain . There are multiple risk factors that are linked to an increased incidence of OA which include age, obesity, acute joint injury, diabetes and abnormal gait which highlights the biomechanical, inflammatory and metabolic aspects of pathology. Degradation of articular cartilage is central to OA pathology. The cleavage of aggrecan, mediated by aggrecanases (ADAMTS-4 and ADAMTS-5), at the pathological $E^{373\_374}A$ site results in loss of chondroitin sulphate rich domains and subsequent reduction in the biomechanical function of cartilage. The loss of aggrecan occurs early in the pathological process, preceding the loss of collagen in OA and is a reversible process; whereas the loss of collagen type II, mediated by matrix metalloproteinases (MMPs), results in irreversible damage to articular cartilage (Karsdal *et al.* 2008).

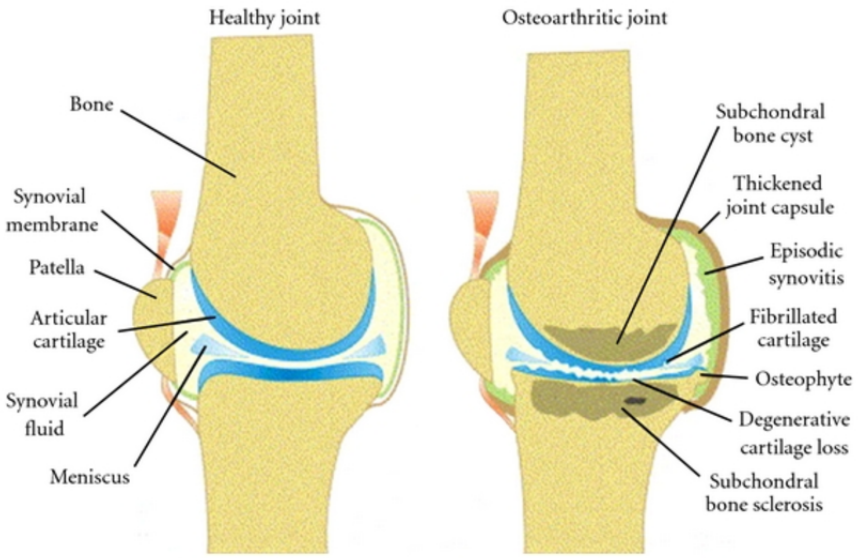

Figure 1.6 – Diagram comparing healthy versus osteoarthritic knee joint (Periyasamy *et al.* 2012).

1.2.1 Cartilage degradation

Aggrecan degradation

Many proteases are capable of degrading aggrecan *in vitro* however in articular cartilage the predominant aggrecan-degrading proteases are MMPs and ADAMTS-4 and 5 also known as aggrecanase 1 and 2, respectively (Durigova *et al.* 2011). There are 5 aggrecanase cleavage sites identified (Struglics *et al.* 2006) (Fig 1.7). Cleavage at the site $E^{373\_374}A$ within the interglobular

domain (IGD) by ADAMTS-4 or ADAMTS-5 results in release of the highly sulphated CS-1 and CS-2 domains from cartilage to the synovial cavity and reduces the mechanical function of articular cartilage. In a murine model where the IGD aggrecanase cleavage site was mutated to resist cleavage, mice were shown to be protected from experimental OA in a destabilisation of the medial meniscus (DMM) model (Little *et al.* 2007). Further cleavage, mediated by MMPs including MMP, at site N^{341}–^{342}F causes the release of a bioactive fragment 32 amino acids in length that has been shown to act as a damage-associated molecular pattern (DAMP) in articular cartilage and can mediate detrimental changes in gene expression of chondrocytes and transmission of pain through a toll-like receptor (TLR) dependant mechanism (Lees *et al.* 2015; Miller *et al.* 2018). Cleavage within the IGD leaves the G1 domain, bound to HA and link protein, within the cartilage and this has been predicted to have a half-life of 20 years and may compete for position on HA chains with newly synthesised aggrecan. Cleavage of aggrecan at sites within the CS2 domain are believed to be non-pathogenic and occur in healthy mature cartilage (Roughley and Mort, 2014).

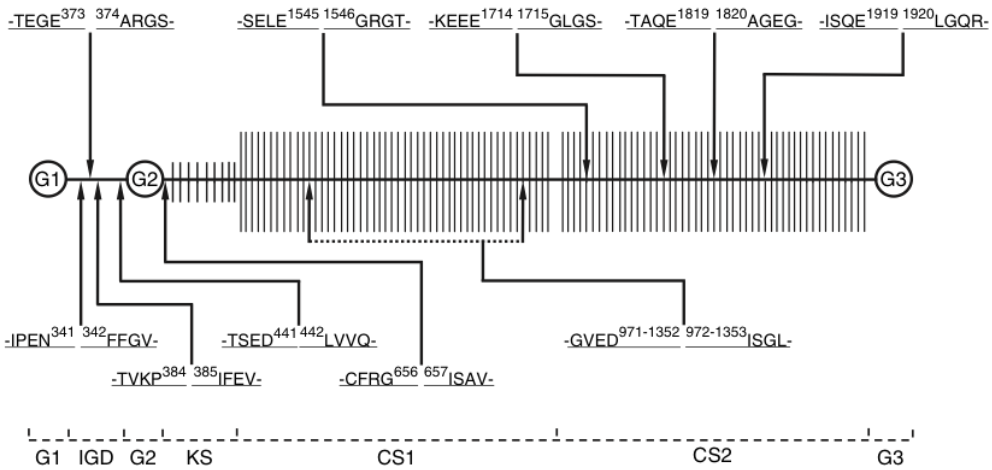

Figure 1.7 – Aggrecan structure showing ADAMTS cleavage sites (top) and MMP cleavage sites (bottom), (Struglics *et al.* 2006).

COMP degradation

Treatment of bovine articular cartilage explants with IL-1 results in COMP degradation and release to media with fragments detected at 300 kDa, 180 kDa and 67-80 kDa. Generation of these fragments was strongly inhibited by the application of broad spectrum MMP inhibitors. It was shown that BB-94, that is known to inhibit ADAMTS activity, mediated a more pronounced reduction in the generation of a 300 kDa fragment whereas CGS 27023A, that has a higher affinity for MMPs, was more potent in the inhibition of 67-80 kDa and 180 kDa fragments, suggesting that COMP is cleavable in explants by MPs of both ADAMTS and MMP sub-families (Ganu *et al.* 1998). MP-mediated cleavage of purified COMP *in vitro* has been shown for ADAMTS-4, 7, 12, MMP-1, MMP-3, MMP-9, MMP-13, MMP-19 and MMP-20 (Dickinson *et al.* 2003; Liu *et al.* 2006; Luan *et al.* 2008; Ganu *et al.* 1998; Stracke *et al.* 2000), although MMP-9 and MMP-13 were less effective in cleavage of cartilage-resident COMP compared to purified COMP (Ganu *et*

al. 1998).

The proteases responsible for cleavage *in vivo* remain unknown for both OA and RA. Di Cesare *et al.* (1996) showed that degradative fragments of COMP of similar molecular weight were detected in the synovial fluid of OA and RA patients suggesting that proteases involved may be similar across the two pathologies (Di Cesare *et al.* 1996). There is increasing evidence for a role of ADAMTS-7 and ADAMTS-12 in COMP cleavage in both OA and RA, with gene expression of both up-regulated in the cartilage of OA and RA patients compared to healthy controls. Inhibition of ADAMTS-7 or 12, using RNAi in human chondrocytes or blocking antibodies in human OA cartilage explants, was protective against COMP degradation with combined inhibition of both proteases resulting in complete inhibition of degradation induced by TNFα or IL-1β (Luan *et al.* 2008). The role of ADAMTS-12 is unclear as its deletion was shown to increase cartilage degradation and synovial inflammation in a collagen-induced arthritis (CIA) mouse model suggesting an anti-inflammatory role for ADAMTS-12 in this model therefore its up-regulation in RA tissue may be protective rather than pathological (Wei *et al.* 2018). The effects of COMP degradation upon OA pathology and cartilage mechanical integrity are unknown.

Collagen degradation

The estimated half-life of collagen type II in human articular cartilage is around 117 years and therefore it is unsurprising that collagen type II degradation and depletion is irreversible. Interestingly, significant degradation and loss of collagen is only evident after significant loss of GAGs suggesting that collagen is not accessible to MMPs in healthy, GAG-replete cartilage as shown by a significant reduction in collagen loss observed upon inhibition of aggrecanase activity in IL-1-treated explants (Pratta *et al.* 2003). Collagen degradation is mediated by the collagenases, a group that includes MMP-1, MMP-8 and MMP-13, that cleave at a ¾ distance from the N-terminus at site $G^{775\_776}L$ in human collagen type II resulting in two fragments that are unstable and therefore susceptible to denaturation allowing for subsequent cleavage by alternative MMPs. *In vitro* it has been shown that MMP-2 and MMP-14 are also capable of cleaving native collagen triple helix but in OA it is suggested that *in vivo* cleavage is predominately mediated by MMP-13 (Wang *et al.* 2013).

MMPs

MMPs are zinc-dependant endoproteinases within the larger metzincin family of proteases. MMPs are synthesised and released as zymogens. There are 24 genes coding for 23 different MMPs in humans with a general modular structure throughout the group (Fig 1.8). The pro-peptide region contains the so-called cysteine switch that associates with Zn^{2+} in the catalytic site and thereby prevents proteolytic activity prior to activation by cleavage of the pro-domain. The conserved sequence HEXXHXXGXXH in the catalytic site binds Zn^{2+}. The catalytic site is further structurally enabled by a methionine 8 amino acids after this sequence. A linker or hinge region is followed by the hemopexin-like domain, which is responsible for substrate specificity of MMPs (Nagase *et al.* 2006). MMPs are highly potent proteases that as a group are capable of degrading most extracellular matrix components, therefore their expression is highly regulated with additional, post-translational regulation of activity provided by the aforementioned cysteine switch and the endogenous tissue inhibitors of metalloproteinases (TIMPs). The catabolic role and in particular

the ability of MMPs to cleave aggrecan and multiple collagen types shows their relevance to OA (Lark *et al.* 1997).

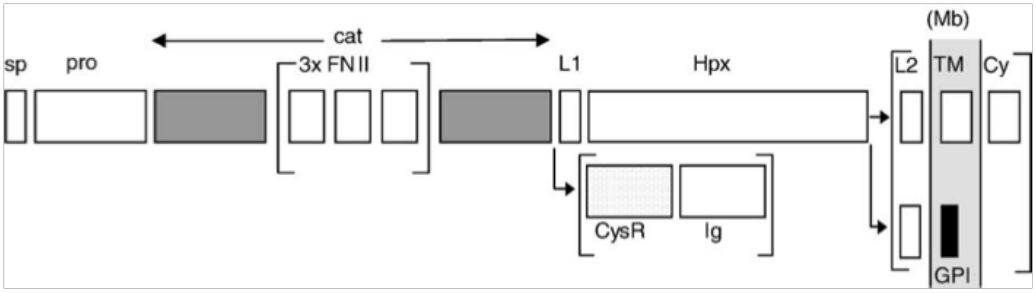

Figure 1.8 – Domain structure schematic of MMPs showing spacer domain (SP), pro-domain (PRO), catalytic domain (CAT), hemopexin-like domain (HPX). Modified from Nagase *et al.* 2006.

Collagenases

The collagenase MMPs include MMP-1 (interstitial collagenase), MMP-8 (neutrophil collagenase) and MMP-13. The collagenases are capable of cleaving the collagen triple helix at a site ¾ of the length from the N-terminal where the proline and hydroxyproline content is reduced. At this site the collagenases are able to partially unwind the helix and cleave which then allows for subsequent cleavage by non-collagenase type MMPs (Nagase *et al.* 2006). MMP-1 levels are elevated in the synovial fluid of OA patients (Tchetverikov *et al.* 2005) and the expression of MMP-1 is responsive to pro-inflammatory cytokines when assessed in chondrocyte monolayers or cartilage explants treated with IL-1β or TNF-α. The preferred substrate for MMP-1 is collagen type III although this MMP is capable of cleaving collagen type I, II, III, VII, IX and X to varying degrees (Klein and Bischoff, 2010). MMP-8 is produced at low levels by both healthy and osteoarthritic chondrocytes in addition to neutrophils. The preferred substrate for MMP-8 is collagen type I although this MMP is also capable of cleaving collagen type II, III, VIII, X, aggrecan and link protein (Cole *et al.* 1996). Interestingly, MMP-8 is capable of cleaving aggrecan at the aggrecanase site $E^{373\_374}A$ but has a much higher affinity for the traditional MMP site at $N^{341\_342}F$ (Fosang *et al.* 1994) (Fig 1.7). The ability of MMP-13 to cleave collagen type II with high efficiency in addition to increased expression at the gene and protein level in human OA patient cartilage reflects its crucial role in the pathogenesis of OA. In addition to mediating cleavage of collagen type II, MMP-13 is capable of cleaving collagen type I, III, VII, X and aggrecan (Rose and Kooyman, 2016). The rate at which MMP-13 cleaves collagen type II is roughly 5 to 10 times the rate of MMP-1 mediated collagen type II cleavage and therefore this MMP has been the focus of many OA studies. MMP-13 deficient mice were shown to be protected from cartilage degradation in a murine DMM model of OA (Little *et al.* 2009). In a rat anterior cruciate ligament transection (ACLT) model of OA, increases of MMP-13 expression were detected early (1 week) suggesting this MMP may have a role in the initiation of disease (Pickarski *et al.* 2011). MMP-13 expression in chondrocytes is shown to be induced upon mechanical loading via cyclic stress (Tetsunaga *et al.* 2010) or treatment with the pro-inflammatory cytokine IL-1β (Chan *et al.* 2017). MMP13 expression is also employed as a marker of chondrocyte hypertrophy (Van der Kraan and Van den Berg, 2012).

Gelatinases

The gelatinases, MMP-2 and MMP-9, are proteases that can cleave denatured collagen post-cleavage of the triple helix by the collagenases. Both MMP-2 and MMP-9 have 3 fibronectin type II repeats within the catalytic domain that mediate binding to gelatin and collagen and these MMPs are capable of cleaving collagen type IV, V and XI. MMP-2 is able to cleave collagens I, II and III by a similar mechanism to collagenases but with a much reduced efficiency. Pro-MMP-2 is associated with the cell membrane and is activated via cleavage by MT1-MMP (MMP-14) or MT2-MMP (Bauvois, 2011). Both MMP-2 and MMP-9 cleave aggrecan at the classical MMP site $N^{341}\_^{342}F$ (Fosang *et al.* 1992).

ADAMTS

A disintegrin and metalloproteinase with thrombospondin motifs (ADAMTS) proteases are members of the metzincin superfamily along with MMPs. They share with MMPs a zinc-dependant catalytic domain and are also released as zymogens that must be activated via removal of a pro-domain, which in the case of ADAMTS is mediated by pro-protein convertases such as furin and PACE-4. The basic modular structure of ADAMTS comprises of pro, catalytic, cysteine-rich, disintegrin, thrombospondin and spacer domains (Fig 1.9). The composition of these ancillary domains convey ADAMTS substrate specificity (Kashiwagi *et al.* 2004). The aggrecanase activity of some ADAMTS proteases is key to their role in OA pathogenesis although many ADAMTS have a role in normal ECM homeostasis (Kelwick *et al.* 2015). There are 19 members of the ADAMTS family which can be further grouped according to substrate (Fig 1.9). For the purposes of this thesis a focus will be made upon the aggrecanases; ADAMTS-4 and 5 due to their known pathological role early in OA.

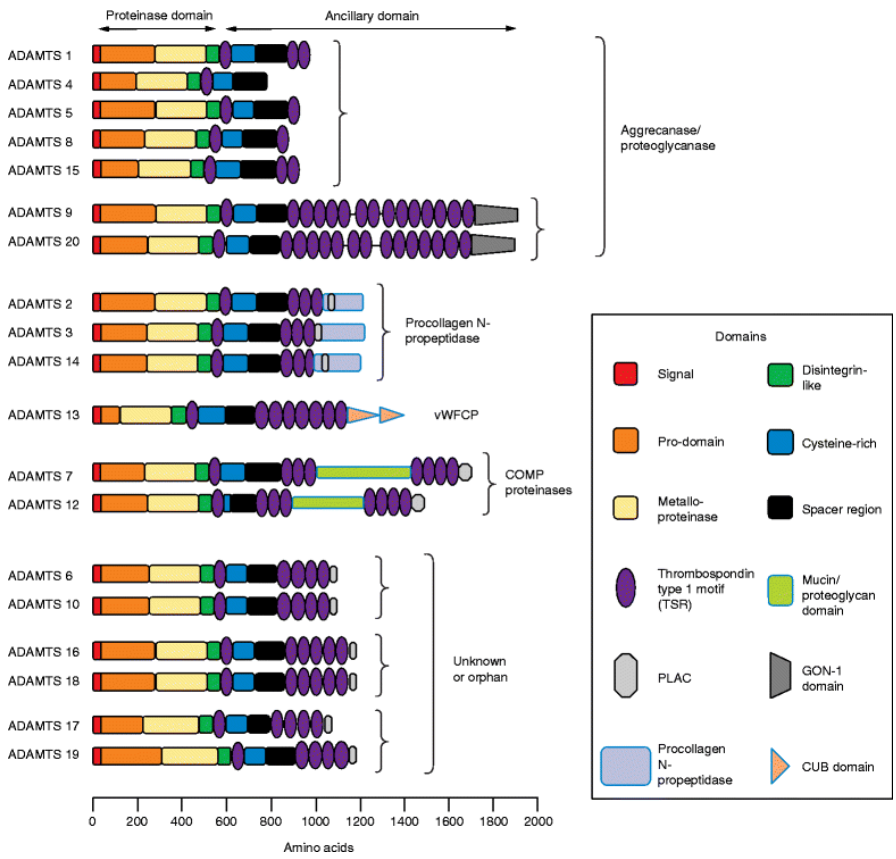

Figure 1.9 – Domain structure of all known ADAMTS proteases (Kelwick *et al*. 2015).

Aggrecanases

Several ADAMTS have been shown to cleave aggrecan *in vitro* including ADAMTS-1, 4 and 5. The initial discovery of a protease capable of cleaving aggrecan at the pathological $E^{373–374}A$ site led to the initial designation of ADAMTS-4 as aggrecanase 1. Further work identified aggrecanase 2 which is now designated ADAMTS-5. Initially postulated to be the main aggrecanase responsible for aggrecan degradation in arthritic disease ADAMTS-4 is capable of self-catalysis which results in multiple C-terminal truncated isoforms present in tissue. Full length ADAMTS-4, after pro-domain removal and activation by pro-protein convertases, has a molecular weight of 68 kDa. Cleavage, mediated by ADAMTS-4 or MT4-MMP (Patwari *et al.* 2005), within the C-terminal spacer domain at $K^{694–695}F$ results in a 53 kDa isoform with further cleavage at site $T^{581–582}F$ resulting in a 40 kDa form of ADAMTS-4. The ancillary domains provide substrate specificity and indeed studies have shown that C-terminal truncation of ADAMTS-4 alters substrate specificity with removal of the spacer domain increasing activity at the IGD cleavage site (Kashiwagi *et al.* 2004). Full length active ADAMTS-4 is found bound to the cell membrane and pericellular ECM, removal of the spacer domain or treatment of cartilage with heparin releases ADAMTS to the media suggesting the spacer domain mediates interactions with the ECM. The spacer domain is also required for cleavage in the heavily glycosylated CS-2 region of aggrecan with the p53 and p40 isoform showing a much reduced efficiency in cleavage at site $E^{1480-1481}G$ compared to active full length ADAMTS-4 (Gao *et al.* 2002). The role of glycosylations in substrate recognition and cleavage was further confirmed by degradation studies using aggrecan that was deglycosylated by treatment with chondroitinase

ABC showing a reduced cleavage mediated by full-length ADAMTS-4 in the CS2 region of deglycosylated aggrecan (Kashiwagi *et al.* 2004). A splice variant of ADAMTS-4, which bears an alternative spacer domain, has been detected in the synovium of OA patients, it was not detectable in OA cartilage or in healthy control synovium. This splice variant is capable of cleaving aggrecan at the $E^{373\_374}A$ site and therefore may contribute to damage in OA through degradation of cartilage upon release from the inflamed synovium (Wainwright *et al.* 2006). The activity of ADAMTS-4 is regulated in tissue by TIMP-3 and not TIMP-1 or 2 (Kashiwagi *et al.* 2001).

Aggrecanase 2 or ADAMTS-5 has a similar structure to ADAMTS-4 but includes an additional thrombospondin type I domain at the C-terminal (Fig 1.8). ADAMTS-5 contains four potential sites for glycosylation. Similarly to ADAMTS-4, full length ADAMTS-5 is associated with the cell membrane and ECM and can be released through the addition of heparin suggesting interactions with GAGs mediate this association (Gendron *et al.* 2007). In contrast to ADAMTS-4, the domains responsible for ADAMTS-5 binding to ECM are the Cys R and spacer domains, the removal of which results in release of ADAMTS-5 from the cell surface and ECM into culture media. The spacer domain in ADAMTS-5, like ADAMTS-4, is also involved in substrate recognition, particularly cleavage at site $E^{1480\text{-}1481}G$ as removal of this domain reduced cleavage activity at this site. Full-length ADAMTS-5 was shown to be over 1000 times more active in general aggrecan degradation compared to full length ADAMTS-4. ADAMTS-5 was also 600 times more active than ADAMTS-4 p53 at the pathological IGD site (Gendron *et al.* 2007). C-terminal truncation removing the TSP-2 and spacer domains of ADAMTS-5 to produce a domain structure very similar to ADAMTS-4 p53 resulted in an enzyme that was still 150-fold more active than ADAMTS-4 p53 at the IGD site (Gendron *et al.* 2007).

Attempts to identify the ADAMTS responsible for aggrecan degradation *in vivo* have shown that mice deficient in ADAMTS-5 are protected against experimental OA, induced by DMM (Glasson *et al.* 2005), whereas ADAMTS-4 deletion provided no such protection. This data, combined with the observed increased *in vitro* cleavage activity of ADAMTS-5 would suggest this is the ADAMTS responsible for pathological cleavage of aggrecan in OA, however, a role for ADAMTS-4 in addition to ADAMTS-5 has been demonstrated in human cartilage using RNAi strategies to down regulate ADAMTS-4 and ADAMTS-5 individually, where the down-regulation of either aggrecanase was shown to significantly reduce aggrecan degradation (Song *et al.* 2007). The lack of observed changes in gene expression of ADAMTS-5 in response to cytokines such as IL-1, led many to postulate that ADAMTS-4, which is up-regulated by pro-inflammatory cytokines, was the major aggrecanase in human OA (Tortorella *et al.* 2000). Post-translational regulation of ADAMTS may play a role in pathology and may potentially mediate a greater effect on protease availability and hence activity than gene expression. The discovery of ADAMTS-4 and ADAMTS-5 recycling by LRP1 in a mechanism to control the level of proteases in the ECM may explain discrepancies in gene expression, protein level and activity *in vivo* (Yamamoto *et al.* 2014). Cytokine-induced shedding of LRP1 reduces the endocytic clearance of ADAMTS-4 and ADAMTS-5 from the ECM and although the effect of this mechanism on aggrecan degradation *in vivo* is unknown, LRP1 levels were shown to be reduced by up to 90% in chondrocytes of OA patients suggesting this mechanism likely contributes to pathology (Yamamoto *et al.* 2013).

1.2.2 Osteoarthritis as an inflammatory disease

Long considered a "wear and tear" disease it is now widely recognised that OA is a whole joint disease with contributions to pathology from the synovium, cartilage and subchondral bone. The role of the inflamed synovium in OA pathology is clear with cells of the synovium, synovial fibroblasts and macrophages, producing and releasing into the synovial fluid of the joint cavity metalloproteinases (MPs) and pro-inflammatory cytokines that can further pathology by direct degradation of articular cartilage or via induction of a catabolic phenotype in chondrocytes, respectively. In contrast to RA, there is no obvious large-scale contribution to OA pathology by the adaptive branch of the immune system, however there is a clear implication for inflammation in disease progression originating from the innate immune system activated by multiple potential sources.

Synovitis

Inflammation of the synovium, detectable in patients by MRI or ultrasound, is a common feature of OA although not often as severe as that observed in RA and it is much less common to observe pannus-like synovitis in OA than RA. Whether synovial inflammation is the initiator of cartilage degradation or a consequence of it remains controversial. A commonly accepted model for synovial inflammation is that cartilage degradation products (such as aggrecan 32mer or fibronectin fragments) and alarmins (such as S100A8 and S100A9) are released to the synovial fluid where they act as damage-associated molecular patterns (DAMPs) to activate cells of the synovium via toll-like receptor (TLR) dependant mechanisms (Sokolove and Lepus, 2013). TLRs and the predominantly intracellular NOD-like receptors (NLRs) are pattern recognition receptors of the innate immune system that are capable of recognising danger signals in the form of pathogens (PAMPs: pathogen-associated molecular patterns) or damaged cells (DAMPs) and initiate innate immune responses. This leads to recruitment of macrophages to the synovium through production of chemokines such as monocyte chemoattractant protein 1 (MCP-1). Activated macrophages, particularly of the M1 inflammatory phenotype, produce inflammatory cytokines which in turn induce the production of proteases by synovial fibroblasts and superficial zone chondrocytes resulting in further cartilage degradation and release of DAMPs in a cycle of inflammation and degradation. During acute synovial inflammation there is an increase of neutrophils within the synovium, however, in chronic inflammation macrophages are present in higher numbers (Bonnet and Walsh, 2005). The role of macrophages in joint degradation has been confirmed by the amelioration of symptoms in mice where macrophages have been depleted by administration of liposomes containing cytotoxic clodronate. In these mice cartilage degradation was reduced as was the detection of the MMP generated aggrecan neo-epitope DIPEN- in the articular cartilage (Bondeson *et al.* 2010).

Crystal deposition

Inorganic crystals in the joint and joint fluid have been shown to activate the innate immune system. Basic calcium phosphate (BCP), calcium pyrophosphate dihydrate (CPPD) and monosodium urate crystals (MSU) have all been shown to activate the Nod-like receptor protein 3 (NLRP3) inflammasome that mediates the activation and release of IL-1β through induction of caspase-1

(Sokolove and Lepus, 2013) . CPPD crystals were detected in 93% of OA patients in contrast to only 24% of minimal or no OA controls (Gordon *et al.* 1984), although it remains to be elucidated if crystal deposition is a causal factor in OA or a consequence of OA pathology.

Ageing and inflammation

"Inflammaging" is the recently coined term for the phenomenon of chronic, sterile low-grade inflammation observed with increasing age. Detection of C-reactive protein and IL-6, (both up-regulated in OA) in the serum of aged patients in the absence of obvious infection does indeed suggest the occurrence of low grade persistent inflammation. Cellular senescence and in particular the acquirement of a senescence associated secretory phenotype (SASP) by senescent cells of the joint results in the secretion of pro-inflammatory cytokines such as IL-1β and IL-6 (Toh *et al.* 2016). Advanced glycation end (AGE) products are the result of non-enzymatic glycation of proteins, Briefly, carbonyl groups of sugars react via the Maillard reaction to a free amine group of amino acids in proteins, predominantly lysines, ultimately forming Schiff bases or Amadori products which are then available to react with free amines in other proteins resulting in protein conjugates or protein cross-linking (Gkogkolou and Böhm, 2012). Advanced glycation end products have been shown to accumulate with age and also in individuals with diabetes and particularly affect proteins that have an exceptionally long half-life such as collagens. These chemical modifications result in increased stiffness and brittleness of the matrix that can lead to increased degradation. Furthermore, the activation of the receptor for advanced glycation end products (RAGE) by binding AGE resulted in significant increases in GAG loss from cartilage cultures and over 200% increase in MMP1 expression (Steenvoorden *et al.* 2006). High mobility group box 1 (HMGB1), released from necrotic cells or secreted in response to cytokines has been shown to bind RAGE and results in the activation of NFκβ and the subsequent expression of pro-inflammatory cytokines. HMGB1 was shown to up-regulated in the synovium of knee OA patients (Xue-Hui Sun *et al.* 2016). Interestingly, the binding of HMGB1 to RAGE and its activation is dependent upon HS (Xu *et al.* 2011). Within inflammaging there appears to be a convergence of signalling via activation of the NFκβ transcription factor. NFκβ results in production of pro-inflammatory cytokines such as TNF-α, IL-1β and IL-6 which induce increased transcription of aggrecanases such as ADAMTS-4 and ADAMTS-5 and MMPs such as MMP-13 in chondrocytes. Importantly, NFκβ activation features prominently in many animal models of OA (Olivetto *et al.* 2015). The induction and resolution of inflammation is tightly controlled to clear infections successfully whilst minimising tissue damage induced by chronic inflammation. Resolution of inflammation is in part mediated by a shift from pro-inflammatory lipid mediators such as PGE2 and leukotrienes to pro-resolving lipid mediators including resolvins, maresins and lipoxins derived from eicosapentaenoic acid, docosahexaenoic acid and arachidonic acid, respectively (Recchiuti, 2014). The pathway and key enzymes and mediators are shown below (Fig 1.10) These lipids have been shown to increase the expression, nuclear translocation and activity of PPARγ, a key transcription factor in inflammation resolution that can directly inhibit the expression of NFκβ and AP-1 target genes and also promotes the transition of M1 inflammatory macrophages to the M2 anti-inflammatory subset (Croasdell *et al.* 2015).

AA, the precursor of lipid inflammatory mediators, potentiates TGFβ signalling via its disassociation

from the α2-macroglobulin inhibitory complex (Ling *et al.* 2003). Cellular levels of AA are tightly regulated with the predominant source of AA being the phospholipid bilayer. AA is liberated via hydrolysis by phospholipase A2 (PLA2) and to a lesser extent phospholipase C, upon release AA is metabolised by 5-lipoxygenase to produce pro-inflammatory leukotrienes such as LTA4 or by 15-lipoxygenases to produce lipoxins such as LXA4 and LXB4. Cytochrome p450 enzymes also play a role in the AA pathway by generating HETEs and EETs which have been shown to be anti-inflammatory (Divanovic *et al.* 2013). The role of pro-inflammatory lipid species, particularly PGE2, are well known in OA and indeed the success of COX-2 inhibitors is based upon their inhibition of PGEH2 production which is a precursor for PGE2 and thromboxin production. Similarly, aspirin mediates acetylation of COX-2 that results in the production of 15-epi-LXA4 and 15-epi-LXB4, the so called aspirin triggered lipoxins (ATL) that contribute to the anti-inflammatory effects of aspirin (Gilroy, 2005), although the action on both COX-1 and COX-2 likely contributes to the observed side-effects of aspirin comparable to those observed in non-specific inhibition of COX by NSAIDs. It must be noted that there is a requirement for both the enzymes and metabolites of the pro-inflammatory lipid pathways to induce the switch to anti-inflammatory mediator production and this may account for the increased damage in cartilage mediated by COX inhibition at later stages of OA and the limited therapeutic benefit of NSAIDs (Chan and Moore, 2010). Interestingly, a proteomics study has shown that PLA2 expression is heavily down-regulated in the chondrocytes of OA patients compared to non-OA controls (Tsolis *et al.* 2015) and a recent study has shown significant reductions in the AA concentration in the synovial fluid of OA patients versus non-OA controls (Vyver *et al.* 2018), which when combined implicate a deficiency in AA pathway-mediated generation of anti-inflammatory eicosanoids in OA pathology. It has been shown in human synovial fibroblasts that LXA4 treatment, at nanomolar concentrations, down-regulated IL-1β-induced expression of IL-6 and MMP-3 (Sodin-Semrl *et al.* 2000). Poly(lactic-co-glycolic acid) (PLGA) microparticles loaded with the anti-inflammatory lipoxin LXA4 were shown to decrease IL-1β and TNFα expression whilst increasing TGFβ expression and collagen deposition in a rat skin lesion wound healing model, with these effects attenuated in the presence of a specific LXA4 inhibitor, suggesting that LXA4 contributes to immune resolution and tissue repair in this model (Reis *et al.* 2017). Additionally, mice deficient in 12/15-Lox, the murine ortholog of 15-Lox-1, showed increased cartilage degradation and synovial inflammation compared to control mice in a transgenic TNFα model of arthritis. Conversely, pro-inflammatory gene expression of macrophages derived from 12/15-LOX deficient mice was reduced in the presence of exogenous LXA4 (Krönke *et al.* 2009). Chondrocytes have been show to express 15-LOX-1and 15-LOX-2 and a metabolite of the linoleic acid pathway generated by 15-LOX-1, 13-(S)-HODE was capable of inhibiting IL-1β induction of MMP-1 and MMP-13 expression in a PPARγ-dependant mechanism (Chabane *et al.* 2008). Collectively, these observations suggest a role for delayed or attenuated resolution of inflammation in the pathology of arthritic disease and the observations of aberrant lipid mediator synthesis and lipid signalling in both ageing and metabolic syndromes deriving from diabetes or obesity, all known risk factors for OA, suggest a potential role for eicosanoids in chronic inflammation of the joint and a therapeutic target.

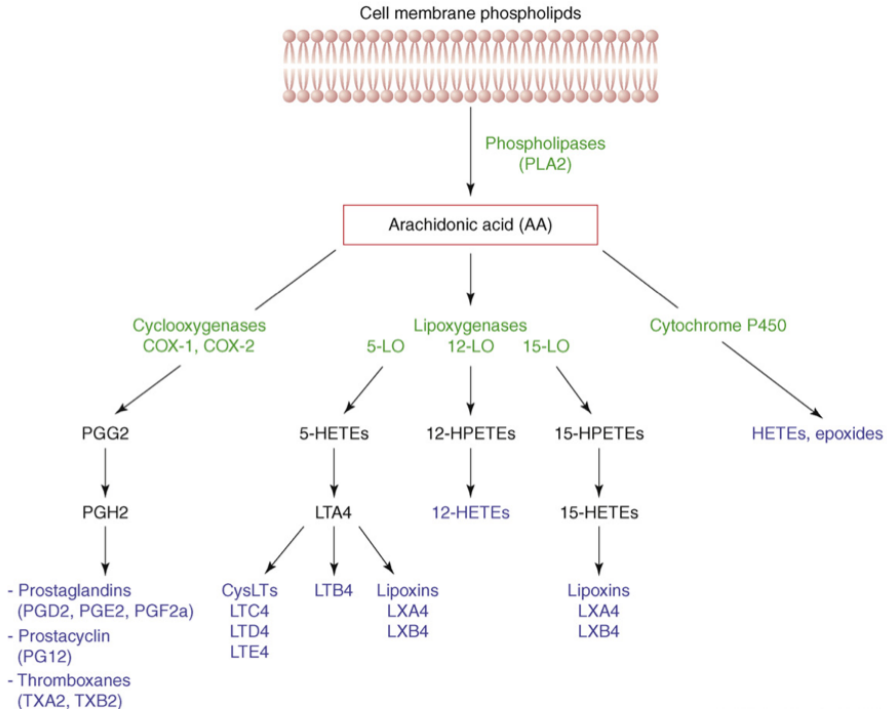

Figure 1.10 – Biosynthesis of eicosanoids from arachidonic acid (Harizi *et al.* 2005).

1.2.3 Cytokines in OA

Interleukin-1

The Interleukin-1 (IL-1) family of pro-inflammatory cytokines consists of 11 members although the most relevant to OA and the focus of this section are IL-1α and IL-1β which are often collectively termed IL-1. These two proteins often mediate the same effects in cells through binding of the same receptor despite only having 26% sequence homology. IL-1β is produced in a pro-form that requires cleavage for activation and secretion. Cleavage of Il-1β pro-domain mediated by NLRP3 inflammasome association with Caspase 1, also referred to as interleukin- converting enzyme (ICE), results in the secretion of a 17 kDa active form. In contrast IL-1α is produced as an active membrane bound pro-form that is cleaved by calpains at the cytosolic side of the cell membrane resulting in a mature soluble form that is secreted into the extracellular space. The cell membrane has two receptors for IL-1; IL-1 R1 and IL-1 R2, that both form duplexes with IL-1 RAcP. IL-1α or β binding to IL-1 R1 activates Myd88 and a subsequent signalling cascade leading to activation of NFκβ through Iκβ/p50/p65 or activation of AP-1 transcription factor through JNK and p38 pathways (Wojdasiewicz *et al.* 2014) (Fig 1.11). The activation of these transcription factors results in up-regulation of cytokines, MMPs and ADAMTS proteases in chondrocytes (Fig 1.11). Furthermore, IL-1 mediates the down regulation of the ECM components collagen type II and aggrecan.

The IL-1 R2 receptor lacks a cytoplasmic signalling domain and therefore acts as decoy receptor, sequestering IL-1 without mediating activation. Additional regulation of IL-1 activity is provided by IL-1RA, a soluble receptor antagonist that competes with IL-1 for receptor binding and thereby preventing activation.

IL-1 and in particular IL-1β have long been implicated in OA progression and is detected at

increased levels in the synovial fluid, synovium and cartilage of OA patients (Tsuchida *et al.* 2014). There are some observed differences in the literature between IL-1α and β, for example, in the synovial fluid of pigs presenting with mild or moderate spontaneous OA, IL-1α was detected at levels of around 0.05ng/ml in mild OA pigs whereas in pigs displaying moderate OA this was increased to a median level of almost 0.300ng/ml, conversely IL-1β levels were unchanged between OA stage with 0.109 and 0.122ng/ml in mild and moderate, respectively (Mcnulty *et al.* 2013). Additionally, it has been shown that IL-1α is 5 times more potent in the induction GAG loss from bovine articular cartilage compared to IL-1β (Smith *et al.* 1989), however IL-1β is more potent in inducing inflammatory response in human chondrocytes and is therefore more commonly employed in *ex vivo* studies where human or murine tissue are employed. In a study of human OA patients the level of IL-1α and β was increased in the synovial fluid but further increases, particularly for IL-1α were observed in the cartilage of OA patients versus healthy controls (Tsuchida *et al.* 2014). The success observed by the use of anti-TNFα antibody based therapies in RA has not been replicated in OA with the use of anti-IL-1 antibodies or the use of IL-1RA as a therapy to reduce IL-1 inflammatory activity. Clinical trials assessing the efficacy IL-1 receptor agonist construct, Anakinra, in knee OA patients showed no improvement in pain over placebo when assessed using the Western Ontario and McMaster Universities Osteoarthritis Index (WOMAC) (Chevalier *et al.* 2009) score but one trial did see a statistically significant improvement where the Knee Injury and Osteoarthritis Outcome Score (KOOS) was applied for Orthokine; an IL-1RA-enriched autologous conditioned serum (Frizziero *et al.* 2012). The lack of clear benefit of IL-1 RA therapeutics could be due to the short half-life of the constructs of around 4 hours, however, Anakinra did show efficacy in a trial conducted on RA patients so this is likely not the case. IL-1 RA is up-regulated in the synovial fluid of OA patients so the benefit of exogenous IL-1 RA is likely limited. A monoclonal antibody (AMG 108) targeting IL-1 R1 to inhibit the action of IL-1α and β has been trialled and showed improvements in patient pain score but not to significant levels and was deemed not clinically viable (Cohen *et al.* 2011).

The role of IL-1 in OA, however, remains contentious and indeed a recent study in mice deficient in either IL-1α, IL-1β and NLRP3 showed no protection compared to wild type mice in a murine meniscectomy model of OA (Nasi *et al.* 2017). Observations in the literature suggest that the role of IL-1 is potentially relevant early in the disease pathology within the acute inflammation phase and therefore the studies above in knee OA patients may have missed the therapeutic window. This however does not explain the lack of protection in IL-1 and NLRP3 deficient mice. However, caution must be applied when comparing studies of murine and human immune systems, where significant differences have been observed, for example mice are much less sensitive to LPS stimulation than humans suggestive of differences in TLR activation and response to stimuli that may be relevant when studying the effect IL-1 responses in mice. In summary, despite some contradictory studies and the lack of effective of anti-IL-1 biologics to date, there is overwhelming evidence in the literature derived from *in vivo*, *ex vivo* and *in vitro* studies showing some role for IL-1 within OA at some stage in the disease pathology.

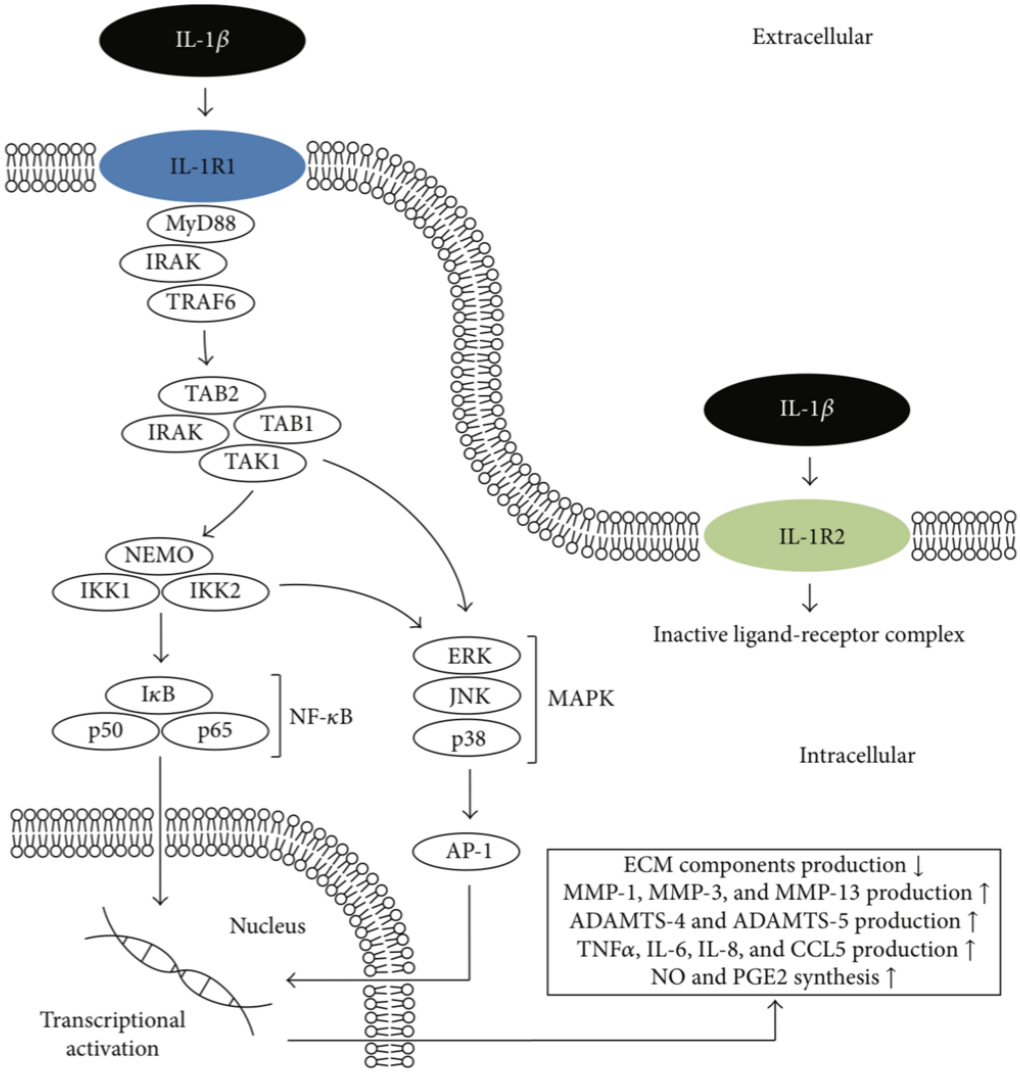

Figure 1.11 – IL-1β signalling pathway. IL-1β signalling through IL-1R1 results in activation of NFκβ and AP-1 transcription factors and subsequent expression of MMPs, ADAMTS, ROS and pro-inflammatory cytokines (Wojdasiewicz *et al*. 2014).

TNF-α

TNF-α is predominantly associated with rheumatoid arthritis (RA) where the use of anti-TNF-α monoclonal antibody therapeutics have had great success, confirming the pathological role of TNF-α in this disease. Studies have shown that TNF-α is up-regulated in OA and it is found in the same tissue compartments, SF, SM and cartilage, as IL-1β and co-localisation studies have shown that the same cells producing IL-1β are also producing TNF-α. Similar to IL-1β, TNF-α is produced in a non-secretable form but in contrast to IL-1β, TNF-α pro-form is active but associated with the cell membrane and requires cleavage by the "sheddase" TACE/ADAM17 to release the soluble form for subsequent binding and activation of target cells. Two TNF-α receptors are present on almost all nucleated cells. TNF-R1 is responsible for the majority of pro-inflammatory effects mediated by soluble TNF-α leading to activation of NFkB via recruitment of adapter proteins, including TRADD and TRAF2, ultimately leading to the phosphorylation of IKK which in turn activates NFκβ (Fig1.12) leading to gene expression in a similar mechanism to IL-1β. Further similarities between IL-1 β and TNF-α is the ability to activate both JNK and p38, through TAK1 and TAB1/2 resulting in activation of AP-1 (Wojdasiewicz *et al*. 2014). The binding of TNF-α to TNF-R2 results in cellular death via apoptosis mediated by pro-caspase-8. TNF-R2 has a much higher affinity for membrane-associated TNF-α as opposed to soluble TNF-α that is preferentially bound by TNF-R1 (Lang *et al.* 2016).

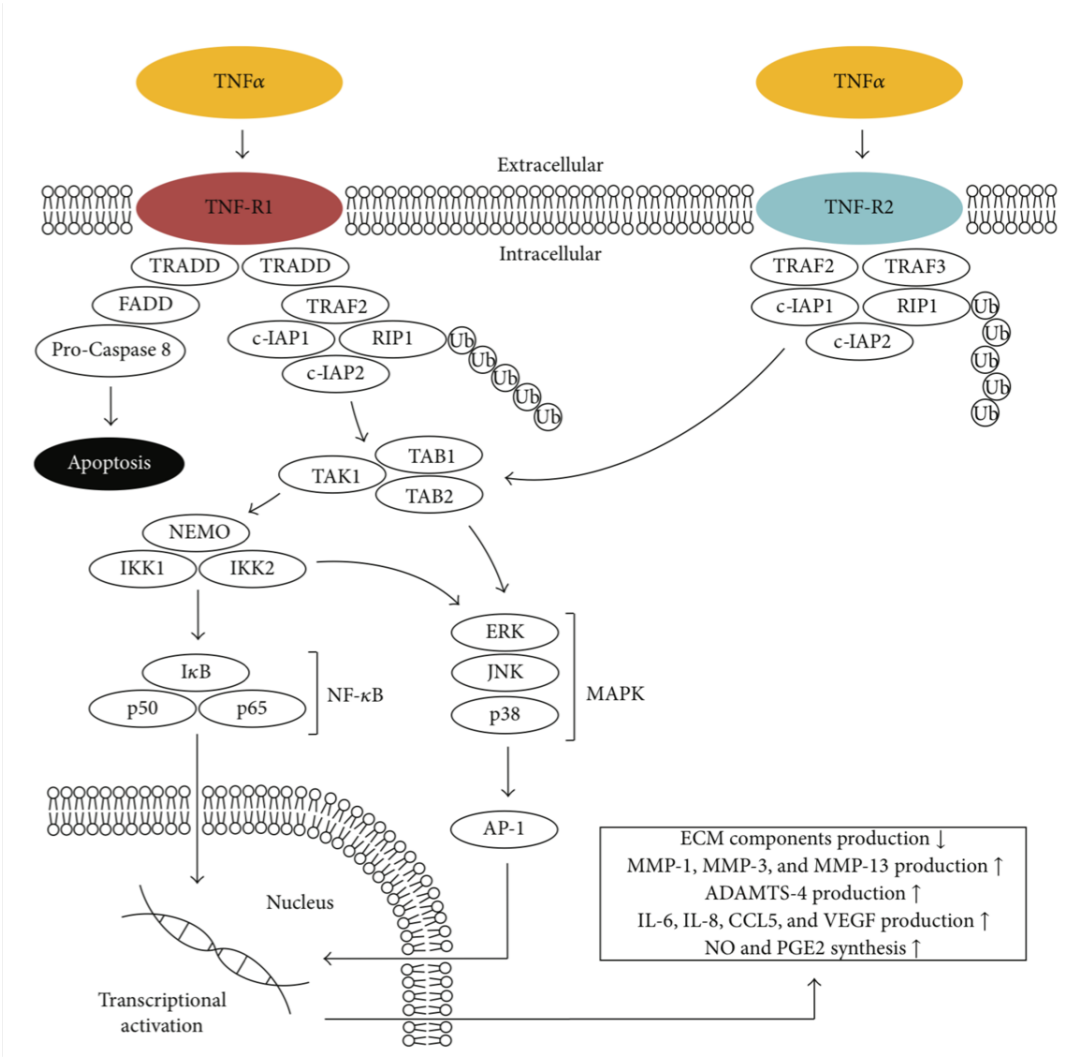

Figure 1.12 – TNF-α signalling through TNF-R1 and TNF-R2 results in activation of NFκβ and AP-1 transcription factors and subsequent expression of MMPs, ADAMTS, ROS, chemokines, growth factors and pro-inflammatory cytokines (Wojdasiewicz *et al*. 2014).

IL-6

IL-6 is a member of the gp130 family of cytokines and similarly to other members of this group, such as OSM and LIF, acts in a pleiotropic way dependent upon cell type and inflammatory state of target cells. IL-6 has been confirmed in multiple studies as being up-regulated in OA and has been shown to be up-regulated by IL-1 β and TNF-α. The classical mechanism of IL-6 activation in cells occurs via binding of IL-6 to the IL-6R receptor, that lacks a signal transduction domain and therefore recruitment of gp130 is required to initiate the signalling cascade. IL-6R can be released from the cell membrane by the "sheddases" ADAM-10 and ADAM-17 and circulating IL-6 bound to sIL-6R can be sequestered and inactivated by binding circulating gp130 (Wojdasiewicz *et al.* 2014). Conversely sIL-6R bound to IL-6 can complex with membrane bound gp130 and mediate signalling in a non-classical mechanism. IL-6 mediated signalling results in activation of STAT3, PI3AKT and MAPK pathways (Africa, 2017). *In vitro* studies using cartilage explants with the addition of IL-6 alone (classical signalling through the membrane form of the receptor) or in conjunction with its soluble receptor (an alternative pathway termed trans-signalling) leads to an increase in cartilage degradation and can synergise with TNFα resulting in greater degradation that either cytokine alone (Flannery *et al.* 2000). Conversely, the neutralisation of IL-6 in synovial fluid of OA patients caused a reduction in GAG content of explants whilst the addition of exogenous IL-6 to healthy chondrocytes increased GAG synthesis highlighting the context-dependent pleiotropic functions of IL-6. IL-6 has been proposed as a predictive biomarker for knee osteoarthritis and successfully used as a marker for disease progression in OA, when levels were assessed in the serum of OA patients versus healthy controls (Livshits *et al.* 2009).

Oncostatin M

OSM, so named from its observed ability to inhibit the growth of some solid tumours, is a member of the IL-6/gp130 family of pleiotropic cytokines. Up-regulation of OSM has been observed in the synovial fluid of OA and RA patients. OSM has been shown to bind and activate signalling through LIF-R and OSM-R, both of which require gp130 for signal transduction. Whereas human OSM can bind both LIF-R and OSM-R, LIF cannot bind and activate through OSM-R, however, the requirement of gp130 by both of these cytokines may explain the some of the observed redundancy between OSM and LIF. Interestingly, murine OSM cannot bind LIF-R, whereas rat OSM does and therefore more closely matches the human system. This may have implications for signalling mechanism studies using mice or murine cells. The mechanism of inhibition of IL-6 by soluble gp130 is not apparent with OSM and soluble gp130 resulted in only a partial inhibition of OSM-mediated proliferation at concentrations significantly higher than those required for IL-6 inhibition. Binding of OSM to LIF-R or OSM-R results in recruitment and activation of JAK1, JAK2 and TYK2 which in turn leads to Akt, STAT1 and STAT3 activation. In contrast, only binding of OSM to OSM-R results in the activation of STAT5b (Richards, 2013). Activation of signalling mediated by OSM can result in the activation of NFkB, STAT1, STAT3, STAT5b, AP-1 and HIF1-α transcription factors that induce the expression of pro-inflammatory genes and cartilage degrading proteases such as ADAMTS-4, ADAMTS-5, MMP-1, MMP-3 and MMP-13 in addition to chemokines such as MCP-1 (Fig 1.13). OSM has also been shown to down-regulate cartilage matrix macromolecule expression with neutralisation of OSM with antibodies increasing matrix

production *in vitro* (Beekhuizen *et al.* 2013).
Levels of OSM have been shown to increased in the synovial fluid of OA patients but to a lesser level than those observed in RA patients. Studies comparing the levels of OSM in the synovial fluid and cartilage of OA patients versus healthy controls found increases in synovail fluid (Ni *et al.* 2015) and cartilage (Tsuchida *et al.* 2014) for OA versus control but interestingly an increased amount of OSM in the cartilage versus synovial fluid (Tsuchida *et al.* 2014). The main source of OSM in the joint is the cells of the synovium with little to no production observed by chondrocytes. OSM has been shown to bind matrix components and remains active upon binding and this may provide a mechanism for increased concentrations in the cartilage compared to the synovial fluid and therefore caution must be applied when deciphering the relevance of cytokines based upon synovial fluid concentrations alone (Ryan *et al.* 2015).
The potential importance of the gp130 family of cytokines, including IL-6 and OSM, has led to the development of gp130 antagonists as potential therapeutics for OA which in mouse studies have shown a reduction in osteophytes, that have been shown to be induced by IL-6 and OSM treatment, and interestingly an increased regeneration of cartilage (Shkhyan *et al.* 2018).

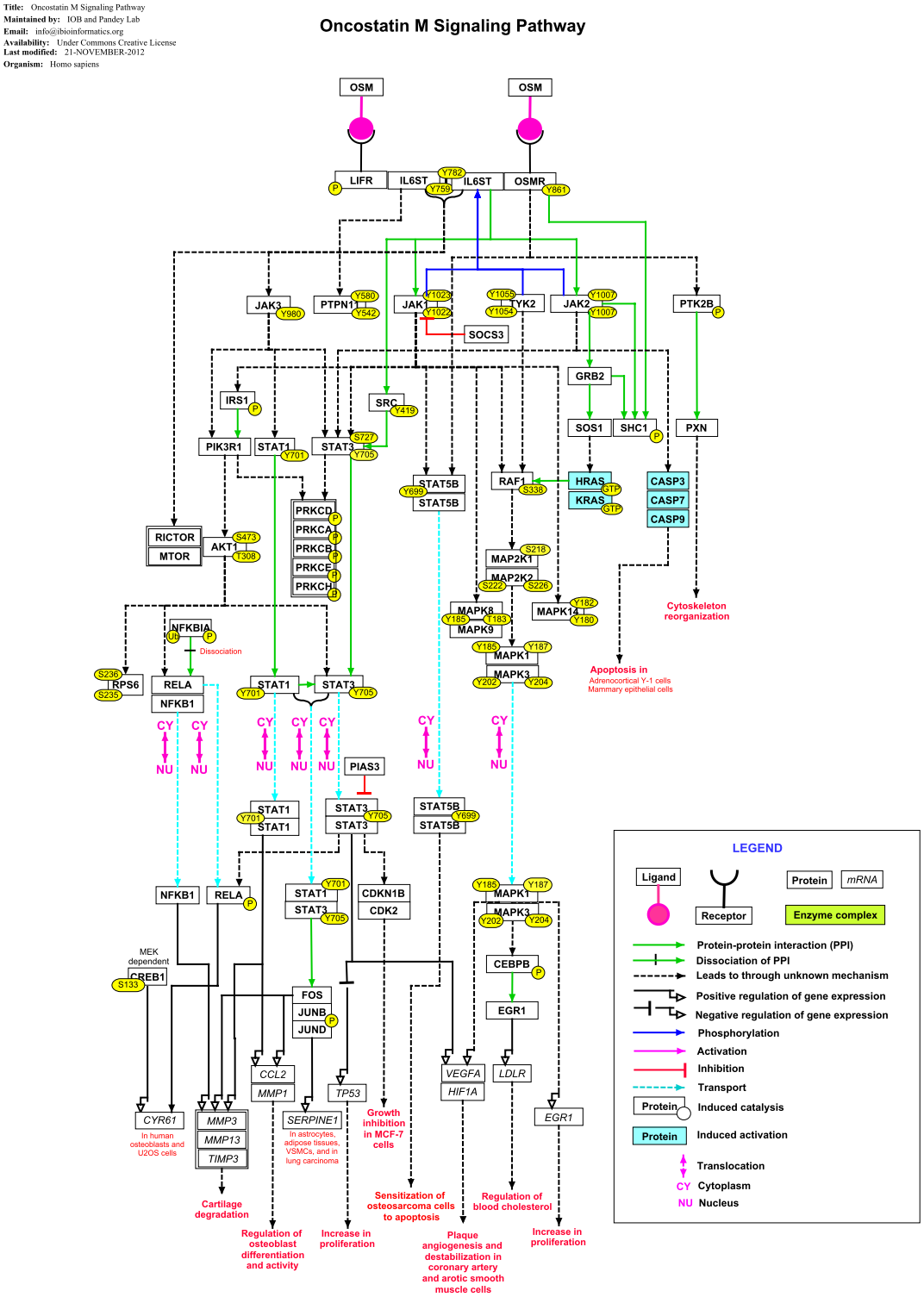

Figure 1.13 – Oncostatin M signalling pathway (Dey *et al*. 2013).

1.3 Osteoarthritis Therapeutics

1.3.1 Current therapeutic strategies for OA

There is a lack of disease-modifying osteoarthritis drugs (DMOADs) and the use of anti-cytokine therapeutics has not been successful to date. Initial treatments focus upon lifestyle modifications and pain management with analgesics, typically acetinomorphen. Lifestyle modifications recommended by health professionals include weight loss and moderate exercise, it has been shown that weight-bearing exercises such as walking are superior in benefit compared to non-weight bearing exercise such as swimming for the alleviation of OA symptoms, likely due to the mechanical stimulation of cartilage (Peeler and Ripat, 2018). For patients with moderate pain, non-steroidal anti-inflammatory drugs (NSAIDs) are recommended such as ibuprofen which act as analgesics and also anti-inflammatories through inhibition of COX-1 and COX-2 (Lambova *et al.* 2017). The observed side effects, such as gastro-intestinal distress, of general NSAIDs has led to the use of COX-2-specific drugs for example Celecoxib, although these have also been shown to mediate potentially harmful side effects, in particular hypertension (Aweid *et al.* 2018). In patients with moderate to severe pain, opioids are prescribed although the potential for dependence leads to the avoidance of their use where possible. Intra-articular injection of corticosteroids is often the next step in treatment and has shown to be effective in pain relief and reduction of inflammation although side-effects of these therapies, particularly immune suppression, ensures that injections are only provided up to 4 times per year (Lambova *et al.* 2017). Corticosteroid administration via the intra-articular route results in systemic effects due to clearance from the joint of small molecule therapeutics, this is discussed in more detail in Part II of this thesis. Intra-articular injections of hyaluronic acid are clinically approved and have shown some efficacy, although it has been shown to be of short-term benefit due to degradation of HA in OA patients (Tammachote *et al.* 2016). The mechanism of HA as a therapeutic is not fully understood but may add to the lubrication of the articular cartilage surface and increase the resistance to compression of synovial fluid. Intra-articular administration of therapeutics is not without risk as it can result in infection of the joint and requires trained medical staff. Nutraceuticals, such as glucosamine and chondroitin sulphate, although not commonly prescribed by medical professionals, have shown modest efficacy in reduction of pain after long term (>3 months) administration, however some large trials have also shown no effect of these dietary supplements therefore their value as therapeutics is still debated (Henrotin *et al.* 2014). Where defined cartilage defects are present then autologous chondrocyte implantation (ACI) offers a suitable therapeutic strategy. ACI requires the harvest of chondrocytes from a healthy non-weight bearing section of patient cartilage, chondrocytes are then expanded *in vitro* in chondrogenic media prior to mixing in a gel matrix, commonly HA, and applied to the defect to generate cartilage. This procedure has been successful in the repair of small defects but is costly and often the regenerated cartilage is fibrous in nature (Brittberg *et al.* 1994). For the treatment of small defects <2cm^2 stimulation of endogenous repair can be attempted via micro-fracture or ultrasound where degenerated cartilage surrounding the defect is debrided, calcified cartilage removed followed by stimulation of subchondral bone by micro-fracture or ultrasound (Nieminen *et al.* 2014). The final therapeutic option left for those that have limited mobility or severe pain due to OA is total joint replacement. Major surgical procedures of this kind are obviously not without

risk therefore represent a last resort.
In conclusion there remains an unmet need in the treatment of OA as a therapeutic intervention that can both halt disease progression and stimulate repair is lacking.

1.3.2 Emerging therapies and therapeutic targets

There is a lack of DMOADs therefore there is a concentrated effort within the OA research community to develop novel therapeutics and to identify novel targets for therapeutic interventions where possible. Therapeutics can be divided into categories based upon mode of action; direct inhibition of cartilage degrading proteases, anti-inflammatories/pathway inhibitors, regenerative medications and pain medications. Some of the discussed potential therapeutics are relevant to multiple groups and indeed the perfect DMOAD would prevent further damage to cartilage, regenerate damaged tissue and reduce pain.

Direct inhibition of OA proteases

Some of the earliest attempts to develop DMOADs were based upon the inhibition of cartilage degrading proteases, such as MMPs and ADAMTS. The inhibition of metalloproteinases is often achieved by competitive inhibitors that target the catalytic site, most often through a zinc-binding group (ZBG). Human trials using broad spectrum MMP inhibitors of the hydroxamic acid type as potential cancer therapies were unsuccessful with unacceptable side effects observed mainly in the form of musculoskeletal pain (Rasmussen and McCann, 1997). These side-effects were deemed serious enough to halt trials of hydroxamate inhibitors in the treatment of cancer. It was postulated that this musculoskeletal toxicity was due to inhibition of MMP-1 and MMP-7 by broad spectrum MMP inhibitors so compounds were developed with a reduced affinity for these MMPs, however toxicity persisted (Krzeski *et al.* 2007). Since these trials there has been a concerted effort to develop inhibitors specific to individual MMPs, particularly MMP-13, and also towards the aggrecanases ADAMTS-4 and ADAMTS-5, although to date none have progressed to the clinic. The potential that OA is a syndrome that may be instigated by multiple pathways e.g metabolic or inflammatory (age related or as a result of injury) ensures that targeting the proteases involved in cartilage destruction remains an attractive strategy because, regardless of the underlying cause of OA, cartilage degradation remains the pathological outcome.

Regenerative medicines and pathway inhibitors

The capability to regenerate degraded cartilage to restore function is an attractive goal for OA therapeutics. In this field there has been a focus upon the use of anabolic growth factors, however, the prototypical chondrogenic growth factor TGF-β often has deleterious effects in OA cartilage and is implicated in disease progression (Van der Kraan. 2018). FGF18 is a member of the FGF family which, like FGF2, can bind FGFR3 and mediate anabolic and chondroprotective effects in cartilage (Davidson *et al.* 2005). FGF18 has not shown any catabolic effects in contrast to FGF2, which upon binding to FGFR1 results in up-regulation of MMP-13 and ADAMTS-5 (Ellmann *et al.* 2013). A recent trial has shown an improvement in WOMAC score and radiographic joint space narrowing at 2 and 3 year assessments when recombinant FGF18, sprifermin was administered to knee

osteoarthritis patients compared to placebo controls (Hochberg *et al.* 2018) despite earlier studies showing little improvement at earlier time points, 6 and 12 months post intervention (Lohmander *et al.* 2014).

The Wnt signalling pathway is vital for tissue formation although recently it has been associated with OA pathology. A SNP in FRZB gene was shown to be associated with increased incidence of hip OA in Caucasian women (Loughlin *et al.* 2004). Additionally, Wnt signalling via WNT5a is implicated in the production of MMPs in response to fibronectin fragments in human chondrocytes and WNT5a expression was shown to be upregulated in the cartilage of DMM mice (Huang *et al.* 2017). The recent development of a small molecule Wnt inhibitor has shown promise as a DMOAD with initial trials showing good tolerability and promising results in reductions of joint space narrowing and WOMAC pain scores in patients receiving the highest dose of SM0469 compared to placebos (Yazici *et al.* 2017). Two larger trials to assess efficacy are underway.

GDF5, a member of the BMP family (BMP-11), has been identified as a genetic risk factor for the development of OA. A single nucleotide polymorphism (SNP) in this gene has to date shown a correlation with OA in Japanese and Han Chinese populations (Miyamoto *et al.* 2007). Therapeutics based upon GDF5 have shown some promise such as the cartilage protective effect mediated by recombinant GDF5 in a rat medial meniscus transection (MMT) model of osteoarthritis, interestingly the highest dosing regimen of 3 bi-weekly injections of 100µg rhGDF5 not only halted damage but also stimulated cartilage repair (Parrish *et al.* 2017). In human chondrocyte pellets GDF5 was shown to reduce expression of *MMP13* and *ADAMTS4* and increased the expression of chondrogenic markers, *ACAN* and *SOX9*. These effects were determined to be via inhibition of Wnt signalling mediated by induced expression of *DKK1* and *FRZB* (Enochson *et al.* 2014). The genetic disposition of populations with polymorphisms in GDF5 and FRZB, whose function is to indirectly or directly inhibit Wnt signalling, respectively, suggests a role for aberrant Wnt signalling in the development of OA or at least a subtype of OA.

Pain reduction

Often the most serious concerns of OA patients is pain and therefore safe pain reduction remains an unmet need, however, the transmission of pain itself in OA is poorly understood. Recent developments have shown a role for MCP-1/CCL-2, nerve growth factor (NGF) and ion channels such as Transient Receptor Potential Cation Channel Subfamily V Member 4 (TRPV4) in the transmission of pain in OA. Anti-NGF monoclonal antibody therapies have been successful in ameliorating pain in human trials, However, human trials were ceased temporarily in 2010 due to observed side-effects of accelerated OA and osteonecrosis mediated by Tanezumub (Hochberg, 2015). Work since has confirmed increased tibial cartilage degradation in Tanezumub-treated rats compared to isotype control in a MMT model of OA (LaBranche *et al.* 2016). Further work is being carried out to reduce dosing of Tanezamub and avoidance of NSAIDs during therapy which appears to compound off-target effects. Therefore, despite the promise of anti-NGF therapies there remains a lack of suitable safe pain therapies for OA. Targeting of TRPV4 using a small molecule inhibitor, that also inhibits the associated channel protein TRPA1 has shown to be a novel and effective therapeutic strategy for the reduction of pain and particularly pain associated with inflammation, when assessed in a trigeminal irritant (formalin) murine model (Kanju *et al.* 2016).

1.4 *In vitro* and *ex vivo* Models of OA for the Assessment of Therapeutics.

For the successful identification and assessment of potential OA therapeutics suitable *in vitro/ex vivo* models are required that mirror the pathology of disease and therefore can generate relevant preliminary data showing efficacy that may translate into a therapeutic benefit when progressing into a suitable animal model of OA. Multiple *in vitro/ex vivo* models are available for the study of chondrocytes and cartilage in response to pathological stimuli including mechanical stress and inflammatory cytokines. The choice of culture system and stimuli should be carefully selected based upon the predicted effect of therapeutic and outcome to be assessed.

1.4.1 Chondrocyte monolayers

The simplest *in vitro* model is the culture of chondrocyte monolayers after harvest from OA patient human cartilage or cartilage of animal origin. Chondrocytes in 2D culture have been shown to lose their chondrocyte phenotype as passage number increases resulting in a loss of the characteristic round cell shape to a more fibroblast-like spindle-shaped cell morphology. Additionally, changes in gene expression are also evident with a decrease in collagen II and aggrecan expression with an increase in collagen type I expression as culture period is extended (Castagnola *et al.* 1988; von der Mark *et al.* 1977). The culture of cells at high density and presence of chondrogenic media (often including ITS, ascorbate and growth factors such as TGF-β, although for gene expression studies growth factors are omitted) aids in preservation of the chondrocyte phenotype (Jakob *et al.* 2001; Schulze-Tanzil *et al.* 2002). Chondrocytes in monolayer can be stimulated through the application of inflammatory cytokines such as TNF-α, IL-1α or β, IL-6, OSM, retinoic acid alone or in varying combinations with co-treatment often resulting in synergistic effects upon gene expression (Johnson *et al.* 2016). Additionally, mechanical stimulation applied through cyclic tensile stretching of chondrocytes in monolayer can be employed to simulate damage induced by aberrant mechanical loading of cartilage (Bleuel *et al.* 2015). The expression of catabolic and anabolic genes can then be quantified using qPCR or ELISA for protein products. The benefits of chondrocyte monolayer culture are the ease of set up and the ability to harvest RNA free from interference from cartilage matrix macromolecules, specifically matrix GAGs that can interfere with RNA isolation and inhibit reverse transcriptase. Disadvantages are that the absence of the endogenous matrix and culture in 2D can affect chondrocyte phenotype and response to stimuli (Zien *et al.* 2001).

1.4.2 Cartilage explants

Cartilage explants derived from articular cartilage of animal or human OA patient origin have long been used in the study of cartilage degradation due to the ability to maintain chondrocytes in their native matrix and the ability to study cartilage matrix macromolecule degradation in response to pathological stimuli such as static load at pathological levels or inflammatory stimuli, through the application of cytokines. Limitations of these systems are the observation of cell death at the cut edge of cartilage explants (Gilbert *et al.* 2009) and the lack of physiological load during culture. Common cytokines used in cartilage explants are IL-1α/β, TNFα, OSM and IL-6. Some cytokine combinations result in synergistic induction of catabolic gene expression and cartilage degradation.

OSM in combination with IL-1 or TNFα results in increased GAG loss and more rapid collagen loss than cytokines added alone (Durigova *et al.* 2008). To better represent *in vivo* conditions, where the contribution of the inflamed synovium contributes to cartilage degradation, then co-culture systems have been developed where cartilage explants are cultured in the same well as synovium explants. In these systems it was shown that culture of normal cartilage with OA patient synovium resulted in catabolic gene expression and cartilage degradation compared to those cultured with normal synovium explants (Beekhuizen *et al.* 2011). The use of co-cultures does make the interpretation of data difficult as the factors produced by the synovium that initiate or augment cartilage degradation are not fully defined.

Sources of cartilage

Explants derived from human OA patients present a method to assess the response of diseased tissue to stimuli and assess the expression and production of catabolic factors such as proteases and cytokines and to assess cartilage degradation, however, the use of human OA tissue is not without limitations. The patient-to-patient variance is large and confounded by patient age, disease stage, sex, therapeutic regimen and weight amongst other factors. The lack of normal tissue controls is also a limiting factor- the practice of harvesting "normal" tissue proximal to diseased tissue is not representative of a healthy control (Geyer *et al.* 2009*;* Sato *et al.* 2006) as pathological changes that are not yet evident macroscopically may well be present at the level of transcription (Tsuchiya *et al.* 1997). Human OA cartilage is often obtained during total knee replacement (TKR) surgery and often represents a late stage of OA and therefore its use in the assessment of therapeutics that can slow disease progression and reduce onset are limited. Cartilage derived from animals sources is often used for initial studies, however, the choice of animal can have an effect upon its representation of human tissue. For example, the cartilage of mice is around 70 times thinner than that of humans and lacks the defined chondrocyte zonal morphology as seen in humans and the cartilage of larger mammals (McCoy, 2015). Porcine, bovine and equine cartilage are similar in thickness to human cartilage, although slightly thinner (Frisbie *et al.* 2006). The cartilage of rabbits is highly cellular in comparison to human cartilage (McCoy, 2015). Bovine cartilage is also more cellular than human cartilage but has very similar permeability properties, whereas, this is much changed in porcine cartilage. In studies where the diffusion of a therapeutic into cartilage is required the permeability of the cartilage will likely affect the observed therapeutic efficacy. The age of animal donors is also of importance and to obtain skeletally mature cartilage it is suggested that pigs, sheep and horses be of at least two years old and mice 10 weeks old, however, it must be noted that the growth plate of most mouse breeds does not fully close, even in animals deemed skeletally mature (Cope *et al.* 2018). The use of immature cartilage and chondrocytes for OA studies is not recommended as the structure, cell density and phenotype of chondrocytes is altered compared to that of mature animals (Fermor *et al.* 2013). The use of cytokines to induce OA like degradation in healthy bovine cartilage explants provides a simple and defined method to assess therapeutic effect in response to a controlled known stimuli.

For the purpose of this thesis, where the effects of therapeutics aimed at inhibiting the earliest stages of OA where the effects of pathology are reversible, namely aggrecan degradation, are to be tested, then the use of human OA cartilage is precluded as the disease state of TKR patient

cartilage is beyond this therapeutic window. Therefore, chondrocytes and cartilage explants from skeletally mature cows (>18 months old) were selected to be stimulated by defined combinations of pro-inflammatory cytokines. Although the concentrations of cytokines commonly used in these assays are at supra-physiological levels this does provide a suitably robust and rapid response to successfully assess therapeutic effects. This system provides a ready source of chondrocytes/cartilage and allows for the investigation of cytokine-specific effects in cartilage degradation, signalling pathways and gene expression assays, whilst additionally providing a suitable matched source of healthy controls which further aid in the assessment of a potential therapeutic. Of greatest importance is the thorough characterisation of the model to be used in the assessment of potential therapeutics to maximise the likelihood of identifying a bona fide therapeutic effect and to elucidate the mechanism of such an effect.

1.5 Surfen as a Potential OA Therapeutic

1.5.1 Historical use of Surfen and GAG interactions

Surfen hydrate (Fig 1.14) was originally developed as a less immunogenic and synthetic replacement for the animal-derived protein protamine in its use as an excipient in insulin delivery in the 1930's. The formation of complexes through electrostatic interactions between insulin and Surfen enabled a sustained release of insulin into the blood and therefore reduced the frequency of injection required (Umber *et al.* 1938). There are no reports of serious adverse events or toxicity with the use of Surfen although several reports of limited allergic reactions (Goerz *et al.* 1981; Kasa and Borda, 1990). Although, a study in mice in 1966 did show that Surfen administered at very high doses resulted in lymphoma development (Hunter and Hill, 1961), however, the concentrations used in this study (150mg/kg/day) were significantly higher than those likely to be used in therapeutic applications.

It was shown as far back as 1961 that Surfen had heparin-neutralising properties and recently there has been a renewed interest in Surfen hydrate due to its documented ability to bind negatively charged sulphated GAG chains. A change in conformation upon Surfen binding to GAGs results in fluorescence emission at 488nm when excited at 360nm allowing for facile quantification of binding. A hierarchy of binding from high affinity to lower affinity was noted Heparin>DS>HS>CS which closely matches the sulphation level of each GAG, with heparin, containing 2.4 sulphates per disaccharide, being the most highly sulphated suggesting that an increase in net negative charge of GAGs results in increased binding, via electrostatic interactions, to the net positively charged Surfen (Weiss *et al.* 2015). In addition, it was shown that Surfen could neutralise heparin and the synthetic anti-coagulant fondaparinux, to which no antidote is currently available (Weiss *et al.* 2015). In many recent papers Surfen has been applied as a tool to delineate the effects of extracellular GAG antagonism and particularly the effects of HS blocking upon HSPG-dependant signalling for example by FGF-2. The growth factor FGF-2, that requires HS co-binding for receptor activation, can elicit anti-chondrogenic effects, therefore the action of HS binding of Surfen on FGF receptors may be a mechanism by which Surfen stimulates chondrogenesis through dampening of FGF-2 signalling. It was shown by Schuksz *et al.* (2008) that Surfen hydrate is an inhibitor of FGF-2 receptor binding assessed by reduced ERK1/2 phosphorylation in cells treated

with FGF-2 in the presence of increasing concentrations of Surfen hydrate (Schuksz *et al.* 2008). FGF-2 release from ECM stores during cartilage damage, induced by cutting or mechanical load, was shown to be pathological and resulted in increased GAG loss from cartilage explants (Vincent *et al.* 2002) and therefore blockade of FGF2 signalling by Surfen may be beneficial in OA cartilage, although there are some discrepancies in the literature as to whether FGF2 acts in a catabolic or anabolic way. Fgf2$^{-/-}$ mice displayed increased articular cartilage degradation compared to wild type mice in both a spontaneous age associated OA model and a post-traumatic surgical instability model of OA (Chia *et al.* 2009). The determination of a net catabolic or anabolic effect of FGF-2 is further complicated by the presence of 4 receptors on the cell surface for FGF-2, FGFR1-4, although FGFR1 and FGFR3 show the highest expression on chondrocytes. During OA an increase in FGFR1 is observed at the chondrocyte surface. FGF2 signalling through FGFR3 results in an anabolic response whereas signalling via FGFR1 results in a catabolic response in chondrocytes, therefore the effects of FGF-2 are context dependent and in OA conditions likely detrimental.

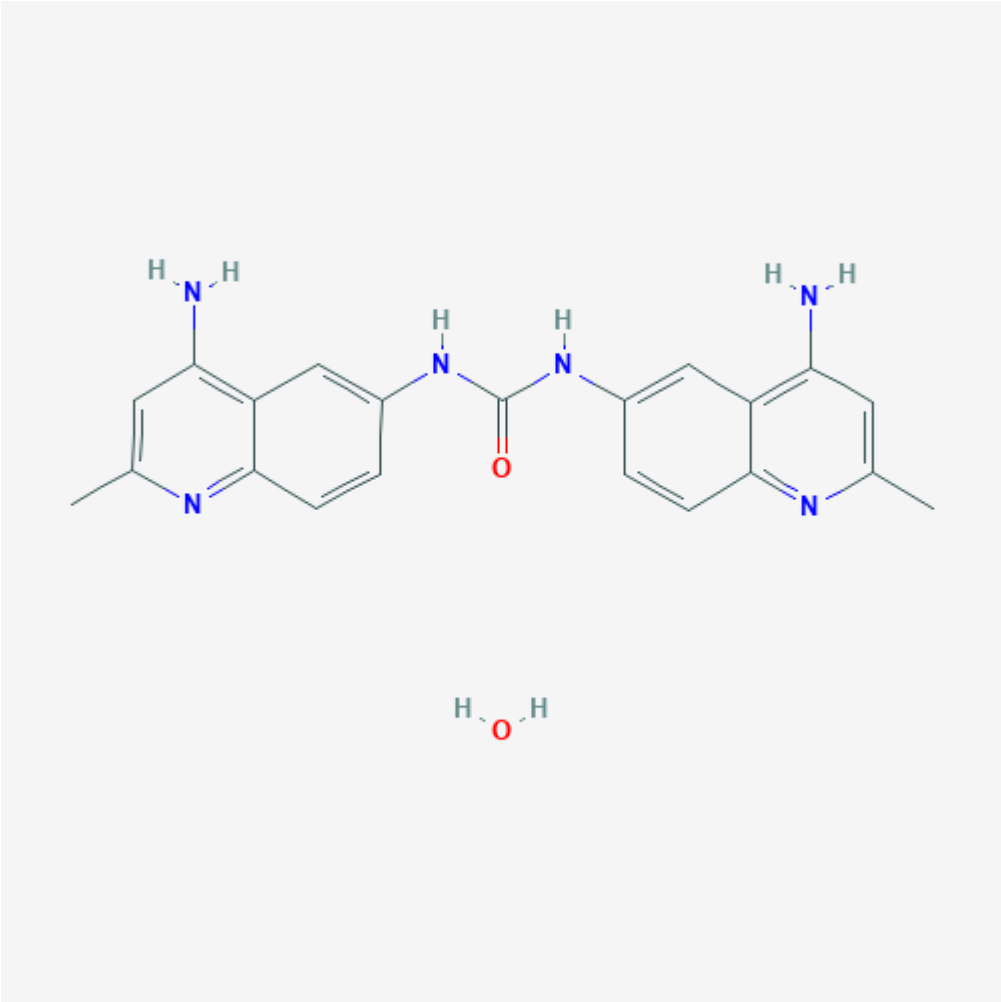

Figure 1.14 – Structure of Surfen hydrate.

1.5.2 Anti-inflammatory effects of Surfen

A study in 1992 aimed at identifying inhibitors of radio-labelled complement factor C5a binding to its receptors, CD88 and C5L2 , showed Surfen to have an IC50 of 3.3µg/ml (9.65 µM). Functional

studies of neutrophil degranulation confirmed Surfen acted as a C5a receptor antagonist (Lanza *et al.* 1992). C5a is a pro-inflammatory anaphylatoxin that acts as a neutrophil and macrophage chemoattractant through the GPCR CD88. C5a is a product of all three complement activation pathways, interestingly, C5a can be generated independent of complement activation via direct degradation of C5 by thrombin and also dust mite proteases. One of the first antagonists of C5aR developed, 3D53, reduced C5a chemotaxis of human polymorphonuclear leukocytes (PMNs) as expected but also reduced pro-inflammatory cytokine production by macrophages in response to LPS and IL-1 co-treatment suggesting a role of C5a beyond anaphylaxis and chemotaxis (Monk *et al.* 2007). The same inhibitor proved efficacious in reducing joint swelling in an antigen-induced rat model of arthritis. Small molecule antagonists have shown species- dependent effects and therefore the ability of Surfen to antagonise C5aRs in non-human species would require validation. C5 concentration is increased in the synovial fluid of OA patients and chondrocytes, both healthy and OA, are known to express C5aR and this expression is increased upon IL-1β treatment. C5-deficient mice showed reduced cartilage degradation and decreased expression of *Mmp3*, *Mmp13*, *Mmp14*, *Adamts4*, *Adamts5*, *Ccl2* and *Ccl5* in a murine medial meniscectomy model of OA, although the contribution of C5a in this model was unknown and protective effects may be a result of MAC inhibition alone (Wang *et al.* 2011). Finally, C5a has been shown to sensitise nociceptors and therefore may contribute to pain transmission in disease states.

Whilst investigating the role of GPCR signalling in the chemotaxis of neutrophils, Surve *et al.* (2016) showed that Surfen, which the authors had previously showed to bind Gβγ in a high throughput screening assay (Surve *et al.* 2014), activated Gβγ signalling independently of GPCR and Gα activation. They demonstrated a Surfen-mediated Ca^{2+} release from intracellular stores as assessed using Fura-2 and that this response was sensitive to the PLC inhibitor U73122 and Gβγ inhibitor M119. Interestingly, Surfen treatment alone resulted in rapid ERK1/2 and AKT phosphorylation (Surve *et al.* 2016). PLC and PLA2 phospholipases are both activated by Gβγ and both result in liberation of arachidonic acid (AA) from the phospholipid bilayer leading to the production of lipid mediators such as the pro-inflammatory PGE2 and leukotrienes and also anti-inflammatory lipoxins. How Surfen-mediated activation of Gβγ would therefore contribute to or potentially attenuate inflammation is unknown but may depend upon inflammatory state of cells. GPCRs are classic chemokine-type receptors and the effect of their activation by Surfen, albeit of only the Gβγ subunit, is largely unknown although it was shown that in a murine experimental autoimmune encephalomyelitis (EAE) model of inflammation that Surfen resulted in significant decreases in CCL2 and CCL5 production and release (Warford *et al.* 2018). Clinical scores were reduced in Surfen treated mice compared to controls, suggesting a reduction in immune cell recruitment and infiltration that was confirmed by flow cytometry of spinal cord extracts. Interestingly, in the EAE model Surfen resulted in a reduced proliferation of $CD4^+$ T-cells and this was also observed *in vivo* and *in vitro* in $CD3^+$ cells (Warford *et al.* 2018) and confirming Surfen-mediated reduction in murine T-cell proliferation observed in an earlier study by the same authors (Warford *et al.* 2014) . In the EAE model Surfen treatment resulted in an increased release of the TH2 cytokine IL-4, which drives M2 differentiation in macrophages promoting resolution of inflammation and tissue repair via IL-10 and TGFβ production (Warford *et al.* 2018). Additionally, Surfen was shown to down-regulate the expression of the pro-inflammatory cytokines IL-6, IL-

10, TNFα and the chemokines CCL2, CCL4 and CCL5 in bone-marrow derived macrophages (BMDMs) when stimulated with LPS *in vitro*. Surfen also mediated a reduction in expression of iNOS and NO release in BMDMs (Warford *et al.* 2018). Collectively, this data suggests that Surfen mediates an anti-inflammatory effect both *in vivo* and *in vitro*. Surfen mediated down-regulation of pro-inflammatory cytokines may be beneficial in the treatment of OA via a reduction in cytokine-induced expression of cartilage-degrading metalloproteinases. Likewise, the down-regulation of chemokines such as CCL2 and inhibition of C5a, combined with an increased expression of IL-4 may reduce synovial inflammation via inhibition of immune cell recruitment and inducing an anti-inflammatory M2 phenotype in synovial macrophages, respectively.

1.5.3 Chondrogenic effects of Surfen

It has been shown that application of Surfen alone may be sufficient to drive chondrogenic differentiation of mouse limb bud MSCs. The group of Maurizio Pacifici, Childrens Hospital of Philadelphia, have shown that addition of Surfen results in SMAD1/5/8 phosphorylation, indicative of TGFβ super family, though most commonly BMP, signalling, with a subsequent increase in the expression of the traditional markers of chondrogenesis; aggrecan, collagen type II and SOX9. Surfen treatment also resulted in an increase in collagen type X and RUNX2 expression, both markers of chondrocyte hypertrophy which suggests that although Surfen is chondrogenic it may also promote differentiation into hypertrophic chondrocytes which may be detrimental (Huegel *et al.* 2013; Mundy *et al.* 2018). The increased expression of aggrecan translates to increased deposition of sulphated GAGs as assessed by increased alcian blue staining of Surfen-treated MSC pellet cultures and this increase in GAG deposition was sensitive to the inhibitor of BMP signalling, Noggin (Huegel *et al.* 2013). The proposed mechanism of Surfen-mediated chondrogenesis was via GAG antagonism and indeed addition of heparitinase to cultures resulted in similar chondrogenic effects suggesting a role for HS and HSPGs. Surfen treatment also resulted in an increased expression of heparanase (HSPE) (Huegel *et al.* 2015). A recent study by the same group proposes a mechanism by which Surfen antagonism of HS prevents sequestration of endogenous BMP by an unknown HSPG allowing for binding of BMP2 to BMPR and resultant signalling. Other groups have observed that application of exogenous HS or heparanase increases the intensity of BMP-mediated SMAD1/5/8 phosphorylation, they also showed this effect to be significantly reduced in cells pre-treated with siRNA against syndecan 3 implicating this HSPG in sequestration and regulation of BMP-2 signalling (Mundy *et al.* 2018). In the absence of data showing the constitutive expression and extracellular concentration of BMPs by these cell types it is difficult to determine if Surfen acts only to increase the effectiveness of endogenous BMPs to activate SMAD or if Surfen acts via a secondary mechanism to increase BMP production by these cells, though Surfen was shown to increase BMP-2, BMPRI and BMPRII expression (Mundy *et al.* 2018). The observed increase in HPSE expression mediated by Surfen and the known inverse link between HSPE and EXT1 expression and the known chondrogenic effects of EXT1 down-regulation (Wang *et al.* 2018) is suggestive of secondary mechanisms but this remains unproven. Regardless of mechanism it is confirmed that Surfen mediates chondrogenic effects on cells, although how TGFβ superfamily signalling might be in disease states is not clear. TGFβ levels are increased in OA cartilage and therefore not perceived to be chondroprotective or is ineffective in pathological conditions (Kraan,

2018). However, Surfen mediated anti-inflammatory effects when coupled with chondrogenic effects on gene expression may lead to attenuation of damage and instigation of tissue repair and due to the distinct lack of truly regenerative OA therapies this warrants further investigation.

1.5.4 Surfen-mediated protease and ion channel inhibition

Interestingly, Surfen hydrate has been shown to be potent inhibitor of anthrax lethal factor (LF), a metalloproteinase, through chelation of zinc in the catalytic domain mediated by the ureic acid moiety present on Surfen (Williams *et al.* 2014) (Fig 1.15). Many first generation metalloproteinase inhibitors were hydroxamate-based inhibitors that function via hydroxamic acid binding of the catalytic site zinc in MMPs and also ADAMTS proteases and many of those inhibitors were promiscuous in their targets. Therefore, Surfen may exhibit inhibitory effects on other metalloproteinases which warrants further investigation. The lack of reported side-effects, particularly musculoskeletal effects, in human use and the lack of observed toxicity observed in multiple animal studies in mice and zebra fish suggest Surfen may be a candidate metalloproteinase and pro-protein convertase inhibitor for use in OA potentially avoiding toxic side effects often encountered with hydroxamate inhibitors but this is entirely dependant upon if Surfen inhibits OA-relevant proteases.
Additionally, Surfen is an inhibitor of both low and high voltage gated calcium ion channels. The implication of ion channels and in particular calcium channels in the transduction of pain led the authors to assess the effects of Surfen blockade of calcium channels in both acute (formalin induced) and chronic pain (thermal hyperalgesia induced by peripheral inflammation) murine models (Rivas-Ramirez *et al.* 2017). Matching that observed *in vitro* using DRG neurons, Surfen was indeed capable of blocking calcium channels and reduced the pain response of mice to thermal hyperalgesia and formalin induced pain stimuli (Rivas-Ramirez *et al.* 2017). This inhibition of calcium release from internal stores does not support the increase in calcium release observed by Surve *et al.* (2014) in the study of Surfen activation of Gβγ, indeed the effects of Surfen upon blockade of calcium channels was confirmed to be independent of Gβγ and therefore suggests potential cell type specific differences in Surfen effects upon calcium signalling.

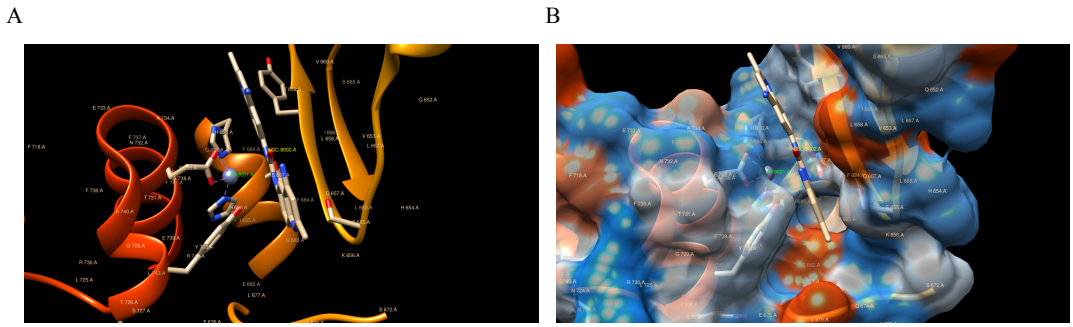

Figure 1.15 – Crystal structure showing Surfen binding proximal to active site zinc of anthrax lethal factor metalloproteinase depicted as ribbon structure (A) and hydrophobicity surface contour map (B). Images generated using PDB 1PWP from the RCSB repository using UCSF-Chimera.

In conclusion, the effects of Surfen as anti-inflammatory whether mediated via GAG interactions, Gβγ activation or calcium channel antagonism may present Surfen as a potential therapeutic for the reduction of cartilage degradation in OA, an effect which may be augmented by potential

direct protease inhibition mediated by Surfen. Additionally, the potentially regenerative effects of Surfen via SMAD activation through BMP or TGFβ signalling pathways and whether these effects are protective in inflammatory conditions warrants further investigation. However, many of the anti-inflammatory effects of Surfen are not quantifiable or relevant to the *ex vivo* cartilage model proposed in this thesis for example the effects of IL-4 induction upon macrophage phenotype could be evaluated *in vivo* or in synovium/cartilage co-cultures but not cartilage explants alone. Similarly, the effects of Surfen upon immune cell infiltration into the synovium via a reduction in chemokines such as CCL2 or even C5a is likewise not relevant to explant cultures but should be considered when selecting suitable animal models later in the project. Direct inhibition of OA-relevant proteases requires investigation using *in vitro* assays to confirm, the inhibition of degradative proteases, directly or via down-regulation of transcription, is essential for the treatment of OA as regenerative therapies such as TGFβ are likely ineffective in highly inflammatory and catabolic conditions. The potential mechanisms whereby Surfen may result in attenuation of cartilage degradation described within this Introduction are myriad and therefore the elucidation of the contribution of individual mechanisms is likely problematic. Therefore, the development and full characterisation of an *ex vivo* model of OA prior to the assessment of Surfen is likely critical in deciphering a mode or modes of action.

1.6 Hypothesis and Objectives

1.6.1 Hypothesis

The hypothesis of Part I of this thesis is that *Surfen may present as a potential therapeutic for the treatment of OA through its anti-inflammtory and pro-anabolic properties and that its mode action likely extends beyond HS antagonism*. Furthermore, it is postulated that the elucidation of a mode of action of potential therapeutics can be enabled through the development and thorough characterisation of cell signalling pathways, gene expression and cartilage matrix macromolecule degradation in cytokine induced *ex vivo* and *in vitro* models of OA. This hypothesis will be investigated through the completion of the following objectives;

1.6.2 Objectives

1. Extensive characterisation of a cytokine-induced *ex vivo* cartilage explant model of OA for the assessment of cytokine-induced cartilage matrix degradation that will provide a characterised method to assess the efficacy of Surfen in reducing cartilage degradation.

2. Determine the effects of cytokine application upon the induction of catabolic gene expression and down-regulation of anabolic gene expression to determine pathological gene regulation and provide a model for the assessment of anti-catabolic or pro-anabolic effects of Surfen.

3. Elucidation of the signalling pathways activated by addition of pro-inflammatory cytokines to isolated primary chondrocytes to identify pathological pathways that mediate the synergistic effects of cytokine combinations upon catabolic gene expression and cartilage degradation.

4. Identify if Surfen mediates direct inhibition of OA relevant MPs using molecular docking studies followed by experimental validation of inhibition using *in vitro* FRET based cleavage assays.

5. Assess the effects of Surfen upon cartilage matrix degradation using assays developed in Objective 1.

6. Attempt to elucidate a mode or modes of action of Surfen-mediated inhibition of cartilage degradation, if any, through assessment of cell signalling pathways and chondrocyte gene expression assays.

Chapter 2

Materials and Methods

2.1 Chapter 3 and General Methods

2.1.1 Cell and cartilage explant culture media

Table 2.1 – Media preparations used within the thesis including notes on application.

Name	Basal Media	Supplements	Notes	Tissue/Cell
Standard chondrocyte media (SCM)	Gibco DMEM Glutamax 4.5g/l Glucose (Thermo)	1X Insulin trasnferrin selenium (ITS) (Sigma). 50µg/ml Gentamicin (Sigma). 14µg/ml Ascorbate (Sigma).	ITS is often a component of chondrogenic media and has been shown to aid in maintainance of the chondrocyte phenotype. Ascorbate is required for collagen synthesis.	Bovine primary chondrocytes and articular cartilage explants.
Full DMEM Media (FDM)	Gibco DMEM Glutamax 4.5g/l Glucose (Thermo)	10% FBS (Thermo). 0.01U/ml PenStrep (Sigma).		J774.A2 HEK293
Full RPMI Media (FRM)	Gibco RPMI-1640 (Thermo)	10% FBS (Thermo). 0.01U/ml PenStrep (Sigma).		THP-1
HEK293 Expression Media (HEM)	Gibco DMEM Glutamax 4.5g/l Glucose (Thermo)	10% FBS (Thermo). 0.01U/ml PenStrep (Sigma). 250µg/ml G-418 (Thermo). 200µg/ml Hygromycin B (Thermo).	Selection agents G-418 and Hygromycin B select for successfully transfected HEK293 cells and ensure expresion of ADAMTS-4 constructs.	HEK293 cells expressing rADAMTS-4 p40, p53 or EtoQ.
Full Hybridoma Media (FHM)	Gibco RPMI-1640 (Thermo)	20% FBS (Thermo), 2 mM Glutamine (Thermo), 0.01U/ml PenStrep (Sigma), 0.01U/ml Fungizone (Sigma), 0.001 M Beta-Mercaptoethanol (Sigma).	Beta-Mercaptoethanol is a reducing agent added to culture to reduce the effects of oxidative stress induced by cell culture in high oxygen conditions.	Ag8 Hybridomas
HAT Media	Gibco RPMI-1640 (Thermo)	20% FBS (Thermo), 2 mM Glutamine (Thermo), 0.01U/ml PenStrep (Sigma), 0.01U/ml Fungizone (Sigma), 0.001 M Beta-Mercaptoethanol (Sigma). 1 X HAT Supplement (Thermo).	Selection media for AG8 and lymphocytes. Aminopterin (A) blocks nucleic acid synthesis which can be rescued via the salvage pathway using hypoxanthine (H) and thymidine (T). Non-fused AG8 cells lack HGPRT and therefore can not process H or T and die in culture.	Fusion Media
Serum Free Hybridoma Media (SFM)	Hybridoma-SFM (Thermo)	2 mM Glutamine (Thermo). 0.01U/ml PenStrep (Sigma), 0.01U/ml Fungizone (Sigma).	SFM is a low-protein (20µg/ml) defined medium and as such contains no bovine albumin or immunoglobulins that can interfere with downstream purification	Hybridomas
Chemically Defined Hybridoma Media (CDM)	Gibco CD Hybridoma (Thermo)	8 mM Glutamine (Thermo) . 0.01U/ml PenStrep (Sigma), 0.01U/ml Fungizone (Sigma).	Animal protein free media for the culture of hybridomas allowing for purification without interference from bovine immunoglobulins presnt in FBS.	Hybridomas
Freezing Media	FBS (Thermo)	10% DMSO (Sigma)	DMSO acts as a cryoprotectant by reducing the formation of crystals during the freezing process.	All cells for freezing

2.1.2 Bovine articular cartilage harvest

Cartilage was harvested under sterile conditions from the metacarpophalangeal (MCP) joint of 18 month old cows (Fig 2.1) obtained from a local abattoir (Maddock and Kembrey, Maesteg) prior to 6mm, 4mm or 2mm diameter biopsies taken using biopsy punches (Miltex), placed in 24, 48 or 96 well plates (Corning), respectively, and equilibrated in SCM (Table 2.1) for 48 hours prior to treatments.

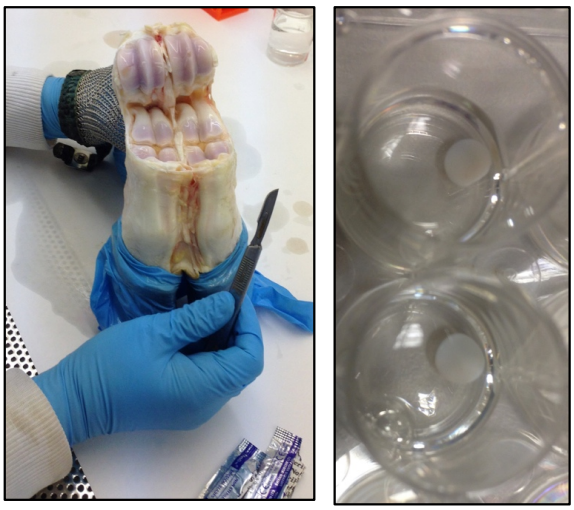

Figure 2.1 – Image showing bovine articular cartilage harvest from metacarpophalangeal joints (left) and 4mm diameter cartilage explants (right).

2.1.3 Bovine primary chondrocyte isolation

Cartilage was harvested from the metacarpophalangeal joints of 18 month old cows with cartilage pooled from a minimum of 3 animals prior to incubation in 0.1% (w/v) pronase (from *Streptomyces griseus*, Sigma) in DMEM + 5% FBS (Thermo) + 50µg/ml Gentamicin (Sigma) for 2 hours. Media was replaced with 0.04% (w/v) collagenase type II (Worthington) in DMEM + 5% FBS + 50µg/ml Gentamicin overnight. Both pronase and collagenase media solutions were added at 7.5ml per gram tissue. The digested cartilage was then passed through a 40µm nylon strainer to remove undigested cartilage and strained cells pelleted by centrifugation at 400 x g for 10 minutes. Cells were washed in DMEM then pelleted by centrifugation and counted using a haemocytometer. Cells were seeded in 24, 12 or 6 well plates dependent upon downstream application at $1x10^6$ cells/cm^2 in SCM and allowed to adhere overnight prior to treatments. The seeding of chondrocytes at high density has been shown to aid in maintenance of the chondrocyte phenotype (Watt. 1988) which was assessed by a round morphology of cells under bright field microscopy. Additionally, chondrocytes were used in cellular assays within 48 hours of harvest to further ensure chondrocyte phenotype was maintained.

2.1.4 BCA total protein assay

The bicinchoninic acid (BCA) protein assay (Pierce) was performed as per manufacturer's instructions. Briefly, a BSA standard curve was generated at concentrations 0, 25, 125, 250, 500,

750, 1000, 1500 and 2000µg/ml. 25µl of standard or sample were added to a clear 96 well plate (Corning) in triplicate. BCA working reagent was prepared by combining reagent A and B at a ratio of 50:1. 200µl of working reagent was added to each well and plates incubated for 30 minutes at 37°C prior to reading absorbance at 560nm using a FluoSTAR Optima plate reader (BMG Labtech). Absorbance values of standards were plotted against concentration and linear regression analysis employed to determine protein concentration of test samples.

2.1.5 Pathscan intracellular signalling array analysis of cytokine treated chondrocytes

The Pathscan intracellular signalling array (Cell Signaling Technology) is a slide-based sandwich array that allows for the simultaneous quantification of the phosphorylation level or cleavage product of 18 signaling proteins (Fig 2.2). Chondrocytes harvested from bovine cartilage, as described in section 2.1.3, were seeded in 6 well plates at a density of $1x10^6/cm^2$ in SCM overnight. Media was then removed prior to addition of IL-1α (10ng/ml), OSM (50ng/ml) or IL-1α +OSM (all Peprotech) or SCM media alone and incubated for 10, 30, 60 or 120 minutes. Upon harvest plates were placed on ice and cell lysis buffer (CST) containing Halt protease inhibitor cocktail and EDTA (Thermo) added to a final concentration of 5mM. Cell lysates were centrifuged at 14,000 x g for 15 minutes to remove cell debris. Total protein was quantified using BCA assay (2.1.4). Array blocking buffer was added to each well for 15 mins prior to addition of 50µg of protein to each well of the Pathscan array and incubation for 2 hours at room temperature (RT) with shaking. Wells were then washed 4 x 5 minutes with array wash buffer prior to addition of detection antibody and incubation for 1 hour at RT with shaking. Wells were then washed 4 x 5 minutes with array wash buffer prior to addition of DyLight 680™-linked Streptavidin and incubation for 30 mins followed by 4 x 5 minutes washing with array washing buffer and assessment of fluorescent intensity at 700nm using a LiCor Odyssey and quantification of the average total fluorescence of duplicate spots performed using LiCor Image Studio.

Intracellular Signaling

	Target	Phosphorylation Site	Modification
1	Positive Control	N/A	N/A
2	Negative Control	N/A	N/A
3	Erk1/2	Thr202/Tyr204	Phosphorylation
4	Stat1	Tyr701	Phosphorylation
5	Stat3	Tyr705	Phosphorylation
6	Akt	Thr308	Phosphorylation
7	Akt	Ser473	Phosphorylation
8	AMPKα	Thr172	Phosphorylation
9	S6 Ribosomal Protein	Ser235/236	Phosphorylation
10	mTOR	Ser2448	Phosphorylation
11	HSP27	Ser78	Phosphorylation
12	Bad	Ser112	Phosphorylation
13	p70 S6 Kinase	Thr389	Phosphorylation
14	PRAS40	Thr246	Phosphorylation
15	p53	Ser15	Phosphorylation
16	p38	Thr180/Tyr182	Phosphorylation
17	SAPK/JNK	Thr183/Tyr185	Phosphorylation
18	PARP	Asp214	Cleavage
19	Caspase-3	Asp175	Cleavage
20	GSK-3β	Ser9	Phosphorylation

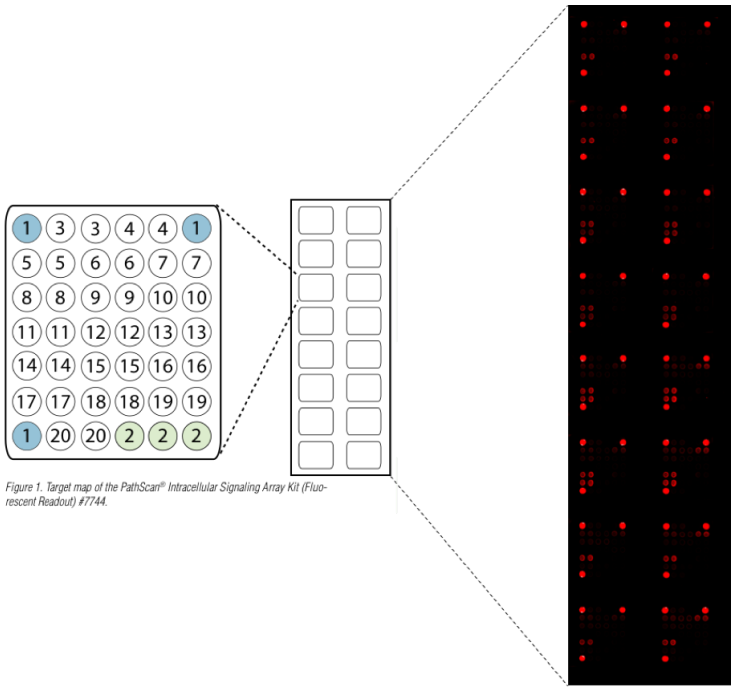

Figure 2.2 – Schematic of Pathscan intracellular signalling array showing signalling molecules assessed according to site of phosphorylation or cleavage event. Modified from www.CST.com.

2.1.6 RNA isolation

Total RNA was isolated from bovine primary chondrocytes by dissolution in TriReagent (Sigma) as per manufacturer's instructions. Briefly, 1ml per $1x10^6$ cells TriReagent was added followed by addition of 0.2ml Chloroform (Sigma) and centrifugation at 14000 x g for 15 minutes (4°C). The upper aqueous phase was collected and 500µl 70% molecular biology grade ethanol (Sigma) added prior to loading on RNAeasy columns (Qiagen) and isolation as per manufacturer's instructions. Harvested RNA was quantified by Nanodrop (Thermo) and protein contamination assessed by 260/280 absorbance ratios with values above 1.7 deemed acceptable for subsequent cDNA generation and analysis.

2.1.7 cDNA generation

cDNA was generated from 50ng or 100ng of isolated RNA using GoScript Oligo(dt) Reverse Transcription system (Promega) as per manufacturer's instruction. Briefly, RNA in nuclease-free water (Promega), 10µl was added to microtubes containing 10µl Go Script master mix (4µl nuclease free water, 4µl Oligo(dt) reaction buffer and 2µl Go Script enzyme mix) and placed in a thermal cycle for the following thermal profile; 25°C for 5 minutes (primer annealing), 42°C for 60 minutes (extension) and 70°C for 15 minutes (inactivation of reverse transcriptase enzyme). cDNA was stored at 4°C until use.

2.1.8 qPCR

cDNA was diluted 1:5 (50ng input RNA) or 1:10 (100ng input RNA) and 5µl added per well with 200 nM forward and reverse primers (Table 2) and 2x JumpStart Sybrgreen mastermix (Sigma) in a

total reaction volume of 30µl. Annealing was performed at 60°C for all primer sets except *COL2A1* and *MMP13* which were run at 62°C and 58°C, respectively. Primers used have been previously validated with the exception of *EXT1* primer pair which were designed using NCBI Primer blast (Table 2.2). Thermal profile was as follows; 95°C for 3 minutes (1 cycle). 95°C for 15 seconds, 60°C for 30 seconds and 72°C for 30 seconds (40 cycles). All experiments were performed using the Stratagene Mx3000 (Agilent). Disassociation curves were analysed for single products (an example of a disassociation curve is provided for *ADAMTS-5* primer set in Fig 2.3). *GAPDH* was used as reference gene (Al-Sabah *et al.* 2015) with fold change of genes of interest calculated using $2^{-\Delta\Delta Ct}$ method (Livak and Schmittgen, 2001) with the mean and *sd* of three experiements plotted. Statistical analysis was performed on ΔCt values prior to exponentiation of data to fold change. Probability that data is normally distributed was assessed using D'Agostino-Pearson omnibus K2 test with statistical significance of data subsequently assessed using ANOVA. Both tests performed using GraphPad Prism 7.0.

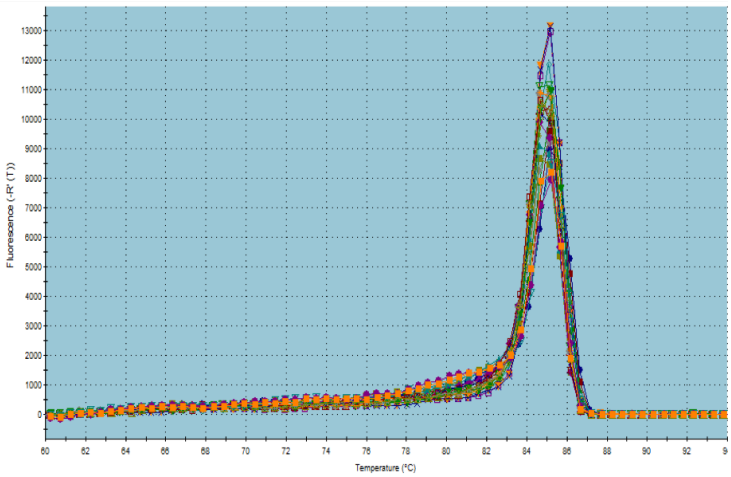

Figure 2.3 – Disassociation curve generated by *ADAMTS-5* primer pair using cDNA derived from bovine chondrocyte RNA showing single product.

Table 2.2 – Primer pairs used in this thesis. * additional experimentally validated *ADAMTS-7* and *ADAMTS-12* primer sets to confirm results were obtained from BioRad.

Gene	Forward 5'-3'	Reverse 5'-3'	Ref
ADAMTS-4	CTCCATGACAACTCGAAGCA	CTAGGAGACAGTGCCCGAAG	(Gilbert *et al.*, 2012)
ADAMTS-5	CTCCCATGACGATTCCAAGT	TACCGTGACCATCATCCAGA	(Gilbert *et al.*, 2012)
*ADAMTS-7**	CCACGTGGTATACAAGCGCC	GGTCCTCCTCCTCATCTTCC	(Willis, Bridges and Fortune, 2017)
*ADAMTS-12**	GTGCAGCAAGGACTATATCA	GCGTTTTCTTTCTCCAGTGC	(Willis, Bridges and Fortune, 2017)
MMP1	CAAATGCTGGAGGTATGATGA	AATTCCGGGAAAGTCTTCTG	(Natoli, Scott and Athanasiou, 2008)
MMP3	TGGAGATGCTCACTTTGATGATG	GAGACCCGTACAGGAACTGAATG	(Al-Sabah *et al.*, 2016)
MMP13	CCCTTGATGCCATAACCAGT	GCCCAAAATTTTCTGCCTCT	(Blain, Ali and Duance, 2010)
iNOS	TGTTCAGCTGTGCCTTCAAC	AAAGCGCAGAACTGAGGGTA	(Hailemariam *et al.*, 2014)
PGE2	GGACGCTCAGAGACATGGAG	TATGCCACGGTGTGTACCATA	(Blain, Ali and Duance, 2010)
ACAN	CAGCCAGGCCACCCTAGAG	GGGTGTAGCGCGTGGAGAT	(Park *et al.*, 2005)
COLL2A	AGCAGGTTCACATATACCGTTCTG	CGATCATAGTCTTGCCCCACTT	(Park *et al.*, 2005)
PRG4	GAGCAGACCTGAATCCGTGTATT	GGTGGGTTCCTGTTTGTAAGTGTA	(Hwang *et al.*, 2009)
EXT1	GAAGTCTTTACGGGCGGGAA	CCTAAACTGCAAGCCTCCG	-
GAPDH	TTGTCTCCTGCGACTTCAACAGCG	CACCACCCTGTTGCTGTAGCCAAAT	(Al-Sabah *et al.*, 2016)

2.1.9 Cytokine-mediated cartilage explant degradation assays

Bovine articular cartilage explant biopsies were treated with control media (SCM alone), IL-1α 10ng/ml) (Peprotech), OSM (50ng/ml) (Peprotech) or IL-1α+OSM in SCM with media harvested and treatments refreshed every 7 days unless otherwise indicated. Upon termination of experiments cartilage explant wet weights were taken. Media samples and cartilage explants were then stored at -80°C until required. The use of IL-1α was selected based upon the observed 5 fold increase of GAG loss from bovine articular cartilage when treated with IL-1α compared to IL-1β (Smith *et al.* 1989).

2.1.10 Papain digestion of cartilage explants

Upon termination of experiments, cartilage explants were harvested and incubated with 300µl of 1U/ml Papain in 0.05 M sodium acetate, 0.025 M Na_2EDTA, 5 mM Cysteine (all Sigma), pH5.6 for 18 hours at 65°C to digest and solubilise tissue allowing for quantification of total GAG and hydroxyproline.

2.1.11 DMMB assay

The 1,9-dimethylmethylene blue assay allows for the colourmetric detection of GAGs enabled by the change in absorbance upon dye binding to GAGs inducing a shift from 650nm (dye monomer absorbance) and 590nm (dye dimer absorbance) to 525nm (Farndale *et al.* 1986). The level of metachromasia is relative to the amount of dye bound to GAGs and hence DMMB can be employed in the quantification of GAGs. Briefly, a standard curve was generated by adding 40µl of 0, 10, 20, 30 and 40µg/ml shark chondroitin sulphate (Sigma) in Ultrapure water to a clear 96 well plate (Corning). Media and papain digest samples were diluted in Ultrapure water, 40µl total volume, prior to addition of 200µl DMMB solution. Absorbance was read immediately at 525nm on the FluoSTAR Optima plate reader (BMG Labtech) to avoid interference by precipitates that form after DMMB solution addition. Media samples and papain digests were subjected to DMMB assay to provide a quantification of % GAG loss.

2.1.12 Hydroxyproline assay

Hydroxyproline assay was employed as an estimation of collagen content in media samples and papain digested cartilage explants. Hydroxyproline is believed to be found exclusively in collagens. Hydroxyproline is released via hydrolysis using strong acid followed by oxidation, mediated by chloramine T, that yields a pyrole that can be detected using Erhlich's reagent to produce a chromophore. The relatively stable proportion of hydroxyproline allows for calculation of collagen content via multiplication of hydroxyproline concentration by 7.5 due to approximately 13.5% hydroxyproline content in collagen type II. All reagents were from Sigma unless otherwise stated. Media and papain samples were diluted 1:1 in concentrated HCl-11.8 M (Fisher) in screw cap tubes and hydrolysed overnight at 110°C. After cooling, samples were freeze dried overnight using a Heto Powerdry 3000 (Thermo). Dried samples were reconstituted in 100µl Ultrapure water and centrifuged at 10,000 x g for 5 mins to remove particulates. Samples and 4-hydroxyproline standards (0, 2, 4, 6, 8 and 10 µg/ml), 30µl total volume, were added to a clear 96 well plate

followed by addition of 70µl of diluent (66% v/v propan-2-ol) and mixing for 5 mins. 50µl of oxidant [18 mM chloramine T, 10% v/v Ultrapure water, 50% (v/v) stock buffer (0.42 M sodium acetate trihydrate, 0.13 M tri-sodium citrate dihydrate, 26 mM citric acid, 4% (v/v) propan-2-ol)] was then added and samples mixed for a further 5 mins. 125µl developing reagent [3.7 mM dimethylamino benzaldehyde, 15% (v/v) perchloric acid, 85% (v/v) isopropanol] was added to each well and plates were sealed and incubated at 70°C for 20 mins. Absorbance was read at 540nm using FluoSTAR Optima plate reader (BMG Labtech) and sample concentration determined by linear regression of the hydroxyproline standard curve.

2.1.13 LDH assay

LDH (lactate dehydrogenase) release assay is a colourmetric method to quantify the viability of cells through the measurement of LDH, a cytosolic enzyme, released through damaged cellular membranes. LDH enzyme catalyses the conversion of lactate to pyruvate which converts NAD+ to NADH. NADH is used by diaphorase to convert INT (tetrazolium salt) in the substrate to a red formazan which can be quantified through reading of absorbance at 490nm. The use of Triton-X detergent-treated samples provides a positive control for toxicity. The release of LDH to the media from cartilage explants provides a facile method of quantifying the toxicity of compounds when applied to intact cartilage explants whilst leaving the cartilage available for alternative assays such as DMMB post papain digestion. Alternative methods to asses toxicity such as live dead staining require harvest and sectioning of cartilage therefore precluding its assessment in other assays. Cartilage explants were incubated with test compounds at the indicated concentrations and incubated for 5 days or one week dependent upon experimental setup. Positive controls for cell death were generated by the incubation of cartilage explants with 10% Triton-X 100 (Sigma) for 2 hours to solubilise chondrocyte cell membranes within cartilage leading to release of LDH. Media or positive control, 50µl, was removed then incubated with LDH substrate (Pierce), 50µl, incubated in the dark for 30 mins prior to absorbance measurement at 490nm. Toxicity was calculated as a percent release of LDH compared to non-treated cells.

2.1.14 Greiss assay

The Greiss assay provides a method for the quantification of nitrite (NO_2^-) release from cells. Nitrite is a stable breakdown product of nitric oxide (NO), a free radical which is produced by cells in response to inflammatory stimuli. The quantification of nitrite in media samples allows an indirect assessment of NO production and therefore the inflammatory state of cells. Greiss assay kit was obtained from Promega. Media from stimulated chondrocytes in monolayer or cartilage explants was harvested with 50µl added to a 96 well plate prior to addition of 50µl sulphanilamide solution and incubation in the dark for 10 mins. 50µl of N-1-napthylethylenediamine dihydrochloride (NED) solution was added and incubated in the dark for a further 10 mins prior to reading of absorbance at 520nm. A standard curve was generated using a nitrite standard at concentrations of 100, 50, 25,12.5, 6.25, 3.13, 1.56 and 0 µM. Linear regression of the absorbance of the standard curve was employed to calculate nitrite concentration in media samples.

2.1.15 SDS-PAGE and Western blot

Samples were diluted 1:1 in 2x SDS sample buffer [0.125 M Tris-HCl, 4% SDS (w/v), 20% glycerol (w/v), 0.01% bromophenol blue (w/v)]. Where samples were run under reducing conditions β-mercaptoethanol was added to a final concentration of 5% (v/v). Samples were heated for 5 mins at 100°C prior to loading onto 4-12% Bis-Tris pre-cast gradient gels or 3-8% Tris-Acetate gels (both Novex, Thermo) dependent upon the molecular weight of the target protein. Gels were run using the XCell SureLock™ Mini-Cell Electrophoresis System (Thermo) in 1x MOPS running buffer (Thermo) or 1x Tris-Acetate running buffer (Thermo) for Bis-Tris or Tris-Acetate gels, respectively. Precision plus all blue re-stained protein ladders (Biorad) were run to allow for visualisation of transfer and as molecular weight markers. Proteins were then transferred to a nitrocellulose membrane using the semi-dry iBLOT transfer system (Invitrogen) with a transfer time of 7 minutes. Membranes were blocked in 5% (w/v) Bovine serum albumin (BSA) in Tris buffered saline plus azide [50 mM Tris-HCl, pH 7.4, 0.2 M NaCl, 0.02% NaN_3 (w/v)] (TSA) for one hour prior to incubation with primary antibody at the indicated concentration (Table 2.3) in 1% BSA/TSA (w/v) for one hour at room temperature or overnight at 4°C with shaking. Membranes were then washed 3 x 10 minutes in TSA prior to addition of species-specific alkaline phosphatase (AP) conjugated secondary antibody (Table 2.4) diluted 1:5000 in 1% BSA/TSA (w/v) for one hour at room temperature. Membranes were washed 3 x 10 minutes in TSA followed by development of blots using BCIP/NBT in AP-buffer (100 mM Tris-HCl, pH 9.55, l00 mM NaCl, 5 mM MgCl2) as per manufacturer's instructions (Promega). ImageJ (NIH) was used for semi-quantitative densitometric band analysis. Calculation of fragment molecular weight was also performed using ImageJ by plotting the relative distance migrated by known molecular weight standards against the log(Mw). Linear regression was used to determine the molecular weight of unknown fragments.

2.1.16 Deglycosylation of samples prior to Western Blot

Detection of the aggrecanase generated aggrecan BC-3 neo-epitope requires deglycosylation of aggrecan to enable detection through removal of chondroitin sulphate and keratan sulphate. The 2B6 anti-chondroitin sulphate antibody recognises chondroitin sulphate stubs (C4S) after cleavage by chondroitinase. For 2B6 and BC-3 Western blot, 20μg of GAG in media, calculated using the DMMB assay, was deglycosylated with 0.002U Chondroitinase ABC (Sigma), Keratanase and 0.0002U Keratanase II (both Seikagaku) overnight at 37°C in 0.1 M Tris-Acetate pH 7.5. Samples were then dialysed against ultra-pure water using membranes with a 10 kDa molecular weight cut off (Spectrum Labs), dried overnight using a speed vac (Savant) at ambient temperature and re-suspended in 2x SDS buffer prior to running of gels as described in 2.1.15. 18μg of GAG equivalent was loaded per well for BC-3 analysis and 2μg GAG equivalent was loaded per well for 2B6 analysis.

Table 2.3 – Primary antibodies used within this thesis.

Primary Antibodies	Target	Species	Supplier/Reference	Dilution	Clonality
BC-3	-ARGSVIL Aggrecan neo-epitope	Mouse	Hughes *et al.* 1995	1:200	Monoclonal
2B6	Chondroitin sulphate CS4 Stub	Mouse	Kratz *et al.* 1986	1:200	Monoclonal
3A4	Non reduced (NR) Lubricin	Mouse	Jones *et al.* 2007	1:100	Monoclonal
6A1	Reduced (R) and NR Lubricin	Mouse	Jones *et al.* 2008	1:100	Monoclonal
Anti-COMP AF3134	R and NR COMP	Goat	R and D Systems	1:2000	Polyclonal
Anti COMP AB74524	R and NR COMP	Rabbit	Abcam	1:2000	Polyclonal

Table 2.4 – Secondary antibodies used within this thesis.

Secondary Antibodies	Product Code	Supplier	Dilution
Anti-Mouse IgG Alkaline Phosphatase	S3721	Promega	1:5000
Anti-Mouse IgG AlexaFluor546	A11030	Thermo	1:200
Anti-Mouse IgM AlexaFluor488	A21042	Thermo	1:200
Anti-Mouse IgG AlexaFluor633	A21052	Thermo	1:200

2.1.17 Metabolically inactive cartilage degradation assay

Bovine cartilage slices (equal wet weight) were subjected to three rounds of freeze thaw at -80°C prior to incubation in media conditioned by rADAMTS4-p53 or rADAMTS4-E/Q expressing HEK293 cell lines (Wainwright *et al.* 2013) at 37°C. Aliquots were harvested at 6 and 24 hours and subjected to SDS-PAGE under non-reducing conditions followed by Western blot for COMP as per section 2.1.15.

2.1.18 Human OA patient synovial fluid Western blot

Synovial fluid (SF) was obtained from 4 consenting OA patients undergoing total knee replacement (TKR) with ethical approval. Synovial fluid was treated with bacterial hyaluronidase (Sigma) to reduce viscosity by degradation of hyaluronic acid. 20µl of 50µg/ml hyaluronidase in PBS was added per 500µl SF and incubated at 37°C for 20 minutes with agitation. 2µl of SF was diluted in 2x SDS loading buffer and subjected to SDS-PAGE under non-reducing conditions using 3-8% Tris-acetate gels (Thermo) prior to transfer to nitrocellulose membranes and Western blotting for COMP degradation with detection using anti-COMP AF3134 or anti-COMP AB74524.

2.2 Chapter 4 Methods

2.2.1 Molecular docking studies

Molecular graphics and analysis were performed using the UCSF Chimera package (Pettersen *et al.* 2004) and molecular docking performed using Autodock Vina (Trott *et al.* 2010). Crystal structures were obtained from the RSCB protein data bank as PDB files. Where co-crystal structures were used, ligands were removed prior to docking. Protein structures were prepared for docking using DockPrep to add hydrogens, remove solvent and remove non-complexed ions. Incomplete side chains were replaced using Dunbrack rotamer library (Shapovalov and Dunbrack. 2011) and charges added to standard residues using AnteAmber ff14SB and charges added to non-standard residues using Gasteiger. Ligand chemical structures were obtained from www.pubchem.com and

were then minimised with default settings of 100 steps at 0.02 Å step size with no atoms fixed. Charges were then added using AnteAmber and Gasteiger. Molecular docking was performed using Autodock Vina using a search area covering the entire protein domain unless otherwise stated with settings as follows; Number of binding modes=9, Exhaustiveness=5 and maximum energy difference 3kcal/mol. Unless otherwise stated the top scoring docking result with RMSD=0 and energy of bonds expressed as ΔG kcal/mol. Comparative dockings were made using Swiss-dock Web-service which is based upon the EADock DSS engine (Grosdidier *et al.* 2011). Settings; Accurate fit and fixed receptor structure unless otherwise stated. Ligand structures were obtained from ZINC database (Irwin and Shoichet. 2005), Surfen accession number 608170.

2.2.2 ADAMTS-4 *in vitro* inhibition assay

For assessment of Surfen-mediated inhibition of ADAMTS-4, the Sensolyte aggrecanase assay 520 (Eurogentic) was used. The conjugation of a donor fluorophore and quencher at either side of the protease cleavage site ensures that low background fluorescence is emitted until cleavage separates the FRET pair and therefore results in fluorescent emission that is relative to the quantity of FRET peptide cleaved (Fig 2.4). 1 ng Recombinant ADAMTS-4-p40 (Sigma) or 10µl of HEK293, expressing ADAMTS-4 p40 or p53 conditioned media was added to glass vials in PBS and pre-incubated for 10 mins with Surfen at the indicated concentrations in a total volume of 50 µl. This was then transferred to a 96 well plate prior to addition of aggrecanase substrate and measurement of fluorescence at 5 minute intervals (Ex-488nm, Em-520nm) using a Fluorostar Optima (BMG-Labtech). Percent activity was calculated compared to no inhibitor controls and IC_{50} was determined using non-linear regression using GraphPad Prism 7.0.

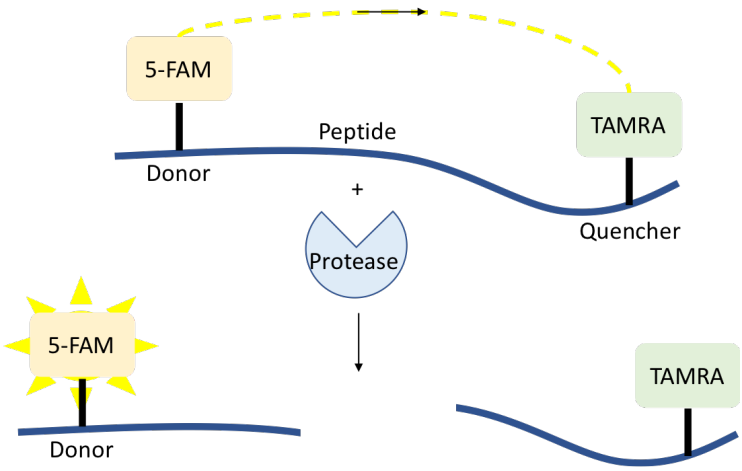

Figure 2.4 – Diagram showing principle of FRET based peptide protease activity assays. Proximity of fluorophore donor and quencher on non-cleaved peptide prevents fluorescence emission. Cleavage of peptide by protease results in emission of fluorescence relative to amount of peptide cleaved allowing for quantification of protease activity.

2.2.3 ADAMTS-5 *in vitro* inhibition assay

A FRET based assay was employed using a peptide sequence derived from the pathological $E^{373-374}A$ cleavage site of aggrecan to assess potential inhibition of ADAMTS-5 mediated by Surfen. 10ng recombinant ADAMTS-5 (R & D Systems) was pre-incubated with Surfen or ADAMTS-5 inhibitor CAS-929634-33-3 (Cayman Chem) at the indicated concentrations in glass vials for 10 mins prior to addition of 50 µl WAAG-3R- Abz - TEGEARGSVI-Dpa-KK-NH2 (Anaspec) at a concentration of 50 µM in 50 mM HEPES, pH 7.5, 100 mM NaCl, 5 mM $CaCl_2$, 0.1 % CHAPS, 5% glycerol. Fluorescence was measured every 5 minutes (Ex-340nm, Em-420nm) using a Fluorostar Optima (BMG-Labtech). Percent activity was calculated compared to no inhibitor controls and IC_{50} was determined using non-linear regression using GraphPad Prism 7.0. Mean and *sem* of duplicate wells were plotted.

2.2.4 Furin *in vitro* inhibition assay

The assessment of Surfen-mediated inhibition of furin was assessed using a FRET peptide (Boc-Arg-Val-Arg-Arg-AMC: Bachem) containing the putative furin cleavage motif Arg-X-X-Arg. 1U (1U=1 pmole/minute cleavage of fluorogenic peptide BOC-RVRR-AMC 30 °C) of furin (Sigma) was pre-incubated with Surfen at the indicated concentrations for 30 minutes in glass vials prior to transfer to black 96 well plates (Thermo) and addition of 50 µM Boc-Arg-Val-Arg-Arg-AMC in assay buffer (100 mM HEPES, pH 7.5, 1 mM $CaCl_2$ 0.1 M β-mercaptoethanol and 5% Triton X-100: all Sigma). Fluorescence was measured every 5 minutes (Ex-360nm, Em-440nm) using a Fluorostar Optima (BMG-Labtech). Percent activity was calculated compared to no inhibitor controls and IC_{50} was determined using non-linear regression using GraphPad Prism 7.0. Mean and *sem* of duplicate wells were plotted.

2.2.5 MMP *in vitro* inhibition assay

The assessment of Surfen mediated inhibition of MMP protease activity was performed using the Matrix metalloproteinase (MMP) inhibitor profiling kit, fluorometric RED (Enzo). This kit provides a FRET peptide that is cleavable by all MMPs tested (although with slightly varying efficiencies) with the sequence TQ3-GABA-Pro-Cha-Abu-Smc-His-Ala-Dab(6'-TAMRA)-Ala-Lys-NH2 (TQ3=tide quencher 3; GABA=4-aminobutyric acid; Cha=L-cyclohexylalanine; Abu=2-aminobutyric acid; Smc=S-methyl-L-cysteine; Dab=2,4-diaminobutyric acid; 6'-TAMRA=6'-tetramethylrhodamine). MMPs tested and included with the kit were MMP-1, MMP-3, MMP-7, MMP-9 and MMP-13. MMPs provided were expressed in *E. coli* and comprise of the catalytic domain only. Inhibition studies were performed as per the manufacturer's instructions. Briefly, MMPs (final concentrations of MMPs per well are given in Table 2.5 below) were incubated for 30 minutes with the indicated concentration of Surfen in glass vials in 1x assay buffer (50 mM HEPES, 10 mM $CaCl_2$, 0.05% Brij-35, pH 7.5) prior to transfer to black 96 well plates (Thermo) and addition of MMP substrate to a final concentration of 0.75 µM in 1x assay buffer. Fluorescence was measured every 5 minutes (Ex.540nm, Em.590nm) using a Fluorostar Optima (BMG-Labtech). Percent activity was calculated compared to no inhibitor controls and IC_{50} was determined using non-linear regression using GraphPad Prism 7.0. Mean and *sem* of duplicate wells were plotted.

Table 2.5 – Concentration of MMPs used in inhibition assays.

Protease	Concentration (mU/µl)
MMP1	128
MMP2	11
MMP3	12.6
MMP9	3.4
MMP13	3.4

1 U=100 pmoL/min cleavage of 100 µM substrate (Ac-Pro-Leu-Gly-[2-mercapto-4-methyl-pentanoyl]-Leu-Gly-OC2H5) determined by ENZO

2.2.6 *In vitro* aggrecan degradation assays

Bovine aggrecan derived from the A1D1 fraction, solated from bovine cartilage via separation on associative followed by dissociative (A1D1) caesium chloride gradients as previously described (Roughley and White, 1980), 20µg (protein concentration determined by BCA assay) in 50 mM Tris-HCl, 10 mM $CaCl_2$, pH 7.4 was incubated with 1ng ADAMTS-4 (Sigma) or 1ng ADAMTS-5 in the presence or absence of Surfen at the indicated concentrations overnight at 37°C. Reactions were stopped by addition of 1 mM EDTA then samples were deglycosylated and subjected to Western blot using antibodies BC-3 or 2B6 as per section 2.1.15.

2.3 Chapter 5 Methods

2.3.1 MTT viability assay

The MTT (3-(4,5-dimethylthiazol-2-yl)-2,5-diphenyltetrazolium bromide) assay is a colourmetric assay used to detect the viability of cells in culture. MTT (yellow) is converted to formazan (purple) by oxidoreductase enzymes in metabolically active cells. Formazan crystals produced are solubilised by the addition of DMSO and the resulting colour change quantified on an absorbance plate reader at 572nm. Cytotoxicity of a compound is assessed by comparison of absorbance between treated and untreated control cells. Often referred to as a proliferation assay, it is more correctly a measurement of respiration of cells although this is highly increased during proliferation. Chondrocytes were seeded at a density of 10,000 cells per well in 96 well plates then incubated for 24 hours at 37˚C prior to addition of Surfen or control media for the indicated time points. Cell culture medium was removed and 200 µl of 0.5% MTT solution in PBS was added. Cells were returned to a 37˚C incubator for 30 mins. MTT solution was removed from all wells and formazan crystals were solubilised using 200 µl DMSO. Plates were placed on a shaker to ensure complete solubilisation after which the absorbance was read at 572nm. All results were normalised to untreated cells.

2.3.2 ADAMTS-4 activity assay

Bovine cartilage explants or bovine chondrocytes were harvested as per section 2.1.2 and 2.1.3, respectively. Explants (4mm) or cells ($1x10^6$) were cultured in control media (SCM alone), IL-1α 10ng/ml) (Peprotech), OSM (50ng/ml) (Peprotech) or IL-1α + OSM in SCM with media harvested

and treatments refreshed every 7 days for explants or harvested after 4 days for cell assays. Surfen was added at the indicated doses concurrently with cytokines. Where multiple doses of Surfen were required the second dose was applied 24 hours after the initial dose. ADAMTS-4 activity was then assessed using the Sensolyte aggrecanase assay 520 (Eurogentic). The sequence of the proprietary peptide is unknown but was shown to be minimally cleaved by recombinant ADAMTS-1 and ADAMTS-5 allowing for the selective quantification of ADAMTS-4 activity in cartilage explant media. 50µl of culture media was added per well of a black 96 well plate (Thermo) prior to addition of aggrecanase substrate and measurement of fluorescence intensity at 5 minute intervals (Ex.488nm, Em.520nm) using a Fluorostar Optima (BMG-Labtech). Means and *sd* were plotted as percent activity relative to controls (explants treated with SCM only)

2.3.3 Surfen *in vitro* GAG binding assays

A1 (Aggrecan, link protein and HA aggregate) and A1D1 (Aggrecan) were isolated from bovine cartilage via separation on associative (A1) or associative followed by dissociative (A1D1) caesium chloride gradients as previously described (Roughley and White, 1980). Chondroitin sulphate (CS), heparin and hyaluronic acid (HA) were all purchased from Sigma. Proteoglycans or GAGs were prepared in Dulbecco's phosphate buffered saline (PBS) (0.16 M NaCl, 3 mM KCl, 8 mM Na_2HP0_4, KH_2P0_4, pH 7.3 purchased as tablets from Oxoid) and added to the wells of a black 96 well plate at the indicated concentrations. Surfen hydrate was added to the wells at the indicated concentration prior to incubation for 30 minutes at room temperature and analysis on plate reader with excitation at 360nm and emission 488nm.

2.3.4 Surfen inhibition of histone deacetylases

Histone deacetylase (HDAC) inhibition was assessed using the HDAC glo I/II system (Promega). HeLa nuclear lysates, 50µl of a 1:3000 dilution of stock, were incubated with Surfen or known HDAC inhibitor trichostatin A (TSA) for 30 minutes. Inhibitor concentrations tested were generated by a 1:2 dilution series from 50 to 0.098 µM for Surfen and 50 nM to 0.098 nM for TSA in HDAC glo buffer. Samples were transferred to a white-walled 96 well plate (Thermo) prior to addition of 100µl HDAC glo reagent. Plates were then sealed and incubated for 20 minutes at room temperature prior to quantification of luminescence using a Fluorostar Optima (BMG-Labtech). Percent activity was calculated compared to no inhibitor controls and IC_{50} was determined using non-linear regression using GraphPad Prism 7.0.

2.3.5 Statistical Analysis

Unless otherwise stated in figure legends, data presented are the mean and *sd* of three independent experiments each performed in technical triplicate (technical replicates n=3, experimental replicates N=3). In experiments where assays were only run in duplicate the mean and *sem* is shown as *sem* reflects an uncertainty of the estimate of the mean and is dependent on sample size i.e reduces as sample size increases (Altman and Bland, 2005). Probability that data was normally distributed was assessed using D'Agostino-Pearson omnibus K2 test. To determine statistcal significance levels comparing more than two groups, ANOVA with Tukey's post-hoc test for multiple comparisons

was employed, when comparing two groups, Students t-test was applied. Statistical significance of qPCR data was performed upon dCt values prior to calculation of fold change. All statistcal analysis were performed using GraphPad Prism 7.0.

Chapter 3

Characterisation of a Cytokine Induced *Ex Vivo* Model of Osteoarthritis

3.1 Introduction

Cytokines have long been implicated in OA progression and there is likely a contribution to joint cytokine levels from cells of the synovium (FLS and macrophages) in addition to chondrocytes themselves. Cytokines released from cells of the joint can act in a paracrine or autocrine way to further increase the expression of cytokines, chemokines and cartilage-degrading proteases in recipient cells. Most *in vitro* and *ex vivo* models to date have used IL-1ß to induce OA-like changes in gene expression and indeed many studies have detected increased levels of IL-1ß and IL-1-converting enzyme (ICE), that activates IL-1ß, in the synovial fluid of OA patients. Other cytokines implicated and detected at increased levels in osteoarthritis patients include IL-6, OSM and TNFα. *In vivo*, cytokines are unlikely to act in isolation and therefore the combinatory effects of cytokines *in vitro* may provide a more accurate representation of cell signalling and gene expression of chondrocytes in response to the pro-inflammatory environment of the OA joint.
Studies in the chondrocyte-like cell line T/C28a4 revealed a significant increase in expression of ADAMTS and MMP proteases in the presence of IL-1β in combination with OSM compared to either cytokine alone. *Ex vivo* cartilage explant models of OA have been used extensively in the literature, based upon the induction of aggrecanases and MMPs by pro-inflammatory cytokines alone or in concert resulting in the degradation and loss of matrix components such as cartilage oligomeric matrix protein (COMP), aggrecan and collagen type II from articular cartilage explants (Durigova *et al.* 2008; Ganu *et al.* 1998; Song *et al.* 2007) thus modelling the pathological processes observed in OA. The combination of IL-1 and OSM results in increased GAG loss and accelerated collagen loss from cartilage explants compared to either cytokine alone in bovine cartilage explants. This synergism between IL-1 and OSM was confirmed *in vivo* by articular adenoviral mediated over-expression of IL-1 and OSM alone or in combination in murine joints that showed an increased proteoglycan degradation and collagen release from cartilage in joints where OSM and IL-1 were co-expressed compared to either cytokine alone. Furthermore, an increased positive staining for MMP-3 and MMP-13 was observed in the cartilage and synovium of IL-1 and OSM over-expressing mice compared to either cytokine alone, as assessed by IHC (Rowan e*t al.* 2003). A later study by the same authors showed remarkably similar results in mice over

expressing TNFα and OSM with increased proteoglycan loss, collagen loss and increased MMP-3 and MMP-13 expression in the cartilage of mice co-expressing TNFα and OSM compared to either cytokine alone (Hui *et al.* Dec 2003). The observed similarities in pathways activated by TNFα and IL-1, namely the activation of IκB, JNK, p38 and ERK1/2 by both cytokines, combined with this data, suggests similar pathways of synergistic induction between OSM and IL-1 or TNFα may be implicated, and highlights a relevance to both OA and RA of the synergistic effects of these pro-inflammatory cytokines. Treatment of bovine nasal cartilage explants with IL-1α in combination with IL-6/sIL-6R resulted in increased collagen loss compared to either cytokine alone confirming that synergy with IL-1α is observed for other members of the IL-6/gp130 family of pleiotropic cytokines (Rowan *et al.* 2001).

It has been shown that OSM treatment (10ng/ml) of normal human chondrocytes results in phosphorylation of AKT, ERK1/2, STAT3 and to a lesser extent p38, whereas, treatment with IL-1β (10ng/ml) resulted in phosphorylation of ERK1/2, p38 and JNK, highlighting the specificity of AKT and STAT3 activation to OSM treatment and JNK activation to IL-1β treatment. In this study no synergistic effects were observed in chondrocytes treated with IL-1 and OSM in combination.

It therefore remains that the cell signalling pathways responsible for the synergistic effect of IL-1 and OSM in combination are unknown and warrant further investigation as the elucidation of points of convergence of signalling pathways that lead to increased cartilage degradation may further our understanding of OA pathology and potentially identify novel therapeutic targets that can ameliorate the effects of multiple cytokines simultaneously.

The aim of this section is to confirm and characterise the synergistic effect of IL-1α and OSM in combination upon cartilage matrix degradation and furthermore to assess the effects of this cytokine combination on the degradation of COMP which to date has not been studied. The mechanisms contributing to the synergistic degradation will be assessed through relative quantification of gene expression changes mediated by IL-1α in combination with OSM and the cell signalling pathways implicated in this synergistic induction which are to date unknown. Furthermore, the comprehensive characterisation of cartilage matrix degradation products, gene expression and cell signalling pathways induced by the application of IL-1α and OSM alone and in combination will provide a comprehensively characterised *in vitro* and *ex vivo* models for the subsequent assessment of Surfen as a potential OA therapeutic.

3.1.1 Aim and Objectives

Aims

The Aims of Chapter 3 are firstly to investigate the potential synergistic effects mediated by IL-1α in combination with OSM in mediating cartilage degradation and to determine the pathological pathways implicated. Furthermore, it is the aim of Chapter 3 to provide an extensively characterised *ex vivo* model for assessment of potential therapeutic effects of Surfen later in this Thesis.

Objectives

These Aims will be investigated through the completion of the following Objectives;

1. Evaluate the effects of IL-1α and OSM alone or in combination upon the degradation of articular cartilage matrix macromolecules in bovine cartilage explants.

2. Assess gene expression in primary bovine chondrocytes of known catabolic and anabolic factors in response to IL-1α and OSM alone or in combination.

3. Elucidate cytokine-mediated signalling pathway activation in primary chondrocytes in response to cytokines and identify pathways where cytokines act synergistically.

4. Develop assays and characterise matrix degradation products released from cytokine stimulated primary articular cartilage explants to identify markers of pathology that could be used to assess therapeutic potential and elucidate the mechanism of action of small molecule therapeutics.

3.2 Results

3.2.1 Cytokine-induced GAG loss and aggrecanase activity in bovine explant cultures

Bovine articular cartilage explants treated with IL-1α and OSM alone or in combination resulted in an increased GAG loss, assessed by DMMB assay, over a three-week culture period compared to control tissue (Fig 3.1). Treatment with IL-1α or OSM resulted in a loss of 45% and 25% total GAG within week 1, respectively, whereas the combination of IL-1α and OSM resulted in 66% GAG loss in the same time period (Fig 3.1A) suggesting an additive effect of IL-1α and OSM in mediating GAG loss. During week 2 IL-1α treated explants released a further 26% GAG to the media whereas GAG loss from OSM and IL-1α+OSM was 34% and 11%, respectively (Fig 3.1B). During week 3 of culture the GAG loss from IL-1α and IL-1α+OSM treated explants was the same or less than that released from control explants. OSM treated explants in week 3 showed a significant increase in GAG loss compared to all other conditions at this time point ($p<0.001$) (Fig 3.1C). GAG loss from explants did not show a synergisitc effect of IL-1α in combination with OSM at anytime point studied. This may be the result of GAG levels in explants and an almost total depletion of GAG in IL-1α+OSM treated explants at week 1. Time course studies trhoughout week 1 may elucidate differences and potentially synergistic effects of IL-1α+OSM are observed at earlier time points but this requires confirmation.

Aggrecanase activity at site $E^{373\_374}A$ is evident in IL-1 and IL-1+OSM treated explants at week 1 and week 2 of culture

Assessment of cartilage explant media by Western blot for the aggrecan neo-epitope -ARGSVIL, generated by ADAMTS-4/5 cleavage of aggrecan at site $E^{374\_374}A$, using our in-house BC-3 monoclonal antibody with equal loading of GAG (20µg) showed positive banding in IL-1α and IL-1α+OSM treated explants in weeks 1 and 2 whereas no BC-3 epitope was detected in non-treated controls or OSM-treated cartilage explants in week 1 or 2 (Fig 3.1D and E), this data closely matches the pattern observed in GAG loss as assessed by DMMB suggesting GAG loss in IL-1α and IL-1α+OSM treated explants is, at least in part, mediated by ADAMTS-4 or ADAMTS-5 in

weeks 1 and 2. The use of equal GAG loading negates the effect of variation in media samples due to differential GAG release according to treatment and explant size.

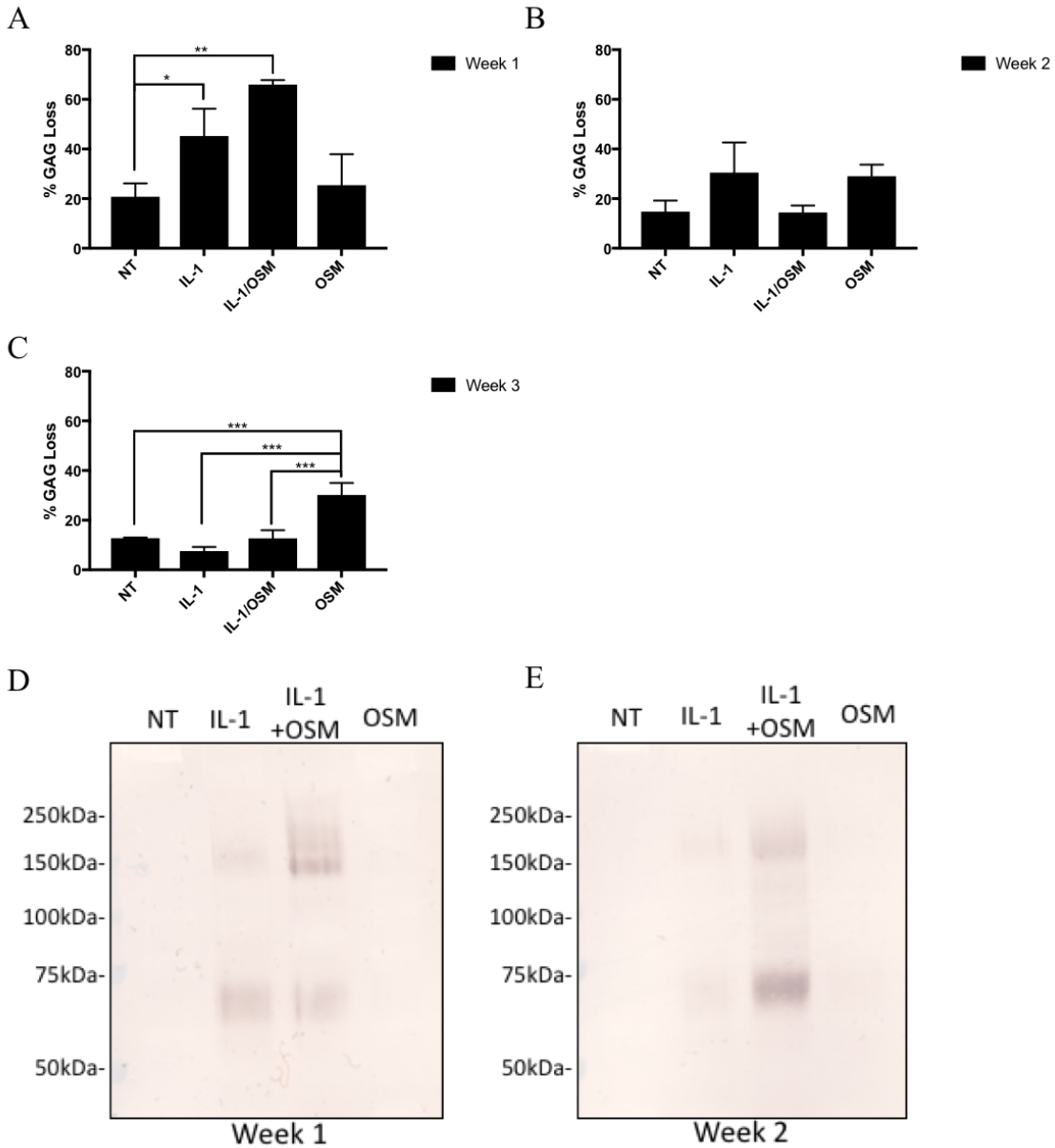

Figure 3.1 – Cytokine mediated degradation of GAG in bovine articular cartilage explants assessed by DMMB assay and Western blot detecting aggrecanase generated -ARGSVIL neo-epitope released to media. GAG loss from explants assessed by DMMB assay of culture media harvested at week 1 (A), week 2 (B) and week 3 (C) from 4mm diameter mature bovine cartilage explants treated with control media, IL-1α (10ng/ml), OSM (50ng/ml) or IL-1α+OSM. Results expressed as % GAG loss. Mean and *sd* of three experiments shown. Statistical significance was determined using ANOVA with Tukey's post-hoc test for multiple comparisons performed using GraphPad Prism 7.0 software. * $p<0.05$. ** $p<0.01$. Western blot of control (NT) or cytokine treated cartilage explant media samples at week 1 (D) and week 2 (E) using antibody BC-3 against –ARGSVIL neo-epitope generated by aggrecanase-mediated cleavage of $E^{373\_374}A$ of aggrecan. Equal loading of 20µg GAG equivalent per lane derived from pooled triplicate wells from one independent experiment.

3.2.2 Cytokine-induced collagen degradation in bovine explant cultures

IL-1+OSM treatment of cartilage explants results in a more rapid and an increased collagen release than either cytokine alone

The loss of collagen type II from explants, assessed by hydroxyproline release to the media, in week 1 of culture was minimal loss in all conditions, <0.6% (Fig 3.7A+D). There was an increased collagen loss in IL-1α+OSM treated explants compared to all other treatments, however, this difference was not significant (Fig 3.7D). Collagen loss in week two was 7.9%, 25.3% and 2.3% for IL- 1α, IL-1α+OSM and OSM treated explants, respectively (Fig 3.7B). The percentage collagen loss in IL-1α and IL-1α+OSM treated explants was significant in week 2 compared to control explants ($p<0.05$ and $p<0.001$, respectively) (Fig 3.7B). Collagen loss in week 2 of explants treated with IL-1α+OSM was also significantly higher than that observed for IL-1α or OSM treated explants ($p<0.001$) with a synergistic increase in degradation observed in explants treated with IL-1α in combination with OSM (Fig 3.7B). In week 3, collagen loss increased in IL-1α (13.2%) treated cultures and OSM (14.6%) treated cultures, whereas it was maintained at 23% for IL-1α+OSM treated explants (Fig 3.7C). The amount of collagen loss in week 3 was significant for all cytokine treatments compared to control media treated explants, ($p<0.05$) (Fig 3.7C).

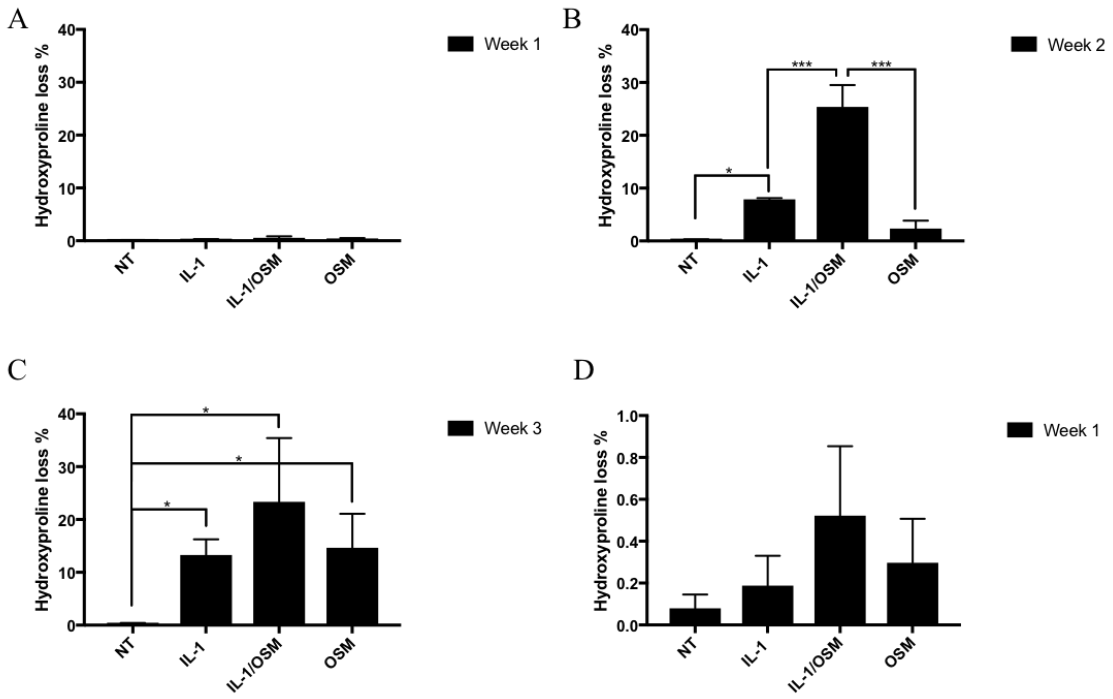

Figure 3.2 – Assessment of cytokine-induced collagen degradation in bovine articular cartilage explants assessed by hydroxyproline assay. Media was harvested at week 1 (A+D), week 2 (B) and week 3 (C) from 4mm diameter mature bovine cartilage explants cultured in the presence of IL-1α (10ng/ml), OSM (50ng/ml) or IL-1α+OSM. Results expressed as % hydroxyproline loss to represent collagen loss. Mean and *sd* of three experiments shown. Statistical significance was determined using ANOVA with Tukey's post-hoc test for multiple comparisons performed using GraphPad Prism 7.0 software. * $p<0.05$. ** $p<0.01$.

3.2.3 Cytokine-induced COMP degradation in bovine explant cultures

Western blot analysis shows IL-1 and IL-1+OSM treatment of cartilage explants results in COMP degradation within one week of culture

The proposed potential of COMP release from cartilage and particularly release of COMP neo-epitopes generated by pathological cleavage of COMP as biomarkers of OA progression led to the development of a Western blot assay to detect COMP fragmentation patterns generated by cytokine treatment of bovine articular cartilage to identify which cytokines mediate degradation and potential synergistic effects between IL-1α and OSM.

Western blot under reducing conditions showed a strong doublet band for control media and OSM incubated explants with fragments of ~95 and 87 kDa and a less intense positive staining at ~75 kDa when blotted with an antibody raised against full length human COMP (Fig 3.3 upper panel). The positive staining at 87 kDa was absent in both IL-1α and IL-1α+OSM treated explants, however the fragment at 75 kDa was clearly visible. The predicted molecular weight of human COMP is 110 kDa when reduced, however this discrepancy in size may be due to species specific differences between human and bovine COMP.

When explant media was assessed by Western blot using a polyclonal antibody raised against a synthetic peptide corresponding to amino acids 1-100 of human COMP (AB74524), the fragment of ~95 kDa is visible in all conditions although the intensity is reduced in IL-1α+OSM treated explants. A less intense positive staining can be seen for the fragment of ~75 kDa in control, IL-1α and OSM treated explants but not IL-1α+OSM treated explants (Fig 3.3 lower panel). The inability of the polyclonal AB74524 to detect the band at ~87 kDa would suggest that this fragment is missing a proportion of the N-terminus within amino acids 1-100 although as this is a polyclonal antibody the exact epitope/s are unknown. Interestingly, this potential cleavage event is detected in control treated explants suggesting cleavage occurs within healthy cartilage potentially in turnover of COMP. The oligomerisation of COMP into its natural pentameric form is mediated by the N-terminal domain and therefore to further assess the effects of cleavage whilst retaining N-terminal domain oligomerisation a Western blot under non-reducing conditions was employed.

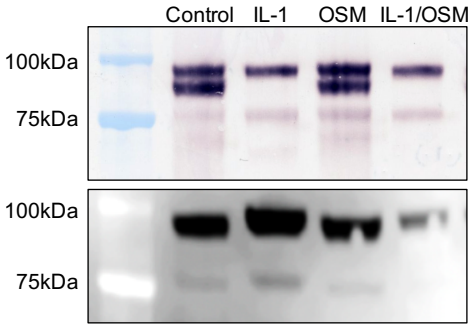

Figure 3.3 – Western blot assessment of COMP release and fragmentation from cytokine-treated bovine cartilage explants performed under reducing conditions. 4mm bovine cartilage explants were incubated with control media, IL-1 (10ng/ml), OSM (50ng/ml) or IL-1+OSM for 7 days prior to harvesting of media and Western blot analysis under reducing conditions using primary polyclonal antibody AF3134 (upper panel), that was generated by immunisation of goats using full length human recombinant COMP, or antibody AB74524 (lower panel) that was generated by immunisation of rabbits using a synthetic peptide corresponding to amino acids 1-100 of human COMP. Loading of media was normalised to explant total GAG content derived from DMMB assay each lane respresents pooled triplicates from one experiment (n=3, N=1).

Western blot under non-reducing conditions reveals multiple sized COMP fragments are generated by IL-1α and IL-1α+OSM treatment

Western blot for COMP under non-reducing conditions showed release to media of COMP in all conditions, however, extensive fragmentation of COMP was noted in IL-1α and IL-1α+OSM treated explants in week 1 with fragmentation appearing in week 2 in OSM treated explants (Fig 3.4A). Fragments generated were of ~260, 190 and 75 kDa (designated Fragment 3,4 and 5 respectively) compared to the predicted weight of intact non-reduced COMP of over 500 kDa, two additional fragments were evident of size greater than 250 kDa (Fragments 1 and 2) however, the lack of molecular marker in this range means the molecular weight cannot be accurately estimated. In week 2, IL-1α treated explants showed only one fragment at 75 kDa whereas no fragments were detected in IL-1α+OSM treated cultures suggesting complete degradation of released COMP or total loss of COMP from explants in week 1. Semi-quantitative Western blot densitometric analysis of COMP fragment release from cartilage explants in week 1 showed a significant reduction of COMP Fragment 1 in explants treated with IL-1α and IL-1α + OSM corresponding to an increased amount of Fragments 3, 4 and 5 that were conversely undetected in control and OSM treated explants. There were no significant differences in the intensity of fragment bands between IL-1α and IL-1α +OSM treated explants (Fig 3.4B). This data combined shows that the application of IL-1 and IL-1+OSM results in degradation of COMP within one week of culture and that the use of Western blot under non-reducing conditions enables the detection of multiple fragments over a wider range of sizes compared to those observed under reducing conditions and is therefore more sensitive to detecting cleavage events that were not detected using Western blot under reducing conditions.

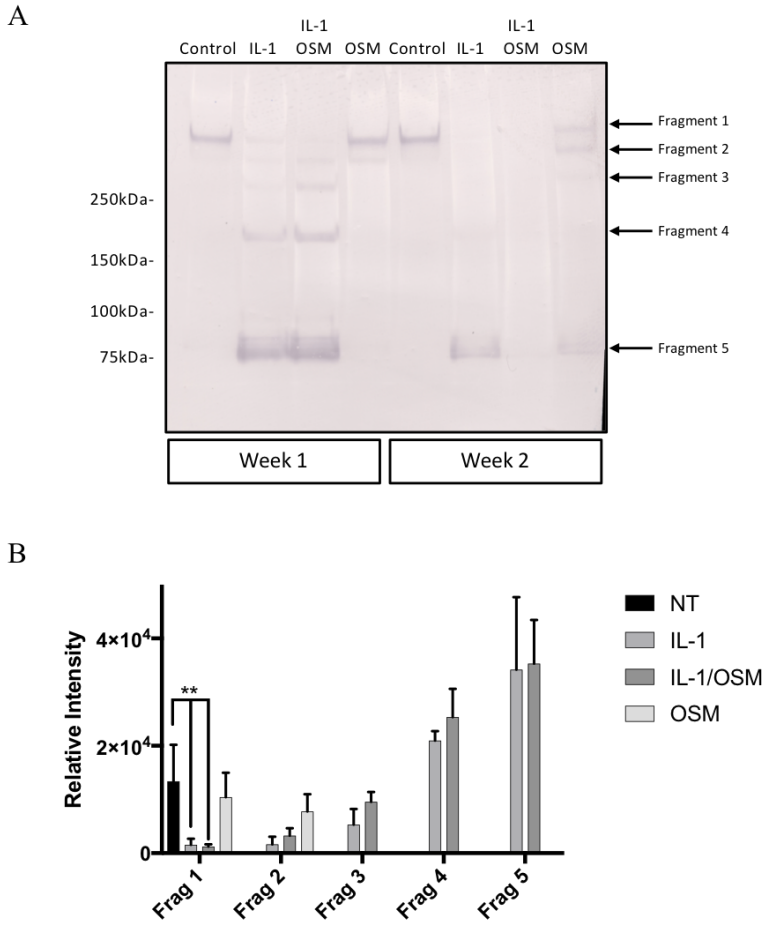

Figure 3.4 – Western blot assessment of COMP release and fragmentation from cytokine treated bovine cartilage explants performed under non-reducing conditions. Western blot under non-reducing conditions against COMP using rabbit polyclonal AB74524 anti-COMP (immunised with synthetic peptide aa's 1-100 of human COMP) of control (NT) , IL-1α (10ng/ml), OSM (50ng/ml) or IL-1α+OSM treated cartilage explant media samples at week 1 and week 2. Loading volume was normalised to cartilage explant total GAG each lane shows pooled triplicate wells from one representative experiment (n=3, N=1) (A). Semi-quantitative densitometric analysis at week 1 with analysis performed using Image J (NIH). Mean and *sd* of 4 experiments shown. Statistical significance determined by ANOVA with Tukey's post-hoc test for multiple comparisons performed using GraphPad Prism 7.0 software. ** $p<0.01$.

3.2.4 Cytokine-induced effects on gene expression in primary bovine chondrocytes in monolayer

IL-1α and IL-1α+OSM mediate significant increases in the expression of metalloproteinases and a synergistic induction of ADAMTS-4 and 5 is mediated by IL-1 in combination with OSM

The effects of cytokines applied alone or in combination on the expression of proteases involved in matrix degradation was assessed. Gene expression analysis by RT-PCR of primary bovine chondrocytes cultured in monolayer for 24 hours in the presence of control media, IL-1α (10ng/ml), IL-1α (10ng/ml) +OSM (50ng/ml) or OSM (50ng/ml) alone showed a significant increase in expression *ADAMTS4* mediated by IL-1α, 154.96 mean fold increase ($p<0.01$), and IL-1α+OSM, 979.36 mean fold increase ($p<0.01$), compared to control cells. The expression of *ADAMTS4* mediated by the combination of IL-1α+OSM was significantly higher than that of cells treated with IL-1α or OSM alone ($p<0.05$) (Fig 3.5A). The effects of cytokine treatment upon *ADAMTS5* expression showed IL-1α up-regulated mean expression by 4.74 fold ($p<0.01$) and the combination of IL-1α+OSM significantly increased the mean expression by 45.9 fold ($p<0.01$). OSM alone treatment of cells resulted in a 7.3 mean fold increase in expression of *ADAMTS5* ($p<0.05$) (Fig 3.5B). Mean fold change expression levels in cytokine treated cells (all conditions) were more pronounced for *ADAMTS4* compared to *ADAMTS5* although *ADAMTS5* showed a higher expression in control cells as determined by dCt value suggesting constitutive expression was higher than that of *ADAMTS4*.

Significant increases in expression were shown for the collagenase *MMP1* in IL-1α ($p<0.01$) and IL-1α+OSM ($p<0.01$) treated chondrocytes, with higher expression observed in cells treated with IL-1α+OSM compared to IL-1α alone with a mean fold increase in expression of 2034.6 and 260.99, respectively, representing a synergistic induction (Fig 3.5C). *MMP13* mean fold expression was increased by 149.9 in IL-1α ($P<0.01$) treated cells and by 777.5 in IL-1α+OSM ($p<0.01$) treated cells (Fig 3.5E) although there was no significant difference in expression between IL-1α and IL-1α+OSM the increases were synergisitc rather than additive. *MMP3* expression was also significantly increased in IL-1α ($p<0.01$) and IL-1α+OSM ($p<0.01$) treated cells, mean fold expression of 73.4 and 110.38 respectively, but there were no significant increases in expression of *MMP3* in IL-1α+OSM treated cells compared to those treated with IL-1α alone and expression levels showed an additive effect of IL-1α and OSM (Fig 3.5D). The observed increases in *ADAMTS4* expression in bovine chondrocytes translated to an increased detection of ADAMTS-4 activity, using the Sensolyte Aggrecanase 1, in the media of IL-1α and IL-1α+OSM treated bovine cartilage explants, though the increased ADAMTS-4 activity observed in IL-1α+OSM compared to IL-1α treated chondrocytes was additive rather than synergistic(Fig 3.5F).

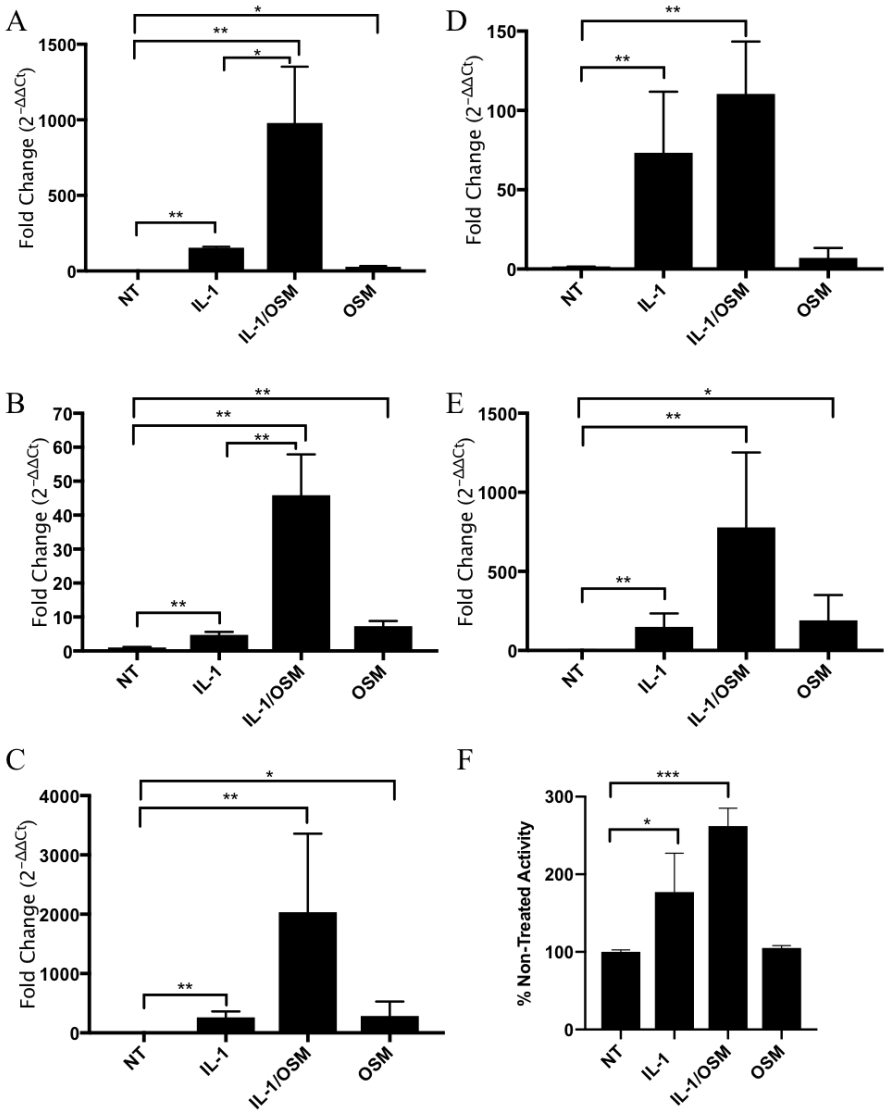

Figure 3.5 – Effects of cytokine treatment upon the expression of metalloproteinases in bovine primary chondrocytes assessed by RT-PCR. Analysis of primary bovine chondrocytes treated for 24 hours with IL-1α (10ng/ml), OSM (50ng/ml) or IL-1α+OSM. Relative expression of *ADAMTS4* (A), *ADAMTS5* (B), *MMP1* (C), *MMP3* (D) and *MMP13* (E). Expression normalised to *GAPDH* and fold change calculated using $2^{-\Delta\Delta Ct}$ method. Mean and *sd* of 3 experiments shown. ADAMTS-4 activity was assessed in the media of cytokine treated explants using the Sensolyte Aggrecanase 1 assay with activity expressed as % of explants cultured in ITS media in absence of cytokines assessed at 24 hours (F). Statistical significance was determined using ANOVA with Tukey's post-hoc test for multiple comparisons performed on dCt values using GraphPad Prism 7.0. * $p<0.05$. ** $p<0.01$.

IL-1α+OSM treatment of chondrocytes results in increased down-regulation of aggrecan and collagen type II expression compared to either cytokine alone

Pro-inflammatory cytokines have been shown to decrease the expression of matrix macromolecules in chondrocytes which contributes to OA pathology through reduced synthesis of matrix structural components and therefore a reduced capacity for repair. The treatment of chondrocyte monolayers with IL-1α, OSM and IL-1α+OSM resulted in down regulation of aggrecan and collagen type II expression. IL-1α mediated a significant reduction in aggrecan mean fold expression (2.5 fold reduction) and collagen type II expression (3.47 fold reduction) compared to normalised expression control cells. The effects were more pronounced in IL-1α+OSM treated cells with an observed reduction in aggrecan mean fold expression by 5.55 fold and collagen type II expression by 18.87 compared to normalised expression of control cells (Fig 3.6A and B). OSM alone significantly reduced mean fold expression of aggrecan by 3.36 and collagen type II by 6.71 fold. DMMB analysis of GAG released to culture media by chondrocytes cultured for 48 hours in the presence or absence of cytokines revealed a significant reduction in GAG release from cells treated with IL-1α and IL-1α + OSM compared to control cells, no significant differences were observed in cells treated with OSM compared to control cells (Fig 3.6D). These data shows a synergistic reduction in the expression of collagen type II mediated by IL-1α in combination with OSM.

IL-1α treatment of chondrocytes down-regulates *PRG4* expression, whereas OSM increases its expression and production

The application of OSM to chondrocytes for 24 hours resulted in a significantly increased expression of *PRG4*/lubricin, 6.24 mean fold increase, an increase was also observed in IL-1α+OSM treated cells to a lesser and non-significant extent, 1.73 mean fold increase. IL-1α treatment of cells resulted in a significant down regulation of lubricin, 3.46 fold reduction, at 24 hours compared to control cells (Fig 3.6C). Western blot analysis of media samples of chondrocytes cultured for 48 hours in the presence of cytokines confirmed the increased production of lubricin by OSM treated cells shown by positive staining when blotted with anti-lubricin 6A4 antibody whereas no positive bands were detected in all other conditions tested including control cells (Fig 3.6E).

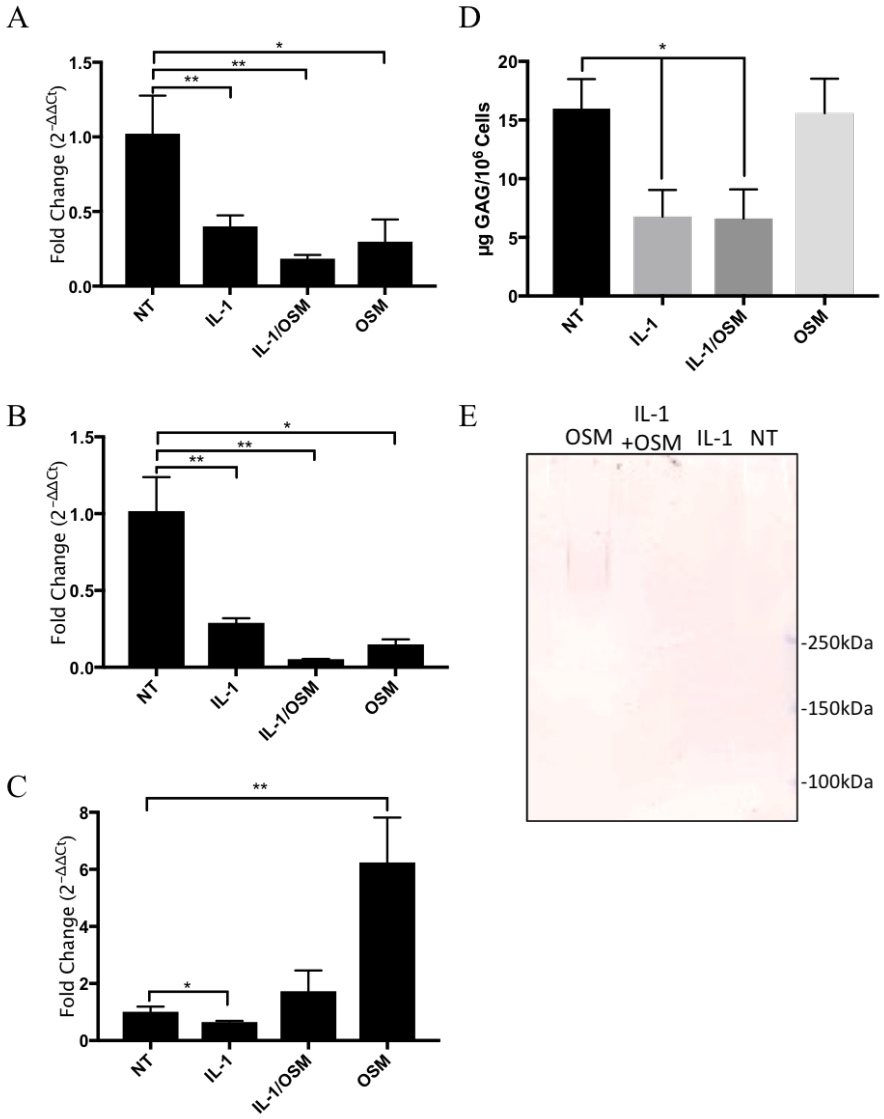

Figure 3.6 – Effects of cytokine treatment upon the gene expression of matrix macromolecules in bovine primary chondrocytes assessed by RT-PCR. Effects of cytokine treatment upon GAG production quantified by DMMB assay and lubricin production assessed by Western blot. RT-PCR analysis of primary bovine chondrocytes treated for 24 hours with IL-1α (10ng/ml), OSM (50ng/ml) or IL-1α+OSM. Relative expression of aggrecan (A), collagen type II (B), and lubricin (C). Expression normalised to *GAPDH* and fold change calculated using $2^{-\Delta\Delta Ct}$ method. Mean and *sd* of 3 experiments shown. Statistical significance was determined using ANOVA with Tukey's post-hoc test for multiple comparisons performed on dCt values using GraphPad Prism 7.0. * $p<0.05$. ** $p<0.01$. DMMB analysis of culture media to assess GAG production by $1x10^6$ primary bovine chondrocytes treated with the indicated cytokines for 48 hours, mean and *sd* of 3 experiments shown (D). Western blot under reducing conditions using anti-lubricin 6A1 antibody of cell culture media, equal volume from pooled triplicate wells (n=3, N=1) from $1x10^6$ primary bovine chondrocytes treated with the indicated cytokines for 48 hours (E).

3.2.5 Cell signalling pathway analysis in primary bovine chondrocytes in monolayer

Cell signalling analysis reveals IL-1α and OSM specific pathways whilst identifying synergistic activation of SAPK/JNK mediated by IL-1α in combination with OSM

Analysis of cell signalling pathways in cytokine stimulated primary bovine chondrocytes using the Pathscan intracellular signalling array, plotted as a time course of activation (Fig 3.7 and 3.8), revealed cytokine specific pathways such as AKT (Thr^{308}/Ser^{473}) and STAT3 signalling activated exclusively in OSM treated chondrocytes with little or no increased induction in combination with IL-1α. The activation of AKT, both Ser^{473} and Thr^{308}, signalling was rapid with the highest level of phosphorylation observed at 10 minutes with decreasing levels observed at 30, 60 and 120 minutes. The phosphorylation of AKT-Ser^{473} and Akt-Thr^{308} decreased to almost control levels by 60 minutes (Fig 3.7). STAT3 phosphorylation was observed at high levels for both OSM and IL-1α+OSM treated cells at 10 minutes and slowly declined through to 120 minutes, however, the level of phosphorylation at 120 minutes was increased compared to control and IL-1α treated cells at this time point (Fig 3.7). STAT1 phosphorylation was modestly increased in IL-1α+OSM and OSM treated chondrocytes compared to controls at 10 and 30 minutes but levels of phosphorylation closely followed those of controls at all other time points (Fig 3.7). OSM treatment resulted in a phosphorylation peak of ERK1/2 at 10 minutes and was evident at similar levels in OSM and IL-1α+OSM treated cells. IL-1α treatment mediated an increase in ERK1/2 phosphorylation at 30 mins compared to controls. The activation of ERK1/2 by IL-1α was not as early or as pronounced as that seen with OSM or IL-1α+OSM treated cells but IL-1α mediated phosphorylation persisted to 120 mins, as did IL-1+OSM treated cells, whereas OSM treated cells returned to baseline phosphorylation levels by 120 mins (Fig 3.7). The activation of SAPK/JNK was minimally increased in the presence of OSM. A greater increase was shown in IL-1α treated cells. The combination of IL-1α and OSM, however, resulted in supra-induction of SAPK/JNK at all time-points (Fig 3.7). The activation of SAPK/JNK in both IL-1α and IL-1α+OSM treated cells spiked at 30 minutes post-cytokine treatment followed by a secondary spike of SAPK/JNK phosphorylation observed at 120 minutes (Fig 3.7). p38 phosphorylation was induced by OSM and IL-1α+OSM treatments at 10 minutes with the highest phosphorylation level observed with IL-1α+OSM. IL-1α induced activation of p38 was delayed compared to OSM and IL-1+OSM and increased only at 30 mins but to similar levels to IL-1α+OSM at this time point. OSM induction of p38 phosphorylation decreased steadily from 10 minutes and was close to control levels from 30 through to 120 minutes. A secondary spike in phosphorylation was seen for IL-1α and IL-1α+OSM treated cells from 60 to 120 minutes. Levels of phosphorylation of p38 at 120 minutes were similar for both IL-1α and IL-1α+OSM treated cells (Fig 3.7). PRAS40 showed similar levels of activation, R.F.I>$1x10^6$, in all conditions at all time-points (Fig 3.8). In other pathways assessed the phosphorylation levels closely correlated with those of control cells with the exception of ribosomal protein S6 kinase beta-1 (P70 S6) where an increased level of phosphorylation was detected for IL-1α, IL-1α+OSM and OSM treated cells at 60 minutes compared to control cells and GSK-3B where an increased activation was observed at 10 and 30 minutes for OSM that was reduced for IL-1α+OSM treated chondrocytes compared to controls.

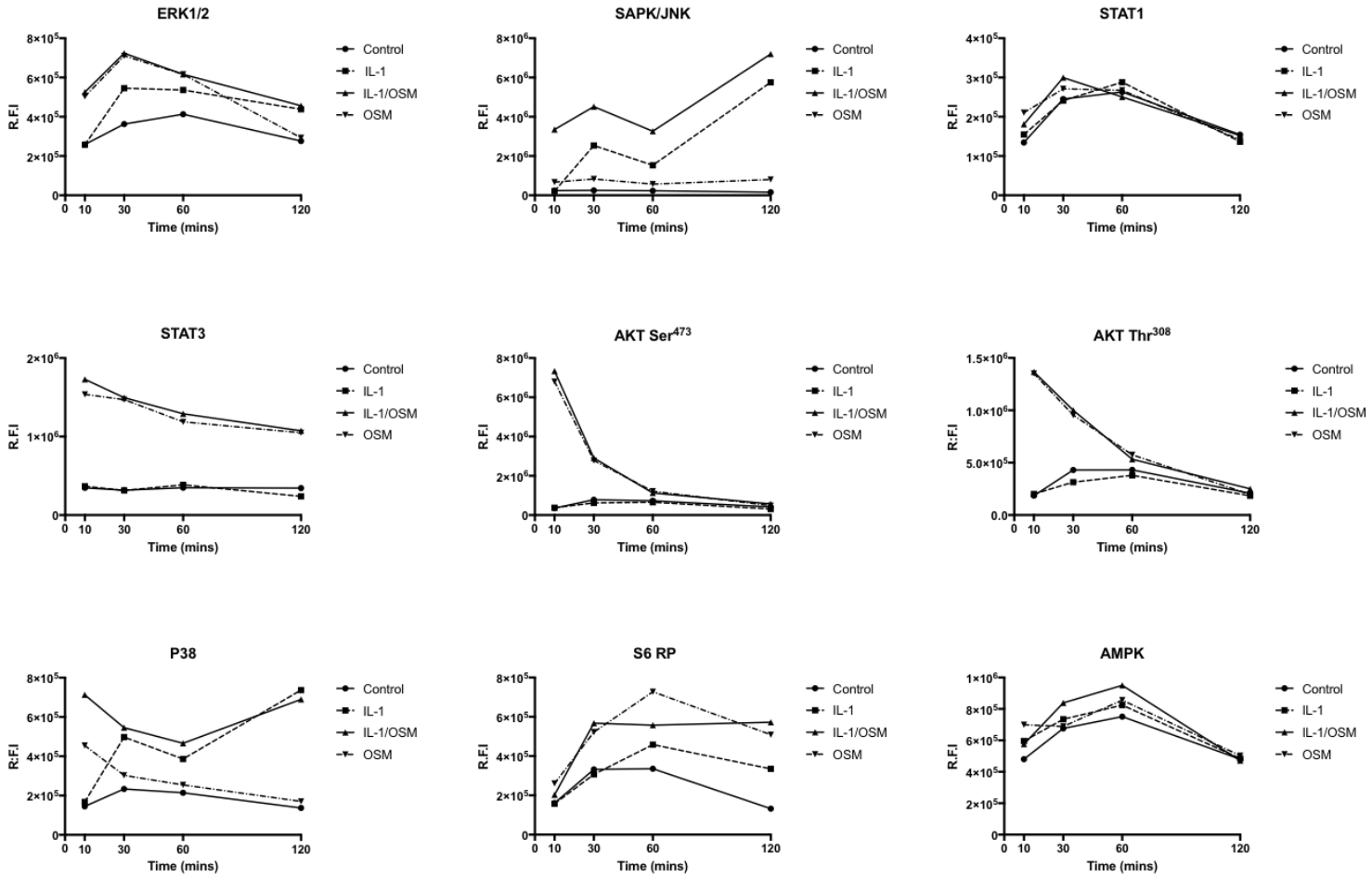

Figure 3.7 – Pathscan intracellular signalling array analysis of cytokine stimulated bovine primary chondrocytes. Pathscan intracellular signalling array analysis of bovine primary chondrocytes cultured in monolayer and treated with IL-1α (10ng/ml), OSM (50ng/ml) or IL-1α+OSM. Chondrocytes were harvested at 10, 30, 60 or 120 minutes and fluorescent intensity measured using a LiCor Odyssey CLx imaging system and ImageStudio. Mean of techincal duplicates plotted representing one independent experiment (n=2, N=1).

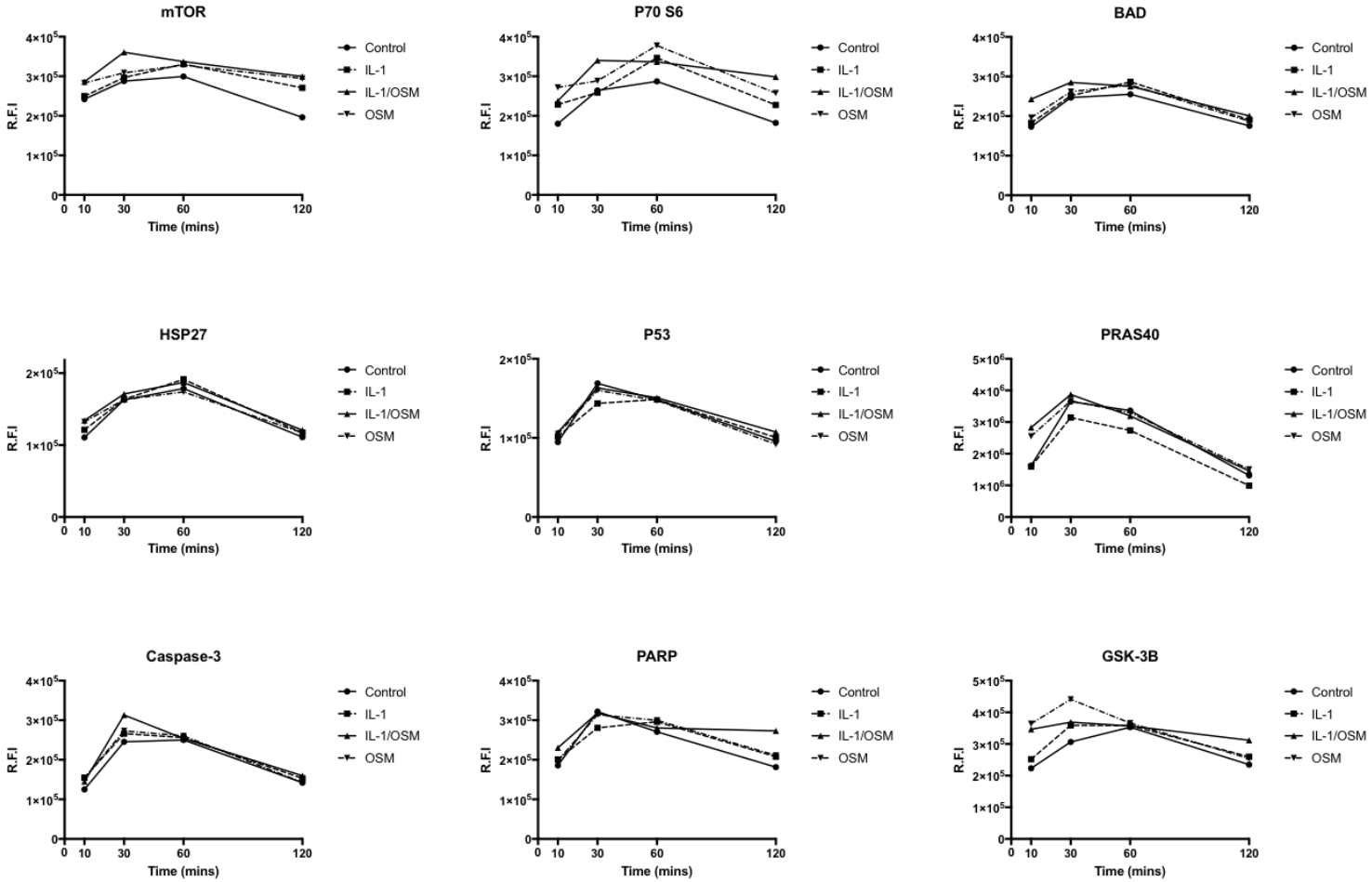

Figure 3.8 – Pathscan intracellular signalling array analysis of cytokine stimulated bovine primary chondrocytes. Pathscan intracellular signalling array analysis of bovine primary chondrocytes cultured in monolayer and treated with IL-1α (10ng/ml), OSM (50ng/ml) or IL-1α+OSM. Chondrocytes were harvested at 10, 30, 60 or 120 minutes and fluorescent intensity measured using a LiCor Odyssey CLx imaging system and ImageStudio. Mean of techincal duplicates plotted representing one independent experiment (n=2, N=1).

3.2.6 Effect of SAPK/JNK inhibition upon cytokine-induced chondrocyte gene expression

Inhibition of SAPK/JNK reduces the expression of *ADAMTS-4, ADAMTS-5, MMP1, MMP3* and *MMP13* in IL-1α and IL-1α+OSM treated chondrocytes

Of all 18 signalling molecules assessed, the phosphorylation of SAPK/JNK was consistently increased in IL-1α+OSM compared to IL-1α or OSM treated chondrocytes therefore pharmacological inhibition was employed to confirm the role of SAPK/JNK in cytokine mediated increases in matrix protease gene expression by primary bovine chondrocytes. Where inhibitors were added, the final volume of DMSO was below 0.5% to avoid potential effects of DMSO upon gene expression (Sumida *et al.* 2011) and control cells received the same concentration of DMSO alone as a carrier control. The incubation of primary bovine chondrocytes 15 minutes prior to IL-1α+OSM stimulation with the JNK1,2 and 3 specific inhibitor SP600125 resulted in a reduction in the expression of *ADAMTS5* by 91.4%, *MMP13* by 72% and *ADAMTS4* by 48.1% compared to IL-1α+OSM treated chondrocytes cultured in the absence of JNK inhibitor assessed after 24 hours in culture (Fig 3.9). JNK inhibition mediated significant reductions in expression of *ADAMTS4*, 5, *MMP1*, *MMP3* and *MMP13* in IL-1α and IL-1α+OSM treated chondrocytes when compared to carrier control (Fig 3.9). No significant differences were observed in the expression of aggrecan or collagen type II in SP600125 treated cells versus carrier control (Fig 3.9) suggesting that SAPK/JNK pathway activation was not implicated in the down-regulation of these genes.

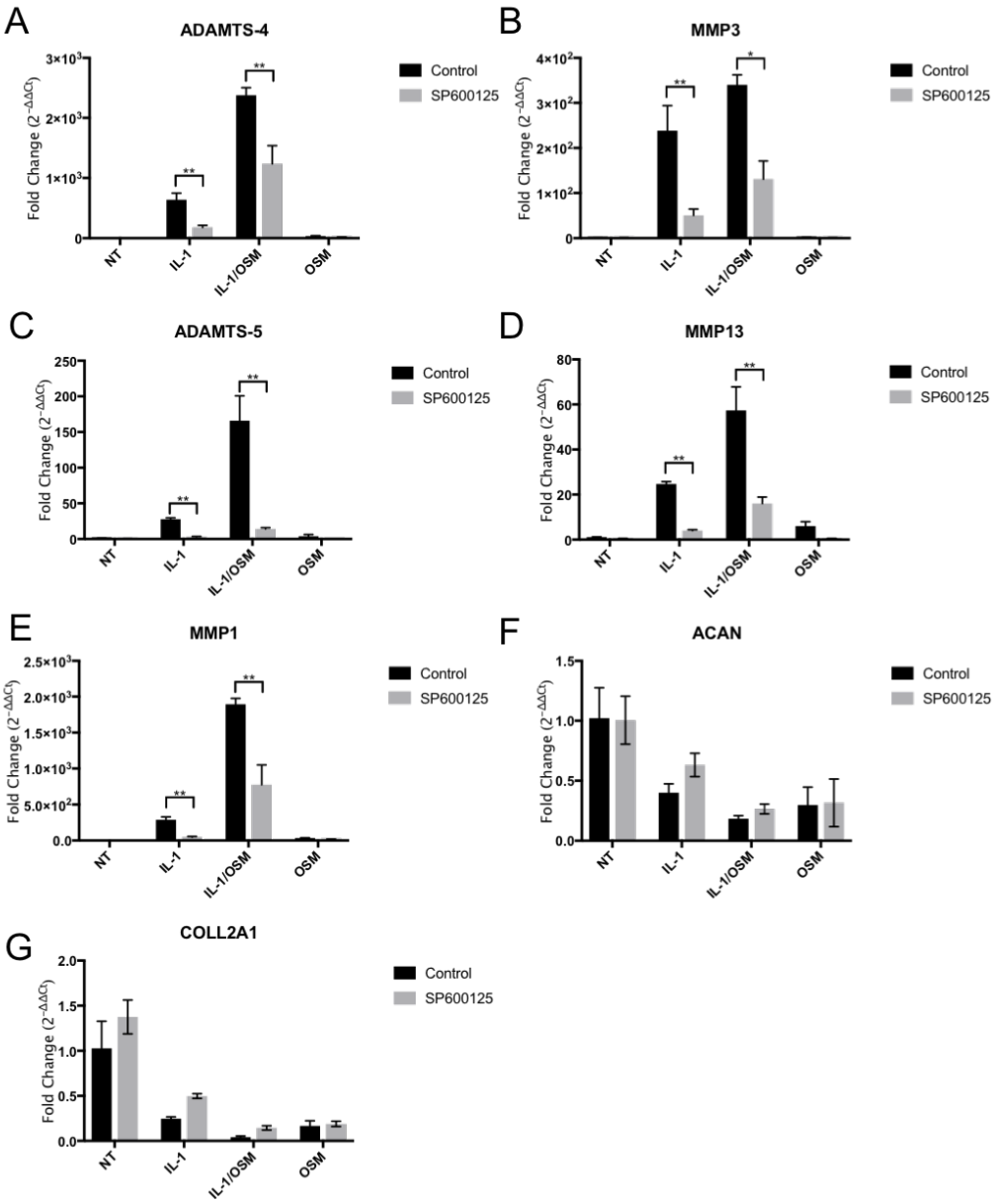

Figure 3.9 – Effects of SP600125 mediated SAPK/JNK inhibition upon cytokine-induced gene expression in primary bovine chondrocytes. RT-PCR analysis of primary bovine chondrocytes treated for 24 hours with IL-1α (10ng/ml), OSM (50ng/ml) or IL-1α+OSM in the presence (black bars) or absence of 10 µM SP600125 added 15 miutes prior to cytokine stimulation (grey bars). Expression normalised to *GAPDH* and fold change calculated using $2^{-\Delta\Delta Ct}$ method. Mean and *sd* of 3 experiments shown. Statistical significance was determined by ANOVA with Tukey's post-hoc test for multiple comparisons using GraphPad Prism 7.0. * $p<0.05$. ** $p<0.01$.

3.2.7 Effects of SAPK/JNK inhibition upon cytokine-induced cartilage degradation in bovine explant cultures

SP600125 mediated SAPK/JNK inhibition in cartilage explants reduces GAG loss and NO production in IL-1α and IL-1α+OSM treated explants

To confirm the role of the SAPK/JNK pathway in cartilage degradation mediated by IL-1α and IL-1α+OSM, cartilage explants were cultured with the indicated cytokines in the presence or absence of the pan-JNK inhibitor SP600125 (inhibitor added 15 minutes prior to cytokine stimulation). The addition of 10 μM SP600125 to bovine articular cartilage explants prior to cytokine treatment significantly reduced the GAG loss, assessed by DMMB assay, to media in IL-1α and IL-1α+OSM treated explants when assessed at day 5 of culture (Fig 3.10A). NO production was assessed by Greiss assay as a marker of inflammation. This showed an increased production and release of NO to media by IL-1α and IL-1α+OSM treated explants that was significantly reduced in the presence of SP600125 (Fig 3.10B), however it must be noted that the NO release by non-cytokine stimulated cartilage explants was similar in level to that of IL-1α stimulated explants and was slightly increased by JNK inhibition suggesting cellular stress under these culture conditions. The assessment of LDH release to media from explants was employed as an indicator of chondrocyte viability. Treatment with IL-1α, IL-1α+OSM or OSM did not result in increased LDH release from explants and no differences in LDH release were observed for explants cultured in the presence of 10 μM SP600125 suggesting this inhibitor is not cytotoxic at this concentration. A positive control was included where explants were incubated for 30 mins in 10% Triton X to dissolve cellular membranes and stimulate LDH release prior to conducting the assay (Fig 3.10C).

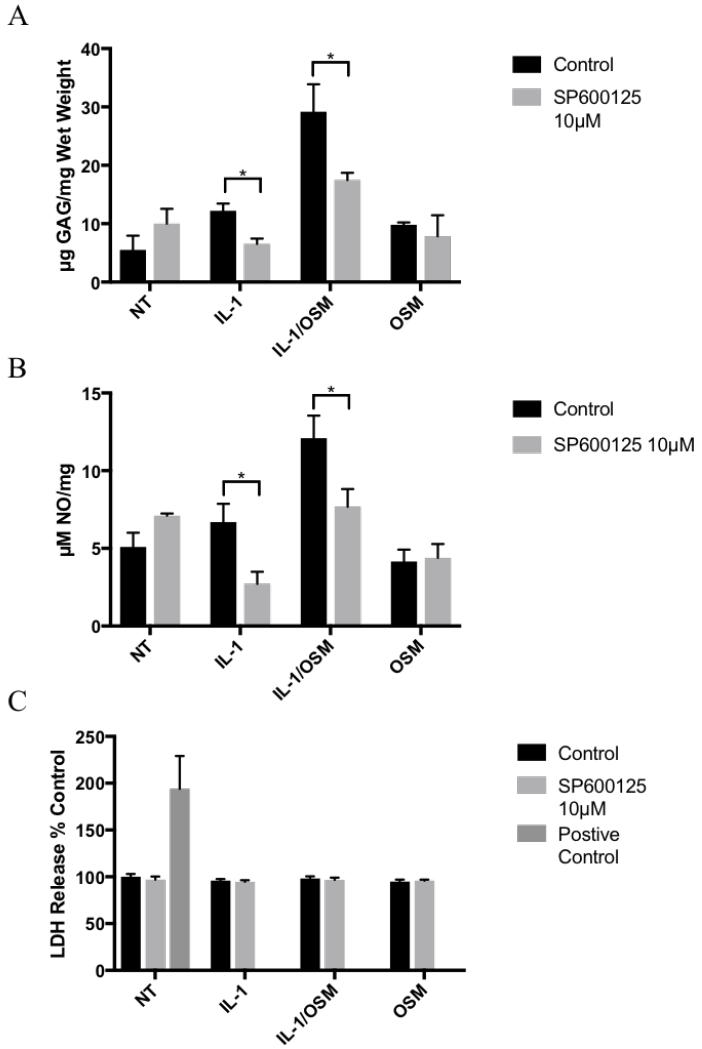

Figure 3.10 – Assessment of pharmacological inhibition of SAPK/JNK in cytokine treated bovine cartilage explants upon GAG loss, NO production and viability. GAG loss assessed by DMMB assay of cell culture media harvested at day 5 from 2mm diameter mature bovine cartilage explants cultured with IL-1α (10ng/ml), OSM (50ng/ml) or IL-1α+OSM in the presence or absence of 10 µM SP600125. Inhibitor was added 15 mins prior to cytokine application (A). NO release from explants in (A) assessed by Greiss assay (B). Viability of explants cultured with the indicated cytokines in the presence or absence of 10 µM SP600125 assessed by LDH release (C). Mean and *sd* of 3 experiments shown. Statistical significance was determined using ANOVA with Tukey's post-hoc test for multiple comparisons performed using GraphPad Prism 7.0 software. * $p<0.05$.

Inhibition of SAPK/JNK results in reduced aggrecanase activity at site $E^{373\_374}A$ in IL-1α and IL-1α+OSM treated explants

Western blot using the neo-epitope monoclonal antibody BC-3, that recognises -ARGSVIL neo-epitope generated by aggrecanase mediated cleavage of aggrecan at site $E^{373\_374}A$, in the IGD showed that inhibition of SAPK/JNK could reduce aggrecanase activity in IL-1α treated explants in a concentration dependent manner, however, the inhibition of aggrecanase activity in IL-1α+OSM treated explants was incomplete even at the highest concentration of SP600125 and intensity was increased at the highest dose of SP600125 (Fig3.11A). Western blot using monoclonal antibody 2B6, that recognises the CS4 stub of CS generated post-cleavage with chondroitinase ABC was used as a loading control and assessment of total aggrecan fragmentation confirming that loading was equal and that fragmentation also occurred in OSM treated explants however the lack of bands in BC-3 Western blot confirms that this degradation in OSM treated explants was not the result of aggrecanase activity at site $E^{373\_374}A$ but more likely at the alternative aggrecanase or MMP cleavage sites in aggrecan (Fig3.11B).

Inhibition of SAPK/JNK results in reduced COMP degradation in IL-1α and IL-1α+OSM treated explants

Western blot analysis was performed on the media of cytokine treated explants cultured in the presence or absence of the SAPK/JNK inhibitor SP600125 under non-reducing conditions to identify the fragmentation of pentameric COMP. Similarly to the BC-3 Western blot it was shown that SP600125 was capable of reducing the observed fragmentation of COMP in the explants cultured with IL-1α but inhibition was less effective in IL-1α+OSM conditions (Fig3.10C).

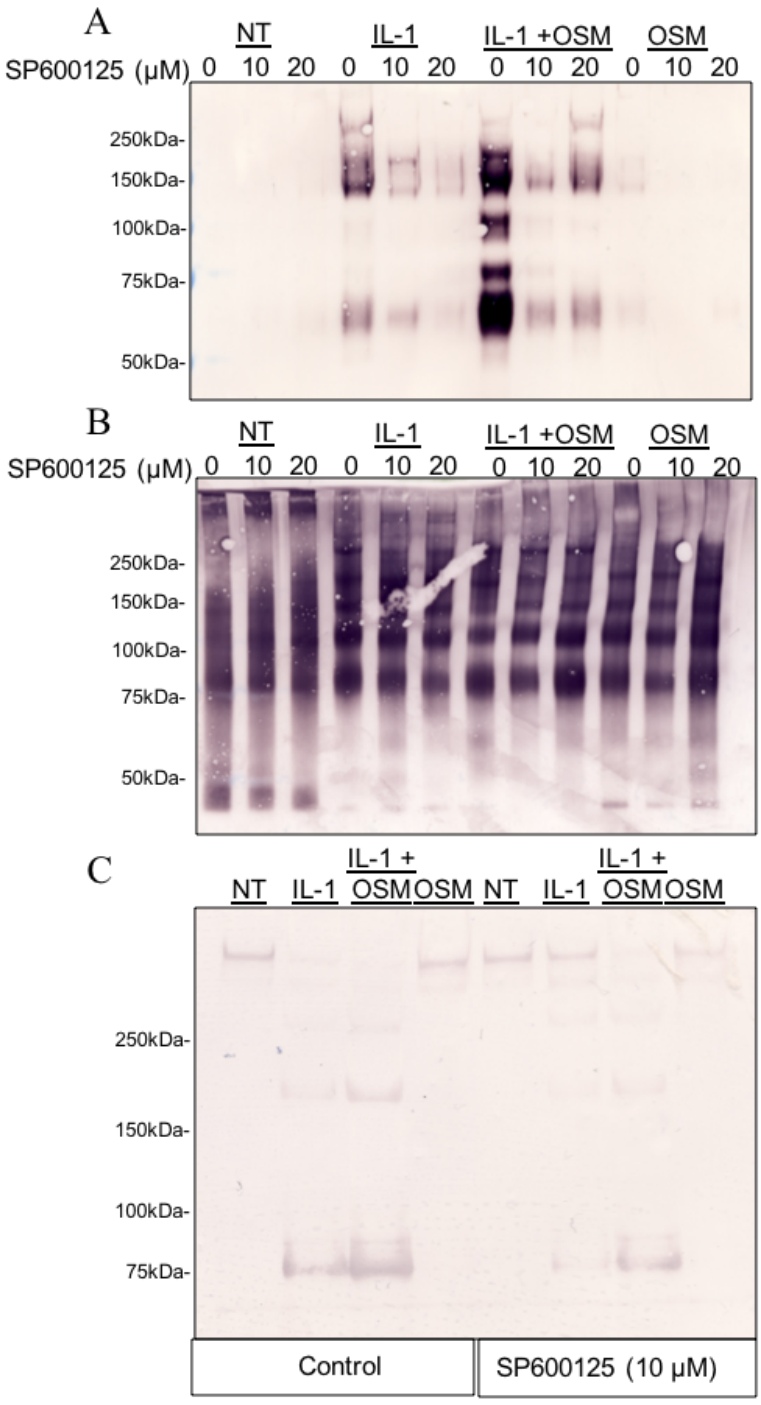

Figure 3.11 – Western blot assessment of SAPK/JNK inhibition on aggrecanase activity and COMP degradation in cytokine treated bovine explants. Western blot of media samples of control (NT) or cytokine treated cartilage explants cultured in the presence of SAPK/JNK inhibitor SP600125 at the indicated doses for 5 days using antibody BC-3 against –ARGSVIL neo-epitope generated by aggrecanase mediated cleavage of $E^{373\_374}A$ of aggrecan. Inhibitor was added 15 mins prior to cytokine application. Equal loading of 18μg GAG equivalent per lane derived from pooled triplicate wells of one independent experiment (A). Media samples from (A) were also blotted with the chondroitin sulphate stub antibody 2B6 as a probe for total aggrecan and aggrecan fragmentation. Equal loading of 2μg GAG equivilant per lane derived from pooled triplicate wells (n=3, N=1) (B). Western blot under non-reducing conditions against COMP of non-treated (NT), IL-1α (10ng/ml), OSM (50ng/ml) or IL-1α+OSM treated cartilage explant media samples cultured in the presence or absence (Control) of 10μM SP600125 for 1 week. Loading volume normalised to cartilage explant total GAG content (n=3, N=1) (C).

3.2.8 *In vitro* ADAMTS-4 mediated COMP cleavage and OA patient synovial fluid analysis

Treatment of metabolically inactive cartilage explants with recombinant ADAMTS-4 results in COMP degradation producing fragments of comparable molecular weight to those observed in cytokine treated live cartilage explants

The incomplete inhibition of IL-1α+OSM mediated *ADAMTS4* expression in chondrocyte monolayers by SP600125 suggested that residual aggrecanase activity detected in BC-3 Western blots of cartilage explants treated with IL-1α+OSM in the presence of SP600125 may be mediated by ADAMTS-4. Reports in the literature of ADAMTS-4 mediated COMP cleavage *in vitro* led to the investigation of ADAMTS-4 cleavage of COMP in its natural, cartilage-bound state by the incubation of metabolically inactive (dead) cartilage explants with conditioned media harvested from HEK293 cells stably expressing recombinant ADAMTS-4 p53. When cartilage, rendered metabolically inactive by multiple freeze-thaw cycles, was incubated with media containing rADAMTS-4 p53, degradation of COMP could be detected by Western blot after just 6 hours of incubation (Fig 3.12A). The pattern of fragmentation matched closely that observed in live cartilage explants treated with IL-1α or IL-1α+OSM showing fragments of ~260 kDa, 190 kDa and 75 kDa (Fig 3.5A) that closely match fragments designated Fragment 3,4 and 5 in the media of IL-1α and IL-1α-OSM stimulated cartilage explants. After culture for 24 hours there was only one fragment visible which was 75 kDa in size (Fig 3.12A) suggesting ADAMTS-4 cannot fully degrade COMP below this molecular weight. Conversely, when equal milligram wet weights of cartilage were incubated with media conditioned by HEK293 cells expressing the catalytically inactive ADAMTS-4 E/Q mutant there were no fragments detected of molecular weight 260 kDa, 180 kDa or 75 kDa further suggesting cleavage produced through incubation of cartilage with rADAMTS-4 expressing HEK293 media was indeed the result of ADAMTS-4. However, there was detection of a faint band at 150kDa in cartilage incubated with the media from HEK293 cells expressing the catalytically inactive EtoQ ADAMTS-4 that was not seen when explants were incubated in media alone (cell free ITS) that may be a result of endogenously produced unknown protease in HEK293 cells (Fig 3.14B).

Synovial fluid of OA patients contains degradation products of COMP

Western blot for COMP of hyaluronidase treated synovial fluid samples obtained from OA patients undergoing total knee arthroplasty was performed using two different primary antibodies. Both primary antibodies employed detected matching banding patterns with positive bands observed in all patient samples at circa 260 kDa, 170 kDa, and 70 kda (Fig 3.12C+D). In 3 of the four patient samples an additional band could be observed at 100 kDa although the staining intensity showed patient to patient variance. This band does not closely correspond to any of the fragments generated by ADAMTS-4 cleavage of metabolically inactive cartilage, whereas the aforementioned three bands match closely to those designated Fragment 3,4 and 5, although a reduced molecular weight is apparent for that designated Fragment 5. This is potentially as a result of lyase activity of bacterial hyaluronidase used to clear synovial fluid prior to Western blot although further work is required to confirm.

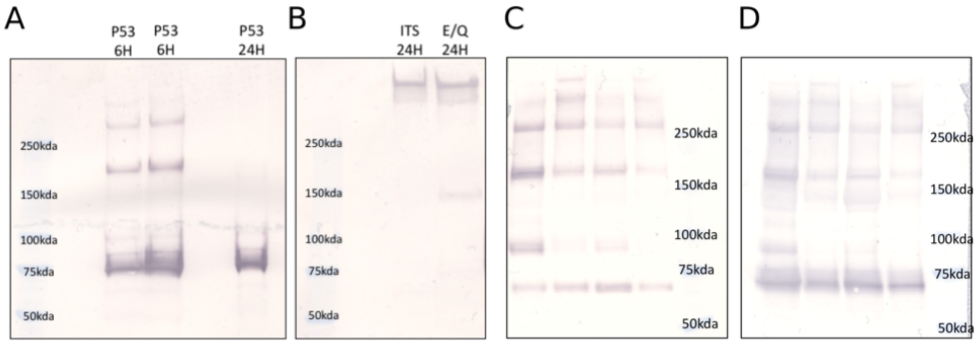

Figure 3.12 – Western blot analysis of COMP fragments present in the media metabolically inactive cartilage treated with recombinant ADAMTS-4 and analysis of COMP fragments present in the synovial fluid of OA patients. Western blot performed under non-reducing conditions against COMP of equal mg wet weights of metabolically inactive bovine cartilage incubated with with conditioned media of HEK293 cells expressing rADAMTS-4 p53 (A), catalytically inactive ADAMTS-4 E/Q or cell free control media (ITS), blots are representative of one independent experiment (n=1, N=1) (B) . Western blot under non-reducing conditions against COMP of hyaluronidase treated synovial fluid from OA patients undergoing total knee replacement equal volume loaded and blotted using rabbit polyclonal anti-COMP (immunised with synthetic peptide aa's 1-100 of human COMP) (C) or goat polyclonal anti-COMP (immunised with recombinant human COMP aa's 21-757) (D).

Treatment of bovine cartilage explants with a commercially available inhibitor specific to ADAMTS-4/5 prevents COMP degradation in response to IL-1α and IL-1α+OSM stimulation.

To further confirm the role of ADAMTS-4 in the cleavage of COMP in IL-1α and IL-1α+OSM treated explants, a commercially available inhibitor (CAS No 929634-33-3), that inhibits both ADAMTS-4 and 5 but has a 40 fold selectivity for ADAMTS-5 was added to cartilage prior to stimulation with the indicated cytokines. Western blot analysis revealed that application of ADAMTS-4/5 inhibitor results in complete inhibition of COMP degradation in IL-1α and IL-1α+OSM stimulated explants when assessed at day 7 of culture (Fig 3.13). This inhibitor has no known activity against MMPs and therefore at day 7 of culture COMP cleavage is not mediated by MMPs even in conditions of ADAMTS-4/5 inhibition although its effect on other cartilage matrix proteases including other ADAMTS proteases are unknown and require validation.

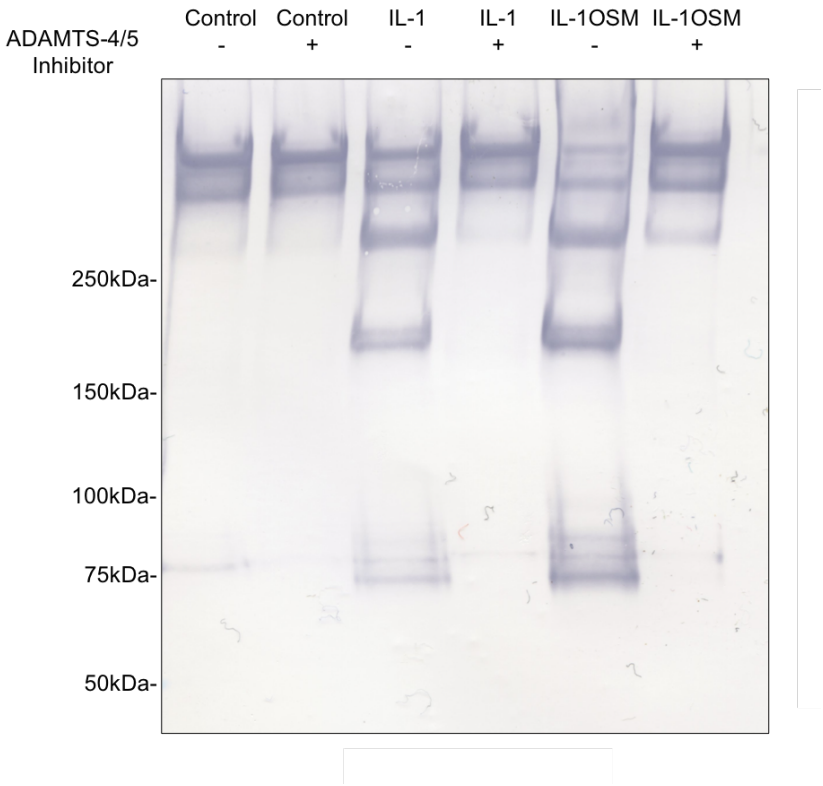

Figure 3.13 – Western blot analysis of COMP degradation and release in IL-1α and IL-1α+OSM stimulated bovine cartilage explants cultured in the presence or absence of a commercial ADAMTS-4/5 inhibitor. The incubation of bovine cartilage explants with a commercial inhibitor selective for ADAMTS-4/5 inhibited COMP degradation from IL-1α and IL-1α+OSM stimulated explants. Lanes represent pooled triplicate wells normalised to total explant GAG content representative of one independent experiment (n=3, N=1).

3.3 Discussion

Cartilage matrix degradation in response to cytokines

The work in this Chapter has replicated that shown in the literature and confirmed the synergistic effects of IL-1α in combination with OSM in the degradation of cartilage matrix, shown by collagen release, that was more rapid and pronounced in explants treated with IL-1α and OSM in combination than either cytokine alone although GAG loss in presence of IL-1α+OSM was additive rather than synergistic this may be a result of assessment at week 1 and further time course experiments are required to confirm. The synergism of cytokines of the IL-6 family of gp130 cytokines in the degradation of cartilage has been shown in the literature for OSM with TNFα and IL-1α and also for IL-6 but not LIF with IL-1 (Rowan *et al.* 2001). The combination of OSM with IL-1α resulted in a rapid loss of articular cartilage collagen that could be the result of an increased and more rapid expression of MMPs, that are capable of cleaving collagen, in the presence of OSM compared to IL-1α alone. Gene expression studies in this Chapter confirmed increased expression of collagenase type MMPs stimulated by IL-1α in combination with OSM compared to either cytokine alone but *MMP3* and *MMP13* were significantly up-regulated by IL-1α alone within 24 hours of application. Although the effect of IL-1α was additive rather than synergistic. However, the potential requirement for aggrecan depletion prior to collagen degradation, (Pratta *et al.* 2003) may suggest that the increased and more rapid aggrecan degradation evident in IL-1α+OSM treated cartilage explants could effect this collagen degradation. Furthermore, MMPs are secreted into the ECM in zymogen form and therefore require activation by ECM proteases which may explain the lag in MMP expression and collagen degradation compared to that of aggrecanase expression and GAG depletion.

Cytokine mediated effects on chondrocyte gene expression

Gene expression analysis in this Chapter showed an increased expression of *ADAMTS4*, *ADAMTS5*, *MMP1* and *MMP13* in primary bovine chondrocytes treated with IL-1α and a further increase in expression when treated with OSM in combination with IL-1α which was significant and synergistic for *ADAMTS4* and *ADAMTS5*. In the T/C28a4 chondrocyte cell line, *ADAMTS4*, *MMP3* and *MMP13* were significantly increased by IL-1α+OSM but *ADAMTS5* and *MMP9* expression was increased by culture of cells in IL-1α compared to IL-1α+OSM (Koshy *et al.* 2002). These differences observed could be due to cell type variance with this chapter using primary bovine cells compared to human immortalised cell lines or differences in concentrations of cytokines used, IL-1α at 10ng/ml and OSM at 50ng/ml were used in experiments in this Chapter, whereas IL-1α concentration was 1ng/ml and OSM was 10ng/ml in the study by Koshy *et al.* (2002). The concentration of OSM used in this Chapter is high and was kept constant at 50ng/ml for both cartilage explant and chondrocyte monolayer assays, the binding of OSM to cartilage matrix (Ryan *et al.* 2015) may result in differences between effective dose of OSM in explants and chondrocytes and should be further investigated. *ADAMTS5* has been previously shown to have a higher constitutive expression and be less responsive to induction via cytokine treatment (Fosang *et al.* 2008), although its relevance to matrix degradation cannot be overlooked, as ADAMTS-5 has been shown to be more efficient in the cleavage of aggrecan *in vitro* compared to ADAMTS-4

(Fushimi *et al.* 2007). Also, caution must be applied when assessing the gene expression of proteins as increased expression does not always correlate to increased production or activity. For example, post-transcriptional regulation of ADAMTS-5 via LRP1-mediated endocytosis has been proposed to rapidly remove constitutively produced ADAMTS-5 from the matrix in non-pathological conditions (Yamamoto *et al.* 2013). LRP1 has also been shown to internalise ADAMTS-4 and may play a role in depletion of free ADAMTS-4 (Yamamoto *et al.* 2014). Gene expression microarrays in SW1353 chondrosarcoma cells revealed multiple genes to be significantly up-regulated by IL-1+OSM compared to either cytokine alone. These genes included metalloproteinases such as *MMP1*, *MMP3*, *MMP10*, *MMP12* and *MMP13* in addition to cytokines such as IL-1, IL-6, IL-8 and the chemokine MCP-1 (Barksby *et al.* 2006). This data confirms the effects of IL-1α+OSM upon MMP expression observed in this Chapter. Aggrecan and collagen type II expression were decreased by the application of cytokines with the effects most pronounced by treatment with IL-1α+OSM. Aggrecan and collagen type II are commonly used as markers of chondrogenesis and their down regulation mediated by cytokines is well documented. The increase in lubricin expression mediated by OSM has been shown previously (Jones and Flannery, 2007), the detection of lubricin protein as early as 48 hours in the culture media from $1x10^6$ cells, however, suggests that this increase in gene expression translates to large increases of lubricin protein. Lubricin production has been shown to occur early in experimentally induced and naturally occurring OA in horse and is suggested as a possible mechanism to abrogate cartilage damage through increased lubrication (Reesink *et al.* 2017). It has been shown in OSMR deficient mice that FOXO1 phosphorylation in response to insulin signalling is impaired (Komori *et al.* 2014) and a recent study showed that ablation of FOXO1 in mice significantly reduced lubricin expression and that lubricin expression was increased *in vitro* by over-expression of FOXO1 in IMACS and ATDC5 cells suggesting a role for FOXO1 in the regulation of lubricin expression by OSM in mice (Matsuzaki *et al.* 2018). Over-expression of *FOXO1* in human OA chondrocytes resulted in a reduced expression of *ADAMTS4* and *ADAMTS5* in response to IL-1β suggesting FOXO1 fulfils an anti-inflammatory/protective role in humans and indeed its expression is reduced in aged and OA tissue (Akasaki *et al.* 2014).

In conclusion, IL-1α+OSM resulted in synergistic induction of *MMP1, MMP13, ADAMTS4, ADAMTS5* but not *MMP3* when assessed at 24 hours post-cytokine stimulation. Collagen loss, assessed by hydroxyproline assay, showed a synergistic effect of IL-1α in combination with OSM but the effect of this cytokine combination on GAG loss was additive when assessed at week 1. Time point assays may reveal a synergistic effect at eariler time points but further investigations are required.

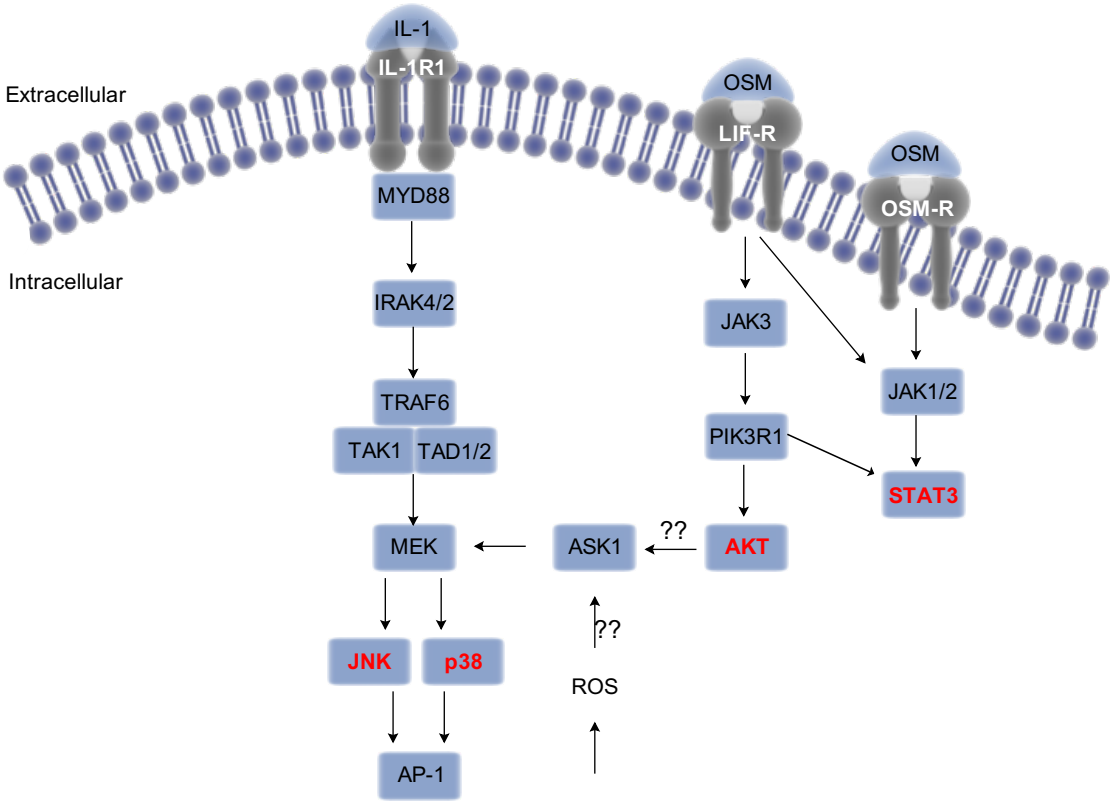

Figure 3.14 – Potential mechanism of synergistic activation of SAPK/JNK mediated by IL-1 and OSM. Text in black depicts pathways known from literature whereas text in red indicates those whose activity was confirmed in this Chapter. ASK1 activation via ROS or an unknown OSM dependent mechanism can subsequently activate MEK that can directly phosphorylate and further activate SAPK/JNK leading to supra-induction in these cytokine conditions.

Cytokine mediated induction of signalling pathways

Signalling pathway activation by cytokines in chondrocytes have been the subject of multiple studies in the literature although the work in this chapter is the first to date to assess simultaneously the activation states of 18 signalling molecules in response to IL-1α and OSM alone and in combination. OSM, a gp130 cytokine of the IL-6 family (including OSM, IL-6 and LIF) is pleiotropic and therefore has differential effects dependent upon target cell type and the inflammatory state of cells (Kishimoto, 2006). The observed OSM mediated increases in AKT, STAT3 and ERK1/2 phosphorylation in this Chapter correspond to those previously observed in the literature (El Mabrouk *et al.* 2007; Miyaoka *et al.* 2006). Through the application of pathway specific small molecule inhibitors, OSM mediated induction of *ADAMTS4* and *MMP13* was shown to be via ERK1/2, JAK3, STAT3, PI3K and AKT activation in human chondrocytes (El Mabrouk *et al.* 2007), though in this Chapter using bovine primary chondrocytes OSM had little effect upon *ADAMTS4* expression. JAK3 was not assessed in this Chapter however the pathways of JAK3 and AKT are linked as observed by a decreased AKT activation mediated by JAK3 inhibition. IL-1α induction of ERK1/2 peaked at 30 mins as opposed to the rapid 10 min peak mediated by OSM and IL-1α+OSM, however the persistence of phosphorylation observed at 120 mins in IL-1α and IL-1α+OSM treated cells suggests a slower but more sustained ERK1/2 activation is mediated by IL-1α compared to OSM. The delay in ERK1/2 activation in IL-1α treatments vs IL-1α+OSM treatments was shown in normal chondrocytes (non-OA) with phosphorylation of ERK1/2 detected in IL-1α and IL-1α+OSM treated cells at 60 mins but not in OSM treated cells confirming that observed in this Chapter (Greene and Loeser 2015). The IL-1α mediated SAPK/JNK activation observed in this Chapter has been shown by others in IL-1α treated normal human chondrocytes, but in contrast to the results in this Chapter, IL-1α+OSM treatment of human chondrocytes resulted in only a moderate increase in phosphorylation of SAPK/JNK and only at one time point, 15 mins, compared to IL-1α mediated levels (Greene *et al.* 2015), this is potentially due to differences in concentration of OSM used in this study, 10ng/ml, compared to work in this chapter where the concentration of OSM was 50ng/ml. Furthermore, the use of an infrared (IR) based detection method for phosphorylation levels provides a more quantitative approach with a much larger linear range and less susceptibility to saturation as compared to the ECL Western blots employed by Greene and Loeser (2015), and therefore differences in phosphorylation level between IL-1 and IL-1+OSM are likely more accurately detected using IR. A role for SAPK/JNK, specifically JNK2, mediated aggrecanase activity was shown in IL-1 treated human chondrocyte cell cultures overlaid with bovine aggrecan (Ismail *et al.* 2015). This study confirmed the role of JNK2 in aggrecan degradation via RNAi and also displayed a dependence on aggrecan degradation on a component upstream of SAPK/JNK-TAK1 in conditions of IL-1 stimulation. TAK1 is also capable of activation of the p38 MAPK pathway although the authors discounted activation of p38 in aggrecan degradation via a lack of reduction on aggrecanase activity after pharmacological inhibition of p38 using the small molecule inhibitor SB201920. In a follow up study Ismail *et al.* (2016) studied the effects of JNK2 in murine destabilisation of the medial meniscus (DMM) models of OA using *Jnk2*$^{-/-}$ mice which showed a reduction in aggrecan degradation, generation of NVTEGE- aggrecanase neo-epitope in cartilage compared to wild type mice and a decrease in 12 of 33 genes tested including *Adamts4* but interestingly not *Adamts5*, the predominant aggrecanase in mice (Ismail *et al.* 2016).

In addition to induction via cytokine treatment it has been shown that SAPK/JNK can be activated by mechanical damage of cartilage. These studies further implicate SAPK/JNK in cartilage degradation and its potential relevance to OA and therefore the effect of SAPK/JNK and its inhibition was selected as a focus of this Chapter. The work in this Chapter showed a secondary spike of SAPK/JNK and p38 phosphorylation mediated by IL-1α and IL-1α+OSM at 120 mins suggesting a potential secondary activation event in SAPK/JNK and p38 pathways after the initial phosphorylation peak at 30 mins. It is known that some pathways and transcription factors display oscillations in activation, this has been demonstrated for NFκβ and p38 MAPK, however, the secondary phosphorylation peaks observed by Tomida *et al.* (2015) are of a lesser intensity than the primary activations, whereas in this Chapter the secondary activation of SAPK/JNK and p38 MAPK are increased in intensity compared to the initial activation (Tomida *et al.* 2015). Early and late responding populations of SAPK/JNK and p38 have been observed in the literature with a secondary activation observed later than 2 hours post the initial response in genotoxin stimulated murine fibroblasts suggesting positive feedback mechanisms in these pathways (Fritz and Kaina, 2005). Scrutiny of signalling pathway networks in the literature revealed ASK1 as a potential convergence point due to its role in activation of both SAPK/JNK and p38 through MKK4/7. Interestingly, using an *Ask1*$^{-/-}$ mouse model Tobiume *et al.* (2001) showed that ASK1 was required for the sustained activation of SAPK/JNK and p38 but also for the secondary and increased spike in phosphorylation that corresponds well to that observed in this Chapter at 120 minutes post-treatment (Tobiume *et al.* 2001). Conversely, AKT is a negative regulator of ASK1, through phosphorylation of Ser83 which inactivates ASK1, therefore the role of ASK1 in IL-1+OSM treated cells, where AKT is highly activated, is unclear and requires further investigation using pharmacological inhibitors of ASK1. In conditions of ROS stimulation, via H_2O_2, AKT depletion via siRNA in human bronchial epithelial cells resulted in a reduction in ASK1 activation (Pan *et al.* 2010) suggesting stimuli dependent differences upon AKT/ASK1 interactions. Betanzos *et al.* (2016) applied a shotgun phosphoproteomics approach to observe concomitant increases in the phosphorylation state of the proposed inhibitory SER83 and the activating THR838 in the presence of increasing H_2O_2 suggesting that in response to ROS SER^{83} phosphorylation is not inhibitory. ASK1 was shown to be expressed by chondrocytes in the superficial zone of OA patients and levels of expression correlated with OA severity, in the same study it was shown that *Ask1*$^{-/-}$ mice were protected from cartilage degradation in partial meniscectomy and joint destabilisation/injury mouse models of OA (Zhang *et al.* 2016) suggesting a role for ASK1and downstream SAPK/JNK and p38 signalling in OA pathology.

Further investigations into the role of SAPK/JNK in cytokine induced cartilage degradation was made by the pre-incubation of cartilage explants with the pan-JNK inhibitor, SP600125 (Bennet *et al.* 2001), that reduced GAG loss significantly and -ARGSVIL neo-epitope release in both IL-1α and IL-1α+OSM treated explants confirming the role of this pathway in aggrecan degradation mediated by IL-1 and IL-1α+OSM. Pharmacological inhibition of SAPK/JNK also resulted in reduced gene expression of MPs but an incomplete inhibition of *ADAMTS4* expression was observed. This incomplete inhibition of *ADAMTS4* expression in chondrocyte monolayers closely matched the BC-3 neo-epitope Western blot data from cartilage explant cultures showing that SP600125 could reduce aggrecanase activity at the $E^{373\_374}A$ site of aggrecan in a dose dependant manner in IL-1α treated

explants but inhibition was incomplete in IL-1α+OSM treated explants. Potentially, the residual aggrecanase activity observed after SP600125 treatment of explants cultured in IL-1α+OSM was due to residual ADAMTS-4 activity resulting from incomplete inhibition of expression. This was also evident for COMP degradation where degradation was still observed after treatment with IL-1α+OSM and SP600125 suggesting that, in the absence of detectable transcripts of ADAMTS-7 or 12, that COMP may be cleaved by ADAMTS-4 in this model system.

Cytokine mediated COMP degradation

The precise function of COMP in cartilage is unknown and it is equally unknown if loss of COMP from mature cartilage is pathological, however, the degradation of COMP and its release to the synovial fluid has been associated with OA pathology and detection of both total COMP and neo-epitopes have been proposed as potential biomarkers of OA, Århmen *et al.* (2014) used N or C-terminal specific antibody enrichment to identify neo-epitopes in the synovial fluid COMP of OA patients. Interestingly, WB of OA synovial fluid identified fragments of a similar molecular weight to those observed in OA synovial fluid in this Chapter, particularly fragments at ~70 kDa, 150 kDa and 300 kDa. Several neo-epitopes were detected in these fragments for example Gly^{202}, $Tyr^{574}$and Phe^{577} were detected in the 300 kDa fragment and ^{91}Cys, ^{523}Asn, Tyr^{574} in the 70 kDa fragment that was also shown to be devoid of the native N-terminal. The detection of a band of 70 kDa in OA synovial fluid using a polyclonal antibody raised against amino acids 1-100 of human in this Chapter is surprising, although still possible, if indeed this fragment as postulated by Århman *et al.* (2014) has an N-terminal of ^{91}Cys. The fragmentation pattern and molecular weights observed in this Chapter using both cytokine treated cartilage explants and human OA synovial fluid also closely match those identified by Di Cesare *et al.* (1996) (designated CF-1 at 150 kDa, CF-2 at 67-94 kDa and CF-3 at 43-67 kDa) when analysing OA patient synovial fluid. In studies in human cartilage stimulated with TNF-α and IL-6/sIL-6R, which result in synergistic degradation of cartilage, Western blot analysis using an N-terminal monoclonal antibody (raised against aa's 48-72 of COMP) and C-terminal antibody (raised against the last 15 aa's of COMP) showed the generation of 5 fragments in stimulated cartilage matching that observed in this Chapter. Differences in size were observed for N-terminal mAb and C-terminal mAb detection with ∼100, 200, and 300 kDa detected with N-terminal mAb and C-terminal mAb detecting 200 and 300 kDa fragments and also a 70 kDa fragment but not 100 kDa. In TNF-α and IL-6/sIL-6R stimulated cartilage the degradation of COMP was much slower, appearing most prominently at 12 days compared to one week in this Chapter (Århman *et al.* 2014). This is potentially due to cytokine differences in protease induction or a reduced sensitivity of monoclonal compared to polyclonal antibody detection methods. Indeed only 3µl of synovial fluid were required for the Western blot in this Chapter suggesting a highly sensitive detection using polyclonal antibodies. In summary, there is a close consensus between the fragmentation patterns and weights observed in OA SF and cytokine treated explants in this Chapter and that observed in the literature. Importantly, the correlation of fragment sizes generated by cytokine treated explants and those in OA synovial fluid in this Chapter, and that observed by others (Århman *et al.* 2014; Ganu *et al.* 1998), would strongly suggest that cleavage of COMP occurs within cartilage and likely from a chondrocyte generated protease.

Although the proteases mediating COMP degradation *in vivo* remain undefined several proteases

have been demonstrated to cleave purified COMP *in vitro* including ADAMTS-4, 7, 12 and MMP-1, 3, 9, 13 and 19 but not ADAMTS-1 or 5 (Dickinson *et al.* 2003). It is difficult to compare the results of this Chapter to the cleavage products generated by Dickinson *et al.* (2003) as a reduced Western blot approach was taken compared to the non-reduced WB in the ADAMTS-4 COMP cleavage assay in this Chapter. Dickenson *et al.* (2003) also observed that the broad spectrum MP inhibitor BB94, that strongly inhibits IL-1α induced GAG loss, from bovine explants (Buttle *et al.* 1993), could partially inhibit COMP release from IL-1 treated nasal cartilage but not articular explants when assessed by ELISA. Western blot analysis of BB94 treated explants in this study confirmed no inhibition of fragmentation compared to IL-1α treated explants. The more specific MMP inhibitors (BB3437 and BB3003), Cysteine protease (E64) and Serine protease (Ep453) inhibitors however showed no effect in nasal or articular cartilage. However, BB94 significantly inhibited IL-1α induced COMP degradation in bovine articular cartilage explants and reduced the appearance of fragments of 300, 180 and 67-80 kDa (Ganu et al.1998). Therefore there are discrepancies in the literature despite use of inhibitors at the same concentration of 10μM in both studies. The observed degradation of COMP in week one of IL-1 treatment, where GAG loss is evident but no collagen loss is observed and therefore an assumed lack of MMP activity, implicates ADAMTS type proteases in the degradation of COMP. A role for ADAMTS-7 and ADAMTS-12 has been demonstrated in IL-1 and TNFα stimulated cartilage explants, which was confirmed by inhibition of COMP cleavage using ADAMTS-7/12 neutralising antibodies in addition to siRNA specific to ADAMTS-7 and ADAMTS-12 (Luan *et al.* 2008). Cleavage of COMP in these systems was fully inhibited when both ADAMTS-7 and ADAMTS-12 were inhibited simultaneously, either by neutralising antibodies in explants or gene silencing in cells, suggesting a role for both proteases in COMP degradation in cytokine treated cartilage explants. The assessment of ADAMTS-7 and 12 transcription in cartilage and synovium by Liu *et al.* (2006) showed a significant up-regulation of *ADAMTS-7* expression in RA cartilage and synovium but not OA cartilage, for *ADAMTS-12* the transcription was significantly up-regulated in OA cartilage but expression was more pronounced in RA cartilage and synovium (Luan *et al.* 2008). However, in this study in bovine chondrocytes and that of Kevorkian *et al.* (2004), in human OA and healthy cartilage, gene expression of *ADAMTS-7* was below detection and *ADAMTS-12* was at very low levels (Ct>40) even in cytokine treated cells suggesting *de novo* synthesis of ADAMTS-7 and ADAMTS-12 was not responsible for COMP degradation (Kevorkian *et al.* 2004). Molecular weights of products observed in ADAMTS-7 and 12 *in vitro* COMP degradation assays by Liu *et al.* (2006) and Luan *et al.* (2008) do not closely correlate to those observed in cartilage cultures or OA synovial fluids in this Chapter, which may be a result of the use of purified COMP compared to cartilage bound COMP or primary antibodies used. ADAMTS-7 and 12 degradation of COMP did show a strong cleavage product at around 100 kDa, interestingly, this correlates with a fragment detected with antibodies specific to the N-terminal observed by Århman *et al.* (2014) detected in OA synovial fluid and in a proportion of acute knee pain patients. A 100 kDa fragment was also present in 3 out of 4 OA patient synovial fluid samples in this Chapter. The 100 kDa band was not detected in IL-1α or IL-1α+OSM stimulated cartilage explants in this Chapter or by Ganu *et al.* (1998), although this is potentially due to antibody recognition. Incubation of metabolically inactive cartilage with rADAMTS-4-P53 resulted in rapid COMP degradation with fragments released matching banding

patterns observed in explant culture suggesting ADAMTS-4 is capable of cleaving COMP in its native cartilage bound state and a commercially available ADAMTS-4 and 5 inhibitor completely abrogated COMP cleavage in cytokine treated explants. However, we cannot rule out the possibility that ADAMTS-4 somehow activate ADAMTS-7 or ADAMTS-12 already present in the ECM although *de novo* protein synthesis was shown to be required for IL-1α induced COMP degradation in bovine explants as incubation in cycloheximide prevented degradation (Ganu *et al.* 1998). Furthermore, although the inhibitor used has been developed to selectively inhibit ADAMTS-4 and 5, its effect on ADAMTS-7, 12 and MMPs are unknown and the difficulty in obtaining recombinant ADAMTS-7 and 12 precluded its testing against these ADAMTS proteases *in vitro*. Likewise, the absence of published crystal structures of ADAMTS-7 and 12 prevented using molecular docking studies to assess the potential binding of inhibitor to these proteases. A study using metabolically inactive human cartilage with digestion by MMP and ADAMTS species independently showed in agreement with the work in this Chapter that ADAMTS-4 p53 digestion resulted in 5 unique peptides when assessed by mass spectroscopy, however the authors also identified two peptides where cartilage was incubated with ADAMTS-5. Other studies have shown no cleavage to be mediated by ADAMTS-5; this may be dependent upon COMP origin as cartilage bound COMP may be cleaved differentially to purified COMP or this may be due to ADAMTS-5 constructs used. The ADAMTS-5 used by Zhen *et al.* (2008) was comprised of aa's 262–554 (after removal of pro-domain) and therefore was lacking in TSP, CysR and spacer domains, whereas the ADAMTS-5 used by Dickinson *et al.* (2003), that showed no degradation of purified bovine COMP, was full length and due to the role in ancillary domains in substrate recognition it is plausible that removal of TSP, CysR and spacer domain would affect substrate specificity. The work in this Chapter clearly demonstrated that COMP degradation in IL-1α and IL-1α+OSM was likely mediated by ADAMTS-4 although we cannot rule out a contribution from ADAMTS-5 it is clear, due to the specificity of the inhibitor used, that COMP degradation was mediated by ADAMTS proteases and not MMPs in week one of culture. However, it is possible that other proteases complete the digestion of COMP in explant cultures as 24 hour digestion with ADAMTS4-p53 resulted in a fragment of around 75 kDa whereas, in week two/three of IL-1α+OSM treated explants no COMP was detectable at any molecular weight. This suggests further digestion in this system, potentially by MMP's as the activity of these enzymes is apparent from week 2 in IL-1α+OSM but not IL-1 treated explants abased upon observed collagen degradation at these time points, althoug total depletion of COMP from explants in IL-1α+OSM conditions is also possible and the levels of COMP in explants should be investigated further using GuHCl extraction and WB. MMP cleavage of COMP has been reported in the literature with evidence of MMP-1, 3, 9, 12, 13, 19 and 19 mediated processing (Dickinson *et al.* 2003; Ganu *et al.* 1998; Stracke *et al.* 2000). Digestion of purified COMP by Ganu *et al.* (1998) using recombinant MMPs showed that at 20 hours there was no complete degradation of COMP mediated by MMP-1, 3, 9 or 13 with the smallest molecular weight band detected being greater in weight than the 94 kDa molecular marker. This would suggest that although the MMPs can cleave COMP they do not generate fragments matching the 75 kDa observed in this chapter and by others in cytokine treated explants (Ganu *et al.* 1998; Århman *et al.* 2014) but MMPs may potentially further degrade COMP post ADAMTS cleavage events, incubation of ADAMTS-4 cleaved COMP with a panel of MMPs would likely reveal if this is the

case but time constraints prohibited this from being assessed in this Thesis.
It must be noted that although the fragments observed in cartilage explants and in rADAMTS-4 p53 digested cartilage closely matched fragments present in the synovial fluid (SF) of OA patients, slight variations in molecular weight were shown, this was potentially a result of the processing of SF for Western blot, which required the use of a bacterial hyaluronidase to reduce the viscosity of SF prior to gel electrophoresis. Bacterial hyaluronidase is capable of acting as a chondroitin sulphate lyase and therefore the slightly lower molecular weights observed in SF may be a result of COMP deglycosylation but further work is required to confirm.

3.4 Summary

The work in this chapter has;

1. Confirmed the synergistic effects of IL-1α and OSM resulting in increased expression of *ADAMTS-4*, *ADAMTS-5*, *MMP-1*, and *MMP-13* compared to either cytokine alone in chondrocytes and results in increased but not synergistic GAG loss in cartilage explants though time points earlier than 1 week are required to confirm the lack of synergistic effect on GAG loss. IL-1α+OSM resulted in synergistic increases in collagen loss from explants.

2. Identified novel synergistic activation of SAPK/JNK mediated by IL-1α in combination with OSM. The pathalogical role of this pathway was confirmed by pharmacological inhibition that reduced metalloproteinase gene expression in bovine primary chondrocytes and cartilage degradation in bovine explant cultures stimulated with IL-1α+OSM.

3. ADAMTS-4 was shown to mediate degradation of COMP in its native state in metabolically inactive articular cartilage resulting in fragmentation patterns matching those observed in the media of IL-1α and IL-1α+OSM treated explants and in the synovial fluid of OA patients. Inhibition of ADAMTS-4/5 completely inhibited IL-1α and IL-1α+OSM induced COMP degradation in cartilage explants at day 7 of culture. Combined these data suggest a role for ADAMTS-4/5 in COMP cleavage in OA and furthermore conclude that MMPs are not responsible for the initial COMP degradation in cartilage explants at day 7 of culture although the effect of ADAMTS-4/5 inhibitor on other matrix degradaing proteases should be further investigated.

4. Additionally, the work in this Chapter has resulted in an extensively characterised cytokine induced OA *in vitro/ex vivo* models for the subsequent assessment of Surfen as a potential therapeutic in this Thesis.

Chapter 4

Protease Inhibition by Surfen

4.1 Introduction

Surfen is an inhibitor of anthrax lethal factor (LF), a metalloproteinase with an IC_{50} of 0.5 µM (Williams *et al.* 2014). The mechanism of inhibition was determined to be competitive and proceeded through sequestration of the LF catalytic site Zn^{2+} by the urea group of Surfen in a mechanism similar to hydroxamate type inhibitors where the hydroxamic acid acts as a zinc binding group to inhibit protease activity. Many hydroxamate inhibitors show little specificity in MP inhibition with the earliest hydroxamate inhibitors to be used in clinical trials, Batimastat and Marimastat, having strong inhibitory effects on multiple MMPs and some inhibitory effect on ADAMs and ADAMTS proteases (Pasternak and Aspenberg. 2009). Indeed it is this lack of specificity that has hindered their clinical development due to off-target effects resulting in musculoskeletal syndrome (MSS) potentially through broad spectrum MP inhibition (Hoekstra *et al.* 2001). Therefore, the ability of Surfen to inhibit LF (Williams *et al.* 2014) suggests it may potentially inhibit other metalloproteinases which combined with the lack of observed toxicity, particularly MSS, in the historical use of Surfen as an excipient in insulin delivery warrants further study as the development of safe inhibitors of aggrecanase or collagenase activity could provide a disease modifying therapeutic for OA treatment. The specificity of an MP inhibitor is provided by the zinc binding group and non-covalent interactions between the inhibitor and hydrophobic substrate pockets of the MP catalytic domain. Substrate pockets are denoted as S1, S2 and S3 or S1', S2' and S3' corresponding to the amino acids of the substrate which are by convention designated from N to C-terminal P3, P2, P1, P1', P2', P3' where the catalytic cleavage site is located between P1 and P1' (Schechter and Berger. 1967). Inhibitor groups that interact with enzyme subsites follow the same nomenclature as that for substrates. The tri-histidine complexed zinc is omnipresent in metzincin MP catalytic domains whereas the S1' pocket shows the most variation in both sequence and structure (particularly depth) between MP catalytic sites and therefore non-covalent interactions between inhibitor P1' groups and MP S1' often convey inhibitor specificity. The distinction of MPs into subgroups based upon S1' pocket depth, for example solved crystal structures, show that MMP-1 and MMP-7 have shallow S1' pockets; MMP-3 and MMP-12 have deep and MMP-2 and MMP-9 have intermediate depth S1' pockets (Park *et al.* 2003). Some compounds are capable of inhibiting groups of MPs based upon pocket depth and access to the catalytic Zn^{2+}. Computational models such as molecular docking can provide indications as to specificity and optimal binding

conformations of inhibitor to protease but are not always accurate due to unpredicted conformational changes in binding pockets as seen with the generation of ADAMTS-5 inhibitors (Shieh *et al.* 2011), therefore *in vitro* screening assays remain the most effective method to test inhibitor specificities. However, the availability of open source molecular docking software with graphical user interface has made this technology available to a wider range of research fields. The accuracy of predicting protease targets of Surfen was therefore investigated in this Chapter and compared to traditional *in vitro* protease activity assays.

4.1.1 Aim and Objectives

Aims

This Chapter aims to identify OA-relevant proteases that may be inhibited by Surfen in a mechanism similar to that observed for LF. This will be performed prior to Surfen cartilage explant studies to aid in the subsequent deciphering of potential therapeutic effects of Surfen as any direct protease inhibition of Surfen is likely to contribute to the effects observed in cartilage explants.

Objectives

This aim will be investigated through completion of the following Objectives;

1. To identify potential protease targets, including MMPs, pro-protein convertase and ADAMTS, of Surfen using molecular docking and to elucidate the optimal binding conformation of Surfen to proteases.
2. To assess ability of Surfen to inhibit proteases identified in Objective 1 using *in vitro* assays to identify potential therapeutic effects of Surfen and to validate molecular docking results.

4.2 Results

4.2.1 Molecular Docking Assessment

Explanation of scoring function and output

Molecular docking was performed to identify potential MP targets of Surfen prior to *in vitro* protease inhibition assays to aid in selection of MPs to be tested and additionally to validate molecular docking as a technique for determining potential inhibitory properties of small molecules. Molecular docking studies were performed using Autodock Vina that presents potential binding conformations of flexible ligand structures to rigid protein structures. Results are scored using a combined empirical and knowledge-based scoring system that estimates the free-binding energy, ΔG, this value is expressed as kcal/mol with a negative value indicating binding. ΔG is derived from the estimated contribution of Van der Waals forces, hydrogen bonding and hydrophobic interactions in addition to steric forces such as repulsion, short range and long range attraction. Equation and weighting of scoring function shown.

$$\Delta G_{binding}\ (kcal/mol) = \Delta G_{gauss(i+ii)} + \Delta G_{repulsion} + \Delta G_{hbond} + \Delta G_{hydrophobic} + \Delta G_{torsion}$$

Weighting

ΔGgauss(i)=−0.0356

ΔGgauss(ii)=−0.00516

ΔGrepulsion=0.840

ΔGhbond=−0.587

ΔGhydrophobic=−0.0351

ΔGtorsion=0.0585

Root-square-mean deviation (RMSD) values are generated that represent the deviation of ligand structure (through bond rotation) from that of its expected resting state derived from structural minimisation using Dockprep. Commonly in the literature a maximum limit of 2Å is set for RMSD although this value is arbitrary. All top scores within this section are shown for ligand conformations with RMSD=0 unless otherwise stated. X-ray Crystal structures in the case of Apo (un-liganded) or co-crystal structures for Halo (liganded) forms of enzymes were obtained from RSCB protein data bank and molecular modelling was performed using a search area that encompassed the whole PDB structure provided, described as blind docking.

The use of Apo versus Halo crystal structures for molecular docking

The use of halo enzyme (ligand bound) structures may introduce bias due to conformational changes brought about by induced fit of inhibitor to protein and therefore initial studies were performed assessing Surfen docking to apo (un-liganded) ADAMTS-4 versus Halo ADAMTS-4 structures. Differences observed in preferential docking pose could suggest bias as a result of inhibitor binding during crystal structure determination. Structural analysis of the Apo form of ADAMTS-4 showed obscuration of the catalytic zinc, this was the result of a looping of S2' across the S1' subsite pocket towards the catalytic zinc and thereby a closed active site configuration (Fig 4.1A+B). Although this phenomena may be exclusive to ADAMTS-4 all subsequent molecular docking experiments were performed using halo enzymes crystallised in the presence of inhibitors known to bind competitively within the catalytic cleft unless otherwise stated where the absence of suitable halo enzyme crystal structures prevented this.

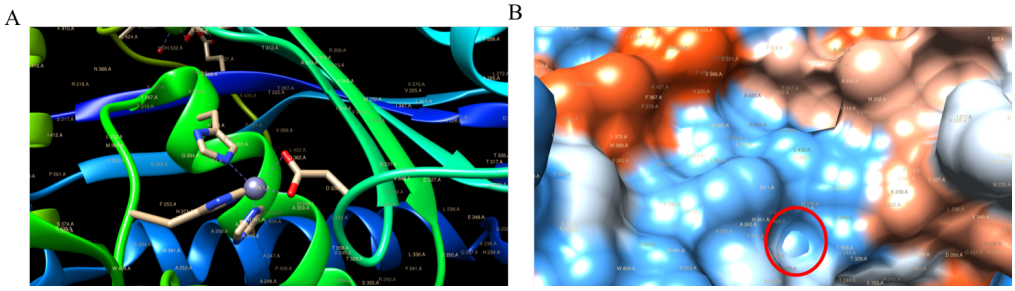

Figure 4.1 – Depiction of crystal structures of ADAMTS-4 in halo and apo forms showing structural differences in catalytic cleft and Zinc accessibility. Crystal structure of Apo ADAMTS-4 showing coverage of catalytic cleft via looping of S2' and chelation of Zn2+ shown in grey (A) Surface representations confirming obscuration of catalytic Zn^{2+} in apo form circled in red (B).

Validation of molecular docking via re-docking of inhibitors

The co-crystal structure 3HY7 depicts the structure of ADAMTS-5 in complex with the known inhibitor Marimastat (Fig 4.2A). To assess the accuracy of molecular docking, Marimastat was removed from 3HY7 followed by molecular docking and comparison of preferential binding results to that of the co-crystal placement of Marimastat within the catalytic cleft of ADAMTS-5. Search area encompassed the entire structure of 3HY7. Results showed that molecular docking does confirm the binding of Marimastat to the catalytic cleft although the conformation is not an exact match for that of the crystal structure location of Marimastat (Fig 4.2B). Similarly when Surfen was removed from the co-crystal structure (Fig4.2 C+D) and re-docked with LAF, it was observed that re-docking can predict binding to the catalytic site but as above the conformations of Surfen did not correlate between co-crystal structure and re-docking experiments (Fig 4.2 E+F). This suggests that although molecular docking can successfully predict binding within the catalytic cleft it does not return the same ligand binding conformation as that observed in the crystal structure. In summary, molecular docking may be useful in the identification of protease targets for Surfen but the binding conformations of top hits within the catalytic cleft may not represent exactly those observed experimentally and therefore caution must be applied when interpreting data and molecular docking prediction must be validated experimentally.

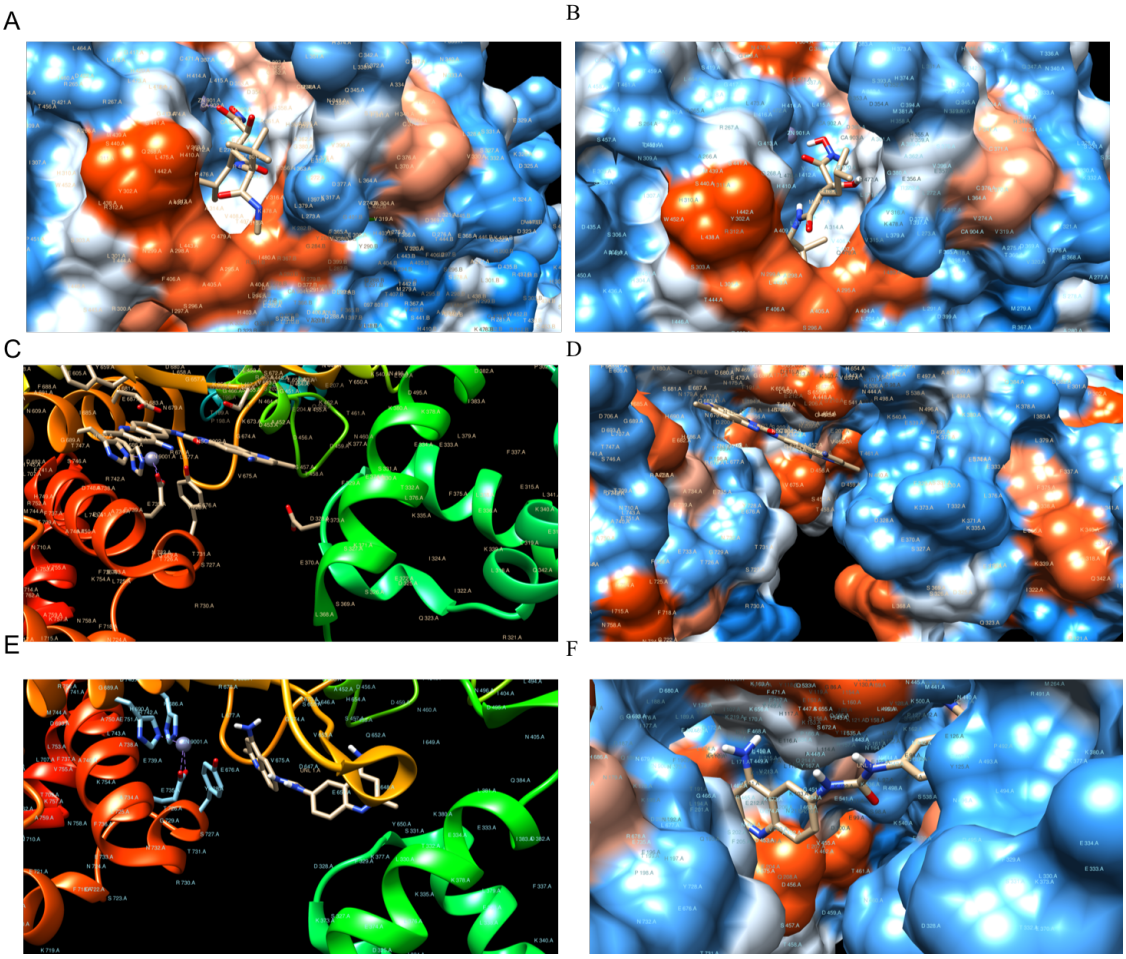

Figure 4.2 – Re-docking of ligands of ADAMTS-5 and anthrax lethal factor using molecular docking. Co-crystal structure 3HY7 of ADAMTS-5 in complex with Marimastat (A). Re-docking of Marimastat with ADAMTS-5 was performed to assess accuracy of molecular docking in predicting target binding compared to known crystal structure (B). Co-crystal structure 1PWP of LAF complexed with Surfen (C+D). Molecular re-docking of Surfen with LAF (E+F). Catalytic Zn^{2+} is depicted in grey.

Molecular docking of ADAMTS-4 and Surfen

Molecular docking of Surfen was performed using the co-crystal structure, 4WK7 (Durham *et al.* 2014), of the halo form of ADAMTS-4 solved bound to the inhibitor 2-(4-chlorophenoxy)-N-{[(4R)-4-methyl-2,5-dioxoimidazolidin-4-yl]methyl} acetamide at a resolution of 1.24 Å (Fig 4.3A). Molecular docking of Surfen with ADAMTS-4 revealed strong binding to the catalytic cleft proximal to Zn^{2+} (Fig 4C+D). A ΔG score of -8.6kcal/mol binding of Surfen in its natural resting state (RMSD=0) would suggest that Surfen could mediate inhibition of ADAMTS-4 via competitive inhibition through binding in the catalytic site (Fig 4.3B). A comparative docking was performed for the known ADAMTS-4/5 inhibitor CAS-929634-33-3 with ADAMTS-4 and surprisingly the top alignment, ΔG=-6.8 kcal/mol(RMSD=0), depicted binding outside of the catalytic cleft. Of 9 predicted binding conformations of CAS-929634-33-3 with ADAMTS-4 only one was within the catalytic cleft (Fig 4.3C), ΔG=-5.6kcal/mol (RMSDi.b =21.955, RMSDu.b =24.077). Such high RMSDs show the requirement of extensive conformational changes of inhibitor in comparison to its assumed resting state structure and therefore not likely to be energetically favourable. This data would suggest that Surfen is potentially a more potent inhibitor of ADAMTS-4 than CAS-929634-33-3.

Molecular Docking of ADAMTS-5 and Surfen

Molecular docking of Surfen was performed using the co-crystal structure, 3HY7 (Tortorella *et al.* 2009), of the halo form of ADAMTS-5 solved bound to the inhibitor Marimastat at a resolution of 1.69 Å (Fig 4.3D). Docking of Surfen revealed a binding site within the catalytic cleft (Fig 4.3E) ΔG=-10kcal/mol (RMSD=0). All 8 alternative binding predictions were within the catalytic cleft with ΔGs ranging from -10 to -8kcal/mol suggesting Surfen could potentially be a potent inhibitor of ADAMTS-5. The known ADAMTS-5 inhibitor CAS-929634-33-3 was shown by molecular docking to preferentially bind to the catalytic cleft, ΔG=-8.3 (Fig 4.3F).

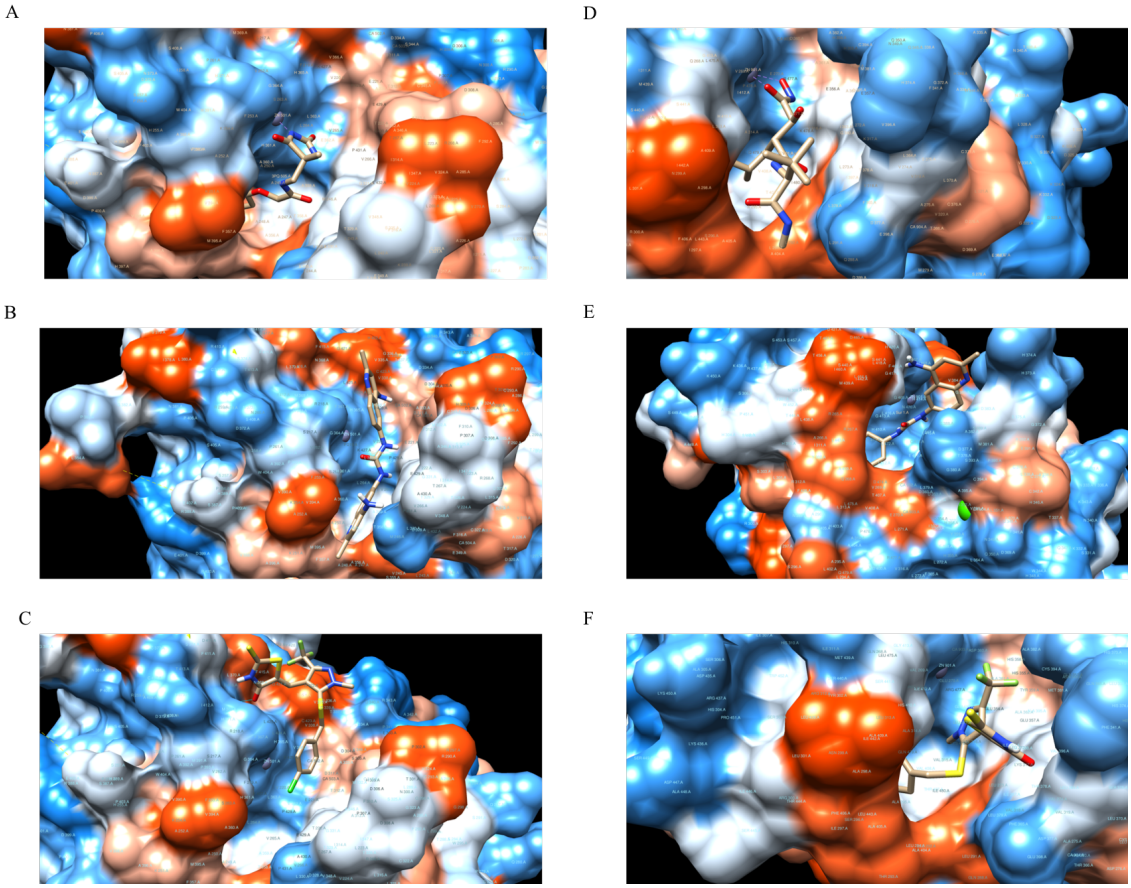

Figure 4.3 – Molecular docking of Surfen with ADAMTS-4 and ADAMTS-5 also a comparative docking of a known inhibitor of ADAMTS-5. Crystal structure of ADAMTS-4 (4WK7) catalytic domain in complex with 2-(4-chlorophenoxy)-N-{[(4R)-4-methyl-2,5-dioxoimidazolidin-4-yl]methyl} acetamide (A), molecular docking of Surfen with ADAMTS-4 catalytic domain (B) and molecular docking of CAS-929634-33-3 with ADAMTS-4 catalytic domain (C). Crystal structure of ADAMTS-5 (3HY7) catalytic domain in complex with Marimastat (D), molecular docking of Surfen with ADAMTS-5 catalytic domain (E) and molecular docking of CAS-929634-33-3 with ADAMTS-5 catalytic domain (F).

MMP-1

It has been shown by Williams *et al.* (2014) that Surfen does not inhibit MMP-1 at concentrations up to and including 100 µM in FRET-peptide assays therefore it was predicted that molecular docking experiments would reveal no or weak binding of Surfen to the catalytic site of MMP-1. Molecular docking using a co-crystal structure of MMP-1 bound to triple-helical collagen peptide, 4AUO (Manka *et al.* 2012), with a resolution of 3 Å revealed a strong potential binding of Surfen to the catalytic cleft of MMP-1 (Fig 4A) ΔG=-8.7 (RMSD=0) (Fig 4A). Binding of Surfen to the catalytic cleft of MMP1 was further confirmed using Apo MMP-1 crystal structure 3SHI (Bertini *et al.* 2012) (Fig 4B). Molecular docking of both Apo and Halo enzyme forms therefore suggests that Surfen could potentially inhibit MMP1 and therefore confirmation is suggested using *in vitro* assays.

MMP-2

Molecular docking of Surfen to MMP-2 was performed using a crystal structure of Apo MMP-2, 1QIB (Dhanaraj *et al.* 1999), at a resolution of 2.8 Å due to the absence of a halo co-crystal structure of MMP-2 bound to a similar inhibitor type. Docking results revealed a potential binding site within the catalytic cleft ΔG= -11.1kcal/mol and RMSD=0 (Fig 4C). Surfen can be seen deep within the catalytic pocket, however, there is minimal interaction with Zn^{2+}. Autodock Vina detected 3 H-bonds between ligand and MMP-2 however an alternative result that had a less favourable ΔG of -10.7kcal/mol showed increased interaction with 5 H-bonds in a location proximal to Zn^{2+} suggesting a strong interaction (Fig 4D). Binding was confirmed to a halo from of MMP-2 bound to decapeptide inhibitor (data not shown) although the size of the inhibitor used may induce conformational changes hence the use of apo-MMP-2 in this instance. Combined, this data suggests that Surfen is potentially a strong inhibitor of MMP-2.

MMP-3

Binding of Surfen to the catalytic cleft of MMP-3 of crystal structure 4G9L (Belviso *et al.* 2013) was predicted with a ΔG -11.0 suggesting strong interactions and therefore Surfen is predicted to inhibit MMP3 in *in vitro* assays (Fig 4E).

MMP-9

Molecular docking of Surfen with crystal structure 4H2E (Antoni *et al.* 2013) of MMP-9 revealed a strong binding conformation (score of -11kcal/mol) with Surfen transcending down and through the S1' subsite with no obvious interactions with the catalytic Zn^{2+} (Fig 4F). Studies by Kridal *et al.* (2001) show positioning of peptide substrates passing along but not down into the S1' pocket as seen with Surfen. This molecular binding data would suggest Surfen may weakly inhibit MMP-9 or not at all dependent upon substrate binding, however, experimental validation is required.

MMP-13

Molecular docking of Surfen was performed using the co-crystal structure of MMP-13 complexed with SC-78080, 3KRY (Becker *et al.* 2010), at resolution 1.9 Å. The predicted binding site was

detected within the catalytic cleft with a score of -8.2, RMSD=0. No interaction between urea group of Surfen and $Zn^{2+}$of MMP13 was observed but the location of predicted binding within the catalytic cleft would suggest Surfen is capable of inhibiting MMP-13 (Fig 4G).

Furin

Moleculqr docking of Surfen with the pro-protein convertase, furin, was performed using crystal structure 6EQV (Dahms *et al.* 2018). The predicted binding site was detected within the catalytic cleft with a score of -8.2, RMSD=0.(Fig 4H) and therefore Surfen is predicted to inhibit furin.

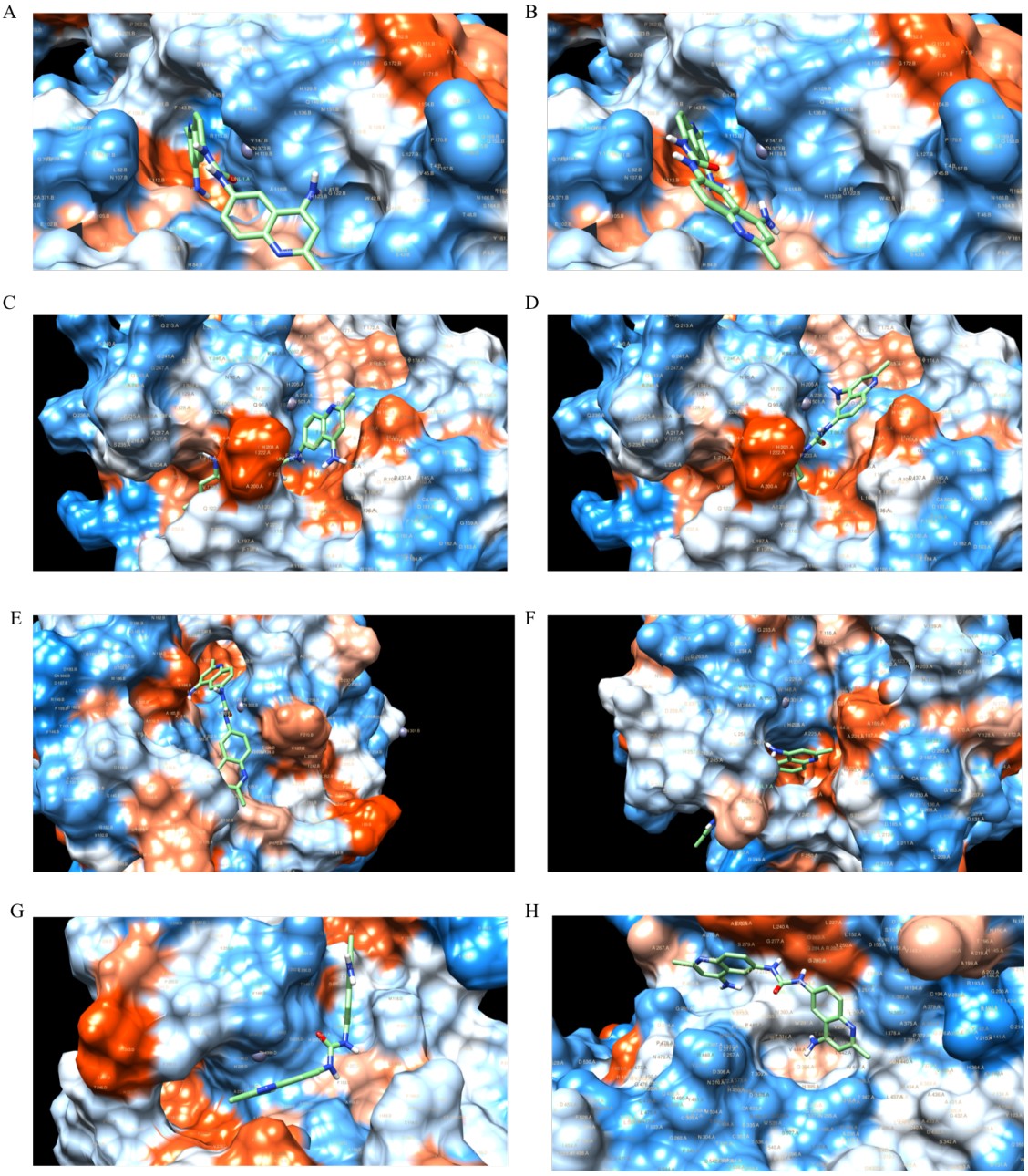

Figure 4.4 – Molecular docking of Surfen with MMP-1, MMP-2, MMP-3, MMP-9, MMP-13 and the pro-protein convertase furin. Crystal halo structure 4AUO of MMP-1 catalytic domain docked with Surfen (A), molecular docking of Surfen with MMP-1 Apo form crystal structure 3SHI catalytic domain (B). Crystal structure 1QIB of apo form MMP-2 catalytic domain docked with Surfen showing 1st (C) and 2nd (D) ranked hits. Crystal structure 4G9L of MMP-3 catalytic domain docked with Surfen (E). Crystal structure 4H2E of MMP-9 catalytic domain docked with Surfen (F). Crystal structure 3KRY of MMP-13 catalytic domain docked with Surfen (G). Crystal structure 6EQV of furin docked with Surfen (H).

4.2.2 *In vitro* inhibition assays

In vitro inhibition of ADAMTS-4 and ADAMTS-5

Initial studies tested the ability of Surfen hydrate to inhibit a recombinant ADAMTS-4 p40 isoform using a commercially available synthetic FRET based peptide substrate, Sensolyte Aggrecanase-1 assay. Cleavage of the peptide substrate results in increased fluorescence, through release of the FRET pair, emitted at 520nm after excitation at 488nm. Surfen possesses intrinsic fluorescent properties which are greatly increased upon binding to GAGs. This property could interfere with FRET assay data interpretation if binding of Surfen to substrates resulted in similar conformational changes and therefore fluorescence emission. Substrate alone plus Surfen and ADAMTS-4 alone plus Surfen confirmed no Surfen mediated fluorescence present in the system. Additionally the use of time-resolved fluorescence assays allows for facile detection of Surfen mediated background fluorescence as initial increases of fluorescence could be detected upon Surfen binding to substrate but this fluorescence would not increase over time. Pre-incubation of recombinant ADAMTS-4 p40 with 15 µM Surfen resulted in a reduction of over 70% in activity compared to enzyme alone suggesting that ADAMTS-4 p40 was inhibited by Surfen (Fig 4.5A). Inhibition of ADAMTS-4 p53 by increasing doses of Surfen or CAS-929634-33-3 was assessed and subsequent dose inhibition curve analysis identified an ADAMTS-4 p53 IC_{50} of 6.15 µM for Surfen hydrate (Fig 4.5B). CAS-929634-33-3 showed a comparable but slightly improved IC_{50} against ADAMTS-4 p53 of 3.48 µM under the same conditions (Fig 4.5C) confirming that molecular docking simulations performed above were not representative of *in vitro* protease inhibitory activity. These studies confirm that Surfen is capable of inhibiting ADAMTS-4 p40 and p53 isoforms.

The ability of Surfen to inhibit recombinant ADAMTS-5 was investigated using a FRET peptide, Abz-TEGEARGSVI-Dap(Dnp)-KK-NH2 (Zhang et al. 2004), derived from the pathological cleavage site within the IGD of aggrecan (Sandy et al. 1992). In the conditions tested Surfen hydrate was incapable of inhibiting ADAMTS-5 activity at all concentrations tested (Fig 4.6A). In comparison, a commercially available inhibitor of ADAMTS-5 (CAS-929634-33-3) was shown to potently inhibit ADAMTS-5 with a IC_{50} of 3.23 µM (Fig 4.6B). To confirm that the lack of inhibition of ADAMTS-5 was not an artefact of an artificial peptide system ADAMTS-5 was pre-incubated with Surfen or commercial inhibitor at increasing concentrations prior to addition of bovine aggrecan derived from A1D1 fraction, reactions were stopped by EDTA followed by deglycosylation using chondroitinase ABC followed by Western blotting for the lyase generated neo-epitope CS-stub using antibody 2B6. Bands showed a clear fragmentation of aggrecan mediated by ADAMTS-5 compared to aggrecan incubated without enzyme. Fragmentation was potently inhibited by the commercial ADAMTS-5 inhibitor (CAS-929634-33-3), whereas Surfen showed no reduction in fragmentation at all concentrations tested (Fig 4.6C). Conversely, an increase of fragment band density, particularly the lowest molecular weight band observed from two independent A1D1 digestion assays showed a concentration dependant increase in band intensity (Fig 4.6D) suggesting Surfen treatment increased ADAMTS-5 activity at a site that resulted in this fragment. Collectively, the inability of Surfen to prevent ADAMTS-5 cleavage of a synthetic substrate and native bovine aggrecan confirms the lack of inhibitory activity

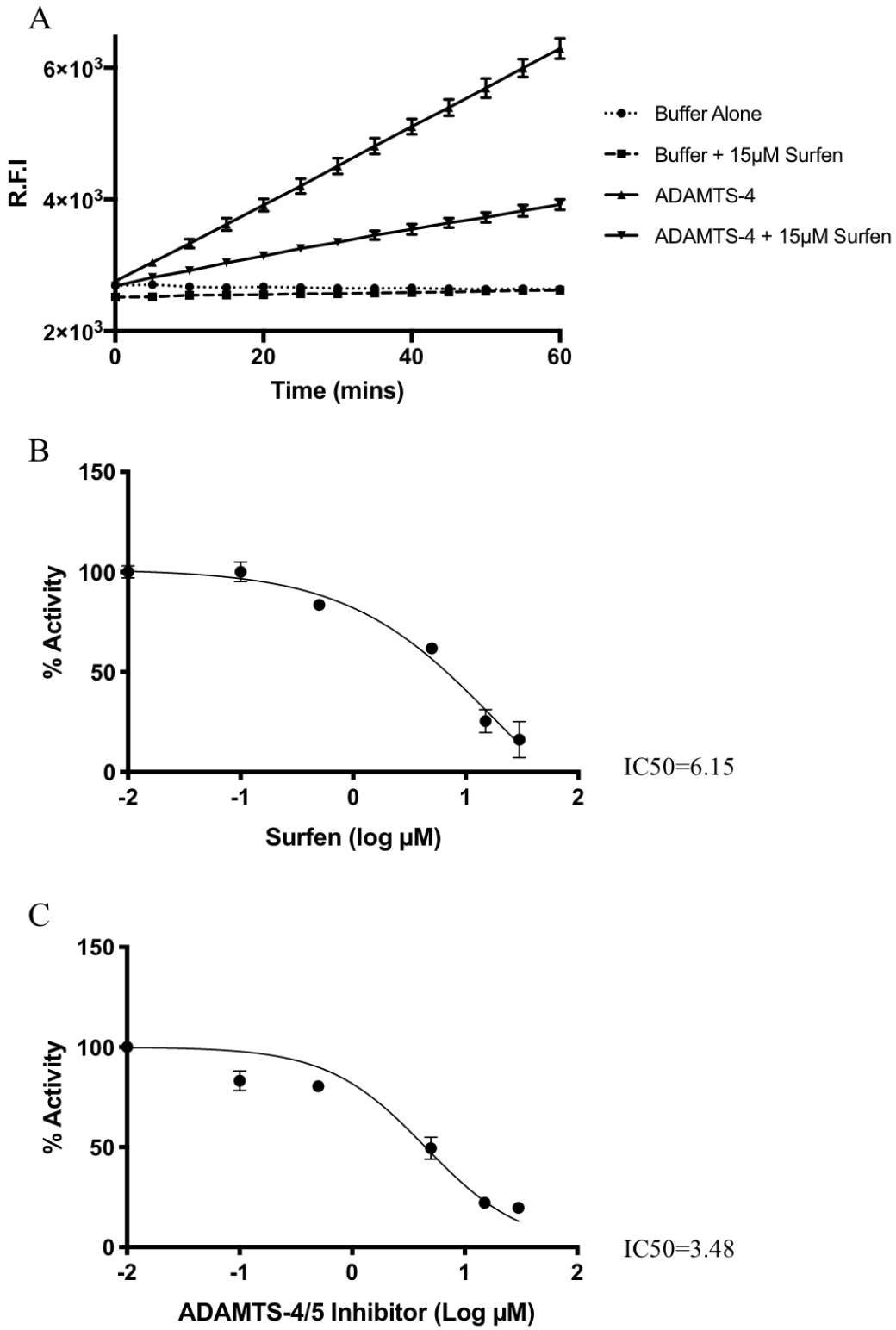

Figure 4.5 – ADAMTS-4 *in vitro* inhibition assays using Surfen and a commercially available ADAMTS-4/5 inhibitor. Sensolyte Aggrecanase-1 assay time course of rADAMTS-4 p40 (1ng/well) in the presence of absence of 15 μM Surfen (A). Dose response curves of rADAMTS-4 p53 incubated with increasing concentrations of Surfen (B) or ADAMTS-4/5 inhibitor CAS-929634-33-3 (C). Mean and *sem* of duplicate wells plotted (n=2, N=1). Measurement of fluorescence was performed at 5 minute intervals (Ex-488nm, Em-520nm). Percent activity was calculated compared to no inhibitor controls and IC_{50} was determined using non-linear regression using GraphPad Prism 7.0 (n=2, N=1).

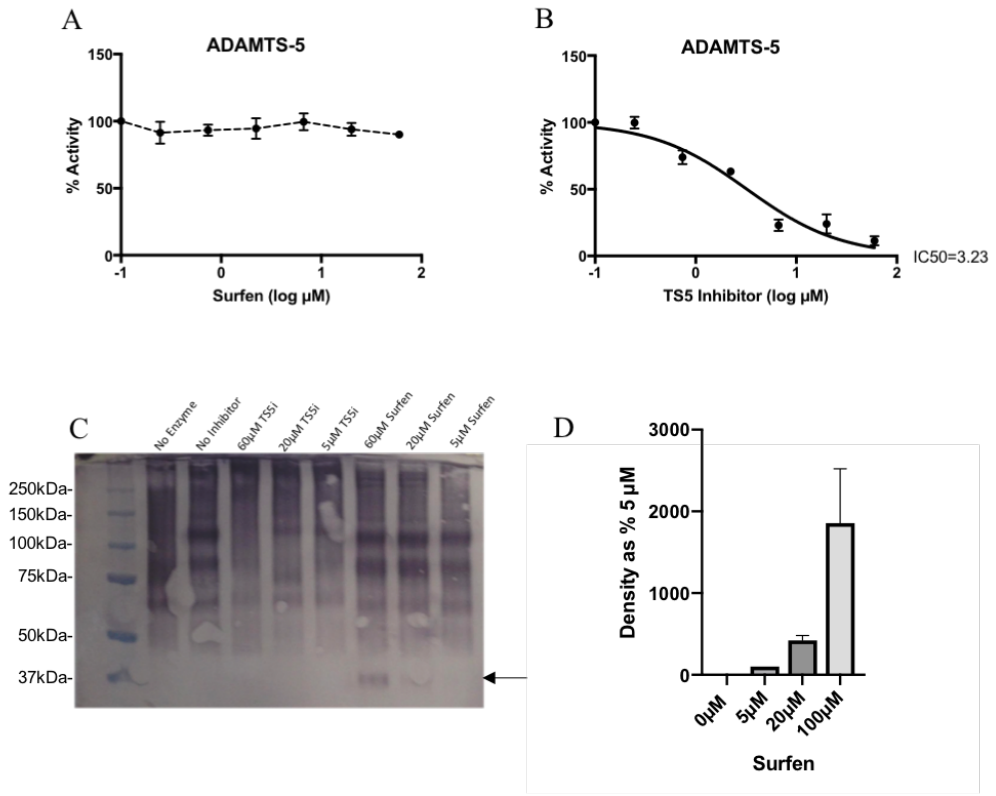

Figure 4.6 – ADAMTS-5 *in vitro* inhibition assays using Surfen and a commercially available ADAMTS-5 inhibitor. ADAMTS-5 (10ng per well) activity assay using WAAG-3R substrate (50µM) in the presence of increasing concentrations of Surfen (A) or ADAMTS-4/5 inhibitor CAS-929634-33-3 Fluorescence was measured every 5 minutes (Ex-340nm, Em-420nm). Percent activity was calculated compared to no inhibitor controls and IC_{50} was determined using non-linear regression using GraphPad Prism 7.0 (n=2, N=1). (B). ADAMTS-5 aggrecan digestion assay visualised by Western blot for the CS4 stub of aggrecan generated by chondroitinase treatment post digestion (C). Densiometric analysis of lowest molecular weight fragment (indicated by arrow) from Western blot (n=3, N=1), mean and *sd* shown (D).

In vitro inhibition of MMPs and Furin

Many inhibitors developed against metalloproteinases, including hydroxamate types, show low specificity for individual metalloproteinases and have a broad activity against multiple MPs. Therefore the effects of Surfen were tested against a panel of OA relevant MMPs selected from molecular docking studies to experimentally confirm targets of Surfen. A Pan MMP cleavable FRET peptide substrate was used to assess Surfen mediated inhibition of recombinant catalytic domains of MMP-1, MMP-2, MMP-3, MMP-9 and MMP-13 (Arafat *et al.* 2014) . Dose inhibition curves revealed that Surfen was capable of inhibiting MMP-2 with an $IC_{50}$of 1.63 µM. Inhibition of MMP-3, MMP-9 and MMP-13 was minimal at the highest concentration of 60 µM Surfen. Surfen mediated a potent dose-dependent increase of MMP-1 activity (Fig 13). Inhibitory activity of Surfen against furin was confirmed using a FRET based peptide substrate assay (Boc-RVRR-AMC) with recombinant furin. Surfen was capable of furin inhibition in this system with dose inhibitory curve analysis showing an IC_{50} of 16.2µM (Fig 13). Summary of Surfen IC_{50}s, substrates and comparisons to molecular docking predictions are shown in Table 4.1.

Table 4.1 – Table summarising molecular docking studies and *in vitro* inhibition assay IC_{50}s and substrates used.

	Molecular Docking			*In Vitro Assays*	
Protease	Score kcal/mol	RMSD	Predicted Inhibition	Substrate	IC50 µM
Furin	-8.2	0	Yes	Boc-RVRR-AMC	16.2
ADAMTS-4	-8.6	0	Yes	Sensolyte 520 Aggrecanase-1	6.15
ADAMTS-5	-10	0	Yes	Abz-TEGEARGSVI-Dap(Dnp)-KK-NH2	>100
MMP1	-8.7	0	Yes	TQ3-GABA-Pro-Cha-Abu-Smc-His-Ala-Dab(6'-TAMRA)-Ala-Lys-NH2	>60
MMP2	-11.1	0	Yes	TQ3-GABA-Pro-Cha-Abu-Smc-His-Ala-Dab(6'-TAMRA)-Ala-Lys-NH2	1.63
MMP3	-11	0	Yes	TQ3-GABA-Pro-Cha-Abu-Smc-His-Ala-Dab(6'-TAMRA)-Ala-Lys-NH2	51.67
MMP9	-10.8	0	No/Weak*	TQ3-GABA-Pro-Cha-Abu-Smc-His-Ala-Dab(6'-TAMRA)-Ala-Lys-NH2	>60
MMP13	-8.2	0	Yes	TQ3-GABA-Pro-Cha-Abu-Smc-His-Ala-Dab(6'-TAMRA)-Ala-Lys-NH2	125.9

** Predicted binding site was not directly within catalytic cleft*

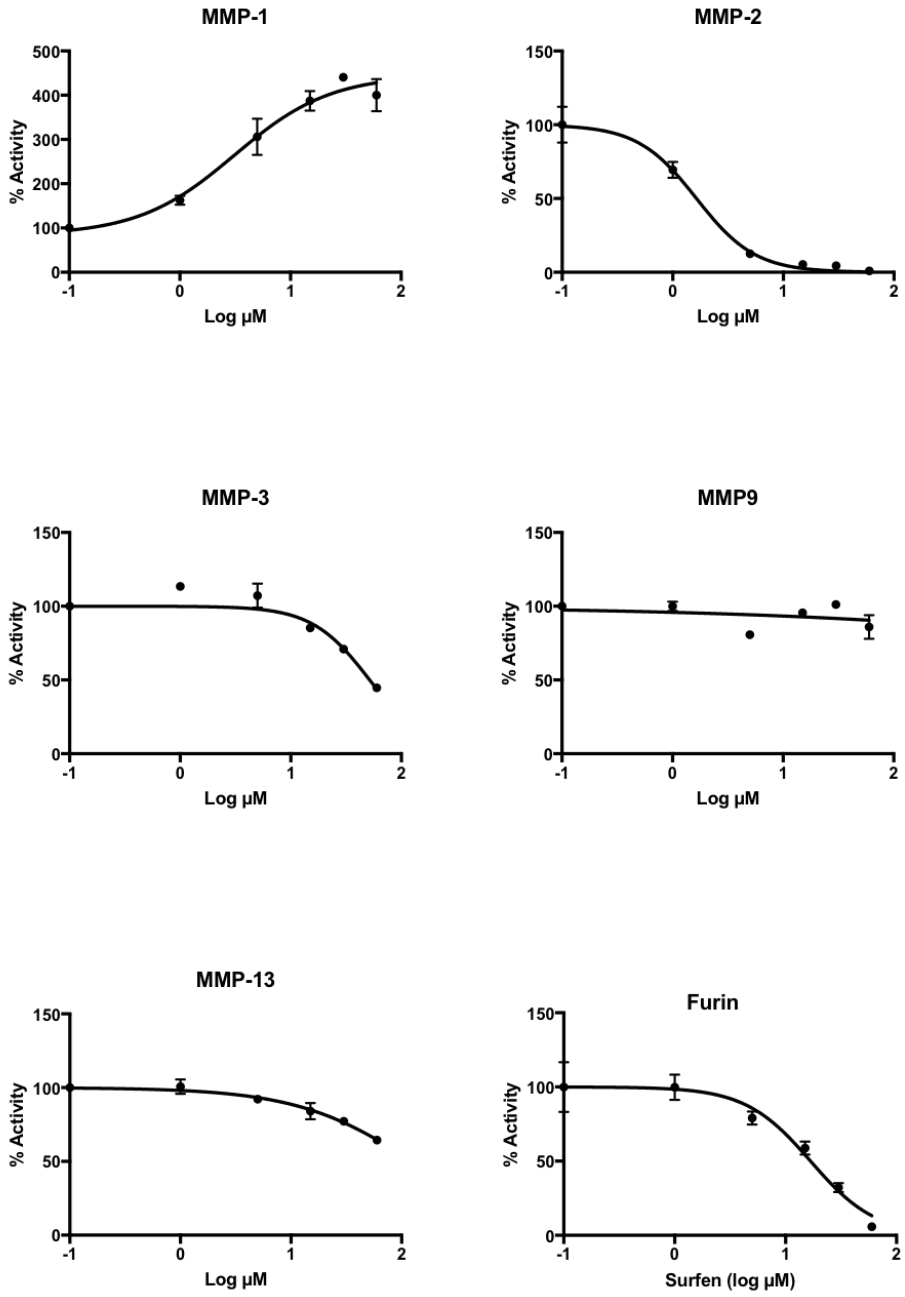

Figure 4.7 – Surfen *in vitro* inhibition assays MMP-1, MMP-2, MMP-3, MMP-9, MMP-13 and furin. *In vitro* MMP inhibition assays using recombinant catalytic domains (concentrations of MMPs shown in table 2.5) and Omni-MMP substrate (0.75 µM). Fluorescence was measured every 5 minutes (Ex.540nm, Em.590nm) using a Fluorostar Optima (BMG-Labtech). Furin inhibition assay using recombinant furin (1U) and substrate Boc-RVRR-AMC (50µM) Fluorescence was measured every 5 minutes (Ex-360nm, Em-440nm). Concentration range of Surfen tested was 0-60 µM. Mean and *sem* of duplicate wells plotted (n=2, N=1). Percent activity was calculated compared to no inhibitor controls and IC_{50} was determined using non-linear regression using GraphPad Prism 7.0

4.3 Discussion

Molecular docking is often used as a tool for virtual pre-screening of compound libraries prior to HTS activity assays. Autodock Vina is one of the most highly cited programs used within molecular docking due to its reported accuracy and its free for academic use format. The validation of molecular docking via the re-docking of Marimastat to ADAMTS-5 and re-docking of Surfen to LAF was successful in predicted binding of inhibitor to the same location as the original crystal structure bound inhibitor, although the conformation of the ligands showed some differences. It must be noted that the crystal structure of complexed inhibitor may not represent the ideal theoretical binding conformation and this may result in the differences observed. It has been shown that molecular docking is often reliable in successfully redocking ligands into the original experimental crystal structures with a 90% success rate demonstrated for Autodock Vina and SwissDock within top 6 results returned (Castro-Alvarez *et al.* 2017). The use of Halo enzyme co-crystal structures was selected where possible due to the conformational change observed in ADAMTS-4 Apo form which resulted in obscuration of the active site. Additionally, where rigid body docking simulations are used, as is the default case for Autodock Vina, then substrate bound structures of enzyme are preferred and likely to be more accurate in predicting ligand binding. The work within this section highlights limitations of this technique. Molecular docking returned multiple poses of Surfen in the catalytic cleft of ADAMTS-5, MMP-1, MMP-3 and MMP-13 which are assumed to be false positives due to lack of significant inhibition mediated by Surfen using *in vitro* activity assays. Docking of ADAMTS-5 with Surfen returned a pose with a very strong predicted binding (ΔG=-10) whereas *in vitro* activity assays showed no inhibitory effect of Surfen at any concentration tested using either synthetic FRET based substrates or native aggrecan. False positive results generated by molecular docking are a well-known limitation of this technique, Ferreira *et al.* (2010) compared molecular docking and HTS activity assays using a library of 197861 compounds against a thiol protease, cruzain, this study revealed 97.5% of molecular docking hits were false positives (Ferreira *et al.* 2010). Attempts to reduce false positive binding conformations included the use of blind docking where predicted binding sites are calculated for the entire PDB protein structure rather than just the known catalytic cleft, however, this did not reduce the occurrence of false positives within the catalytic cleft which confirms that observed in this Chapter. Blind docking more closely reflects *in vitro* activity assays in which Surfen was incubated with the entire catalytic domain in the case of MMPs or entire proteins in the case of ADAMTS-4 and 5. In this system Surfen could potentially bind multiple allosteric sites and therefore molecular docking data predicting strong binding to MPs outside of the catalytic site may indicate low inhibitory capacity despite high binding affinity ΔG. Although allosteric inhibition of enzymes is possible the determination of Surfen's potential to inhibit an MP in this chapter was made solely upon binding to the catalytic cleft in a competitive inhibition mechanism. Surfen was shown to inhibit ADAMTS-4 with an IC_{50} of 6.15 µM whereas no inhibition was observed for ADAMTS-5 at any concentration tested, indeed aggrecan degradation studies suggested that Surfen increased the activity of ADAMTS-5. It has been shown that ADAMTS-5 has the ability to form oligomers and oligomeric forms of ADAMTS-5 show an increased rate of aggrecan cleavage (Kosasi *et al.* 2016). Interestingly, ADAMTS-5 is N-glycosylated at two sites whereas ADAMTS-4 is not glycosylated (Kelwick *et al.* 2015). A potential mechanism of Surfen mediated increases in ADAMTS-5 cleavage of aggrecan

could be the formation of oligomers via interactions with these glycosylations, enabled by Surfens ability to bind sulphated GAG chains. Attempts to detect oligomerisation using dynamic light scattering were unsuccessful due to the high protein concentrations required for detection and therefore further work is required to elucidate this mechanism. Alternatively, Surfen may increase ADAMTS-5 mediated cleavage by stabilisation of aggrecan through interactions with CS and KS GAG chains and thereby increase activity of ADAMTS-5, the lack of increased activity in synthetic peptide assays compared to glycosylated aggrecan would suggest this is a possible mechanism, attempts to confirm by pre-treatment of aggrecan with chondroitinase ABC and keratanase I prior to digestion were unsuccessful as BC-3 neo-epitope was not detected by Western blot presumably due to the reduced cleavage of de-glycosylated aggrecan by ADAMTS-5. Studies using a commercial inhibitor of ADAMTS-5 and ADAMTS-4 showed almost equal IC_{50} for both ADAMTS-4 and ADAMTS-5, IC_{50}=3.48 and 3.23 µM, respectively, although this inhibitor has been shown to have a 40 fold increased effectivity compared to ADAMTS-4 (Gilbert *et al.* 2007). The differences observed in this Chapter are potentially due to differences in substrate, enzyme concentration and isoform used. The use of WAAG-3R in place of the Sensolyte 520 aggrecanase-1 peptide substrate for ADAMTS-4 studies may have shown an increased IC_{50} of ADAMTS-4 compared to ADAMTS-5. ADAMTS-5 is incapable of degrading the Sensolyte 520 aggrecanase-1 peptide substrate so this comparison could not be made. The choice to use the Sensolyte substrate was based upon a greater efficiency of cleavage by ADAMTS-4 compared to WAAG-3R substrate and therefore potentially a more robust system for the assessment of inhibitors of ADAMTS-4.

The effects of Surfen on MMPs tested were variable with very low levels of inhibition observed for MMP-3, MMP-9 and MMP-13 at 60µM suggesting that at Surfen concentrations commonly used in the literature there would be very little effect on MMP-3, MMP-9 or MMP-13 activity in *ex vivo* cartilage explant models of OA and likely collagen degradation directly by these MMPs would not be prevented in this system.

Surfen inhibited ADAMTS-4 but not ADAMTS-5 despite structural similarities between these two enzymes. It has been shown, however, by crystal structures of both ADAMTS-4 and ADAMTS-5 that the S1' binding pocket of ADAMTS-4 is larger than that of ADAMTS-5 and therefore this may account for the inability of the "bulky" aromatic rings of Surfen to inhibit ADAMTS-5. Overlaying the crystal structures of ADAMTS-4 and ADAMTS-5 shows a restricted active site in ADAMTS-5 compared to ADAMTS-4 mediated by a bulky overhang (Fig 4.8A+B).

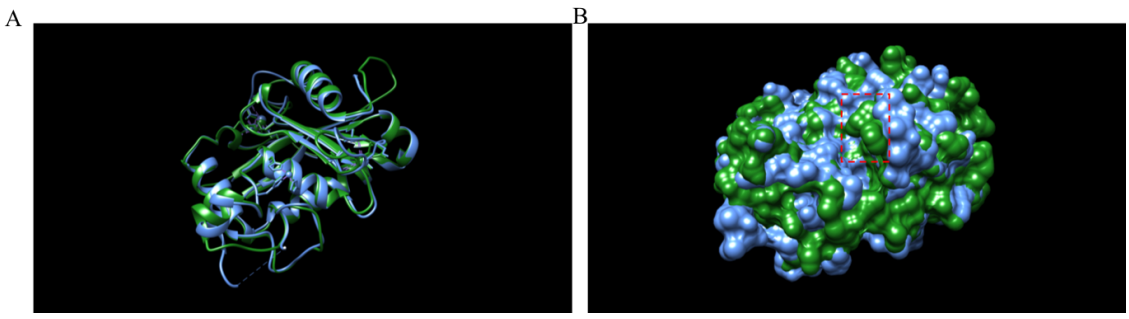

Figure 4.8 – Depiction of structural overlays of ADAMTS-4 and ADAMTS-5. Overlay of ADAMTS-4 in blue and ADAMTS-5 in green shown as a ribbon (A) and surface structure (B) depicting the restricted active site as a result of the overhang (boxed in red) in ADAMTS-5 compared to ADAMTS-4. Overlay and images generated using Chimera.

Conversely, the S1' pockets of MMP2 and MMP9 are very similar in size, sequence and structure so the specificity observed for MMP2 over MMP9 by Surfen is surprising. The presence of Thr^{426} in MMP2 and Arg^{424} in MMP-9 provides some differences to S1' subsites and it has been shown that Arg^{424} of MMP9 may sterically block longer, bulkier P1' interactions of inhibitors that are otherwise capable of inhibiting MMP2.

The lack of an inhibitory effect of Surfen on MMP-1 activity confirmed that shown by Williams *et al.* (2014).[1]The observed increase in MMP-1 activity mediated by Surfen in a concentration dependent manner was surprising. The MMP-1 source for this assay was a recombinant catalytic domain produced in *E. coli* and although MMP-1 can be glycosylated in certain circumstances this construct was not glycosylated and therefore increased activity was not a results of oligomerisation mediated by Surfen/GAG interactions as described as a potential mechanism, for ADAMTS-5 increased activity above. Multiple HTS assays for enzyme inhibitors have identified small molecule allosteric activators of several enzymes, the most studied of which is SIRT1 activation by resveratrol (Borra *et al.* 2005). However, *in vitro* cleavage assays must be interpreted with caution in respect to activators as many small molecule activators have been shown to act non-specifically as surfactants to increase enzyme activity (Thorne *et al.* 2010). The addition of surfactants was shown to abrogate the effects of 7 small molecule activators tested against 8 enzymes. Importantly, the assay buffer used for MMP-1 and ADAMTS-5 activity assays contained surfactants (chaps) and therefore the increased activity observed is not the result of a surfactant-like effect mediated by Surfen. Additionally, this effect is likely specific as no increases in activity were observed for other proteases in this Chapter. This suggests that Surfen does indeed increase the activity of the catalytic domain of MMP1 against a synthetic substrate but further work is required to test if Surfen mediates similar effects on full length MMP1 upon its native substrate.

It was shown that Surfen is capable of inhibiting furin showing an IC_{50} of 16.2 µM. Pro-protein convertase inhibition has been shown by others to be protective in cartilage explant models of OA for example in bovine nasal cartilage explants cultured in the presence of IL-1α+OSM, a peptide based inhibitor of pro-protein convertases including furin and PACE4 significantly reduced GAG loss to media from explants compared to non-treated controls presumably via reducing the amount of active ADAMTS-4 and 5 (Milner *et al.* 2003). The inability of Surfen to inhibit ADAMTS-5 does not preclude its further testing as a potential inhibitor of GAG loss in OA models as a role for both ADAMTS-4 and ADAMTS-5 has been demonstrated in human cartilage (Song *et al.* 2007), however, this data may indicate a lack of effectivity in murine models of OA, where ADAMTS-5 has been shown to be the predominant mediator of GAG loss from cartilage. In conclusion, Surfen hydrate inhibits ADAMTS-4, MMP-2 and furin with IC_{50}values well within the concentration ranges commonly used in the literature for both *in vitro* and *in vivo* studies and therefore Surfen will be tested in cartilage explant model as developed in Chapter 3.

4.4 Summary

The work in this Chapter has;

[1]There is slight confusion as to whether Surfen did inhibit MMP-1 in the studies by Williams *et al.* (2014), Table one states Surfen mediated inhibition with an IC50 of 30µM whereas all other references to Surfen and MMP1 in this paper state IC50>100µM. Therefore it was assumed no inhibition was present.

1. Identified Surfen as a potential inhibitor of multiple OA relevant MPs using molecular docking, however, the limitations of molecular docking are evident as *in vitro* validation confirmed that Surfen only mediated significant inhibition of ADAMTS-4, MMP-2 and furin at concentrations of Surfen observed in the literature in cell based assays.

Chapter 5

Assessment of Surfen in Cartilage Explant Models of OA

5.1 Introduction

In Chapter 3 the use of IL-1α alone and in combination with OSM resulted in increased expression of aggrecanases, increased GAG loss and increased COMP degradation compared to controls mirroring the processes that lead to cartilage degradation in early stage OA. The inhibition of SAPK/JNK led to an almost complete reduction in ADAMTS-5 expression in IL-1α+OSM cells however ADAMTS-4 was only partially inhibited. The incomplete inhibition of aggrecan cleavage in explants treated with IL-1α+OSM where SAPK/JNK was inhibited suggested that residual aggrecanase activity was due to ADAMTS-4 and therefore that ADAMTS-4 contributes substantially to aggrecan degradation in this cytokine induced model of OA. The ability of Surfen to inhibit ADAMTS-4 activity in *in vitro* peptide cleavage assays suggests that Surfen may inhibit ADAMTS-4 mediated aggrecan degradation in cartilage explant models of OA. Additionally, the observed inhibition of furin by Surfen may indirectly reduce cartilage degradation through reduced pro-protein convertase mediated activation of aggrecanases (Wang *et al.* 2004) in combination with Surfen's predicted activation of BMP signalling may result in a net anabolic state and thereby be cartilage protective. Therefore this Chapter will investigate the effects of Surfen upon cytokine induced cartilage matrix macromolecule degradation in bovine cartilage explant cultures.

5.1.1 Aim and Objectives

Aims

The aim of this Chapter is to determine the effects of Surfen upon cartilage matrix degradation in cytokine stimulated bovine cartilage explants to identify potential therapeutic effects.

Objectives

These Aims will be investigated though completion of the following Objectives;

1. Determine the safe upper dose limit of Surfen by assessment of cytotoxic effects in chondrocyte monolayers and cartilage explants prior to explant studies.

2. Determine the therapeutic potential of Surfen by assessing GAG loss, aggrecanase activity and COMP degradation in IL-1α, OSM and IL-1α+OSM stimulated bovine cartilage explants.

5.2 Results

5.2.1 Surfen toxicity assays

Initial studies were performed to determine the effects of Surfen on the viability of cartilage explants and chondrocytes in monolayer to determine a range of concentrations for subsequent experiments that would not affect cell viability. MTT assay analysis, measuring cellular metabolism as an indicator of viability, of bovine primary chondrocytes cultured in monolayer in the presence of increasing concentrations of Surfen for 24 hours showed no negative effects on cell viability at concentrations up to and including 30 μM. A decrease in viability was seen at 60 μM Surfen ($p<0.01$) but there was no difference in the viability of these cells and those receiving the same concentration of DMSO as a carrier control therefore it is unclear whether Surfen in the absence of DMSO would be cytotoxic at 60 μM concentration (Fig 5.1A). LDH release assay analysis of 2mm diameter bovine cartilage explants cultured in the presence of Surfen at the indicated doses for 3 days showed no increased release of LDH to the media in Surfen treated explants at all doses tested (Fig 5.1B). Although a toxic dose was not determined in cartilage explants all subsequent cartilage explant experiments were performed at levels under 60 μM to reduce the amount of DMSO added to cultures. No toxicity was observed at 3 days, however, the effects of Surfen on long term culture were not assessed and require investigation.

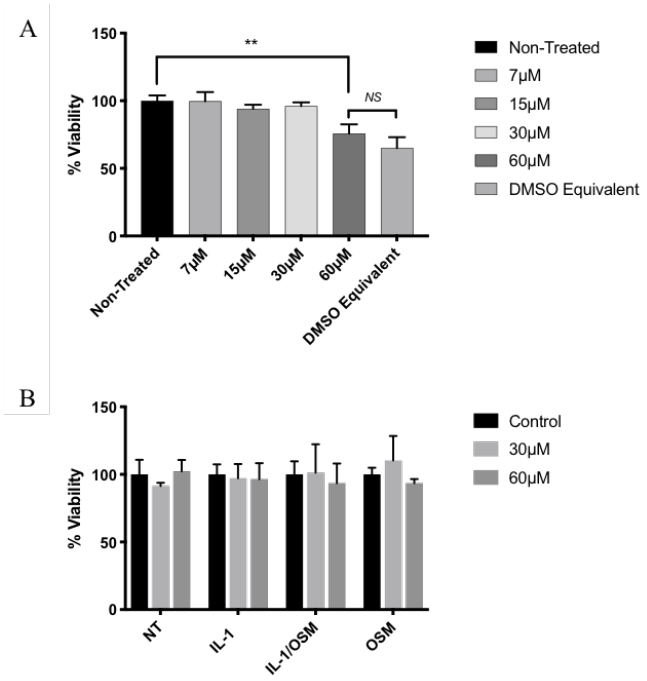

Figure 5.1 – Assessment of Surfen mediated toxicity in bovine primary chondrocytes and cartilage explants. MTT assay analysis of bovine primary chondrocytes incubated for 24 hours with the indicated doses of Surfen or DMSO alone added at the same concentration as that present in 60 μM Surfen dose (A). LDH release assay of bovine cartilage explants cultured in control media (NT), IL-1α (10ng/ml), OSM (50ng/ml) or IL-1α+OSM in the presence of Surfen at the indicated doses for 3 days (B). Mean and *sd* of triplicates shown (n=3, N=1). Statistical significance was determined by ANOVA with Tukey's post-hoc test for multiple comparisons using GraphPad Prism 7.0 (**p<0.01).

5.2.2 Effect of Surfen on cytokine induced cartilage degradation in bovine cartilage explants

Surfen inhibits GAG loss from IL-1α but not IL-1α+OSM stimulated cartilage explants

Bovine cartilage explants were cultured in the indicated cytokines in the presence or absence of 15 μM Surfen for three weeks with treatments and media refreshed weekly (Fig5.2). DMMB analysis at week 1 showed a significant reduction in GAG loss in IL-1α treated explants in the presence of 15 μM Surfen ($p<0.05$), no reduction in GAG loss were observed in IL-1α+OSM treated explants (Fig 5.2A). In weeks 2 and 3 no significant differences in GAG loss to the media were observed in explants cultured in the presence of Surfen compared to those not receiving Surfen treatment in all cytokine conditions (Fig 5.2B+C).

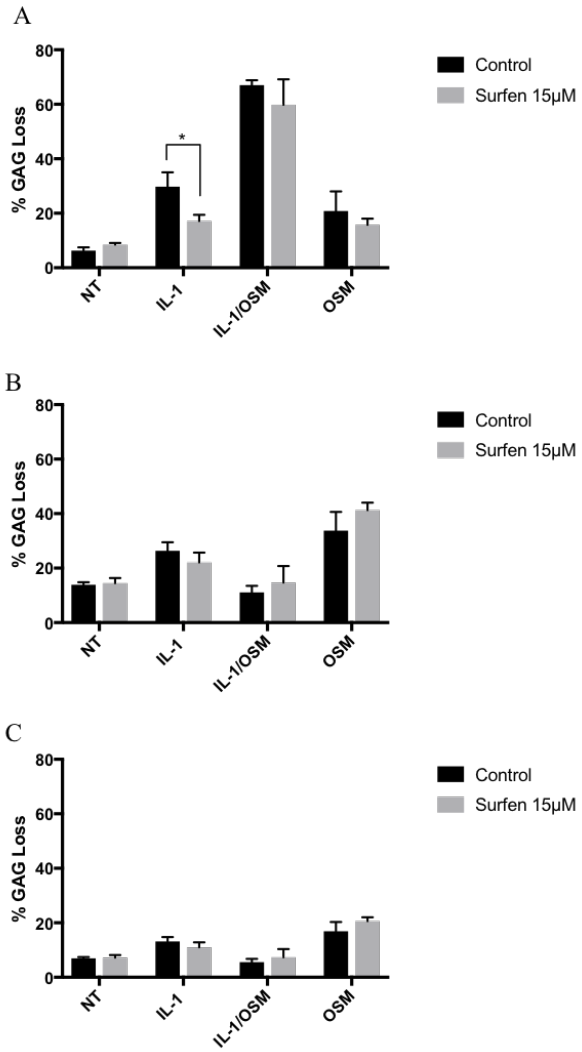

Figure 5.2 – Assessment of Surfen treatment upon GAG loss in cytokine treated bovine cartilage explants over 3 weeks. Assessment of GAG loss by DMMB analysis from cartilage explants (4mm) cultured in the presence or absence of 15 μM Surfen in control media (NT), IL-1α (10ng/ml), OSM (50ng/ml) or IL-1α+OSM at week 1 (A), week 2 (B) and week 3 (C). Mean and *sd* of three experiments. Statistical significance determined by ANOVA with Tukey's post-hoc test for multiple comparisons performed using GraphPad Prism software (* $p<0.05$).

Surfen decreases -ARGSVIL aggrecanase generated aggrecan neo-epitope release from IL-1α treated explants at week 1 and 2 of culture but increases aggrecanase activity in IL-1α+OSM treated explants

Media samples were processed and analysed by Western blot for the BC-3 positive neo-epitope generated by aggrecanase cleavage of aggrecan at site $E^{373\_374}A$ resulting in the release of GAG bearing the -ARGSVIL neo-epitope at the N-terminal. Equal loading of 20μg GAG equivalent per lane allows for equal comparison of the proportion of -ARGSVIL neo-epitope per μg GAG released to media amongst cytokine treatment groups and is independent of amount of GAG released to media. Week one media samples showed no aggrecanase activity in non-treated and OSM treated explants (Fig 5.3A). Positive staining was observed for IL-1α treated explants with an increased density observed for IL-1α+OSM treated explants that was sufficiently high to saturate the signal. (Fig 5.3A). The addition of Surfen to cartilage cultures showed an apparent reduction in aggrecanase activity in IL-1α treated explants compared to those cultured in the absence of Surfen, whereas, a marked increase was observed on the density of staining in Surfen treated explants cultured in the presence of IL-1α+OSM suggesting Surfen mediated an increase in aggrecan cleavage at the pathological IGD site (Fig 5.3A). Analysis of week 2 media samples showed positive staining for IL-1α, IL-1α+OSM and OSM treated explants with no clear differences in staining intensity observed between non-treated control and Surfen treated explants (Fig 5.3B). In week 3 media samples positive staining was seen in non-treated control samples in addition to IL-1α, IL-1α+OSM and OSM (Fig 5.3C).A reduced intensity of positive staining was observed in IL-1α+OSM treated explants compared to IL-1α or OSM despite equal GAG loading. Surfen treatment at three weeks increased the band intensity compared to control explants with clear increases in staining observed in IL-1α, IL1α+OSM and OSM treated cultures. These increases were most prominent for the lower molecular weight fragment at circa 70 kDa in IL-1α and OSM treated explants, whereas for IL-1α+OSM treated explants increases were observed in both higher and lower molecular weight bands compared to control explants (Fig 5.3C). This would suggest that a higher proportion of aggrecan released to media in Surfen treated explants at these time points contain the -ARGSVIL neo-epitope which suggests Surfen treatment increases aggrecanase activity at the IGD in these conditions although it must be noted that this data was derived from a single Western blot of triplicate wells with normalised loading of GAG it is semi-quantitative at best and increased aggrecanase activity did not result in significant increases in total GAG loss as assessed by DMMB (Fig 4.2). A repeat of this assay using infrared (IR) secondary antibodies may provide a more quantitative analysis due to the extended dynamic range of IR compared to colourmetric Western blot techniques.

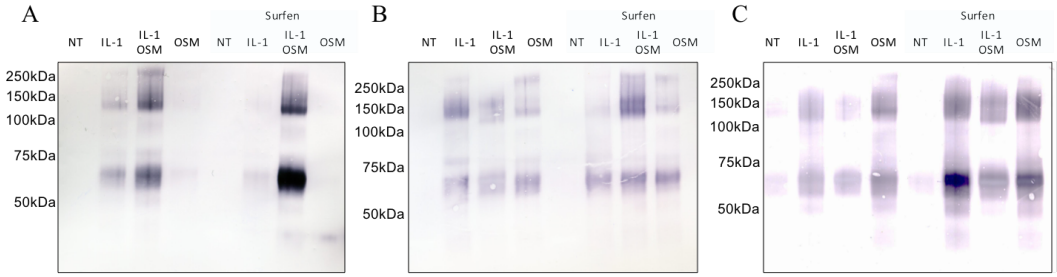

Figure 5.3 – Assessment of Surfen effects on aggrecanase activity at the IGD site of aggrecan in cytokine stimulated bovine cartilage explants over 3 week culture period. Western blot analysis for the BC-3 neo-epitope generated by aggrecanase cleavage of aggrecan within the IGD at site E374_374A from 4mm bovine explants cultured for 1 week (A), 2 weeks (B) or 3 weeks (C) in the presence or absence of 15 µM Surfen in control media (NT), IL-1α (10ng/ml), OSM (50ng/ml) or IL-1α+OSM. 20µg GAG equivalent loaded per lane derived from pooled triplicate wells (n=3, N=1).

Increasing Surfen dose whilst reducing explant size results in increased inhibition of GAG loss in IL-1α but not IL-1α+OSM treated explants

Experiments were repeated using 2mm cartilage explants, which due to a smaller size possess a reduced GAG content that may result in reduced Surfen sequestration by GAG and thereby increasing the effective concentration whilst keeping Surfen concentrations well below toxic levels. Cartilage explants were cultured in control media or media containing IL-1α or IL-1α+OSM for 5 days in the presence or absence of Surfen at the indicated concentrations. DMMB assay analysis showed a significant concentration dependent reduction in IL-1α induced GAG loss when treated with 7 ($p<0.05$) and 15 µM ($p<0.01$) Surfen, however, Surfen showed only a slight and non-significant reduction in GAG loss from IL-1α+OSM treated explants at either concentration (Fig 5.4A).

Inhibition of both ADAMTS-4 and ADAMTS-5 results in significant reduction in GAG loss in both IL-1α and IL-1α+OSM treated explants

A commercially available inhibitor (CAS 929634-33-3), which has a 40 fold increased activity against ADAMTS-5 over ADAMTS-4, was added to cartilage cultures at a concentration of 5µM. The use of CAS 929634-33-3 at a concentration 3 times lower than the highest Surfen concentration despite similar IC_{50} values for ADAMTS-4 was to aid in the determination between the contribution of ADAMTS-5 and ADAMTS-4 to GAG loss as the inhibition of ADAMTS-4 should be reduced compared to that mediated by Surfen at 15 µM. CAS 929634-33-3 showed a significant reduction in IL-1α mediated GAG loss ($p<0.05$) but also significantly reduced IL-1α+OSM ($p<0.01$) induced GAG loss (Fig 5.4B). This data would suggest that ADAMT-5 is the major aggrecanse in IL-1α+OSM treated explants in this system, although this is not possible to confirm as CAS 929634-33-3 is also capable of inhibiting ADAMTS-4. The effective concentration and bioavailability of both inhibitors within cartilage is unknown and likely compounded by chemical stability of the inhibitors in addition to Surfen binding to GAGs. BC-3 Western blot would be required to determine if GAG loss reductions observed are specific to aggrecanase activity at the IGD site of aggrecan or cleavage by other proteases are inhibited by Surfen or CAS 929634-33-3.

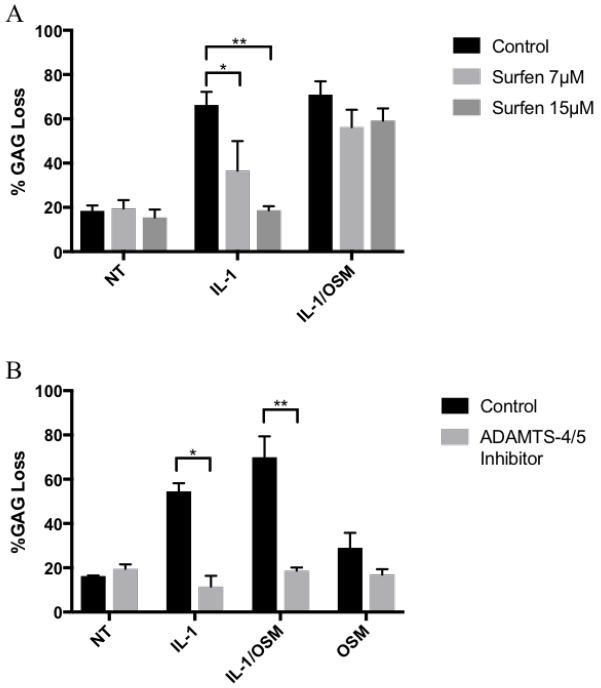

Figure 5.4 – Comparison of GAG loss inhibition mediated by Surfen and a commercial ADAMTS-4/5 inhibitor in cytokine stimulated bovine cartilage explants. GAG loss assessed by DMMB assay from 2mm cartilage explants incubated for 5 days with control media (NT), IL-1α (10ng/ml), OSM (50ng/ml) or IL-1α+OSM and 0, 7 or 15 μM Surfen (A). GAG loss assessed by DMMB assay from cartilage explants incubated for 5 days with control media (NT), IL-1α (10ng/ml), OSM (50ng/ml) or IL-1α+OSM and 0 or 5 μM ADAMTS-4/5 inhibitor CAS 929634-33-3 (B). Mean and *sd* of three experiments shown. Statistical significance determined by ANOVA with Tukey's post-hoc test for multiple comparisons performed using GraphPad Prism software. * $p<0.05$, ** $p<0.01$.

Surfen binds sulphated GAGs *in vitro* and in cartilage explants and therefore likely affects Surfen bioavailability in explants

It has been reported that Sufen binds avidly to sulphated GAGs and that this property likely affects the bioavailability of Surfen, therefore the GAG binding properties of Surfen were investigated to elucidate which cartilage matrix macromolecules Surfen preferentially binds and to investigate methods to reduce or negate this binding in cartilage explant systems to aid in determination of the cartilage protective mechanism of Surfen in IL-1α treated explants. Assessment of the fluorescence spectrum of Surfen showed a much increased emission at 488nm when bound to CS versus unbound Surfen (Fig 5.5A). An excitation sweep was performed with a fixed emission at 488nm. Excitation maximum peaks were observed at 260nm and 360nm (Fig 5.5A) with excitation at 260nm being most efficient but 360nm being most commonly used in the literature due to availability of suitable filter sets on commercially available plate readers and fluorescent microscopes.

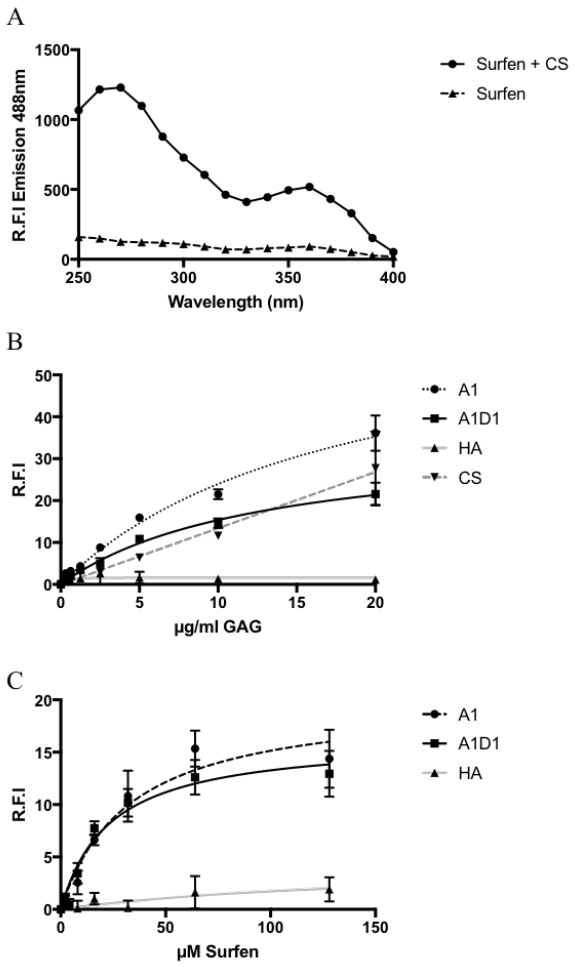

Figure 5.5 – *In vitro* Surfen GAG binding assays. Excitation sweep with fixed emission of 488nm of Surfen in the presence or absence of CS (A). Fluorescent analysis of Surfen (60 µM) binding to increasing concentrations of aggrecan aggregate (A1), aggrecan (A1D1), hyaluronic acid (HA) or chondroitin sulphate (CS) (B). Fluorescent analysis (Ex-360nm, Em-488nm) of increasing concentrations of Surfen binding to fixed equal concentrations (20µg/ml) of GAG A1, A1D1 or HA (C). Mean and *sd* of three technical replicates shown (n=3, N=1).

Fluorescent binding assays using increasing concentrations of GAGs with a fixed concentration of

60 µM Surfen (Ex360nm/Em488nm) showed Surfen binding to aggrecan aggregate (A1), aggrecan (A1D1) and CS but not HA (Fig 5.5B). Studies repeated using a fixed concentration of GAGs (20µg/ml) and increasing concentrations of Surfen confirmed binding of Surfen to A1 and A1D1 but not HA (Fig 5.5C).

Surfen binds to heparin with increased avidity compared to CS and increasing concentration of protamine were shown to compete with Surfen binding to heparin and aggrecan

Work of Weiss *et al.* (2015) showed that Surfen had a higher affinity to heparin and HS than CS, the predominant GAG present on aggrecan, therefore the binding of Surfen to A1D1 was compared to heparin as a substitute for HS. Surfen binding to heparin resulted in an almost 4 fold increase in fluorescence emission compared to A1D1 (R.F.I=424.6 and 112.8 respectively) (Fig 5.6A).
Protamine, a positively charged peptide that binds sulphated GAGs, was added in increasing concentrations to heparin or A1D1 in the presence of a fixed concentration of Surfen. It was shown that addition of protamine reduces Surfen mediated fluorescence suggesting displacement and competition for binding with Surfen for A1D1 and heparin by protamine (Fig 5.6B). Combined, this data suggests that Surfen is capable of binding aggrecan aggregate, aggrecan, CS and HS and therefore it is likely that Surfen added to explant cultures will bind endogenous GAGs and thereby the effective concentration of Surfen available in cartilage will be greatly reduced. The addition of protamine to cartilage cultures may reduce the GAGs interaction of Surfen and improve bioavailability.

Surfen binding to CS does not interfere with DMMB assay quantification at concentrations used in culture

The binding of Surfen to CS may interfere with the assessment of GAG release via DMMB assay. To test this effect CS standards at concentrations used for generating standard curve in DMMB assay were assessed ± 6 µM Surfen. This concentration was selected as it equates to the highest well concentration of Surfen used in this Chapter of 60 µM Surfen when diluted 1:10 as was standard for DMMB assessment of culture media from cytokine treated explants. Importantly, no significant effects of Surfen were observed on DMMB assay at this concentration (Fig 5.6C).

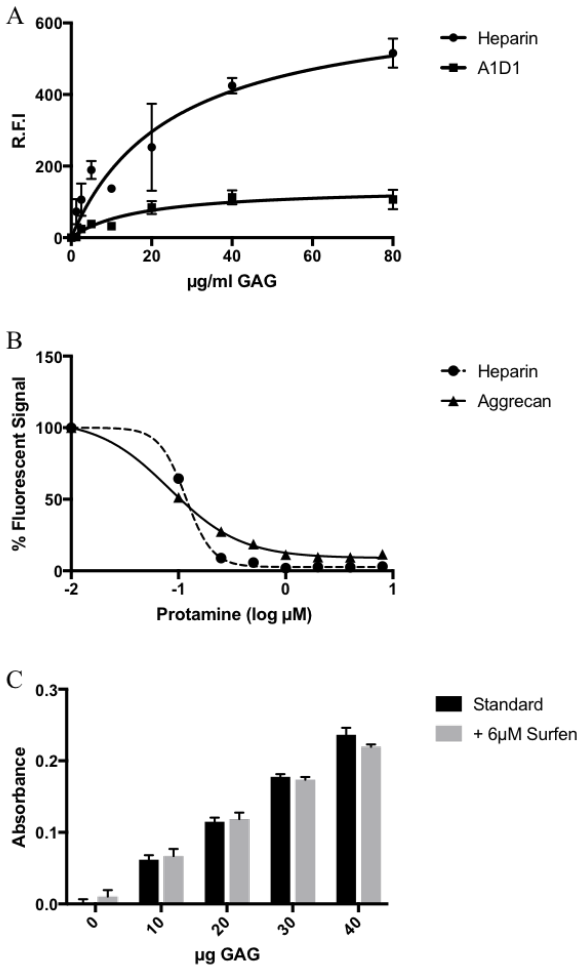

Figure 5.6 – *In vitro* Surfen heparin binding assays and assessment of potential interference of DMMB assay mediated by Surfen. Fluorescent analysis (Ex-360nm, Em-488nm) of Surfen (100 µM) binding to increasing concentrations of heparin or aggrecan (A). Fluorescent analysis of Surfen (50 µM) binding to heparin or aggrecan (both 20µg/ml) in the presence of increasing concentrations of protamine (B). DMMB analysis of chondroitin sulphate standards in the presence or absence of 6 µM Surfen (C), statistical significance determined using ANOVA performed using GraphPad Prism 7.0. Mean and *sd* of three technical replicates shown for A+C (n=3, N=1) and single replicate plotted for B (n=1).

Surfen binds to cartilage matrix-macromolecules but not collagen

To confirm Surfen binding to matrix macromolecules cryosections of bovine articular cartilage were incubated with Surfen alone or in conjunction with picosirius red to counterstain collagen fibres. Picosirius red is often used as a collagen stain in histochemistry and visualised using bright-field microscopy or birefringence, however, picosirius red is also fluorescent and when excited at 561nm emits at 650nm. Therefore fluorescence microscopy could be employed to visualise both Surfen bound to matrix macromolecules and picosirius red staining of collagen. Confocal fluorescence microscopy confirms Surfen binding to cartilage (Fig 5.7A). The highest intensity of staining was seen in the pericellular matrix of cartilage (Fig 5.7A+C). Counter staining with picosirius showed no co-localisation of fluorescence in the ECM suggesting Surfen does not bind collagen (Fig 5.7B+C). The presence of high concentrations of HS within the pericellular matrix combined with the increased avidity of binding of Surfen to HS compared to CS may suggest that Surfen is bound to HSPGs within the pericellular matrix and that Surfen added to cartilage explant models is likely sequestered by GAGs and thereby reducing the concentration of free Surfen within cartilage.

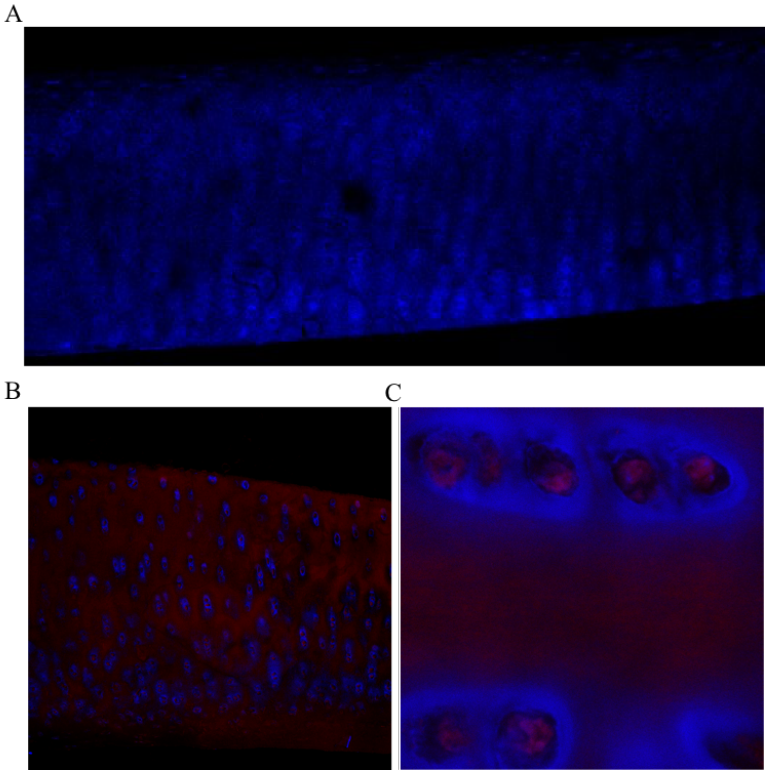

Figure 5.7 – Assessment of Surfen binding to cartilage using fluorescent microscopy. Fluorescent confocal microscopy analysis of bovine cartilage cryosections (10µm thickness) stained with Surfen alone (A) or Surfen counterstained with picosirius red (B+C). (Blue=Surfen, Red=Picosirius red).

5.2.3 Effect of GAG pre-blocking on Surfen activity in cartilage explants

Blocking of Surfen GAG binding by protamine increased its efficacy in preventing GAG loss in IL-1α+OSM stimulated explants but protamine alone was also protective in these conditions

Cartilage explants were incubated in control media, IL-1α, OSM or IL-1α+OSM alone or in the presence of protamine or Surfen + protamine media samples were harvested after 4 days. DMMB analysis revealed a slight but significant decrease in GAG loss mediated by protamine alone ($p<0.05$) but this was increased in the presence of Surfen ($P<0.01$) suggesting that reduction of binding to GAG in cartilage increases the effect of Surfen (Fig 5.8A). Therefore, the consistant lack of effect of Surfen in IL-1α+OSM treated explants in the absence of protamine may be due to increased expression of ADAMTS-4 and an insufficient concentration of free Surfen to inhibit protease activity due to GAG sequestration. Western blot for the BC-3 positive -ARGSVIL neo-epitope revealed a decrease in band intensity in protamine treated explants compared to IL-1α+OSM control explants (Fig 5.8B). The combination of protamine and Surfen appeared to result in a decreased intensity of the lower molecular BC-3 positive fragment compared to controls and protamine alone (Fig 5.8B) but an increase in the higher molecular weight (~150kDa) fragment compared to protamine alone. No positive staining was observed in IL-1α or control media treated explants corresponding with low GAG loss observed in DMMB assay at this 4 day time point (Fig 5.8A+B). The effects of protamine in this system, including effects on viability, are not fully known and appear to mediate an inhibitory effect upon GAG loss and aggrecanase activity although protamine has been shown to be well tolerated by cells (Arbab *et al.* 2004). As the effects of protamine are not fully known a panel of Surfen dosing was devised using one or two doses to maintain levels under the potentially toxic 60 μM whilst increasing the availability through saturation of cartilage GAG binding.

A

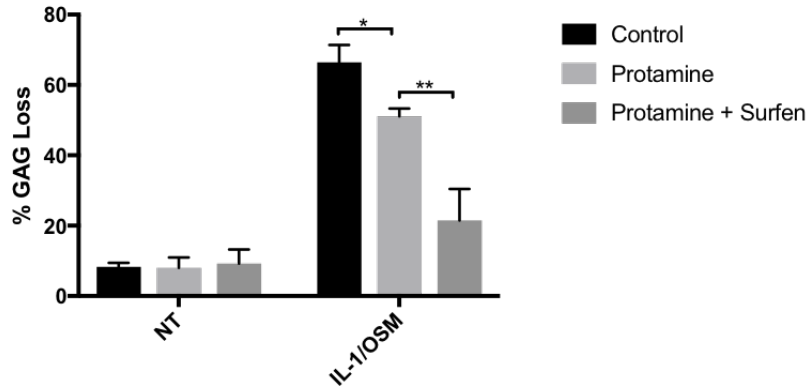

B

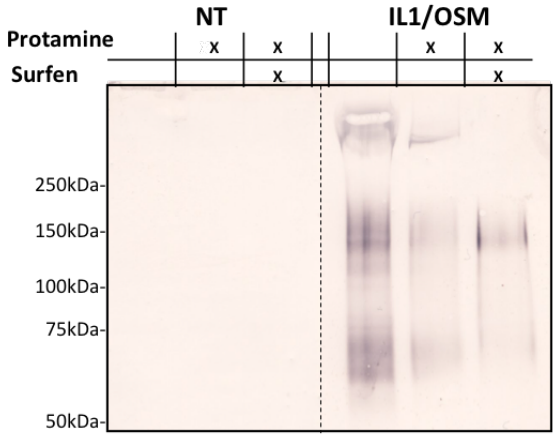

Figure 5.8 – Effects of GAG pre-blocking by protamine on the effects of Surfen on GAG and aggrecanase generated -ARGSVIL neo-epitope release to media in cytokine stimulated bovine cartilage explants. GAG loss assessed by DMMB assay from 2mm bovine cartilage explants cultured in control media (NT), IL-1α (10ng/ml), OSM (50ng/ml) or IL-1α+OSM alone or in the presence of protamine (11 μM) or protamine plus Surfen (7 μM) (A). Representative of two independent experiments with mean and *sd* of triplicate wells shown (n=3, N=2). Statistical significance determined using one-way ANOVA with Tukey's post-hoc test for multiple comparisons performed using GraphPad Prism 7.0. Western blot for BC-3 neo-epitope of explant culture media from (A) 20μg GAG equivalent loaded per lane derived from pooled triplicate wells (B).

5.2.4 Effect of Surfen dose concentration and frequency on cartilage degradation

Multiple dosing of Surfen mediated varying effects in GAG loss compared to equivalent concentration administered once

Multiple dose Surfen explant assays were performed where second dose of Surfen was applied 24 hours post intial cytokine and Surfen treatment. This study revealed varying effects dependent on dosing regimen that appeared independent of total dose concentration. As per previous experiments Surfen at a single dose of 15 μM significantly reduced GAG loss from IL-1α treated explants compared to control in week 1 ($p<0.001$) (Fig 5.9A). Interestingly, increased frequency or concentration of Surfen dose did not significantly inhibit GAG loss compared to controls (Fig 5.9A). A small but significant reduction in GAG loss was observed for IL-1α+OSM treated explants receiving 1 or 2 doses of Surfen at 15μM ($p<0.05$ and $p<0.01$), respectively), however, explants receiving 1 x 30 μM and 2 x 30 μM Surfen showed no significant reduction in GAG loss (Fig 5.9A). No significant differences were observed at any Surfen concentration for OSM treated explants at this time point (Fig 5.9A). At week 2 no significant reduction in GAG loss was observed for IL-1α treated explants receiving 1 x 15 μM Surfen. IL-1α+OSM treated explants receiving 2 x 15 μM Surfen in week 2 showed a significant increase in GAG loss compared to controls ($p<0.05$) (Fig 5.9B). OSM stimulated explants treated with 2 x 15 μM Surfen showed a significant decrease in GAG loss compared to controls in week 2 ($p<0.01$) (Fig 5.9B). When data from week 1 and 2 were combined significant differences in the GAG loss of IL-1α+OSM stimulated explants was observed between those receiving 1 x 15 μM Surfen and 1 x 30 μM Surfen ($p<0.05$), where GAG loss was increased (Fig 5.9C). Conversely, GAG loss was significantly decreased from explants treated with 2 x 30 μM compared to 1 x 30 μM in IL-1+OSM conditions ($p<0.05$) (Fig 5.9C).

Western blot assessing COMP release and degradation from explants cultured in the presence of cytokines for 1 week showed a decreased COMP degradation in IL-1α treated explants when treated with 15 μM and 30 μM Surfen (both single dose). Degradation of released COMP was reduced in IL-1α+OSM treated explants receiving 15μM Surfen, however, explants treated with 30 μM showed little inhibition of degradation compared to controls (Fig 5.10A).

COMP Western blot analysis of 15 μM Surfen treated explants at week 1, 2 and 3 showed similar results as Western blot assays for BC-3 neo-epitope, with a decrease in positive banding in week 1 in IL-1α treated explants receiving 15 μM Surfen compared to IL-1α alone. Whereas, in weeks 2 and 3 there was an increase in positive banding observed for explants stimulated with IL-1α+OSM and treated with 15 μM and 30 μM Surfen compared to cytokines alone (Fig 5.10 B+C). In weeks 2 and 3 COMP degradation appeared to be increased in the presence of 15 μM Surfen treated explants in IL-1α conditions (FIG 5.10 B+C) In a repeat experiement, using 15 well gels that included a 30 μM Surfen treated IL-1α stimulated explants, a slight increase in COMP fragment 5 (75kDa) was seen in the media of IL-1α stimulated explants treated with 30 μM Surfen in week 1 (5.10F).

Western blot performed on the culture media of bovine primary chondrocytes cultured with cytokines in the presence or absence of Surfen showed little change in the production and release of COMP across conditions with the exception being that Surfen appeared to increase COMP production and release in control media cultured explants (Fig 5.10D+E). This data suggests that the increased positive staining observed in IL-1α+OSM treated explants receiving Surfen in week 2 and week 3 was not due to increased production of COMP. It is however possible that the presence

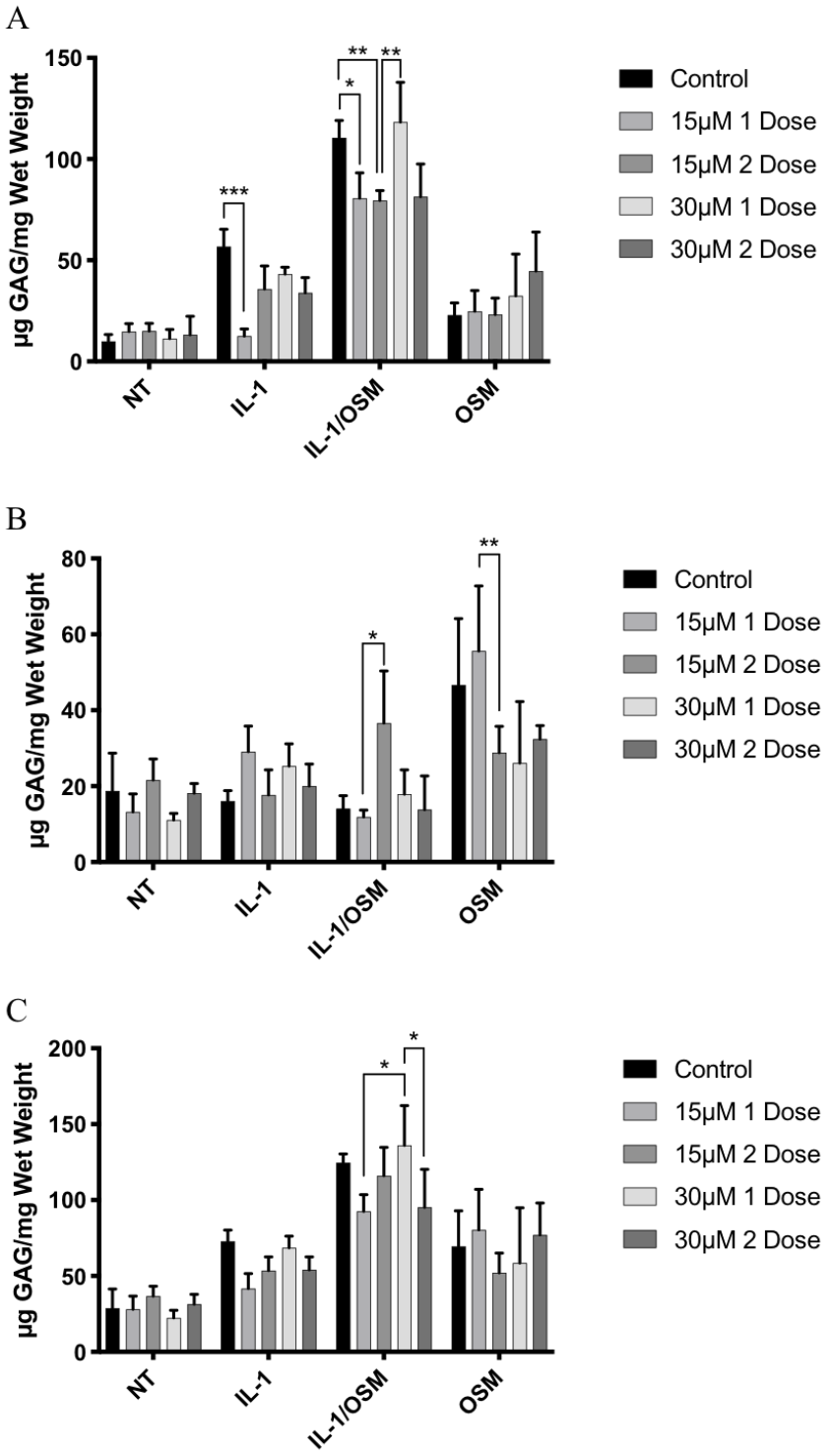

Figure 5.9 – Assessment of multiple dosing of Surfen upon GAG loss in cytokine stimulated bovine cartilage explants. GAG loss assessed by DMMB assay from 4mm cartilage explants incubated with control media (NT), IL-1α (10ng/ml), OSM (50ng/ml) or IL-1α+OSM in the presence of Surfen at the indicated concentrations and dosing regimen at week 1 (A), week 2 (B) and weeks 1 and 2 combined (C). Mean and *sd* of three experiments shown. Statistical significance determined using ANOVA with Tukey's post-hoc test for multiple comparisons performed using GraphPad Prism 7.0. * $p<0.05$, ** $p<0.01$, *** $p<0.0001$.

of Surfen inhibits secondary cleavage of COMP and thereby preventing complete degradation and therefore the appearance of stronger banding of fragments of ~75kDa. The complete degradation observed in week 2 and week 3 of IL-1α+OSM treated explants would suggest a role for MMPs but further work is required to confirm that is not the result of cartilage COMP depletion in week 1 under these conditions.

This data combined suggests a potential increase in COMP degradation dependant on Surfen dose but also duration of culture. Chapter 3 identified a potential role for ADAMTS-4 in COMP degradation which combined with the potentially bi-phasic effect described upon COMP degradation and aggrecanase activity in this Chapter led to the assessment of ADAMTS-4 activity in Surfen treated explant media samples to determine if Surfen increases ADAMTS-4 activity despite its demonstrated inhibitory properties *in vitro*.

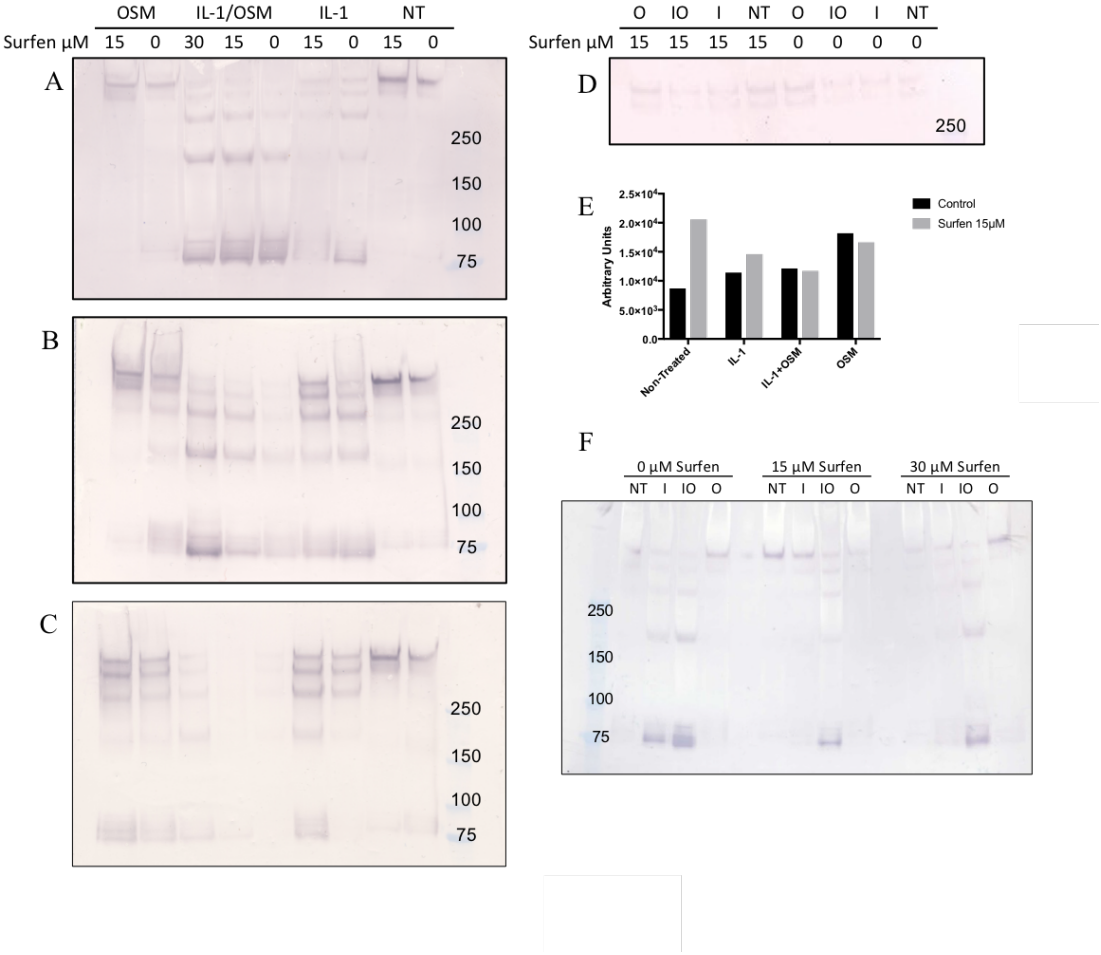

Figure 5.10 – Assessment of Surfen upon COMP release and degradation in cytokine stimulated bovine cartilage explants over 3 week culture period. Western blot showing COMP release and fragmentation from bovine cartilage explants cultured in the indicated cytokine conditions and indicated concentration of Surfen. Media harvested and analysed at week 1(A), week 2 (B) and week 3 (C) each lane represents pooled triplicates with loading normalised to total GAG content. Western blot showing COMP production and release from chondrocytes cultured in monolayer for 48 hours incubated with control media (NT), 10ng/ml IL-1α (I), IL-1α+ 50ng/ml OSM (IO) or OSM (O) in the presence or absence of 15 µM Surfen, each lane represents pooled triplicate wells (D). Densitometric analysis using ImageJ of bands from D (E). Cartilage explants were incubated with control media (NT), 10ng/ml IL-1α (I), IL-1α+ 50ng/ml OSM (IO) or OSM (O) in the presence of Surfen at the indicated concentrations for 1 week prior to analysis by Western blot (F). All blots represent one experiment with triplicate wells pooled per lane (n=3, N=1).

5.2.5 ADAMTS-4 activity assays

Surfen mediated increases in ADAMTS-4 activity in explant media where total concentration of Surfen was 30 µM

Explant culture media was assessed using the Sensolyte Aggrecanase-1 assay which uses a FRET peptide sequence specific to ADAMTS-4 and is minimally cleaved by recombinant ADAMTS-5 and ADAMTS-1 up to 20ng/well, both aggrecanases capable of cleaving at the IGD stie of aggrecan, as shown by manufacturers data. Data showing the potential cleavage of this substrate by MMPs are not provided and should be assessed experimentally. A screen of ADAMTS-4 activity in media samples pooled from triplicate wells from explants cultured in the presence of IL-1α+OSM plus Surfen at the indicated concentrations and dosing revealed a large increase in ADAMTS-4 activity in the media of explants receiving 2 doses of 15µM Surfen at both week 1 and week 2 time points. The activity of ADAMTS-4 in explants receiving 1 dose of 30 µM Surfen decreased and activity decreased further in media from explants receiving 2 doses of 30 µM in both week 1 and week 2. The experiment was repeated as individual well triplicate data points which confirmed the increased ADAMTS-4 activity of explants treated with 2x 15 µM Surfen. The activity of ADAMTS-4 in IL-1α cultured explants receiving 2x 15µM Surfen showed a slight reduction in activity compared to IL-1α alone. In Chapter 4 it was postulated that Surfen may potentially increase the aggrecan degrading activity of ADAMTS-5 and therefore the ability of ADAMTS-5 to cleave the ADAMTS-4 specific Sensolyte substrate in the presence and absence of Surfen was tested. Under the conditions tested there was a slight increase in fluorescence emission and therefore peptide cleavage in ADAMTS-5 containing wells compared to no enzyme controls. This activity showed a slight but not significant increase upon addition of 30 µM Surfen. In Fig 5.11D the activity of IL-1α+OSM treated explants receiving 2 x 15 µM doses of Surfen is given for comparison.

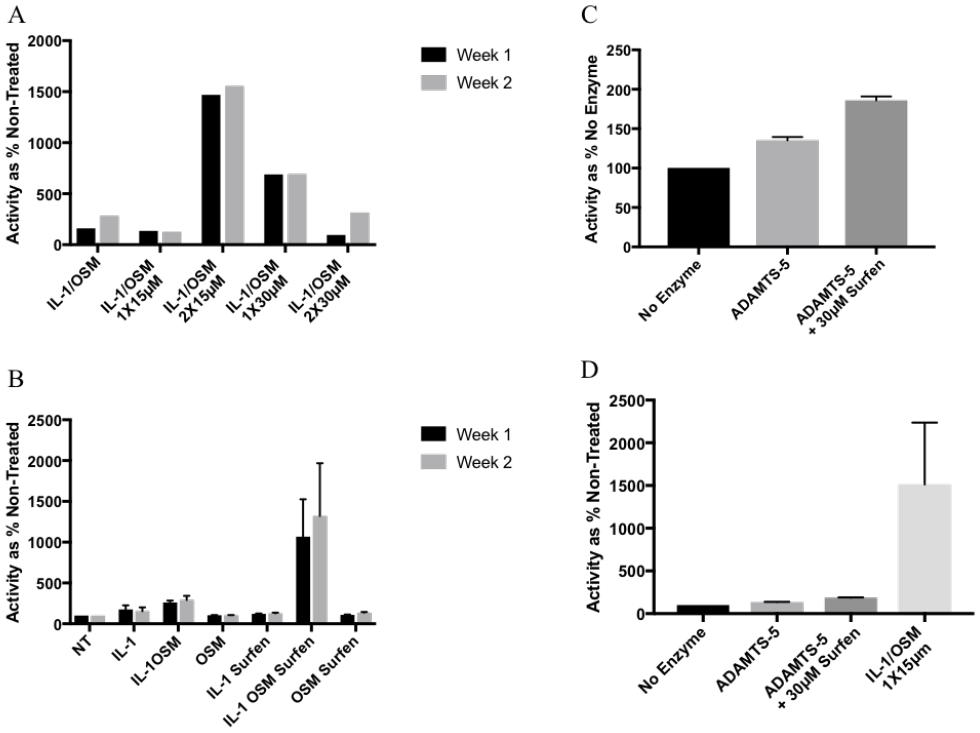

Figure 5.11 – ADAMTS-4 activity in the culture media of cytokine stimulated cartilage explants in the presence or absence of Surfen. ADAMTS-4 activity was assessed using Sensolyte Aggrecanase-1 assay in media from explants treated with IL-1+OSM and Surfen at the indicated concentration and dose regimen. Data represents one experiment (n=3, N=1) (A). ADAMTS-4 activity of media from cartilage explants incubated with the indicated cytokines in the presence or absence of 2 doses of 15 µM Surfen. Mean and *sd* of 3 experiments shown (B). Assessment of ADAMTS-5 (400ng/well) cleavage of Sensolyte Aggrecanase-1 substrate (C). Graph from (C) with the inclusion of media from explants cultured in IL-1+OSM plus 2x15 µM Surfen under the same assay conditions as comparison (D).

5.3 Discussion

The work in this Chapter has demonstrated a consistent inhibition of IL-1α induced aggrecan and COMP degradation mediated by Surfen. It was shown however that Surfen has no significant inhibitory effect upon IL-1α+OSM induced GAG loss, the reason for which is unclear and the effects of Surfen on multiple proteases make any subsequent conclusions highly speculative. It must be noted that in the assays performed using multi-dose Surfen there was a significant inhibition of IL-1α+OSM mediated GAG loss in explants receiving 1 x 15 μM Surfen which was confirmed in repeat experiments, this is potentially a flaw in the experimental design where wet weights were taken at the end of the two week culture period. It is unknown, but possible that Surfen mediates a reduction in collagen loss, inhibition of MMPs was demonstrated *in vitro* and in explant media via zymography in work performed by a BSc student in the Caterson/Hughes lab (data not shown), which thereby preserves the weight of explants and results in underestimation of the amount of GAG lost/ wet weight but this requires validation by hydroxyproline assay. In experiments where % GAG was quantified then no such significant reduction in GAG loss was observed in this Chapter. There are several potential mechanisms that may explain this data. As shown in Chapter 3 the application of IL-1α+OSM results in significantly higher up-regulation of ADAMTS-4 and ADAMTS-5 compared to IL-1α treatment in chondrocytes, therefore the lack of an effect mediated by Surfen in IL-1α+OSM treated explants may be the result of increased ADAMTS-4 production compared to IL-1α conditions and insufficient concentration of Surfen to mediate significant inhibition. The free concentration of Surfen in explants may also be reduced due to GAG binding which was suggested to be the case as blocking of GAGs by application of protamine increased inhibitory effects of Surfen in IL-1α+OSM treated explants, protamine alone mediated inhibitory effects in this system so it is not possible to conclude that this increase in effect was simply mediated by blocking of Surfen GAG binding. Protamine was selected for this assay due to its safe clinical use as a heparin neutralising agent and its small size of 4-5kDa allowing for diffusion throughout cartilage, however protamine has been shown to inhibit furin proprotein convertase which may contribute to inhibition of GAG loss via reduced activation of ADAMTS-4. However, the lack of effect of higher concentrations of Surfen and a seemingly bi-phasic effect of Surfen on GAG loss and COMP degradation would suggest that Surfen concentration is not a limiting factor in its efficacy in IL-1α+OSM treated explants. Alternatively, the IL-1α+OSM mediated induction of ADAMTS-5 could be responsible for the majority of aggrecanase activity in these explants. Full length active ADAMTS-5 has been shown to be 1000 times more potent in cleavage of aggrecan at the pathological $E^{373\_374}A$ site than full length active ADAMTS-4 (Gendron *et al.* 2007), which combined with the inability of Surfen to inhibit ADAMTS-5 could explain the increased GAG loss and BC-3 neo-epitope generation in IL-1α+OSM compared to IL-1α treated explants and lack of effect of Surfen on GAG loss in these explants. The lack of Surfen mediated inhibition of GAG loss and the complete inhibition of GAG loss mediated by an inhibitor of ADAMTS-4/5 that has a 40 fold selectivity for ADAMTS-5 would suggest that indeed ADAMTS-5 is responsible for aggrecanase activity in IL-1α+OSM treated bovine explants. Interestingly, it has been shown that the application of a pro-protein convertase (PC) inhibitor (with activity against furin, PC1/3, PC4, PC5/6 and PACE4 but not PC7) to cartilage explants resulted in release of increased amounts of active ADAMTS-5 suggesting that PC inhibition indirectly increases the release of ADAMTS-5

that is presumably activated by PC7. The mechanism for this is unknown but furin is required for trafficking and presentation of LRP1 at the surface of chondrocytes. LRP1 is believed to control the ECM level of ADAMTS- 4 and ADAMTS-5 via endocytosis and degradation. A decrease in furin activity may therefore lead to accumulation of active ADAMTS-5 in ECM. ADAMTS-4 is activated by furin and PACE4 therefore no increase in active ADAMTS-4 was detected by the authors (He *et al.* 2015). *In vitro* inhibition assays in Chapter 4 have shown that Surfen inhibits furin but it is unknown if it inhibits other PCs and likewise for protamine but this warrants further study as it may shed light upon this mechanism. Full length ADAMTS-5 is known to not cleave COMP and therefore is not proposed to be responsible for Surfen resistant cleavage of COMP in IL- 1α+OSM treated explants but this should be tested experimentally using the Western blot assays developed in Chapter 3 to confirm. The BC-3 Western blot detects aggrecanase activity at the $E^{373\_374}A$ site of aggrecan but it cannot distinguish between the activity of ADAMTS-4 or 5. Analysis of explant media using the ADAMTS-4 selective Sensolyte Aggrecanase-1 assay kit actually revealed a large increase in ADAMTS-4 activity in explants treated with 15 μM Surfen administered twice. This is unexpected due to the observed inhibition of ADAMTS-4 *in vitro* by Surfen. It must be noted that the Sensolyte assay performed only detected activity of ADAMTS-4 in media and the level of ADAMTS-4 activity in the cartilage was unknown, attempts to quantify by GuHCL extraction of protein from cartilage was unsuccessful presumably due to degradation of ADAMT-4 by proteases or self-catalysis. There are two potential mechanisms of Surfen mediated increases in ADAMTS-4 activity in media; Surfen may compete for HS binding with the heparin binding domain of ADAMTS-4, in cartilage and thereby liberating active ADAMTS- 4 to media, additionally the furin mediated effects postulated above may result in increased ADAMTS-4 through reduced recycling. To confirm the increase in activity wasn't mediated by Surfen-activated ADAMTS-5, ADAMTS-5 alone or in the presence of 30 μM Surfen was added to the Sensolyte Aggrecanase-1 substrate. Surfen did increase the activity of ADAMTS-5 in this system (although not significantly) but this is unlikely the cause of the increase observed in explants as the concentration of ADAMTS-5 used was 400ng /well which is well above levels estimated in cartilage. The effects of ADAMTS-4 versus ADAMTS-5 are further complicated by the observed differences in activity between isoforms. Post-translational modification by C-terminal processing, mediated by MT4-MMP or self-catalysis, results in an increased activity of ADAMTS-4 at $E^{373\text{-}374}A$ in aggrecan but reduces the activity of ADAMTS-5 at this site (Fushimi *et al.* 2007). To fully clarify the contribution of each enzyme (in the absence of a specific FRET peptide substrate selective for ADAMTS-5) quantitative Western blot analysis of all isoforms of ADAMTS-4 or 5 would be required on cartilage explant extracts and media samples in the presence and absence of Surfen. As discussed above the potential mechanisms of action of Surfen in IL-1α+OSM treated explants are myriad but these mechanisms proposed above do not fully explain the bi-phasic effect of Surfen at higher concentrations as observed in GAG loss and ADAMTS-4 activity assays. Additionally, in the initial three week Surfen explant assays the effects of 15 μM Surfen on BC-3 neo-epitope generation in weeks 2 and 3 may be the results of an increased effective dose of Surfen due to extensive GAG loss and therefore less sequestered Surfen than at the start of cultures and therefore potentially another example of a bi-phasic Surfen effect on aggrecanase activity. It is unknown whether Surfen has any effects on cytokine-induced gene expression or cell signalling. The observed inhibition of FGF2 signalling

via Surfen/HS interactions and the detection of increased ERK1/2 phosphorylation upon mouse limb bud MSCs suggests that Surfen may mediate effects cell signalling and gene expression so this was investigated further in Chapter 6.

Chapter 6

Effects of Surfen upon Chondrocyte Gene Expression in Response to Pro-inflammatory Cytokines.

6.1 Introduction

The effects of Surfen in multiple models described in the literature and particularly its observed effects on the expression of aggrecan both *in vitro* (Huegel *et al.* 2013) and *in vivo* (Warford *et al.* 2018) in combination with its documented effects upon Gβγ activation, discussed in detail in Chapter 1.5, would suggest that Surfen may be capable of mediating direct changes in cellular gene expression and potentially that these effects proceed via mechanisms other than Surfen mediated extracellular GAG interactions. Furthermore, it was shown in Chapter 5 that increased doses of Surfen resulted in an increased ADAMTS-4 activity in the media of IL-1+OSM stimulated explants compared to non-treated explants, despite the observation in Chapter 4 that Surfen was an inhibitor of ADAMTS-4 activity *in vitro.* This is suggestive of Surfen-mediated effects upon ADAMTS-4 expression under these conditions. The effect of Surfen upon chondrocyte gene expression in response to pro-inflammatory cytokines was therefore investigated in this Chapter. Furthermore, cell signalling pathway analysis was performed in an attempt to elucidate the mechanism of action of Surfen-mediated changes in gene expression.

6.1.1 Aims and Objectives

Aims

In Chapter 5 despite being a direct inhibitor of ADAMTS-4 activity, Surfen mediated increases in aggrecanase and ADAMTS-4 activity in IL-1α+OSM stimulated explants but mediated inhibition of GAG loss and aggrecanase activity in IL-1α treated explants in week 1. This observation was suggestive of Surfen mediated effects upon chondrocyte gene expression in response to cytokines. The aim of this Chapter was to investigate the effects of Surfen upon primary bovine chondrocytes stimulated with IL-1α, OSM or IL-1α+OSM to identify genes regulated by Surfen. Furthermore, this Chapter aims to identify any potential effects of Surfen upon cytokine-induced cell signalling

pathway activation to identify pathways of regulation.

Objectives

These Aims were assessed by completion of the following Objectives;

1. To assess effects of Surfen upon expression of chondrogenic and cartilage matrix-relevant genes in primary bovine chondrocytes treated with pro-inflammatory cytokines.

2. To assess Surfen-mediated effects on the expression of inflammatory mediators in response to pro-inflammatory cytokine treatment of chondrocytes.

3. To assess the effects of Surfen on the expression of cartilage matrix-degrading ADAMTS and MMPs in response to pro-inflammatory cytokines.

4. Signalling pathway analysis was employed to elucidate potential mechanisms of gene regulation by Surfen.

6.2 Results

6.2.1 Chondrocyte uptake of Surfen

Initial studies were performed to assess cell uptake of Surfen as the effects upon cellular targets for example through G$\beta\gamma$ interactions are dependent upon cellular uptake. Surfen fluorescence upon binding allowed for facile assessment of uptake in primary bovine chondrocytes. Staining appeared to bre present in both the cytoplasm and nucleus of Surfen treated cells when assessed by confocal microscopy, although counter staining for nuclear and cytoplasmic structures are required to confirm (the fluorescence emmision spectra of GAG bound Surfen prevented the use of DAPI for nuclear localisation and Surfen mediated background fluorescence was high using filter sets for propidium iodide (PI) nuclear staining) (Fig 6.1 A+B). In parallel, chondrocytes were cultured for 5 days in the presence of sodium chlorate to inhibit GAG synthesis and thereby deplete extracellular GAG levels. Sodium chlorate treatment of cells did not inhibit Surfen internalisation by cells suggesting that GAGs are not required for this process (Fig 6.1 A+B).

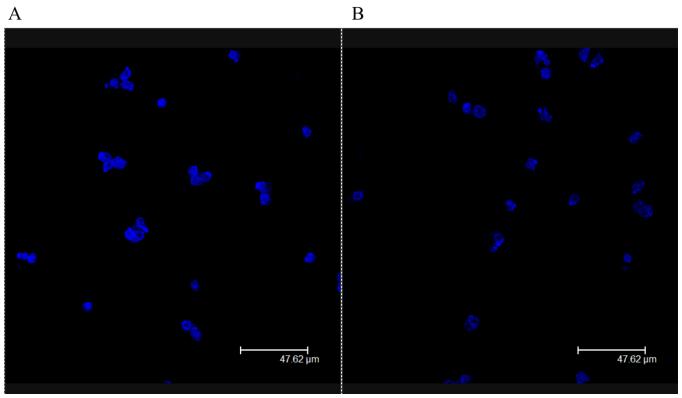

Figure 6.1 – Assessment of Surfen uptake in chondrocytes cultured in the presence or absence of the GAG synthesis inhibitor sodium chlorate assessed by fluorescent microscopy. Surfen was taken up by bovine primary chondrocytes cultured in the absence of sodium chlorate (A) and in the presence of 50mM sodium chlorate (B). Surfen was detected using 405nm laser and depicted as blue.

6.2.2 Surfen effects on chondrogenic gene expression and pro-inflammatory mediators.

Surfen application results in a bi-phasic trend in gene expression of aggrecan and collagen type II in control and cytokine-stimulated chondrocytes, whereas Surfen mediated dose dependant inhibition of *EXT1* and *PGE2* gene expression in cytokine-treated chondrocytes

The observed increases in aggrecan expression and GAG deposition in murine MSC limb bud cultures led to the assessment of chondrogenic gene expression in the presence or absence of Surfen at 7 and 15 µM when cultured in the indicated cytokine conditions (Fig 6.2). Viability assays in chondrocytes, Surfen alone, and in explants in the presence of cytokines and Surfen at concentrations up to 60 µM (Fig 5.1)would suggest that Surfen is not toxic at the doses and incubation times used in this Chapter for gene expression and cell signalling assays.

As observed in Chapter 3 (Fig 3.6), IL-1α and IL-1α+OSM significantly down regulated expression of aggrecan in chondrocytes (Fig 6.2A). Treatment of control media cultured cells with 7 µM Surfen resulted in significant down-regulation of aggrecan ($p<0.01$), however, cells treated with 15 µM Surfen showed a rescue in expression genes compared to those treated with 7 µM ($p<0.05$) (Fig 6.2A). Surfen treatment at 7 µM also resulted in significant down regulation of collagen type II compared to untreated controls ($P<0.01$) in control media cultured cells (Fig 6.2B). In the presence of IL-1α, OSM and IL-1α+OSM there was a non-significant trend in down-regulation of aggrecan expression at 7µM compared to non-treated controls however, 15 µM resulted in increased but non-significant expression of aggrecan compared to 7µM treated chondrocytes. This trend was also observed for collagen type II expression in IL-1α, OSM and IL-1α+OSM treated chondrocytes though the increased expression observed in 15 µM compared to 7 µM treated chondrocytes was significant (all $p<0.05$)(Fig 6.2B).

EXT1 which mediates the synthesis of HS via chain elongation was shown to be up-regulated by IL-1α and IL-1α+OSM treatment and this up-regulation was inhibited in a concentration dependant manner by 7 µM Surfen treatment (both $p<0.01$) and further down-regulated by 15 µM Surfen treatment (Fig 6.2C). 7 µM Surfen also mediated significant reductions in *EXT1* expression in control ($p<0.05$) and OSM ($p<0.05$) conditions (Fig 6.2C). Work in the literature has

ascribed some of Surfens chondrogenic effects to be the result of Surfen mediated up-regulation of heparanase, although when assessed in cytokine treated chondrocytes Surfen attenuated IL-1α and IL-1α+OSM mediated increases in heparanase at 7 μM although this was only deemed significant in IL-1α+OSM conditions ($p<0.01$) (Fig 6.2D). Surfen was also shown to down-regulate the IL-1α+OSM mediated increase in *PGE2* expression at 7 μM ($p<0.01$) with 15 μM Surfen treatment showing no significant further down-regulation (Fig 6.2E). Surfen at 7 μM mediated no decrease in IL-1α induced *PGE2* expression but did significantly down-regulate expression at 15 μM concentrations ($p<0.05$) (Fig 6.2E). NO release was assessed using the Greiss assay as a functional readout of the pro-inflammatory state of chondrocytes and indeed it was shown that Surfen significantly decreased the release of NO from chondrocytes treated with IL-1α and IL-1α+OSM. There were no significant differences in the reduction of NO mediated by 7 μM compared to 15 μM Surfen (Fig 6.2F).

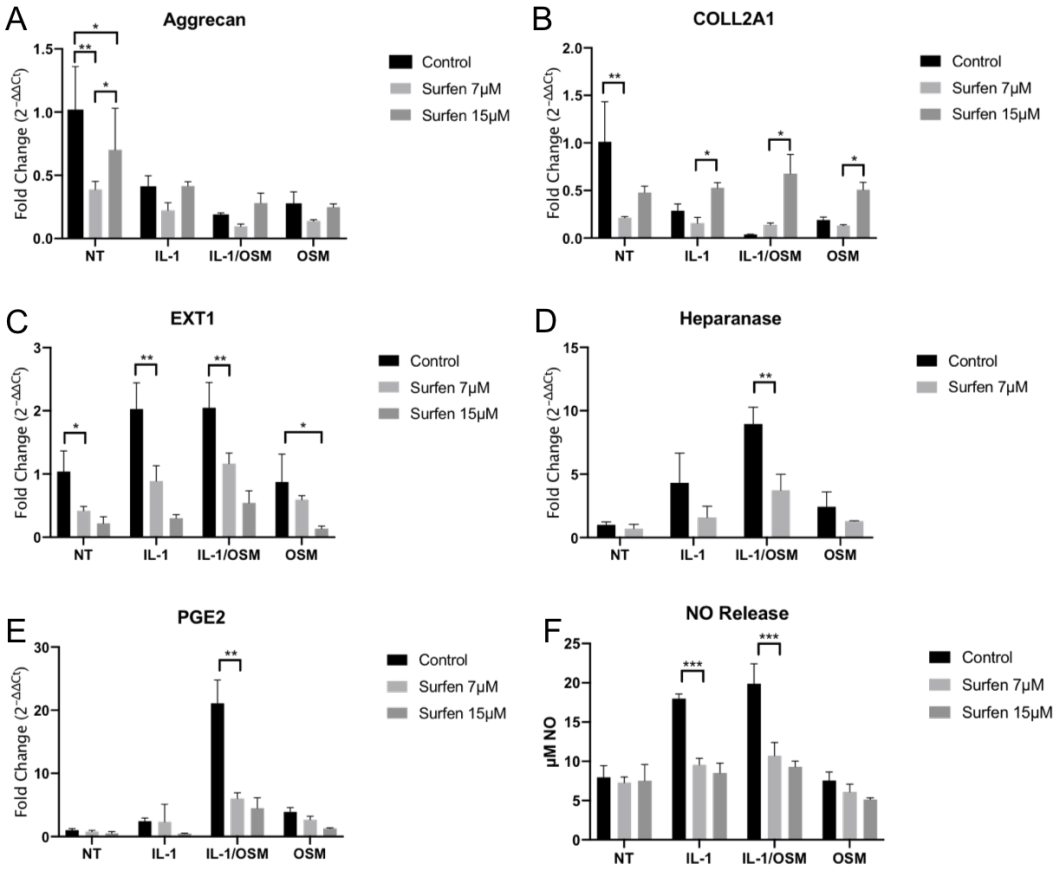

Figure 6.2 – Surfen mediated effects upon gene expression of matrix macromolecules, GAG modulators and inflammatory mediators in cytokine stimulated bovine primary chondrocytes assessed by RT-PCR. Effects of Surfen treatment at 7 or 15 μM upon the gene expression of cartilage matrix macromolecules aggrecan and collagen type II in primary bovine chondrocytes treated with IL-1(10ng/ml), OSM (50ng/ml) or IL-1+OSM for 24 hours. Effects of Surfen treatment upon the the expression of HS synthesis factor *EXT1* and heperanase. Effects of Surfen upon the expression of the pro-inflammatory mediator *PGE2* and Greiss assay to assess the release of NO by chondrocytes in response to cytokine treatment in the presence or absence of Surfen at 7 or 15 μM concentrations. Mean and *sd* of three experiments shown. Statistical significance determined by ANOVA with Tukey's post-hoc test for multiple comparisons performed using GraphPad Prism 7.0.

6.2.3 Surfen effects on catabolic gene expression

Surfen inhibits IL-1α and IL-1α+OSM induced gene expression of ADAMTS-4, ADAMTS-5, MMP1, MMP3 and MMP13 at low dose (7 µM) but ADAMTS-4 expression was increased by high dose (15 µM) Surfen treatment in IL-1α+OSM stimulated chondrocytes

Surfen was shown in Chapter 5 to inhibit GAG loss from IL-1α treated explants and was assumed to be via direct inhibition of ADAMTS-4 activity, however, the increased aggrecanase activity observed at higher concentrations and with multiple doses of Surfen combined with the increase in BC-3 neo-epitope released to media in Surfen treated explants at weeks two and three in IL-1α and IL-1α+OSM culture conditions suggest that Surfen may potentially affect the gene expression of cartilage degrading enzymes and therefore Surfen effects on the expression of selected ADAMTS and MMPs were assessed (Fig 6.3A-E). As shown in Chapter 3, IL-1 results in increased *ADAMTS4* expression in chondrocytes and the combination of IL-1α+OSM further increases this expression. Surfen significantly inhibited IL-1α ($p<0.01$) and IL-1α+OSM ($P<0.01$) induction of *ADAMTS4* at 7 µM, however, increased treatment with Surfen to 15 µM resulted in a slight increase in *ADAMTS4* expression in IL-1α+OSM treated cells compared to control cells cultured in the absence of Surfen and a significant increase in expression compared to 7 µM treated chondrocytes ($p<0.01$) (Fig 6.3A). This bi-phasic effect was not observed for *ADAMTS5* expression where 7 µM and 15 µM Surfen significantly down-regulated *ADAMTS5* expression in IL-1α and IL-1α+OSM treated cells ($p<0.01$ and $p<0.01$, respectively) (Fig 6.3B). Surfen treatment resulted in a dose-dependent and significant attenuation of IL-1α and IL-1α+OSM mediated induction of *MMP1* (Fig 6.3C), *MMP3* (Fig 6.3D) and *MMP13* (Fig 6.3E). 15µM Surfen treatment in IL-1α+OSM treated cells only reduced *MMP1* (Fig 6.3C) and *MMP3* (Fig 6.3D) expression by ~50%, whereas a more complete down-regulation of *MMP13* was observed by 7 ($p<0.01$) and 15 µM ($p<0.01$) Surfen treatment (Fig 6.3E).
To assess if the effects of Surfen upon increased *ADAMTS*4 expression in IL-1α+OSM stimulated chondrocytes resulted in the increased release of active ADAMTS-4, Sensolyte aggrecanase 1 activity assay was used on the media of chondrocytes cultured for 4 days with increasing doses of Surfen in the presence or absence of IL-1α+OSM stimulation (Fig 6.3F). ADAMTS-4 activity in chondrocyte culture media was increased by IL-1α+OSM stimulation and this activity was further increased with Surfen treatment at 5, 15 and 30 µM concentrations. The highest ADAMTS-4 activity was observed for 15 µM Surfen treated explants ($p<0.001$ compared to 5 µM Surfen treated cells). A slight decrease in ADAMTS-4 activity was observed at 30 µM Surfen treatment, potentially as a result of sufficient Surfen concentration in media to mediate direct inhibition of ADAMTS-4 (Fig 6.3F). This data suggests that observed increases in *ADAMTS4* expression in response to Surfen treatment at 15 µM translates to increased ADAMTS-4 activity.

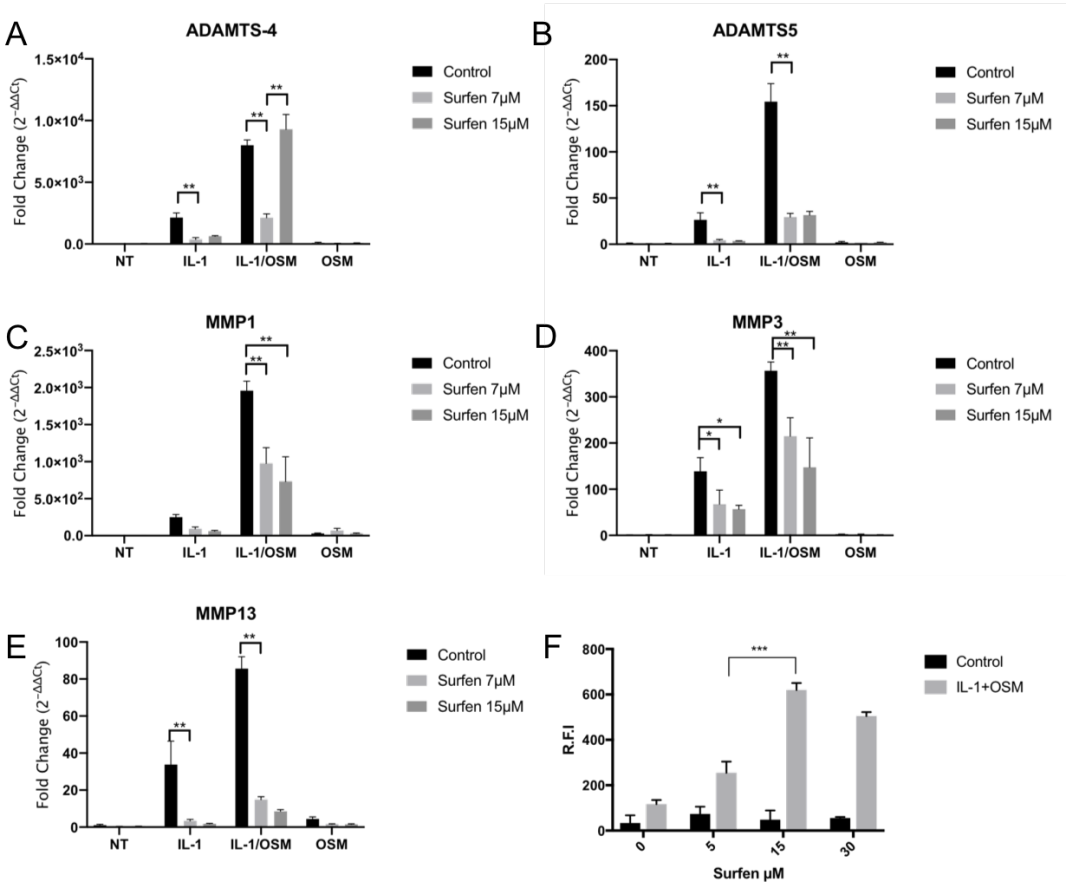

Figure 6.3 – Effects of Surfen on the expression of metalloproteinases in cytokine stimulated bovine primary chondrocytes assessed by RT-PCR. Effects of Surfen treatment at 7 or 15 μM upon the gene expression of *ADAMTS4*, *ADAMTS5*, *MMP1*, *MMP3* and *MMP13* in primary bovine chondrocytes treated with IL-1α(10ng/ml), OSM (50ng/ml) or IL-1α+OSM for 24 hours. ADAMTS-4 activity in media of chondrocytes cultured in control or IL-1α+OSM media for 4 days in the presence of increasing concentrations of Surfen was assessed by Sensolyte Aggrecanase 1 assay (bottom right). Mean and *sd* of three experiments shown. Statistical significance determined by ANOVA with Tukey's post-hoc test for multiple comparisons performed using GraphPad Prism 7.0.

6.2.4 Surfen mediated effects on cytokine induced cell signalling pathways

AKT

Bovine primary chondrocytes were incubated with IL-1α, OSM or IL-1α+OSM in the presence or absence of 7 μM Surfen with cells harvested at 10, 30, 60 and 120 minutes and pathway activation was assessed using the Pathscan intracellular signalling array.

Analysis of AKT phosphorylation at site Thr^{308} showed no differences in activation in the presence or absence of Surfen compared to cells cultured in cytokines alone (Fig 6.4 A-D). Phosphorylation of AKT at Ser^{473} showed a modest increase in phosphorylation mediated by Surfen at 10 minutes in control (Fig 6.4E) and IL-1α media cultured cells (Fig 6.4F). No differences in phosphorylation of AKT at Ser^{473} were observed with Surfen treatment in IL-1α+OSM (Fig 6.4G) and OSM cultured cells (Fig 6.4H), although due to the modest increase in the presence of Surfen observed in non-treated cells (no cytokine stimulation) effects would be likely obscured by the activation of AKT mediated by OSM in these conditions (Fig 6.4).

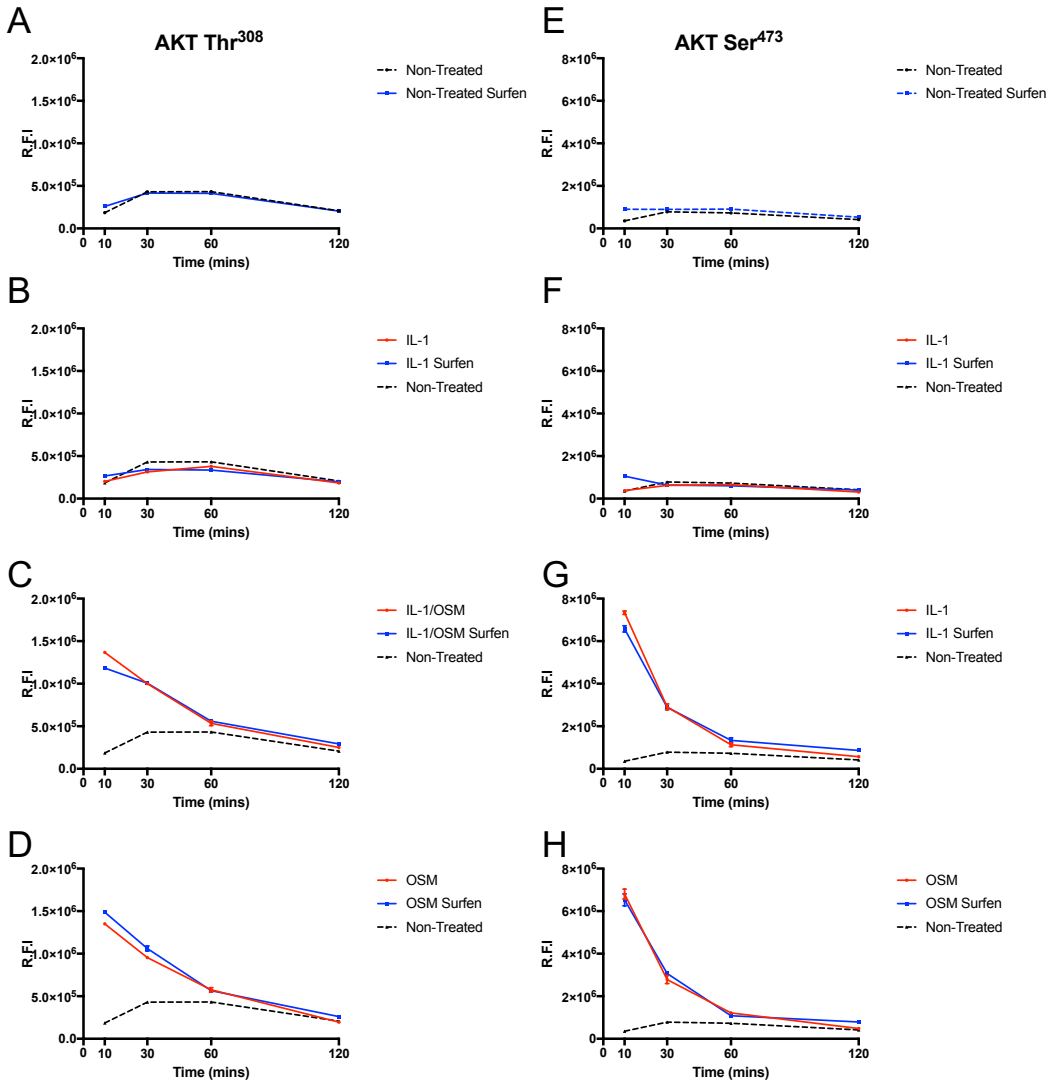

Figure 6.4 – Assessment of Surfen on AKT intracellular signalling pathways in cytokine stimulated bovine chondrocytes. Pathscan intracellular signalling assay time course quantifying phosphorylation of AKT Thr^{308} (left column) and AKT Ser^{473} (right column) in primary bovine chondrocytes treated with IL-1α(10ng/ml), OSM (50ng/ml) or IL-1α+OSM in the presence or absence of Surfen (7 μM) with cells harvested and analysed at 10, 30, 60 and 120 minutes. Mean and *sem* of duplicate spots from one experiment plotted (n=2, N=1).

ERK1/2 and SAPK/JNK

Surfen mediated a large increase in ERK1/2 phosphorylation in non-treated cells with the largest increase observed at 60 minutes of culture (Fig 6.5A). A small increase in ERK1/2 activation was observed in IL-1α cultured cells treated with Surfen at 10 minutes but this increase was minimal compared to subsequent IL-1α mediated increases (Fig 6.5B). The Surfen mediated ERK activation observed in non-treated cells (Fig 6.5A) was higher than that observed in IL-1α (Fig 6.5B) treated cells but not IL-1α+OSM (Fig 6.5C) and OSM treated cells (Fig 6.5C). A small increase in SAPK/JNK activation was observed at 10 minutes in IL-1α treated cells (Fig 6.5F) in the presence of Surfen compared to cells alone (Fig 6.5E), but no difference at all other time points. Surfen mediated an almost 50% reduction in SAPK/JNK phosphorylation in IL-1α+OSM at 10 minutes but no difference at all other time points (Fig 6.5G).

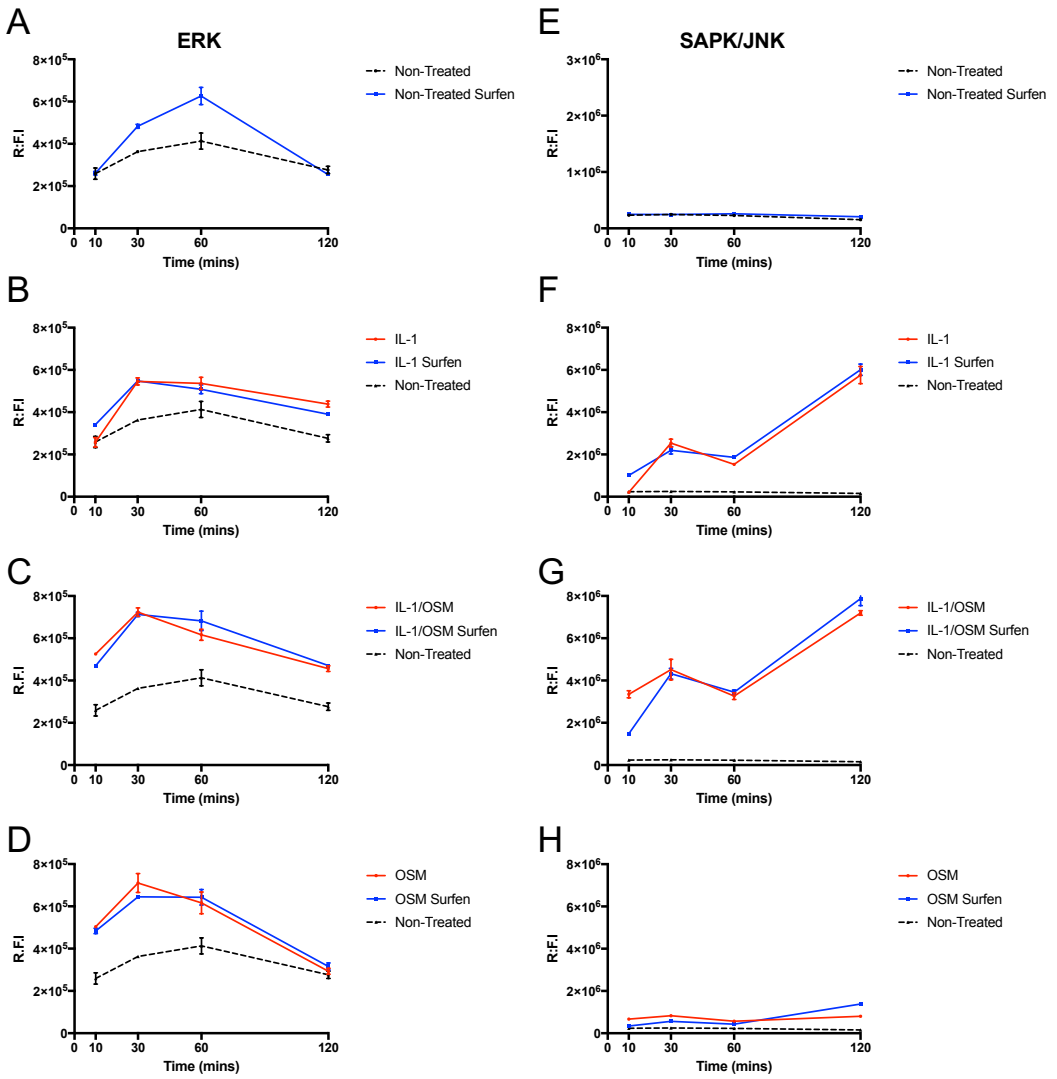

Figure 6.5 – Assessment of Surfen on ERK1/2 and SAPK/JNK intracellular signalling pathways in cytokine stimulated bovine chondrocytes. Pathscan intracellular signalling assay time course quantifying phosphorylation of ERK (left column) and SAPK/JNK (right column) in primary bovine chondrocytes treated with IL-1α(10ng/ml), OSM (50ng/ml) or IL-1α+OSM in the presence or absence of Surfen (7 µM) with cells harvested and analysed at 10, 30, 60 and 120 minutes. Mean and *sem* of duplicate spots from one experiment plotted (n=2, N=1).

P38 and AMPK

Surfen was shown to minimally increase p38 phosphorylation in non-treated cells at 10, 30 and 60 minutes (Fig 6.6). In IL-1α treated cells Surfen mediated a rapid increase in p38 phosphorylation at 10 minutes compared to cells treated with IL-1α alone (Fig 6.6B). This increase was almost 3 fold in intensity though levels of phosphorylation were equal at 30 and 60 minutes and Surfen treated cells showed a decrease in phosphorylation of p38 at 120 minutes (Fig 6.6B). No difference in activation of p38 was shown at 10, 30 and 60 minutes in IL-1α+OSM treated cells in the presence of Surfen compared to cells treated with cytokines alone, a small decrease in phosphorylation was evident at 120 minutes matching that observed in IL-1α treated cells (Fig 6.6C). The secondary spike in p38 activation observed between 60 and 120 minutes in IL-1α (Fig 6.6B) and IL-1α+OSM (Fig 6.6C) treated cells was slightly reduced by Surfen treatment. In OSM treated cells where no secondary spike was observed Surfen treatment slightly increased the phosphorylation at 120 minutes (Fig 6.6D). Initial Surfen-mediated spikes were also observed in AMPK phosphorylation at 10 minutes in non-treated (Fig 6.6E) and IL-1α (Fig 6.6F) treated cells that was not observed in cells cultured in the presence of OSM (Fig 6.6G+H).

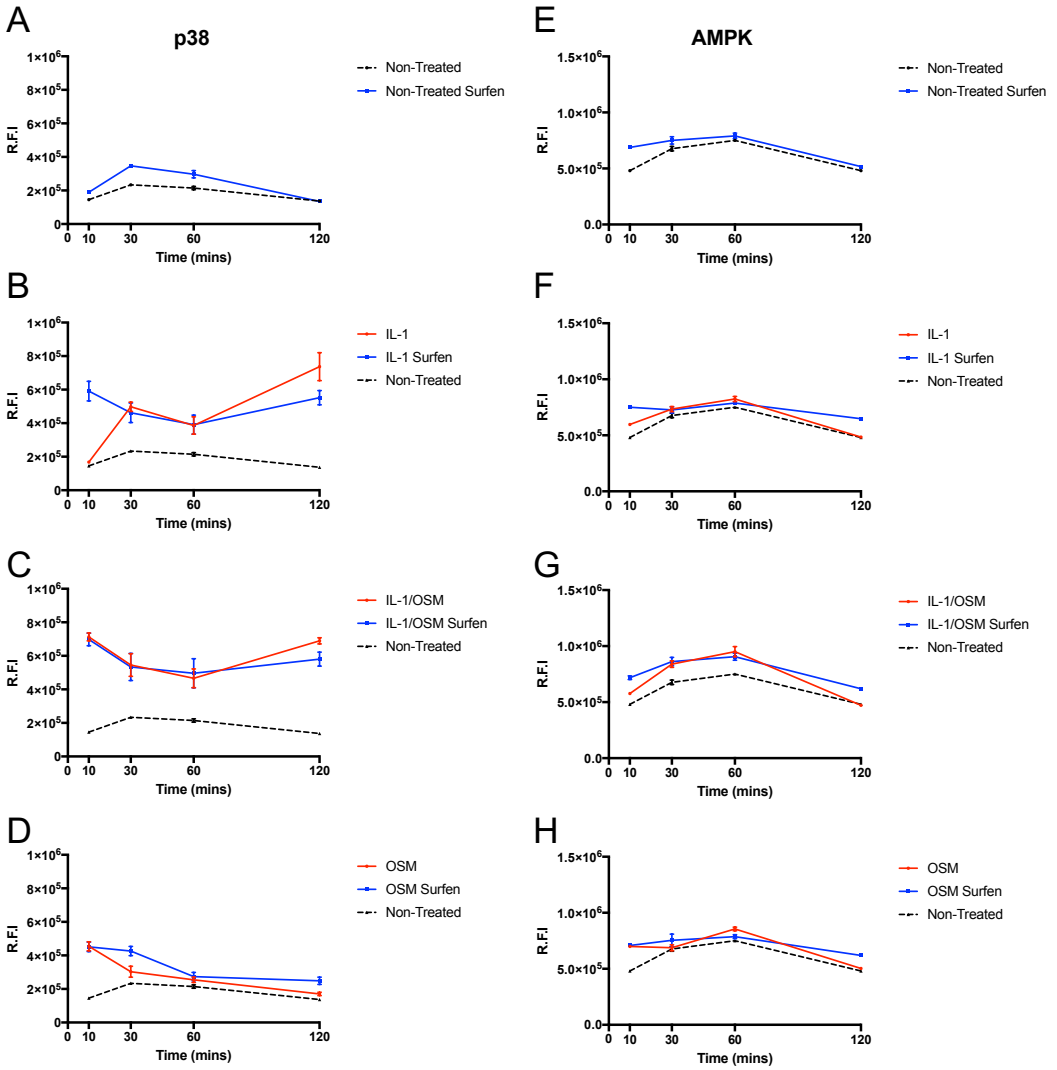

Figure 6.6 – Assessment of Surfen on p38 and AMPK intracellular signalling pathways in cytokine stimulated bovine chondrocytes. Pathscan intracellular signalling assay time course quantifying phosphorylation of p38 (left column) and AMPK (right column) in primary bovine chondrocytes treated with IL-1α(10ng/ml), OSM (50ng/ml) or IL-1α+OSM in the presence or absence of Surfen (7 μM) with cells harvested and analysed at 10, 30, 60 and 120 minutes. Mean and *sem* of duplicate spots from one experiment plotted (n=2, N=1).

STAT1 and STAT3

STAT1 and STAT3 signalling pathways, which were shown to be OSM specific in Chapter 3, were unaffected by Surfen treatment in all conditions tested (Fig 6.7A-F) with the exception of small increases in STAT3 phosphorylation level in IL-1α+OSM (Fig 6.7G) and OSM (Fig 6.7H) stimulated chondrocytes in the presence of Surfen.

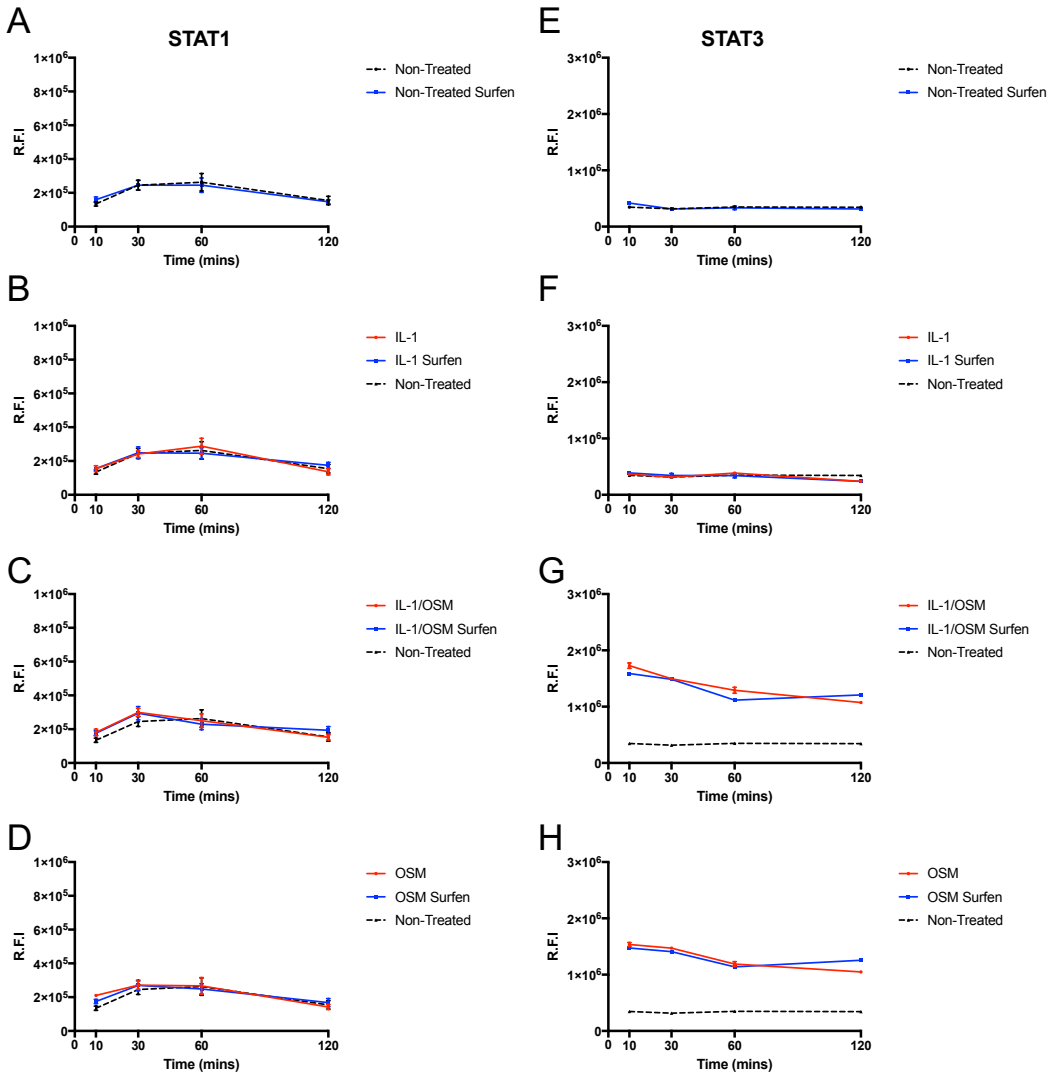

Figure 6.7 – Assessment of Surfen on STAT1 and STAT3 intracellular signalling pathways in cytokine stimulated bovine chondrocytes. Pathscan intracellular signalling assay time course quantifying phosphorylation of STAT 1 (left column) and STAT 3 (right column) in primary bovine chondrocytes treated with IL-1α(10ng/ml), OSM (50ng/ml) or IL-1α+OSM in the presence or absence of Surfen (7 µM) with cells harvested and analysed at 10, 30, 60 and 120 minutes. Mean and *sem* of duplicate spots from one experiment plotted (n=2, N=1).

The lack of clearly defined effects of Surfen in cytokine treated cells, with only modest changes observed in signalling pathway activation, suggested that the mechanism of Surfen effects on gene expression are via pathways not tested or downstream of the signalling molecules assessed in the Pathscan intracellular signalling array assay.

6.2.5 Assessment of Surfen inhibition of HDACs *in vitro*

Surfen showed no inhibitory effect upon HDAC activity *in vitro*

It has been shown that many hydroxamate type inhibitors show inhibitory activity upon histone deacetylases (HDACs) and can mediate gene expression changes through epigenetic mechanisms. Therefore, Surfen was tested as a potential HDAC inhibitor using the Promega HDAC Glo assay. HeLa nuclear lysates provided with the assay kit were incubated with increasing concentrations of Surfen and results clearly showed no inhibitory effect of Surfen at micro-molar concentrations. As a positive control, lysates were incubated with the known hydroxamate type HDAC inhibitor Trichostatin A which showed strong inhibition of HDAC activity in HeLa lysates at a nano-molar concentration range (Fig 6.8). Therefore, the effects of Surfen upon cytokine induced gene expression are not mediated via inhibition of general HDAC activity.

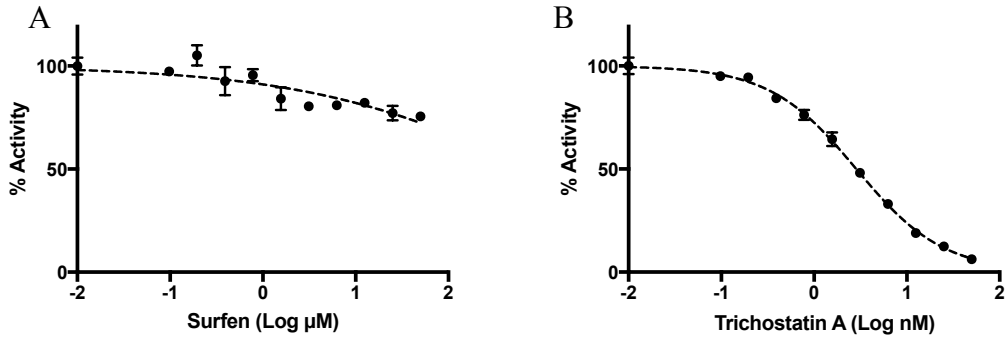

Figure 6.8 – *In vitro* assessment of Surfen as a potential inhibitor of HDACs. HDAC inhibition assay of HeLa nuclear lysates incubated with increasing concentrations of Surfen (A) or known HDAC inhibitor Trichostatin A (B). Mean and *sd* of triplicate wells from one experiment plotted (n=3, N=1).

6.3 Discussion

Surfen mediated effects upon gene expression

It has been shown that the treatment of limb bud MSC micromass culture with Surfen results in increased expression of collagen type II and aggrecan with a concomitant increase in GAG deposition (Huegel *et al.* 2013). This effect was shown to be mediated by BMP signalling as shown by Surfen-mediated phosphorylation of SMAD1/5/8 that was ablated by treatment with the BMP specific inhibitor noggin (Huegel *et al.* 2013). Furthermore, these effects were assumed to be specific to HS interactions as they were replicated by the addition of heparanase to cells (Huegel *et al.* 2015). Indeed, Surfen-mediated activation of BMP signalling correlates well with the work in this Chapter where a significant rescue of IL-1α+OSM mediated down-regulation of aggrecan and collagen type II expression was observed upon treatment of bovine chondrocytes with 15 µM Surfen. It must be noted that the Heugel *et al.* (2013) showed an increase in aggrecan, collagen type II and *SOX9* but also collagen type X and *RUNX2* expression suggesting that although rescuing GAG synthesis, Surfen treatment may also induce a hypertrophic phenotype that warrants further investigation.

15 μM Surfen treatment of IL-1α+OSM cultured chondrocytes resulted in an increase in *ADAMTS4* expression. TGFβ superfamily signalling has been shown to regulate *ADAMTS4* expression with chondrocytes treated with TGFβ showing increased *ADAMTS4* expression compared even to IL-1 stimulated chondrocytes (Moulharat *et al.* 2004). Likewise, a recent study observed leptin mediated increases in *ADAMTS4* and *MMP13* expression were the result of BMP signalling pathways (Su *et al.* 2018). No increases in *MMP13* expression were observed at any concentration of Surfen in this Chapter, however, gene expression was only assessed at 24 hours and a more extensive time course study may reveal delayed Surfen mediated BMP dependent effects. Interestingly, there was a bi-phasic effect upon the expression of *ADAMTS4* in IL-1α+OSM stimulated chondrocytes with expression reduced at 7 μM and increased at 15 μM Surfen concentrations compared to non-treated controls. *ADAMTS4* expression increases translated to an increased ADAMTS-4 activity in the media of treated chondrocytes in a dose dependant manner from 0-15 μM Surfen. This suggests that increased expression results in increased protein production and release from chondrocytes and likely contributes to the lack of Surfen effects upon GAG loss in IL-1α+OSM treated explants and the observed increases in aggrecanase activity and ADAMTS-4 activity in cartilage explants in Chapter 5. Bi-phasic effects of Surfen upon *ADAMTS4* expression were not observed in IL-1α or OSM treated chondrocytes. Both LIF and OSM have been shown to amplify BMP and TGFβ signalling via STAT3 interactions with SMAD1/5 and SMAD3 respectively (Fukuda *et al.* 2007;Bryson *et al.* 2017). Why this effect was not observed in OSM alone treated chondrocytes is unknown but IL-1 mediated increases in BMP-2 expression (Fukui *et al.* 2003) may provide a greater pool of endogenous BMP for Surfen mediated activation. Sufficient BMP levels may not be present in OSM alone conditions although the effects of OSM on BMP expression in this system is unknown and requires confirmation.

Loss of function mutations in EXT1 are associated with Hereditary Multiple Exostoses, a disease characterised by cartilaginous outgrowths from the perichondrium (Wuyts *et al.* 1998). It is therefore assumed that loss of EXT1 can stimulate chondrogenesis and cartilage formation although how the loss of functional EXT1, an enzyme that mediates the elongation step in HS synthesis, induces this is unknown. Interestingly, IL-1α and IL-1α+OSM treatment increased the expression of *EXT1* which was abrogated by Surfen treatment. A recently published abstract showed that shRNA mediated knockdown of EXT1 in ATDC5 cells resulted in increased aggrecan and collagen type II expression and also proteoglycan deposition suggesting knockdown of EXT1 is indeed chondrogenic. Decreased EXT1 expression appeared to effect a decrease in active WNT signalling in these cells (Wang *et al.* 2018). Surprisingly, knockdown of EXT2 resulted in opposing effects on aggrecan, collagen type II expression and WNT signalling (Wang, X *et al.* 2018). Both EXT1 and EXT2 are required for efficient HS chain elongation suggesting that these effects are not related to either proteins role in HS synthesis *per se*. However, specific modifications in HS chain length resulting from specific silencing of EXT1 or 2 may alter the binding of cell surface HSPGs to BMPs and their antagonists, such as noggin and thereby effect changes in BMP signalling. Interestingly, Surfen is employed in its capacity as an HS antagonist, in *in vitro* models of exostosis and is presumed to be effective due to the aforementioned effect on BMP signalling via HS interactions, although the effects observed in this Chapter on *EXT1* expression may also contribute. This data is the first to our knowledge to show a significant increase in *EXT1* expression in chondrocytes

stimulated with IL-1α or IL-1α+OSM which coupled with the known chondrogenic effects of EXT1 ablation warrant further investigation.

The proposed BMP dependent mechanism of Surfen mediated effects upon *ADAMTS4*, aggrecan and collagen type II expression in this Chapter does not satisfactorily explain the observed Surfen mediated down-regulation of *ADAMTS5*, *PGE2*, *EXT1*, *MMP1*, *MMP3* and *MMP13* at both 7 and 15 μM in IL-1α and IL-1α+OSM stimulated chondrocytes. Likewise, the down-regulation of IL-1α+OSM induced *ADAMTS4* expression mediated by 7 μM treatment but an increase at 15 μM does suggest two mechanisms are at play. Indeed, over-expression of *BMP2* in the joints of mice treated with IL-1 results in increased aggrecanase neo-epitope, -NITEGE and collagenase neo-epitope-VDIPEN detected in cartilage compared to wild type suggesting increased aggrecanase and MMP activity, respectively (Davidson *et al.* 2007) and therefore if Surfen acts exclusively via BMP signalling pathways it would be expected that Surfen would not be cartilage protective in IL-1 alone conditions.Therefore signalling pathway analysis was performed to identify potential pathways that may be external to BMP signalling.

Surfen mediated effects upon chondrocyte cell signalling pathway activation

Cell signalling pathway analysis showed that in non-treated cells Surfen was capable of activating ERK1/2 and to a lesser extent AKT Ser^{473}. This confirms that observed by Surve *et al.* (2014) that showed that Gβγ activation, independent of GPCR binding, mediated by Surfen resulted in rapid ERK1/2 phosphorylation at 5 minutes and AKT Ser^{473} phosphorylation at 3 minutes (Surve *et al.* 2014). The modest increase in AKT phosphorylation observed in this Chapter may be time dependent as AKT Ser^{473} was assessed at 10 minutes, a repeat of the experiment with harvest at 3 minutes may reveal a more robust activation. P38 was also activated in IL-1α and non-treated cells in the presence of Surfen. This is potentially also a result of Surfen-mediated Gβγ activation as it has been shown that phosphorylation of p38 by activation of β-adrenergic receptors was dependent upon Gβγ (Yamauchi *et al.* 1997) . However, p38, ERK1/2 and AKT phosphorylation have been observed upon BMP-2 administration in a pathway independent of the SMAD1/5/8 pathway (Boergermann *et al.* 2010). Therefore, further work is required using inhibitors of Gβγ, such as gallein, and BMP-2 using recombinant noggin to confirm the relevance of each pathway to Surfen mediated effects upon cell signalling pathway activation and gene expression.

If the secondary spikes in SAPK/JNK and p38 phosphorylation observed at 120 minutes, as described in this and Chapter 3, were a result of reactive oxygen species activation via ASK1 it would have been expected that Surfen may mediate a reduction in these secondary spikes due to its role in reducing NO production and PGE2 synthase expression, though this was not the case. To confirm however it would be necessary to analyse the effects of Surfen upon the production of all ROS species known to activate ASK1 and particularly the robust activator, H_2O_2, which was prevented by time restrictions. The activation by Surfen of pathways that were also activated in the presence of cytokines (ERK1/2, p38 and AKT) does not offer an obvious mechanism to Surfen mediated effects on gene expression within the context of the inflammatory signalling mediators tested in this Chapter as these pathways were significantly activated by the cytokines tested themselves. Additionally, ERK1/2 has been shown to be a negative regulator whereas p38 was a positive regulator of chondrogenesis (Oh *et al.* 2000) and its inhibition led to osteoarthritis

like changes in a rat model (Prasadam *et al.* 2012), therefore the net effects of Surfen mediated activation on these pathways are unknown and likely context dependent.
Surfen mediated effects may be more pronounced in pathways not studied in this Chapter or Surfen may act downstream of these pathways at the transcription factor level or via epigenetic silencing. Many hydroxamate type inhibitors of MPs are also capable of inhibiting HDACs which led to the assessment of Surfen as a potential HDAC inhibitor (Olson *et al.* 2015). HDAC inhibitors have been shown to inhibit IL-1α mediated induction of ADAMTS-4 and 5 in rat chondrocytes (Wang, P *et al.* 2018) . The metal chelating properties of the urea group in Surfen, comparable to the hydroxamic acid group of known HDAC inhibitors such as trichostatin A and valproic acid, suggested this may be a potential mechanism, although studies using HeLa cell lysates showed no inhibition of HDAC activity at micro-molar concentrations which confirmed conclusively that gene expression effects of Surfen are not mediated at the epigenetic level via general HDAC inhibition. Therefore, we can conclude that Surfen mediates pro-anabolic, anti-catabolic and anti-inflammatory effects in the gene expression of cytokine stimulated primary bovine chondrocytes but the effects are both cytokine and dose dependent. The precise mechanism of Surfen mediated gene regulation is not determinable from the data in this Chapter and remains unknown.

6.3.1 Summary

1. Surfen reduces cytokine induced gene expression of *ADAMTS4*, *ADAMTS5*, *MMP1*, *MMP3*, *MMP13* and *PGE2* Synthase at 7 µM in primary bovine chondrocytes.

2. Bi-phasic effects upon on *ADAMTS4* gene expression showed a decrease at 7 µM but an increase in expression at 15 µM Surfen concentrations in IL-1α+OSM primary bovine chondrocytes. The increased expression resulted in increased ADAMTS-4 activity in the media of Surfen treated chondrocytes stimulated with IL-1α+OSM.

3. Bi-phasic effects were also noted for expression of aggrecan and collagen type II in IL-1α and IL-1α+OSM treated chondrocytes. Surfen rescued expression of collagen type II and aggrecan in cytokine treated primary bovine chondrocytes at 15 µM concentrations but a trend of further down-regulation was shown at 7 µM Surfen concentrations suggestive of multiple mechanisms of gene regulation mediated by Surfen.

4. Surfen modestly activates p38, ERK1/2 and AKT Ser^{473} in non-treated chondrocytes but no other pathways showed Surfen mediated effects in any cytokine conditions tested.

5. Target prediction, literature searches and qHTS datasets suggest Surfen effects are not exclusive to GAG antagonism and therefore further work is required to elucidate the mechanisms of Surfen in chondrocytes.

Chapter 7

Part I General Discussion

The work in Chapter 3 identified the SAPK/JNK pathway as being synergistically activated in bovine primary chondrocytes in response to treatment with IL-1α and OSM in combination, which to our knowledge is the first study to date to identify supra-induction of a signalling pathway mediated by this cytokine combination. Furthermore, inhibition of JNK, using the pan-JNK inhibitor SP600125, was shown to be protective against IL-1α+OSM induced catabolic gene expression in bovine chondrocytes and cartilage matrix degradation in bovine cartilage explants. To date, this is the first study to identify synergistic activation of SAPK/JNK by IL-1α in combination with OSM and may explain the in vivo success of SAPK/JNK inhibition in CIA models of rheumatoid arthritis (Schepetkin *et al.* 2015) as the concentration of OSM in the synovial fluid is known to be higher in RA compared to OA patients, although it is present at higher concentrations in OA synovial fluid compared to normal controls. Jnk2 knockout mice were also shown to be protected against cartilage degradation in a DMM model shown by a reduction in NVTEGE- neo-epitope detection compared to wild type mice and also a down-regulation in *Adamts4* expression, although *Adamts5* expression was unchanged (Ismail *et al.* 2016). Similar to our own observations there was no effect of JNK inhibition on cytokine induced down-regulation of aggrecan and IL-1 suggesting that this down-regulation occurs via JNK independent mechanisms (Ismail *et al.* 2015). Down-regulation of *ADAMTS4* was incomplete in IL-1α+OSM stimulated bovine chondrocytes in the presence of a JNK inhibitor, this observation correlated with residual aggrecanase and COMPase activity in JNK inhibitor treated explants, suggesting that this activity may be a result of ADAMTS-4.

Further assessment of COMP cleavage in its native cartilage bound state via treatment of metabolically inactive cartilage with recombinant ADAMTS-4. This indeed resulted in cleavage of COMP and generation of fragment sizes similar to those observed in IL-1α and IL-1α+OSM treated explants and human OA synovial fluid. Use of a commercially available ADAMTS-4/5 inhibitor that completely inhibited GAG loss and COMP degradation from IL-1α and IL-1α+OSM treated explants suggests a role for ADAMTS-4 in COMP degradation, although it must be noted that in the absence of inhibitor effects on other proteases this cannot be concluded. Furthermore, a mechanism similar to that observed for MMP mediated degradation of collagen, aggrecan degradation may be a pre-requisite for COMP degradation by endogenous ECM enzymes other than ADAMTS-4. The effects of the inhibitor upon the activities of ADAMTS-7 or 12 are unknown and should be determined, however, the lack of detectable ADAMTS-7 and ADAMTS-12 transcripts coupled with the known requirement of *de novo* synthesis in IL-1 mediated induction of COMP degradation

(Ganu *et al.* 1998) would make it unlikely that ADAMTS-7 and ADAMTS-12 are mediating COMP degradation in IL-1α and IL-1α+OSM treated explants in this work. The sensitivity of the non-reduced Western blot developed in this Thesis in its detection of strong fragmentation patterns using less than 3µl of synovial fluid suggests this may detect fragments in the serum or urine of patients and could therefore provide a non-invasive source of a marker for OA progression. Furthermore, COMP degradation occurred early in explant cultures when GAG loss was most evident suggesting COMP degradation may be an early event in OA that warrants further investigation as an early biomarker for detection of OA.

Surfen as a potential OA therapeutic

The work in Chapter 4 of this thesis identified, using molecular docking, many potential metalloproteinase targets of Surfen inhibition. Inhibition at concentrations shown to be below cytotoxic levels, was only validated *in vitro* for ADAMTS-4, MMP-2 and furin which highlights the limitations of molecular docking and the importance of experimental validation. This result is significant however, and should be considered when Surfen is applied as a tool using *in vitro* assays in its role as an HS antagonist. Surfen showed inhibition of GAG loss in week 1 of IL-1α stimulated explants but not at weeks 2 and 3, where GAG loss was unchanged and aggrecanase activity was actually increased in week 3 when assessed by BC-3 Western blot. In IL-1α+OSM stimulated explants no effect on GAG loss was observed and aggrecanase activity was increased. This was shown to be the result of increased expression of ADAMTS-4 in the presence of 15 µM Surfen in IL-1α+OSM treated chondrocytes. It is clear from gene expression data that Surfen appears to have differential effects dependent upon concentration with 7 µM attenuating the cytokine mediated increases in metalloproteinases and PGE2 but also reducing the expression of chondrogenic genes aggrecan and collagen type II at this concentration. Conversely, when treated with 15 µM Surfen we saw increases in expression of these matrix genes in all conditions and ADAMTS-4 in IL-1α+OSM conditions. This is suggestive of two independent mechanisms in the regulation of these genes at 7 and 15 µM. Indeed, the well described effects of Surfen upon increasing BMP signalling (Chapter 6 for discussion) would explain the effects on gene expression at 15 µM, however, this mechanism is not likely mediating the down-regulation of metalloproteinases. Attempts to ascribe a tentative potential mechanism to these observations led to scrutiny of PUBCHEM and CHEMBL High throughput screening (HTS) repositories to search for known activities of Surfen and particularly those complimentary to the published activities of Surfen such as Gβγ activation and HS antagonism. The most potent activity of Surfen of all bioactive assays listed was as an activator of 15-lipoxygenase 1 with an EC_{50} of 0.641 µM (Pubchem:AID 887 and SID 4252577). Lipid mediators of inflammation are well documented with the generation of PGE2 via COX2 and leukotrienes, such as LTB4 produced by 5-lipoxygenase being highly pro-inflammatory. PGE2 and LTB4 are increased in the synovial fluid of OA patients and levels correlated with increased 5-LOX activity in these patients. LTB4 was shown to increase the expression of IL-1β and TNFα in the synovial membrane, additionally glucocorticoid treatments were shown to down regulate 5-LOX expression but had no effect on 15-LOX. Additionally, inhibition of 5-LOX reduced induction of IL-6 and MCP-1 in response to TNFα in C57BL/6 mice (Lin *et al.* 2014).

Metabolites generated from AA by the action of 15-lipoxygenase 1, known to be expressed by

chondrocytes (Chabane *et al.* 2009), result in the production of anti-inflammatory lipoxins such as LXA4 . Through the GPCR ALX the lipoxin LXA4 acts as a potent stop signal to resolve inflammation (Chiang *et al.* 2006). Anti-inflammatory effects of lipoxins include the inhibition of PI3k/AKT, ERK1/2, STAT, NFκβ pathways and activation of PPARγ (Chandrasekharan and Sharma-Wali, 2015), which is implicated directly in resolution of inflammation. LXA4 at nanamolar concentrations was shown to reduce the expression of *IL6*, *MMP1* and *MMP3* in synovial fibroblasts stimulated with IL-1 further implicating lipoxins in reducing catabolic gene expression in response to pro-inflammatory conditions (Sodin-Semrl *et al.* 2000). In Surfen treated chondrocytes the rapid activation of ERK1/2 and AKT may result from Gβγ activation which leads to AA release from the phospholipid bilayer via PLA2 and PLC. Increased AA concentrations coupled with a potent Surfen mediated increase in 15-lipoxygenase 1 activity may result in increased concentrations of LXA4. The expression and activity of PLA2 in human aortic valves correlated with *BMP2* expression, this was confirmed by decrease in *BMP2* expression when PLA2 was inhibited using siRNA (Suzuki *et al.* 2014) suggesting AA pathways may be anti-inflammatory and also result in increased *BMP2* expression and signalling and therefore may provide a mechanism that explains both the anti-inflammatory and pro-chondrogenic effects of Surfen upon cytokine induced gene expression external to HS antagonism but further work is required to confirm. Interstingly, synovial fluid levels of AA and chondrocyte expression of PLA2 are reduced in OA patients (Vyver *et al.* 2018;Tsolis *et al.* 2015).

It is unclear why the biphasic effects upon *ADAMTS4* expression were so pronounced in IL-1α+OSM treated cells compared to cells treated with either cytokine alone, however, oncostatin M treatment resulted in an almost complete reduction of PPARγ expression in 3T3-L1 cells in a ERK1/2 dependant mechanism (Miyaoka *et al.* 2006) and therefore as the anti-inflammatory effects of LXA4 are mediated via a PPARγ dependant mechanism (Chandrasekharan and Sharma-Wali, 2015) then this would be abrogated in IL-1α+OSM culture conditions and *ADAMTS4* expression would be increased by both IL-1α induced NFκβ activity and Surfen induction of BMP signalling pathways. This is a speculative mechanism and would require extensive experimental validation but it does highlight the intricacies of cytokine combinations upon catabolic gene expression in chondrocytes and therefore the complexity of OA pathology *in vivo*.

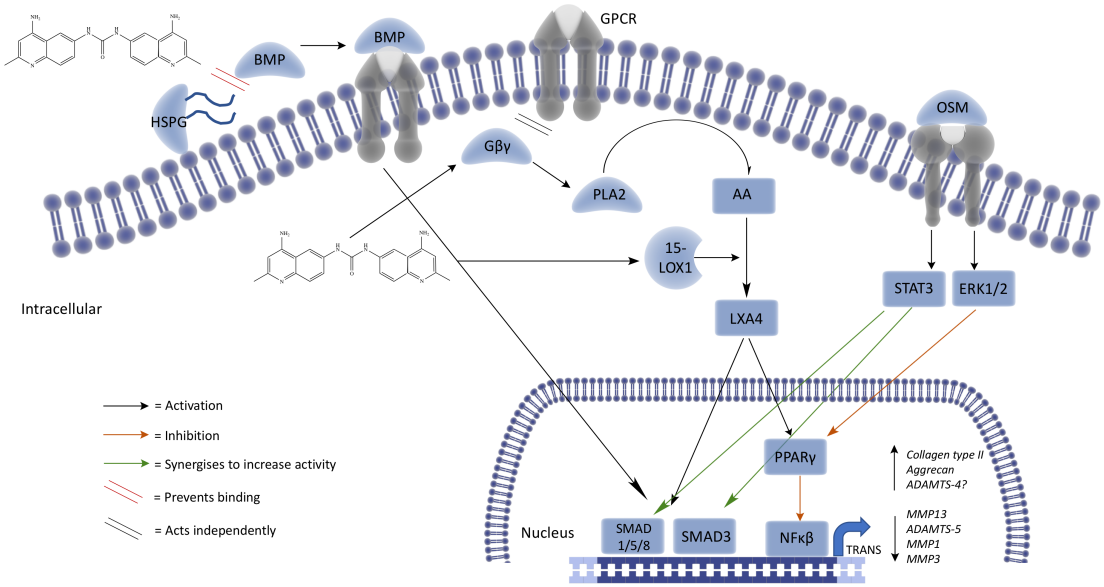

Figure 7.1 – Proposed speculative mechanism of Surfen actions upon gene expression in IL-1α+OSM treated bovine chondrocytes. Surfen treatment results in disassociation and activation of Gβγ, independent of GPCR ligand binding, resulting in activation of phospholipase 2A (PLA2) phospholipase C (PLC). PLA2 and PLC liberate arachidonic acid (AA) from phospholipid bi-layer store which is converted to LXA4 by 15-liopoxygenase 1 whose activity is increased directly by Surfen. LXA4 stimulates PPARγ expression, activation and nuclear translocation where it supresses NFκβ activity resulting in decreased expression of ADAMTS-5, PGE2, MMP1, MMP3 and MMP13. Oncostatin M (OSM) acting through OSMβ receptor or LIFR activates ERK1/2 that downregulates expression of PPARγ thereby reducing the inhibitory effects of LXA4 upon NFκβ mediated gene expression. LXA4 activates SMAD1/5/8 which proceeds to activate BMP regulated genes. Additionally, OSM activates STAT3 which can act synergistically with SMADS to increase the transcription of TGFβ/BMP target genes which are activated at higher doses of Surfen via extracellular HS interaction liberating endogenous BMP, from HSPGs, that subsequently binds BMPRs and activates SMAD1/5/8 leading to increased expression of aggrecan, collagen type II and ADAMTS-4.

Surfen target prediction by 3D and 2D similarity to compounds with known activities

Further complexity to the potential effects of Surfen is offered when using target prediction algorithms that predict potential activity through 3D and 2D chemical structure comparison to compounds with known and experimentally validated targets (Fig 7.2). Although the returned predictions did not offer a clear target that would be beneficial in cytokine treated chondrocytes there were several targets returned that closely reflect recent published activities of Surfen. For example, Surfen has been shown to prevent hyper-phosphorylation of tau, predicted to be pathological in Alzheimer's disease, the mechanism of this inhibition was propsed to be via HS interactions (Naini *et al.* 2018), although, Swiss-Dock target prediction results would suggest direct interactions are likely. Likewise, Surfen inhibition of calcium channels and the observed analgesic effcts in murine models of pain (Rivas-Ramirez et al., 2017) could potentially be mediated by TRPV family antagonism or interactions with opoid receptors (Fig 7.2).

The expanding number of published and potential target interactions of Surfen ensure it is an unlikely candidate to be taken forward for further studies but it may provide a suitable start point for chemical modification experiments to improve specificity.

Target	Uniprot ID	Gene code	ChEMBL ID	Probability	# sim. cmpds (3D / 2D)	Target Class
Microtubule-associated protein tau	P10636	MAPT	CHEMBL1293224		2944 / 58	Unclassified
Tyrosyl-DNA phosphodiesterase 1	Q9NUW8	TDP1	CHEMBL1075138		362 / 6	Enzyme
Inosine-5'-monophosphate dehydrogenase 2	P12268	IMPDH2	CHEMBL2002		42 / 22	Enzyme
Inosine-5'-monophosphate dehydrogenase 1 *(by homology)*	P20839	IMPDH1	CHEMBL1822		42 / 22	Enzyme
Transient receptor potential cation channel subfamily V member 1	Q8NER1	TRPV1	CHEMBL4794		144 / 60	Ion channel
Transient receptor potential cation channel subfamily V member 4 *(by homology)*	Q9HBA0	TRPV4	CHEMBL3119		69 / 60	Ion channel
Transient receptor potential cation channel subfamily V member 2 *(by homology)*	Q9Y5S1	TRPV2	CHEMBL5051		69 / 60	Ion channel
Orexin receptor type 1	O43613	HCRTR1	CHEMBL5113		25 / 2	Membrane receptor
Orexin receptor type 2	O43614	HCRTR2	CHEMBL4792		25 / 2	Membrane receptor
Mu-type opioid receptor *(by homology)*	P35372	OPRM1	CHEMBL233		58 / 21	Membrane receptor
Delta-type opioid receptor *(by homology)*	P41143	OPRD1	CHEMBL236		58 / 21	Membrane receptor
Kappa-type opioid receptor	P41145	OPRK1	CHEMBL237		58 / 21	Membrane receptor
Nociceptin receptor	P41146	OPRL1	CHEMBL2014		58 / 21	Membrane receptor
5-hydroxytryptamine receptor 6	P50406	HTR6	CHEMBL3371		38 / 6	Membrane receptor
Melanin-concentrating hormone receptor 1	Q99705	MCHR1	CHEMBL344		73 / 52	Membrane receptor

Figure 7.2 – Swiss-Dock target prediction of Surfen.

7.0.1 Conclusion

Although it is clear from the work in this thesis that Surfen shows potential in the inhibition of IL-1α stimulated cartilage degradation the temporal effects upon aggrecanase activity in IL-1α conditions and the observed induction of ADAMTS-4 in IL-1α+OSM conditions at higher doses are problematic. This coupled with the GAG matrix binding by Surfen demonstrated in this Thesis ensures that dosing within such a narrow therapeutic range is not trivial and furthermore, in the osteoarthritic joint, where the relative concentrations of cytokines at any one time are unknown, Surfen may exacerbate cartilage damage. Therefore it is unlikely that Surfen is a potential therapy for OA or indeed RA. However, there may be an application for Surfen as an initial protective therapy for the treatment of post-traumatic OA, where the contribution of IL-1 is considered significant although *in vivo* studies would be required to assess and issues of multiple activities described above would likely preclude Surfen from consideration as a therapeutic.

7.0.2 Future Work

The discovery of synergistic activation of SAPK/JNK by IL-1α and OSM in this Thesis will be followed by an investigation into the mechanisms of OSM induction of JNK in the presence of IL-1α. An initial focus will be made upon the ASK1 and TAK1 pathways that are both capable of increasing JNK activation. This work will be performed using small molecule inhibitors against these pathways. This work will further our understanding of cytokine signalling pathways and gene expression induction whilst also potentially identifying a therapeutic target up-stream of JNK that may be beneficial in conditions where cytokines of the IL-6 family interact with IL-1 or TNF-α.
The data in this thesis strongly implicates ADAMTS-4 in the degradation of COMP, however, validation is required. Future studies will focus on the use of RNAi, in particular Gapmers that do not required transfection agents and can be up-taken unaided by cells via a process called gymnosis. Initial studies performed using Gapmers to ADAMTS-4 during this thesis were unsuccessful, however time constraints prevented further testing and optimisation. The knock down of ADAMTS-4 but not 5 should allow for unequivocal confirmation that ADAMTS-4 is responsible for COMP degradation as it is predicted that ADAMTS-5 aggrecan degradation will proceed unhindered and therefore if GAG depletion is a requirement of COMP degradation this would also be apparent in this system.
The work in this thesis has identified anti-inflammatory and cartilage protective effects mediated by Surfen in conditions of IL-1α stimulation. However, as discussed above the effects upon aggrecanase activity, particularly in conditions of IL-1α+OSM preclude its consideration as an OA therapeutic. However, the bi-phasic effects observed upon gene expression do point to multiple mechanisms of Surfen action suggesting that anti-inflammatory effects and chondrogenic effects are potentially uncoupled. In collaboration with Professor Jeff Esko and Dr Ryan Weiss we have received a panel of Surfen analogues to be tested and potentially identify analogues that show an increased efficacy compared to the parent structure or display individual properties such as anti-inflammatory or driving chondrogenesis in isolation. This will further our understanding of Surfen mediated effects observed in this Thesis and may identify novel therapeutics or therapeutic targets for the treatment of OA.

Part II

Development and Assessment of Monoclonal Antibody Targeting Moieties for Intra-articular Drug Delivery Systems

Chapter 8

Development and Assessment of Monoclonal Antibody Targeting Moieties for Intra-articular Drug Delivery Systems

8.1 Introduction

This PhD was conducted as part of the MSCA-ITN, TargetCaRe whose aim was the development of targeted intra-articular drug delivery systems (DDS) for the treatment of OA. As a part of this consortium this PhD was tasked with the discovery of suitable targets and development of monoclonal antibodies and conjugation strategies for DDS developed elsewhere in the consortium to enable targeting of sustained release DDS to specific joint compartments to reduce frequency of administration and increase bioavailability of therapeutics to target cells.

8.1.1 Requirement for drug delivery solutions in OA

At present there are no disease modifying therapeutics available for the treatment of osteoarthritis. Lack of efficacy of current therapeutics is partly attributed to poor delivery and therefore bioavailability of drugs at the target site. The overall aim of a drug delivery system is the improvement of the therapeutic efficacy and reduction of off-target effects of pharmaceuticals. This can be achieved by the concentration of pharmaceuticals in drug carriers combined with passive or active targeting to ensure drug release at the site of disease. The use of sustained release drug delivery systems increases the bioavailability of drugs, reduces the frequency of administration and is particularly important for drugs with a low therapeutic index. Basic requirements of a successful drug delivery system that must be met are; Biocompatibility, efficient drug encapsulation and effective release of drug at site of action. Common factors that determine the design of drug delivery systems will be discussed highlighting the unique requirements and opportunities in design of drug delivery systems for treatment of joint disease and specifically OA.

8.1.2 Modes of administration

The avascular nature of the cartilage matrix precludes systemic delivery via oral or intravenous routes, hence administration is commonly intra-articular, for example in the use of corticosteroids (Arroll and Goodyear-Smith, 2004). Local administration bypasses many of the obstacles of systemic administration, such as requirement of stealth components for avoidance of the mononuclear phagocyte system (MPS), for example Kuppfer cells in the liver, which rapidly remove drug delivery systems from the circulation (Salmaso and Caliceti, 2013). Clearance can still occur in the joint due to resident macrophages and fibroblasts in the synovium (Butoescu et al, 2009) but clearance is likely reduced compared to the sequestration observed at sites such as liver or spleen with systemic administration. Some success, however, has been observed *in vivo* using systemic administration. Near-infrared (NIR) dye loaded liposomes bearing a collagen type II specific mAb as a targeting moiety for diseased tissue, due to potential exposure of collagen type II at the cartilage surface after protease induced matrix degradation, were administered intravenously to young and old Dunkin-Hartley guinea pigs, a strain that spontaneously develops OA, with increased accumulation observed in the diseased joint of the older animals. In this system, fluorescence was also detected in both the liver and spleen of young and old animals (Cho *et al.* 2014) showing clearance of liposomes from the circulation by the MPS thereby highlighting the potential for off-target effects and the requirement for stealth in the design of systemic drug delivery systems. Systems that have a suitable biodistribution profile and targeting mechanism also show potential for systemic administration, such as the use of fulranumab and tanezumab (anti-NGF) therapeutic antibodies which have a plasma half-life of 22-25 days and pico-molar affinity for NGF and are used to block pain (Schnitzer and Marks, 2015). IgG has a naturally long circulatory half-life, due to recycling by the neonatal Fc receptor (FcRn) (Schnitzer and Marks, 2015), and an intrinsic targeting capability therefore is suitable for use as a systemically administered therapeutic or antibody-drug conjugate, particularly in PEGylated systems that further increase the circulatory half-life through prevention of opsonisation and clearance (Ebbesen *et al.* 2013). For non-antibody based therapeutics the ability to directly administer to joints shows promise as a simple and effective method for delivering high concentrations of drug directly to disease sites. However, rapid clearance of therapeutics from the joint hamper current therapies such as corticosteroids, where administration directly to the joint results in intra-articular half-lives of less than 12 hours (Evans *et al.* 2014) corresponding with data showing peak serum levels of the corticosteroid methylprednisolone within 2-12 hours of intra-articular administration (Armstrong *et al.* 1981). The technique of intra-articular injection is not without complications, such as potential for infection, requirement for trained medical staff and low patient compliance (Brandt *et al.* 2000). The use of drug delivery systems could negate or minimise these issues through reducing the frequency of injections. Drug delivery systems to be developed during this PhD will be designed solely for intra-articular administration.

8.1.3 Drug release profile

To reduce the frequency of intra-articular injections, a drug delivery system for OA should incorporate a sustained drug release profile (Fig 8.1). This can be achieved through the use of biodegradable polymer systems such as PLGA that hydrolyse over time into glycolic and lactic acid that is cleared from the body (Ko *et al.* 2013). The use of parathyroid hormone (aa's 1-34)

loaded PLGA particles confirmed a sustained release profile *in vitro* and a sustained therapeutic effect in a rat OA model compared to parathyroid administered alone (Eswaramoorthy *et al.* 2012). Other, more complicated, systems rely upon the use of polymeric systems with cross linkers that are cleavable by reactive oxygen species (ROS) (Saravanakumar *et al.* 2016), UV light or enzyme cleavable linkers which can provide an "on-demand" drug release (de la Rica *et al.* 2012). The use of "slow" (hydrazone) or "fast" (ester) acting cleavable linkers delayed the release of dexamethasone conjugated to avidin and therefore prolonged the therapeutic effect in an OA explant model system (Bajpayee *et al.* 2016). The use of linkers cleavable by enzymes relevant to OA has shown some success in collagen-mimetic hydrogels cross-linked by MMP-7 cleavable peptide sequences mediating localised cell-induced degradation (Parmar *et al.* 2015).

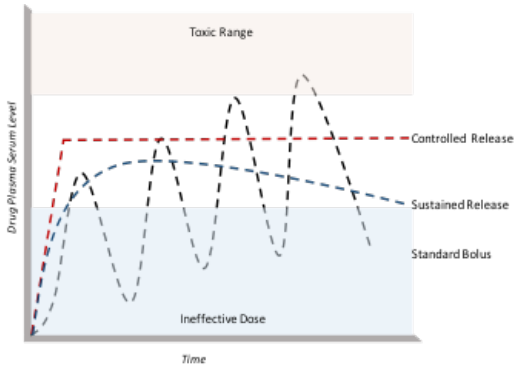

Figure 8.1 – Drug release profiles of drug delivery systems.

8.1.4 Particle size

Standard drug delivery systems for intravenous delivery are often termed nanocarriers due to their size of 50nm to 300nm. This optimum size is derived from the need to avoid cells of the MPS, which more efficiently phagocytose larger particles (Champion *et al.* 2008) and to exploit the leaky vasculature at tumour sites, termed the enhanced permeability and retention (EPR) effect, for passive targeting (Fang *et al.* 2011). Particles greater >6μm are avoided for systemic delivery due to filtration of the particles in the capillary bed of the lungs (Chao *et al.* 2010). The unique anatomy of the synovial joint coupled with local administration negates many of the factors determining the size of current systemic nanocarriers. Micrometre scale drug delivery particles have shown some success due to slower clearance from the joint (Kavanaugh *et al.* 2015), however, for the direct targeting of chondrocytes within the cartilage matrix particles smaller than 50nm are recommended due to the estimated 60nm space between collagen fibres. Polymeric particles of 38nm have shown cartilage penetration whereas particles of 96nm did not enter the cartilage matrix (Rothenfluh *et al.* 2008). However, a recent study showed cartilage penetration of poly cationic particles greater than 100nm (Perni and Prokopovich, 2017), therefore, the size of a drug delivery system must be carefully considered dependent upon location of therapeutic target and its trafficking in cartilage should be assessed where chondrocytes are the therapeutic target.

8.1.5 Retention and targeting

Despite local administration into the joint space, targeting moieties are likely required as it has been shown that small molecules/particles are rapidly cleared by diffusion and larger particles, although showing a greater retention with increasing size, are cleared through the lymphatic system (Evans *et al.* 2014). This is pertinent to OA as many of the therapeutics currently administered directly to the joint show reduced efficacy and systemic effects due to drainage of drug to the circulation. The steroidal nature of many OA therapeutics makes systemic off-target effects potentially harmful.
A mechanism to increase retention in the joint by specific targeting or indirect mechanisms e.g. charge based interactions or size is therefore required to anchor the drug delivery system within specific regions of the joint creating a drug depot combined with sustained release. Charge based interactions have shown success in the increased retention of positively charged avidin compared to its neutral (deglycosylated) analogue in the cartilage matrix, however, in models of OA, with GAG depletion, this charge based retention was abrogated to less than 12% of that retained in non-OA tissue (Bajpayee *et al.* 2014) suggesting that passive, charge based interactions are not sufficient for nanoparticle retention in osteoarthritic cartilage and therefore more specific forms of targeting are required. The use of phage display technologies identified a peptide sequence (WYRGRL) showing specific binding of collagen type II which when subsequently conjugated to 38nm co-polymer [poly(propylene sulphide) and Pluronic] nanoparticles mediated increased accumulation (72 fold increase compared to scrambled peptide) and retention (little to no clearance observed in 96 hours) in cartilage explants (Rothenfluh *et al.* 2008). This finding offers the potential for creating a drug reservoir within the cartilage matrix itself, using targeting moieties specific to matrix components, thus reducing frequency of administration and increasing therapeutic bioavailability to the thus far hard to reach chondrocytes. In addition to increased retention targeting allows for directing therapeutics to specific sites within the joint for example targeting chondrocytes within cartilage matrix or macrophages and fibroblasts resident in the synovium. It is proposed that many of the catabolic factors implicated in OA are in fact released from the synovium such as pro-inflammatory cytokines and degradative enzymes from the synovial macrophages and fibroblasts. This highlights the importance of targeted, specific therapies and the treatment of OA as a whole joint disease.

8.1.6 Targeting of synovial macrophages

The contribution of activated synovial macrophages in joint diseases, particularly RA but increasingly viewed as important mediators of inflammation in OA, present them as suitable targets for depletion or anti-inflammatory therapies to ameliorate the symptoms of inflammation and slow disease progression (Bondoson *et al.* 2010). Therefore, monoclonal antibodies were developed towards resident synovial macrophages for subsequent conjugation to drug delivery systems to enable direct targeting and reduce systemic effects of therapeutics upon intra-articular administration. The contribution of the cells of the synovium in OA pathology is well documented. The presence of an inflamed synovium with increased leukocyte infiltration, particularly macrophages, correlate with presence of inflammatory OA and pain scores in OA patients (Scanzello and Goldring, 2012). The production of pro-inflammatory mediators such as PGE2, iNOS and pro-inflammatory cytokines such as TNF-α, IL-1β and OSM stimulate the degradation of cartilage through stimulating chondrocytes towards a pro- catabolic phenotype in addition to direct production of metalloproteinases by

macrophages themselves (Sokolove and Lepus, 2013). The efficacy of NSAIDs and corticosteroids in reducing pain and inflammation (Østergaard and Halberg, 1998) is potentially attributed to their anti- inflammatory effects on macrophages in the synovium as evidenced by reduced synovial inflammation after therapy (O'Neil *et al.* 2015). However, a negative effect has been shown upon chondrogenic gene expression by the application of corticosteroids such as triamcinalone acetate (TAA), that has been employed as a model drug for initial *in vitro* synovium culture and *in vivo* assays within the TargetCaRe project. Therefore the ability to direct DDS to macrophages in the synovium will increase efficacy whilst reducing off-target effects on chondrocyte gene expression. CD64 (also known as FcγRI) was selected as a potential target for therapies directed at macrophages in the synovium due to the lack of its expression on fibroblast-like synoviocytes and its increased expression on activated macrophages, particularly the pro-inflammatory M1 subtype (Hristodorov *et al.* 2015). This allows for targeting of inflammatory mediators whilst reducing the off target effects on M2 anti-inflammatory subtypes and fibroblast-like synoviocytes. CD64 is a high affinity Fc receptor present in the cell membrane that binds exposed Fc regions of IgG's bound to antigens to mediate phagocytosis and immune cell activation (Stewart *et al.* 2014). In humans there are 7 IgG Fc receptors; FcγRI (CD64), FcγRIIA, FcγRIIB, FcγRIIC, FcγRIIIA, FcγRIIIB and the neonatal Fc receptor (FcRN). In mice there are 5 IgG receptors; FcγRI, FcγRIIB, FcγRIII, FcγRIV and FcRN Antibody subtypes (Bruhns, 2015). The development of a monoclonal antibody that is capable of binding native CD64 in both human and mouse whilst avoiding non-specific bindings through Fc interactions is made difficult due to the observed differences in specificity in IgG subtype Fc binding of human and murine CD64 for example an IgG2a subtype would be preferential in human to avoid Fc binding but conversely would be the subtype with the highest Fc affinity to murine CD64 (Bruhns, 2015). Therefore, to develop an anti-human and anti-mouse CD64 monoclonal antibody using murine hybridomas requires more stringent characterisation techniques than usually applied. The development of an IgM monoclonal antibody may be beneficial in avoiding the non-specific Fc interactions predicted with IgG class antibodies due to the lack of any IgM Fc receptor on monocytes or macrophages in both mouse and humans.

8.1.7 Aims and Objectives

Aims

The overall Aim of Chapter 8 was the development and characterisation of mAb based targeting moieties for conjugation to DDS that may aid in targeted delivery to specific joint compartments and furthermore, may increase retention of DDS proximal to therapeutic target site.

Objectives

This Aim was investigated by completion of the following Objectives;

1. DDS trafficking and diffusion into cartilage explants will be assessed using a unidirectional chamber system to determine if DDS developed within the TargetCaRe consortium are able to penetrate articular cartilage and thereby deliver therapeutics directly to chondrocytes.

2. Potential cartilage surface targets will be identified and validated for retention of micrometre

sized DDS at the cartilage surface. MAbs will be generated and conjugation strategies developed for micrometre sized DDS.

3. Novel mAbs will be generated that specifically bind both human and murine FCγRI/CD64 for subsequent targeting of M1 macrophages by DDS.

8.2 Materials and Methods

8.2.1 Nanoghost trafficking assays

Nanoghosts are nanosized membranous drug delivery vesicles generated by hypotonic treatment of MSCs to remove cellular contents whilst leaving membrane and membrane proteins intact a preocess originally used on red blood cells with the resultant 'empty'cells termed 'ghost cells'. Ghosted MSCs are then sonicated to produce nanovesicles (Kaneti *et al.* 2016). Fluorescent 1,1-Dioctadecyl-3,3,3,3-tetramethylindodicarbocyanine (DiD) (Ex.644nm, Em. 665nm) labelled Nanoghosts were produced by the Machluv lab at Technion University, Haifa as per previously described (Kaneti *et al.* 2016). Cartilage was harvested from the metacarpophalangeal joints of 18 month old cows, punched with a 6mm biopsy punch and cultured in SCM for 2 days prior to addition of IL- 1α (10ng/ml) + OSM(50ng/ml) or culture media alone for 5 days. Explants were cut in half and secured into the unidirectional chamber system (Perni and Prokopovich, 2017) using sterile silicone glue followed by addition of Nanoghosts (35μg/ml total protein assessed by BCA) in SCM media to the superficial side of cartilage and media to the basal chamber for 24 hours (Fig 8.2). Explants were then washed in PBS, snap frozen in OCT (Sigma) and cryosections of 20μm taken. Sections were fixed in 95% ETOH for 10 mins or air fixed prior to DAPI staining, mounting and immediate imaging. Confocal microscopy images were taken using Zeiss DM6000.

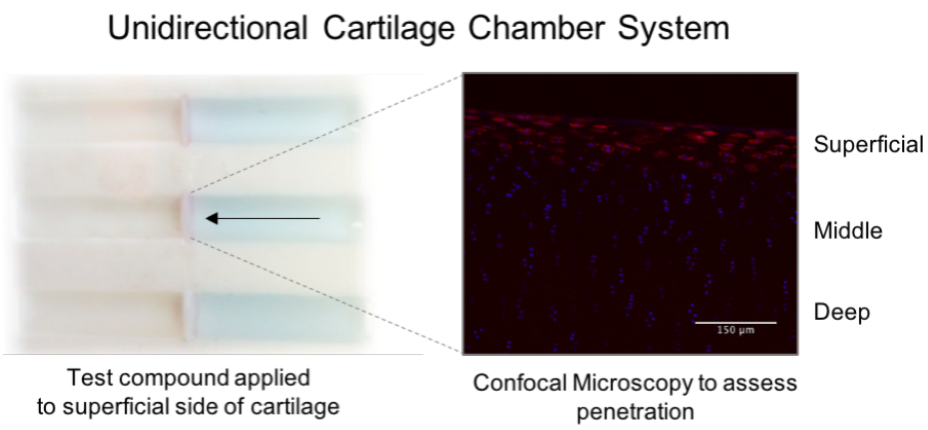

Figure 8.2 – Development of a unidirectional cartilage chamber system. Chamber (left) allows for the study of trafficking of macromolecules or drug delivery systems within cartilage after application to the superficial surface only and therefore replicating conditions observed *in vivo*. Sectioning and confocal microscopy allows for assessment of test compound/drug delivery system cartilage penetration, Blue=Dapi, Red=DiD labelled test compound (right).

8.2.2 Lubricin immunofluorescence

Bovine cartilage was harvested from the metacarpophalangeal joint of 18 month old cows then biopsies taken followed by culture in SCM ± IL-1α (10ng/ml) + OSM (50ng/ml) (Peprotech). for the indicated time points. Explants were harvested, snap frozen in OCT media (Sigma) prior to cryo-sectioning. 20μm sections were mounted on poly L-lysine slides (Thermo) and blocked in 5% (w/v) BSA in PBS for one hour followed by incubation with anti-lubricin monoclonal antibody 3A4 overnight at 4°C. Sections were then washed 3 x 5minutes in PBS+0.05% (v/v) Tween- 20 followed by incubation for one hour with Alexafluor633 anti-IgG secondary (Thermo) in 1%BSA/PBS and washing 3 x 5 minutes in PBS+0.05%Tween-20. Slides were analysed using a Zeiss DM6000 confocal microscope. GAG loss was confirmed by Safranin O staining, briefly, sections were incubated in 0.1% (w/v) Safranin O (Sigma) solution for 5 mins followed by dehydration in 95% ethanol, clearing in xylene followed by mounting in DPX resinous mounting media (Sigma) and analysis by bright field microscopy.

8.2.3 Conjugation of anti-lubricin antibody 3A4 to 1μm carboxylate latex beads

1μm fluorescent carboxylated latex beads (Thermo) were conjugated with anti-lubricin antibody 3A4 or isotype control murine IgG (Sigma) using EDC (1-ethyl-3-(3-dimethylaminopropyl)carbodiimide hydrochloride) and s-NHS (N-hydroxysulfosuccinimide sodium salt) chemistry. 100μl of beads at 10% w/v were added to 900μl of activation buffer (50 mM MES, pH 6.0) and washed twice by centrifugation at 10,000g for 5 minutes. 24μl of 200 mM EDC (Sigma) and 200μl of 200 mM s-NHS (Sigma) were added to the bead solution for 30 minutes. Beads were then washed twice in activation buffer prior to resuspension in 700μl activation buffer and addition of 300μl of a 2mg/ml solution of antibody 3A4 in activation buffer. Beads and antibody solution were then incubated with end over end mixing for 2.5 hours. 30μl of ethanolamine was then added to quench the reaction followed by washing and resuspension of beads in blocking buffer [50 mM Tris, pH 8.0, 1% (w/v) BSA] and incubation for 2 hours with end over end mixing. Beads were then washed in blocking buffer prior to use.

8.2.4 Conjugation of anti-lubricin antibody3A4 to microsomes

Microsomes comprising of a calcium carbonate core encased in polydopamine in a layer by layer method were synthesised by Marco Sorbona of Imperial College London (ICL). Conjugation of antibody to polydopamine beads proceeds though reaction between primary amines present on antibodies and catechol groups present on polydopamine. Microsomes and antibody 3A4 (0.2mg/ml) were incubated in 10 mM Tris-HCl pH 7.5 for 5 hours prior to washing 3 times in PBS by centrifugation at 1000 x g to remove unbound antibody. Microsomes alone or conjugated to 3A4 were incubated for 30 minutes with Alexafluor 633 anti-IgG (Thermo) prior to washing three times in PBS and resuspension in PBS+1%BSA. Flow cytometry was performed using a FACS Canto (BD Bioscience) with untreated microsomes used to gate for forward scatter, side scatter and fluorescent background. Microsome fluorescence was assessed using excitation 633nm and emission quantified in APC channel with mean fluorescence of 10,000 events plotted.

8.2.5 Microsome binding to cartilage explants

4mm diameter bovine articular cartilage explants were harvested as described in section 2.1.2. Anti-lubricin antibody (3A4) or murine isotype control IgG from whole serum (Sigma) were conjugated to microsomes as described in section 8.2.4. Lubricin was stripped from the surface of explants using NaCl extraction for 30 minutes (Jones *et al.* 2007). To recover lubricin at the surface of stripped explants, bovine synovial fluid was added to explants for 1 hour. An equal volume, containing equal number of microsomes, of 3A4 or Isotype control conjugated microsomes were then added to explants prior to incubation overnight, washing 3x 10 minutes in PBS and assessment of binding by bright-field microscopy.

8.2.6 Monoclonal antibody generation

Generation of hybridomas was performed using a modified protocol of that developed by Kohler and Milstein (Kohler and Milstein, 1975). Schematic of workflow is shown in Figure 8.3. Briefly, three 6-8 week-old female BALB/c mice were immunised with the ovalbumin conjugated synthetic peptide, CGGTKAVITLQPPWVS (Altabioscience), corresponding to to aa's 20-32 of human FcγR1 and aa's 30-42 of *Mus musculous* FcγR1 or ovalbumin conjugated CGGVLKRSPELELQVLG, which corresponding to aa's 270-283 and aa's 278-291 of human and murine FcγR1, respectively. Peptides in PBS (200μg/ml) were mixed with Fruend's complete adjuvant (Sigma) and 0.05ml injected in mice as per immunisation scheme in the lateral thoracic, inguinal regions or both (Fig 8.4). The second immunisation (day 3) was performed in incomplete adjuvant (Sigma) and all subsequent immunisations (day 6, 9 and 12) consisted of peptide in PBS. At the end of immunisation mice were sacrificed and lymph nodes harvested. Nodes were ruptured to disassociate cells and then incubated with an equal number of P3-X63-AG8 (IgG- and HGPRT-) murine myeloma cells in the presence of 20% PEG 4000 (Sigma) to aid fusion (Baker *et al.* 1982). Cells were then subjected to limiting dilution in HAT culture media (HAT-RPMI + 20% FBS, 2mM Glutamine, 0.01 unit/ml PenStrep, 0.001 unit/ml Fungizone, 1x HAT and 0.001 M 2- mercaptoethanol) into 8 X 24 well plates and incubated at 37°C in 10% CO_2. After two weeks of culture, media was then assessed by ELISA against the immunising peptide and alternative peptide to screen for cross-reactivity to oval-albumin or the link peptide-CGG.

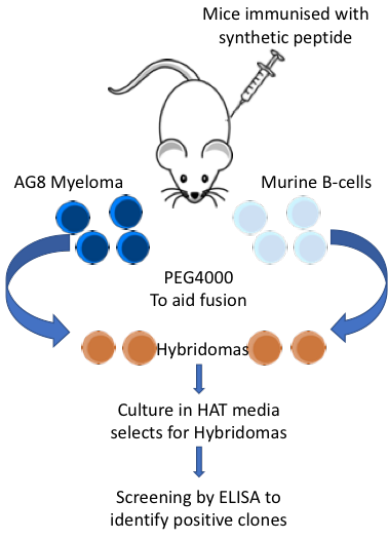

Figure 8.3 – Schematic of workflow and principle of monoclonal antibody generation. Lymphocytes harvested from immunised mouse are fused in the presence of PEG 4000 to IgG- /HGPRT- AG8 myeloma cells. Non-fused myelomas die in culture in presence of HAT selection media and primary lymphocytes naturally die in prolonged culture therefore only hybridomas survive the selection process.

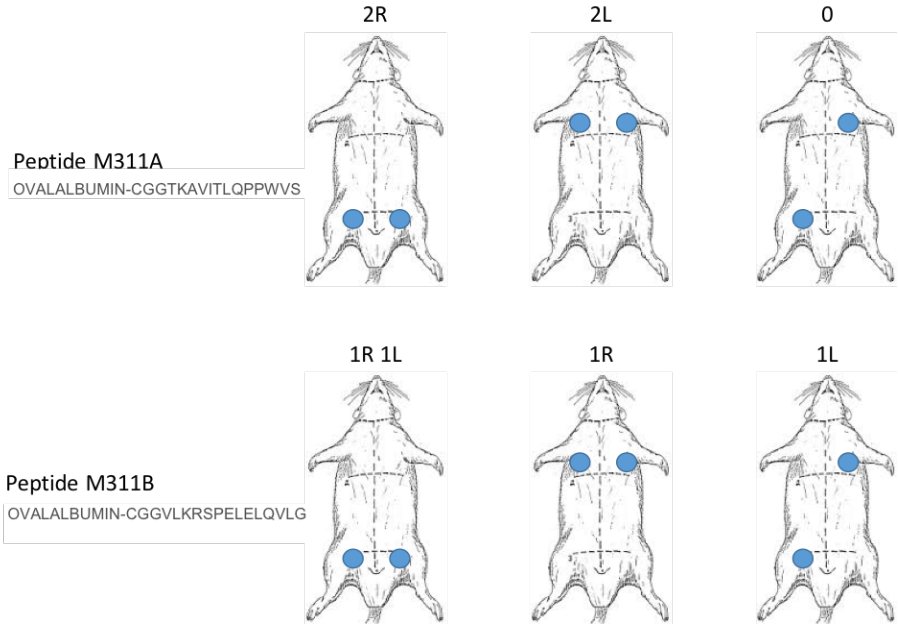

Figure 8.4 – Injection scheme for generation of CD64/FcγRI monoclonal antibodies. Scheme shown for each immunising peptide. Blue circles depict injection sites.

8.2.7 Monoclonal antibody ELISA

Clear 96 well plates were coated overnight at room temperature with 100µl of 5µg/ml immunising peptide in PBS per well then washed with 3x with TSA prior to blocking with 1% BSA/TSA for 1 hour at 37°C. Wells were then incubated with hybridoma culture media for 1 hour at 37°C. Plates were then washed 4x with TSA followed by addition of Alkaline phosphatase conjugated anti-mouse (H+L) secondary (Promega) diluted 1:5000 in 1% BSA/TSA for 1 hour at 37°C. Wells were then washed 4x with TSA and developed using pNPP substrate (Sigma) 1 tablet per 5ml in AP-ELISA buffer (10 mM Diethanolamine, 0.5 mM MgCl2, pH 9.8) (all Sigma). Absorbances were read at 405nm using FluoSTAR Optima plate reader (BMG Labtech) after plates were incubated for 30 minutes at 37°C. 2.3.8 Hybridoma Culture Clones determined positive for the immunising peptide by ELISA were transferred from the fusion 24 well plate to 10cm petri dishes for up-culture in RPMI + 20% FBS, 2mM Glutamine, 0.01 unit/ml PenStrep, 0.001 unit/ml Fungizone, and 0.001 M β-mercaptoethanol (FHM). Media was refreshed as required and upon confluence cells were sub-cultured. Hybridoma lines were secured once culture had reached three confluent 10cm petri dish of cells. Cells were removed, media removed by centrifugation at 300g for 10 minutes prior to addition of freezing media (FBS+10%DMSO). Secured lines were then stored at -80° until required. Recovery of cells was performed by thawing rapidly in a 37°C water bath before adding cells to pre-warmed DMEM, centrifugation at 300g for 10 minutes and resuspension in FHM in 10cm petri dishes.

8.2.8 Monoclonal antibody isotyping

A direct ELISA based method was employed to detect the isotype of monoclonal antibodies produced by hybridomas. Clear 96 well plates were coated overnight at room temperature with 100µl of 5µg/ml immunising peptide in PBS per well then washed with 3x with TSA prior to blocking with 1% BSA/TSA for 1 hour at 37°C. Wells were then incubated with hybridoma culture media for 1 hour at 37°C. Plates were then washed 4x with TSA followed by addition of AP-conjugated mouse isotype specific antibodies (Southern Biotech) (anti-IgG1, anti- IgG2a, anti-IgG2b, anti-IgG3, anti-Kappa or anti-Lambda) in 1% BSA/TSA for 1 hour at 37°C. Wells were then washed 5x with TSA before the addition of pNPP alkaline phosphatase substrate (Sigma) in AP-ELISA buffer and incubation of plates for 30 minutes at 37°C. Absorbance of wells was read at 405nm using FluoSTAR Optima plate reader (BMG Labtech).

8.2.9 Assessment of serum free culture of hybridomas

The presence of bovine IgG in FBS contained in full hybridoma media complicates downstream purification of monoclonal antibodies due to co-isolation of bovine IgG when purifying monoclonal murine IgG using protein G spin columns. Therefore, the suitability of chemically defined media (CDM) and serum free hybridoma (SFM) media was assessed. Cells were thawed prior to seeding of equal cell numbers to T-75 flasks containing SFM or CDM and culture for 1 week. In parallel, equal cell numbers were seeded in full hybridoma media. Growth of hybridomas was assessed visually using bright field microscopy throughout the culture period. Media was harvested and assessed for monoclonal antibody production by ELISA as per section 2.3.4.

8.2.10 FcγR1/CD64 Western blot

240ng of His tagged human recombinant FcγR1/CD64 (Sinai Biological) was loaded per lane on 4-12% Bis-Tris gels (Invitrogen) under reducing and non-reducing conditions and run at 150V for approximately 1 hour followed by transfer to nitrocellulose membranes, blocking with 5% BSA in TSA and blotted for 1 hour with undiluted media from hybridoma cultures. Blots were then washed 3x 10 minutes in TSA, prior to the addition of AP-conjugated anti-mouse (H+L) secondary (Promega) diluted 1:5000 in 1%BSA/TSA for one hour. Blots were washed 3x 10 minutes in TSA and developed colourmetrically using BCIP/NBT (Promega) as described fully in 2.1.15

8.2.11 FcγR1/CD64 immunofluorescence

THP-1 cells were maintained in Full RPMI media (Table 2.1). THP-1 cells were seeded in 8 well chamber slides at 20,000 cells per well, incubated with PMA (100ng/ml) for 24 hours followed by treatment with IL-4 (100ng/ml) or IFNg (100ng/ml) for 3 days to decrease or increase FcGR1 expression, respectively. J774A2 cells were maintained in Full DMEM (Table 2.1). J774.2 cells were seeded at 20,000 cells per well. It has been shown previously that J774.2 cells constitutively express FcγR1 and therefore no stimulation was required for this cell type. After treatments cells were fixed in 4% PFA or cold 95% ETOH +5 % glacial acetic acid for 10 mins followed by washing and blocking in 5% BSA/PBS for 1 hour. After blocking undiluted media from hybridoma cultures [where CDM cultured hybridomas were used then a final concentration of 5% BSA (w/v) was added to reduce non-specific binding] was added for 1 hour followed by washing 3 x 5 minutes with PBS + 0.05% Tween 20 and incubation with Alexafluor 564nm anti-IgG (Thermo) or Alexafluor 488nm anti-IgM (Thermo), dependant upon isotype of hybridoma being assessed, for 1 hour followed by PBS washing. Cells were then mounted with fluoroshield +DAPI mounting media (Sigma) and analysed by confocal microscopy using a Zeiss DM6000. Cells treated with secondary alone served as a negative control for the determination of gain settings.

8.2.12 FcγR1/CD64 Flow Cytometry

THP-1 cells were incubated with PMA (100ng/ml) for 24 hours followed by treatment with IL-4 (100ng/ml), IFNg (100ng/ml) or control media for 3 days followed by mechanical detachment and counting. 100,000 THP-1 or J774.2 cells were used per analysis, blocked with 5% BSA/PBS followed by incubation with undiluted media from hybridoma cultures followed by washing with PBS and incubation with Alexafluor564nm anti-IgG (ThermoFisher) or Alexafluor488nm anti-IgM (ThermoFisher) for 1 hour followed by PBS washing. For peptide inhibition assays, 1ml hybridoma culture media was incubated with 50μg of immunising peptide for 30 mins prior to application as primary antibody. Murine IgG and IgM from whole serum (both Sigma) were used as primary controls. Analysis performed on a FACS Canto (BD Bioscience) flow cytometer and data analysed by Kaluza (Beckman Coulter).

8.3 Results

8.3.1 Nanoghost trafficking in articular cartilage

The delivery of therapeutics directly to chondrocytes within the cartilage matrix requires the diffusion of the drug delivery system (DDS) through the superficial zone and into the dense cartilage matrix therefore trafficking assays were performed using a unidirectional chamber developed at CU. Nano-ghosts (NGs) developed by the Machluv lab and derived from MSCs that have been subjected to hypotonic treatment to remove cellular contents prior to sonication, are the smallest DDS (circa 200nm hydrodynamic size) in the TargetCaRe repertoire and due to their lipid bilayer structure derived from the parent MSCs are predicted to be deformable which may aid penetration of cartilage. Bovine cartilage explants were incubated for 3 days in control media or IL-1α (10ng/ml)+OSM (50ng/ml) to induce GAG loss and therefore represent early stage OA cartilage where therapeutic interventions are most likely to be successful. Toluidine blue staining of explants and DMMB assay to quantify GAG loss to media confirmed GAG depletion in these explants (Fig 8.5 A+B). Collagen content appeared unchanged when assessed by picosirius red staining of sections as expected in the short 3 day culture period (Fig 8.5 C+D). Confirmation of GAG loss from IL-1+OSM treated explants was performed by DMMB assay of explant culture media (Fig 8.5E).

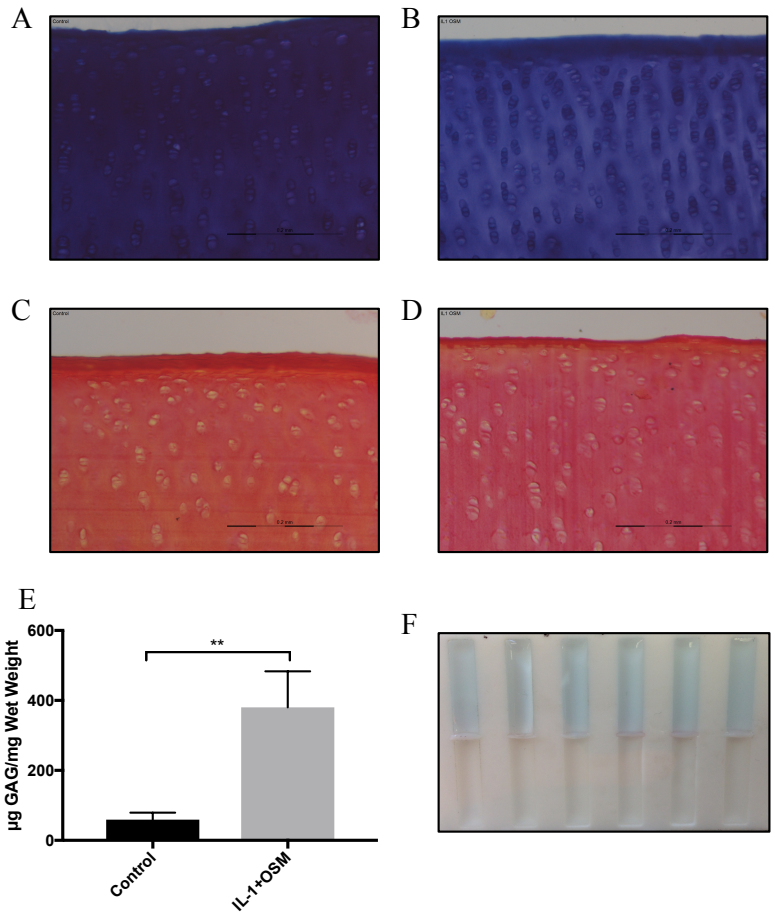

Figure 8.5 – Assessment of cytokine pre-treatment of bovine cartilage explants prior to Nanoghost trafficking assay. Bovine cartilage explants were cultured in the presence of IL-1α (10ng/ml) + OSM (50ng/ml) for 3 days in preparation for Nanoghost trafficking assay. Toluidine blue staining to assess for GAG loss shown in control (A) and IL-1α+OSM (B) explants. Picosirius red staining of collagen in sections of control (C) and IL-1α+OSM explants (D). GAG loss assessed by DMMB assay, data shows mean and *sd* of three explants (E). Image showing cartilage explants fixed into unidirectional chamber and incubated with Nano-ghosts (F).

Nanoghosts do not penetrate intact or GAG depleted bovine cartilage explants

Incubation of control and IL-1α+OSM treated explants showed no penetration of NGs into cartilage after 24 hours suggesting that NGs are too large to penetrate even under conditions of GAG depletion in explants. The presence of fluorescence signal at the surface of explants after washing suggested that NGs were bound to the surface and to confirm that NGs were intact and fluorescent signal detected was not a result of diffusion of free DiD into cartilage, explants were treated with ethanol to lyse intact NGs at the surface. Ethanol treatment reduced staining at the outermost surface but resulted in diffuse staining within the superficial zone suggesting that lysis of intact NGs releases the lipophilic dye which then diffuses into the superficial zone. In this study cartilage degradation was minimal and it must be noted that extended GAG and collagen depletion may permit transport though due to the lack of therapies capable of reversing damage at this later disease stage this was not explored further. This assay confirms that the DDS developed within TargetCaRe are too large to penetrate cartilage and therefore for the targeting of therapeutics to chondrocytes it was required to validate cartilage surface targets that may be employed to anchor DDS at the surface for subsequent degradation and release of therapeutics proximal to chondrocyte targets.

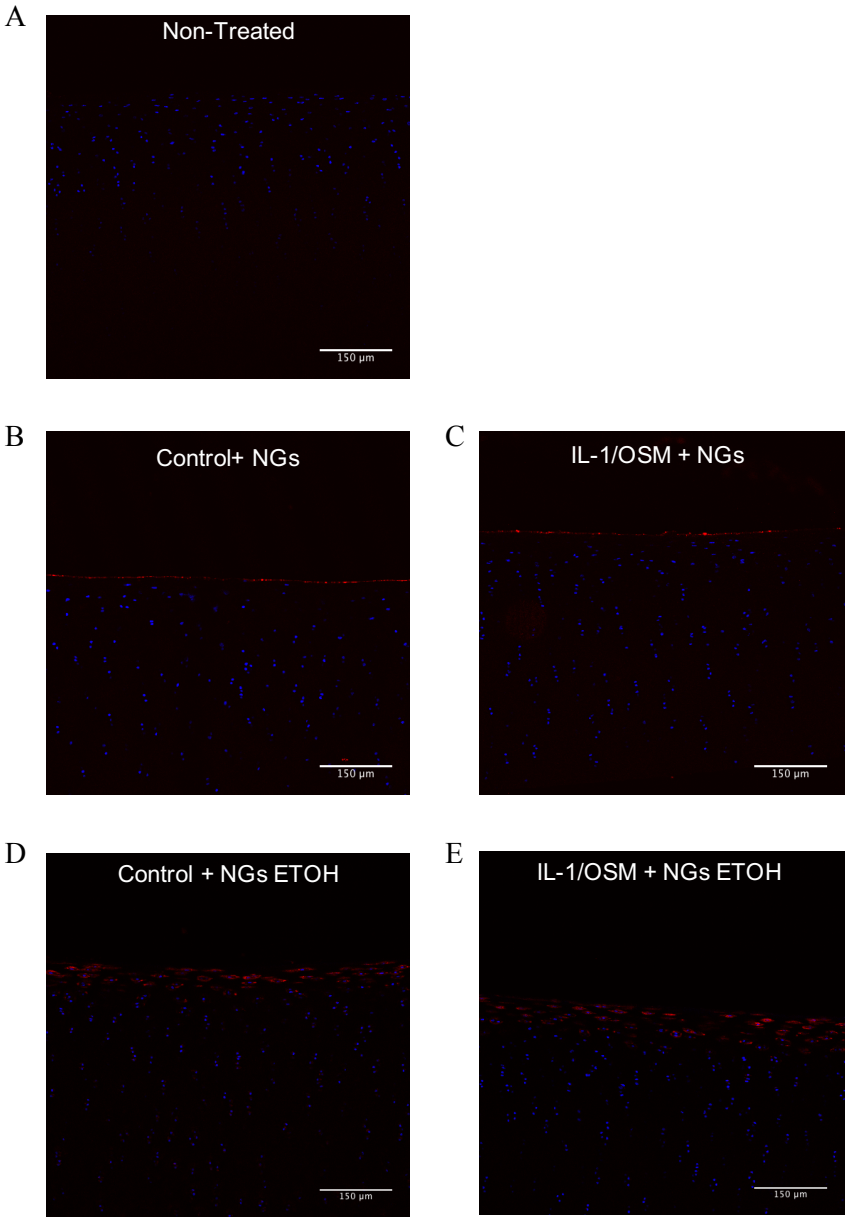

Figure 8.6 – Trafficking of Nanoghosts in bovine cartilage explants assessed by confocal fluorescence microscopy. Bovine cartilage explants cultured in control media or IL-1α (10ng/ml)+OSM (50ng/ml) prior to mounting in unidirectional chamber and addition of Nano-ghosts for 24 hours. Explants were then washed and cryosections taken and analysed for penetration using confocal microscopy (blue=DAPI, red=DiD labelled Nanoghosts). Non treated explants minus Nanoghosts (A), control media cultured explants (B) and IL-1+OSM cultured explants (C). Sections from B+C were fixed with ethanol to lyse surface bound Nanoghosts (D+E).

8.3.2 Validation of lubricin as a potential surface target for DDS

Lubricin is present at the articular cartilage surface in both control and IL-1α+OSM stimulated bovine cartilage explants

Lubricin is located at the surface of articular cartilage where it provides lubrication. It has been suggested that during OA the surface level of Lubricin is decreased, however, there are conflicting reports in the literature as to lubricin levels during OA progression. In Chapter 3 an increase in lubricin expression was observed in OSM treated cells versus controls and although IL-1α down-regulated expression of lubricin the combination of IL-1α+OSM resulted in no change in expression compared to controls. Therefore, the presence of lubricin was assessed on bovine explants after 4 or 14 days cultured in the presence of IL-1α+OSM or control media. Confocal microscopy confirmed that lubricin was present in both control and IL-1α+OSM treated explants at day 4 and day 14 (Fig 8.7A+B). Interestingly, there appeared to be an increase in staining intensity at the surface of cartilage in IL-1α+OSM treated explants at day 14 compared to controls (Fig 8.7B). Additionally, cells at day 4 appeared positive for lubricin staining in IL-1α+OSM treated explants but not in controls suggesting that cytokine treatment induces expression of lubricin at this time point (Fig 8.7A). This data shows that in cytokine induced *ex vivo* models of OA there is no clear decrease in lubricin levels at the surface of articular cartilage after 14 days of culture in the presence of IL-1α+OSM.

Conjugation of anti-lubricin mAb 3A4 to 1µm latex beads increases retention at the surface of bovine articular cartilage explants

To assess the suitability of lubricin as a target for DDS retention at the surface of cartilage 1µm carboxylate modified latex beads were conjugated, using EDC-sNHS chemistry, to anti lubricin monoclonal antibody 3A4 or IgG isotype control. Explants and beads were then incubated for 24 hours and fluorescence analysed at the surface using confocal microscopy. An increased fluorescence was detected at 24 hours at the surface of explants treated with 3A4 conjugated beads compared to IgG controls. In parallel, explants were incubated with beads for 24 hours as per above but then washed and incubated in media for a further 24 hours to assess the retention of 3A4 beads at the surface. Fluorescence signal was detected after 48 hours showing retention of beads mediated via lubricin binding (Fig 8.7C).

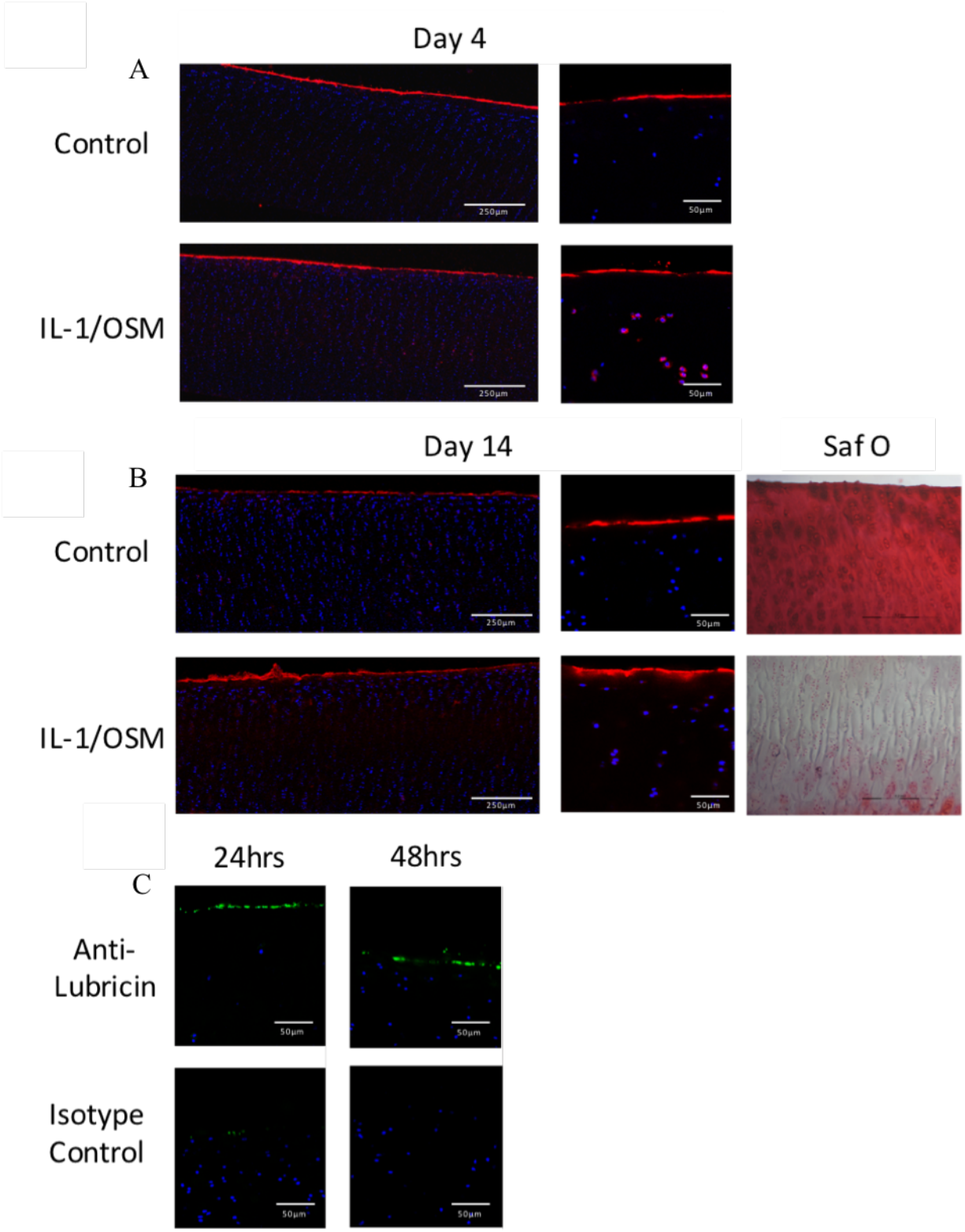

Figure 8.7 – Assessment of the presence of lubricin in cytokine treated bovine cartilage explants and retention assays using anti-lubricin mAb conjugated 1µm fluorescent latex beads. Bovine cartilage explants cultured in presence or absence of IL-1α(10ng/ml) + OSM (50ng/ml) visualised by immunofluorescence confocal microscopy for detection of lubricin using antibody 3A4 at day 4 (A) or day 14 (B) of cultures. Cartilage explants incubated with FITC labelled 1µm latex beads conjugated to antibody 3A4 or Isotype Control (C).

8.3.3 Anti-lubricin antibody 3A4 conjugation to Microsomes

Conjugation of anti-lubricin mAb 3A4 to microsomes was specific and could be detected by flow cytometry

To target microsomes to the surface of articular cartilage conjugation of 3A4 anti-lubricin was performed. The polydopamine shell of microsomes allows for facile conjugation of antibodies via catechol groups present on the microsomes to primary amines present on antibodies. The large size of microsomes 3-4μm allows for assessment of conjugation using flow cytometry (Fig 8.8A). Microsomes were incubated in the presence of 3A4 prior to staining with fluorescently labelled secondary antibody and detection via flow cytometry (Fig 8.8B). Increased fluorescence was detected on microsomes pre-incubated with antibody 3A4 compared to secondary alone controls confirming conjugation (Fig 8.8B). To confirm that conjugations proceeded covalently, as opposed to adsorption, pre-blocking experiments were performed using FITC labelled methoxy PEG- NH_2, 5kDa (PEG-NH_2). PEG-NH_2 reduced binding of 3A4 to microsomes suggesting that antibody binding to microsomes was specific and mediated via amine groups present on antibody (Fig 8.8D+E), however, the reduction of fluorescence mediated by pre-blocking with excess PEG-NH_2 was not as complete as that observed by pre-blocking of microsomes with BSA therefore a proportion of antibody binding is potentially via non-specific adsorption (Fig 8.8C).

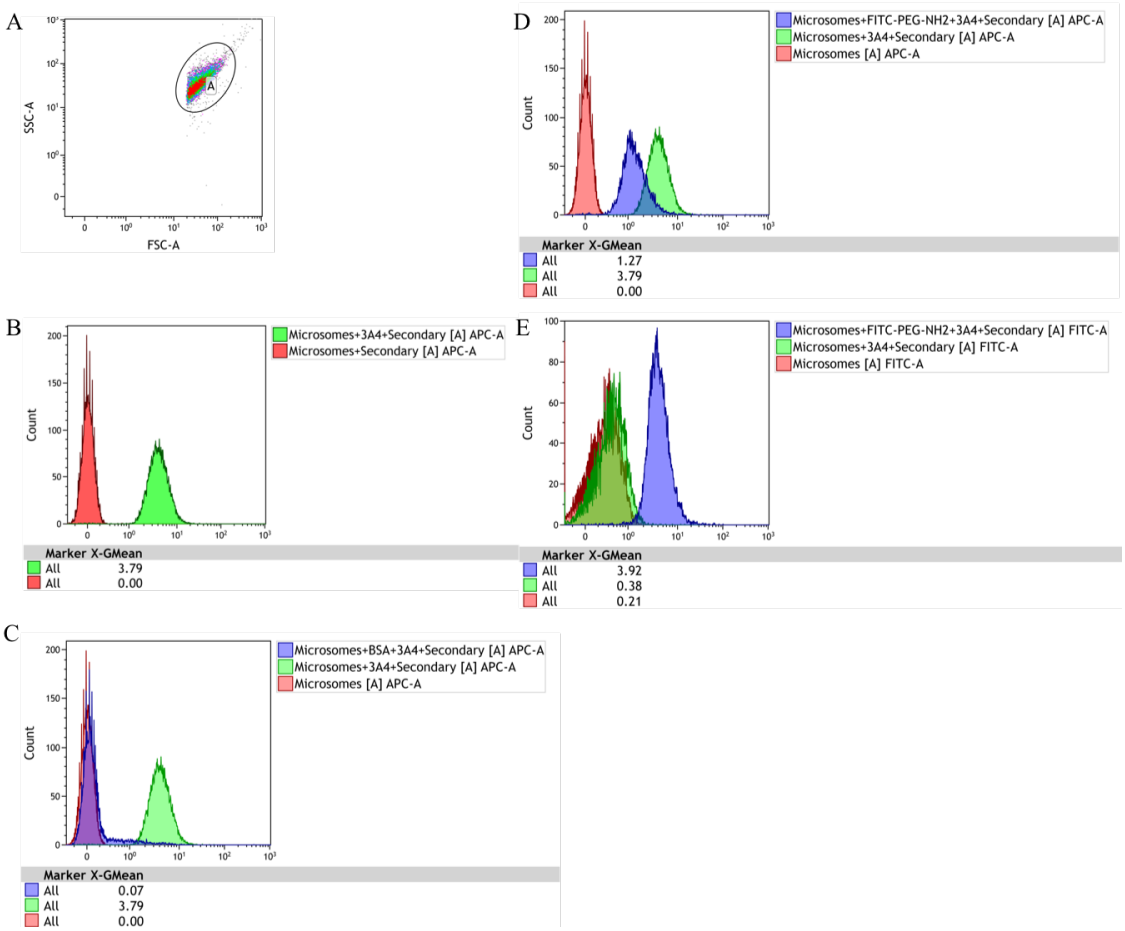

Figure 8.8 – Conjugation of anti-lubricin mAb 3A4 to microsomes using flow cytometry. Forward and side scatter gating for microsomes (A). Microsomes incubated with mAb 3A4 followed by fluorescent secondary antibody staining showed increased fluorescence compared to non-treated and microsomes incubated with secondary antibody alone (B). Blocking of microsomes with BSA prior to addition of 3A4 reduces fluorescent intensity (C). Pre-blocking of microsomes via FITC-PEG-NH reduces fluorescent intensity suggesting reduced 3A4 binding (D). Assessment of 2 FITC-PEG-NH binding in FITC channel (E). 100,000 events recorded per analysis.

8.3.4 Anti-lubricin conjugated microsomes *in vitro* cartilage binding and retention assay

Anti-lubricin conjugated microsomes showed increased binding to the surface of articular cartilage and the binding was dependent upon lubricin.

The binding and retention of 3A4 conjugated microsomes was tested *in vitro* using bovine cartilage explants. Anti-lubricin antibody 3A4 conjugated microsomes showed increased binding to cartilage explants compared to IgG isotype conjugated controls ($p<0.05$) (Fig 8.9A+B). This was confirmed quantitatively through counting of particles in 3x200μm^2 regions of interest per explant, mean and *sd* of 3 explants per condition shown (Fig 8.9F). To further confirm the specificity of binding of 3A4 conjugated microsomes to lubricin at the cartilage surface a 1M NaCl extraction was performed, this has been shown to remove lubricin with minimal effect on GAG levels (Jones *et al.* 2007). Lubricin removal abrogated 3A4 microsome binding to cartilage which was recovered via the incubation of NaCl extracted explants with bovine synovial fluid that replenishes cartilage surface lubricin levels (Fig 8.9C+D). This study confirms the specific binding of lubricin at the cartilage surface and confirms the suitability of lubricin as a target for larger DDS anchorage at the surface of articular cartilage.

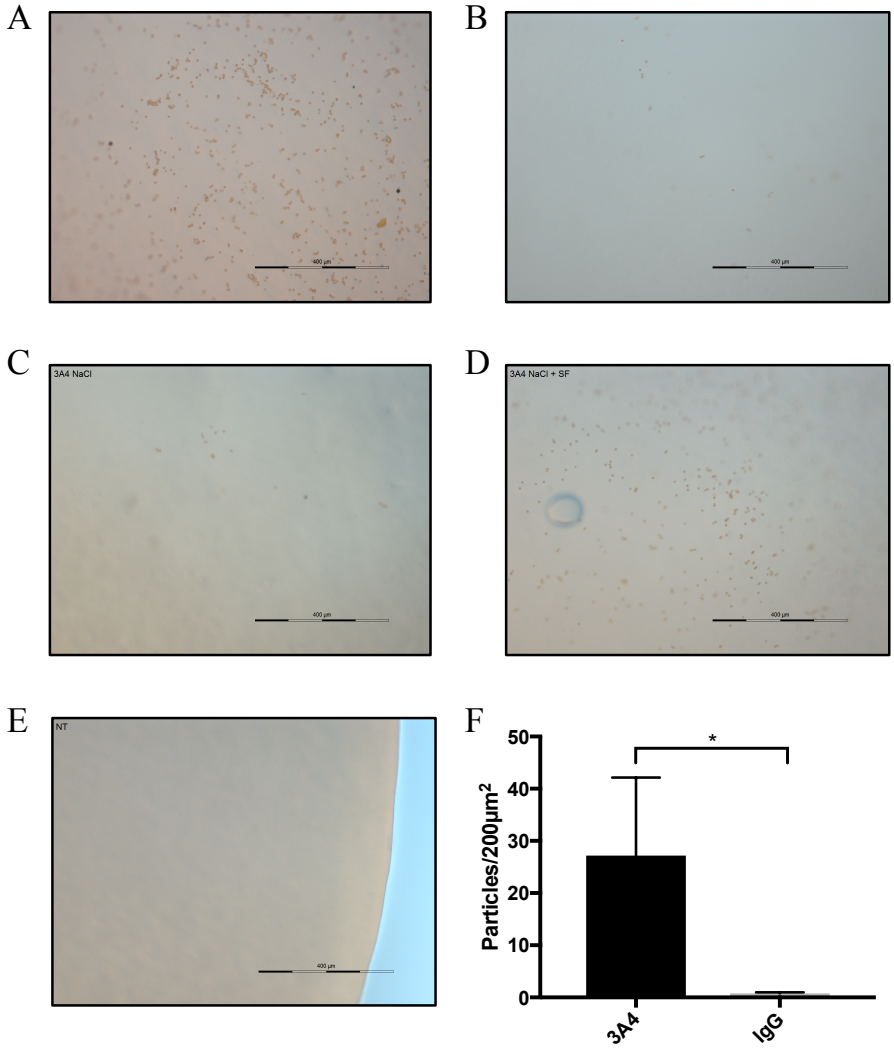

Figure 8.9 – Binding and retention assay of anti-lubricin mAb 3A4 conjugated microsomes at the surface of bovine cartilage explants. Bovine cartilage explants incubated with anti-lubricin 3A4 conjugated microsomes (A) or Isotype Control conjugated microsomes (B). 3A4 conjugated microsomes incubated with cartilage explants stripped of surface lubricin via NaCl extraction (C) or lubricin stripped explants with surface lubricin replenished via incubation with bovine synovial fluid (D). Non-treated explants (E). Quantification of binding and retention of 3A4 and IgG conjugated microsomes from triplicate explants. Mean and *sd* of three cartilage explants per condition shown. Statistical significance determined by students t-test using GraphPad Prism 7.0 software, *$p<0.05$.

8.3.5 Generation of monoclonal antibodies targeting CD64/FcγR1

To target DDS to the inflamed synovium CD64/FcγR1 was selected due to its increased expression on the pro-inflammatory M1 macrophage subtype. There are no commercially available mAbs that recognise both murine and human FcγR1. *In vitro* studies in the TargetCaRe consortium will use human and murine tissues, whereas *in vivo* studies will be performed in mice therefore the development of an antibody capable of recognising both murine and human FcγR1 will allow for all *in vitro* studies to be performed using the same antibody as will be used for *in vivo* studies. Two peptide sequences within the extracellular domain were chosen as immunogens based upon specificity for FcγR1 and homology between murine and human sequences.Regions containing cysteine were avoided due to use of cysteine for conjugation of peptides to ovalbumin carrier protein and cysteine di-sulphide bridges in protein that could obscure epitopes. Prolines within a peptide sequence often represent a kink/turn or exposed region that could be beneficial as an immunogen therefore homologous sequences containing prolines or flanked by two prolines were selected (Fig 8.10).

```
Mouse   10   MWLLTTLLLWVPVGGEVVNATKAVITLQPPWVSIFQKENVTLWCEGPHLPGDSSTQWFIN  69
             MW LTTLLLWVPV G+V + TKAVITLQPPWVS+FQ+E VTL CE  HLPG SSTQWF+N
Human   1    MWFLTTLLLWVPVDGQV-DTTKAVITLQPPWVSVFQEETVTLHCEVLHLPGSSSTQWFLN  59

Mouse   70   GTAVQISTPSYSIPEASFQDSGEYRCQIGSSMPSDPVQLQIHNDWLLLQASRRVLTEGEP  129
             GTA Q STPSY I  AS  DSGEYRCQ G S  SDP+QL+IH  WLLLQ S RV TEGEP
Human   60   GTATQTSTPSYRITSASVNDSGEYRCQRGLSGRSDPIQLEIHRGWLLLQVSSRVFTEGEP  119

Mouse   130  LALRCHGWKNKLVYNVVFYRNGKSFQFSS-DSEVAILKTNLSHSGIYHCSGTGRHRYTSA  188
             LALRCH WK+KLVYNV++YRNGK+F+F   +S + ILKTN+SH+G YHCSG G+HRYTSA
Human   120  LALRCHAWKDKLVYNVLYYRNGKAFKFFHWNSNLTILKTNISHNGTYHCSGMGKHRYTSA  179

Mouse   189  GVSITVKELFTTPVLRASVSSPFPEGSLVTLNCETNLLLQRPGLQLHFSFYVGSKILEYR  248
             G+S+TVKELF  PVL ASV+SP  EG+LVTL+CET LLLQRPGLQL+FSFY+GSK L  R
Human 180    GISVTVKELFPAPVLNASVTSPLLEGNLVTLSCETKLLLQRPGLQLYFSFYMGSKTLRGR  239

Mouse   249  NTSSEYHIARAEREDAGFYWCEVATEDSSVLKRSPELELQVLGPQSSAPVWFHILFYLSV  308
             NTSSEY I  A RED+G YWCE ATED +VLKRSPELELQVLG Q   PVWFH+LFYL+V
Human   240  NTSSEYQILTARREDSGLYWCEAATEDGNVLKRSPELELQVLGLQLPTPVWFHVLFYLAV  299

Mouse   309  GIMFSLNTVLYVKIHR-LQREKKYNLEVPLVSEQGKKA-NSFQQVR  352
             GIMF +NTVL+V I + L+R+KK++LE+ L S   KK  +S Q+ R
Human   300  GIMFLVNTVLWVTIRKELKRKKKWDLEISLDSGHEKKVISSLQEDR  345
```

Key:
Blue=Signal Peptide
Bold=Extracellular Domain
Highlight=Selected Immunising Peptide Sequence
Red=Transmembrane Domain

Figure 8.10 – Human and murine CD64/FcγRI amino acid sequence alignment. Human and murine CD64/FcγRI amino acid sequences showing selected immunising peptides in yellow within the extracellular domain of CD64.

Post-fusion ELISA revealed 22 positive hybridoma clones

After fusion and limiting dilution, cultures were incubated for 2 weeks prior to an initial ELISA screen using the immunising peptide as the plate coating antigen, plates were run in parallel coated with the alternative peptide, for example M311A fusions were screened against M311A and M311B to identify cross reactivity which would indicate positive clones that bind an epitope within the carrier ovalbumin or link peptide region and therefore not specific to FcγR1. Initial screening showed multiple positive hybridomas which when cross reactive positives were removed, 22 potential successful hybridomas remained. Interestingly, the fusion resulting from M311A immunised mice produced 18 positive clones compared to just 4 for M311B (Fig 8.11) . Peptide property calculators confirmed that M311A was highly hydrophobic, a property reflected in its low solubility (1mg/ml) compared to M311B (5mg/ml). Hydrophobic peptides are highly immunogenic which may explain the success of this peptide in generating positive clones.

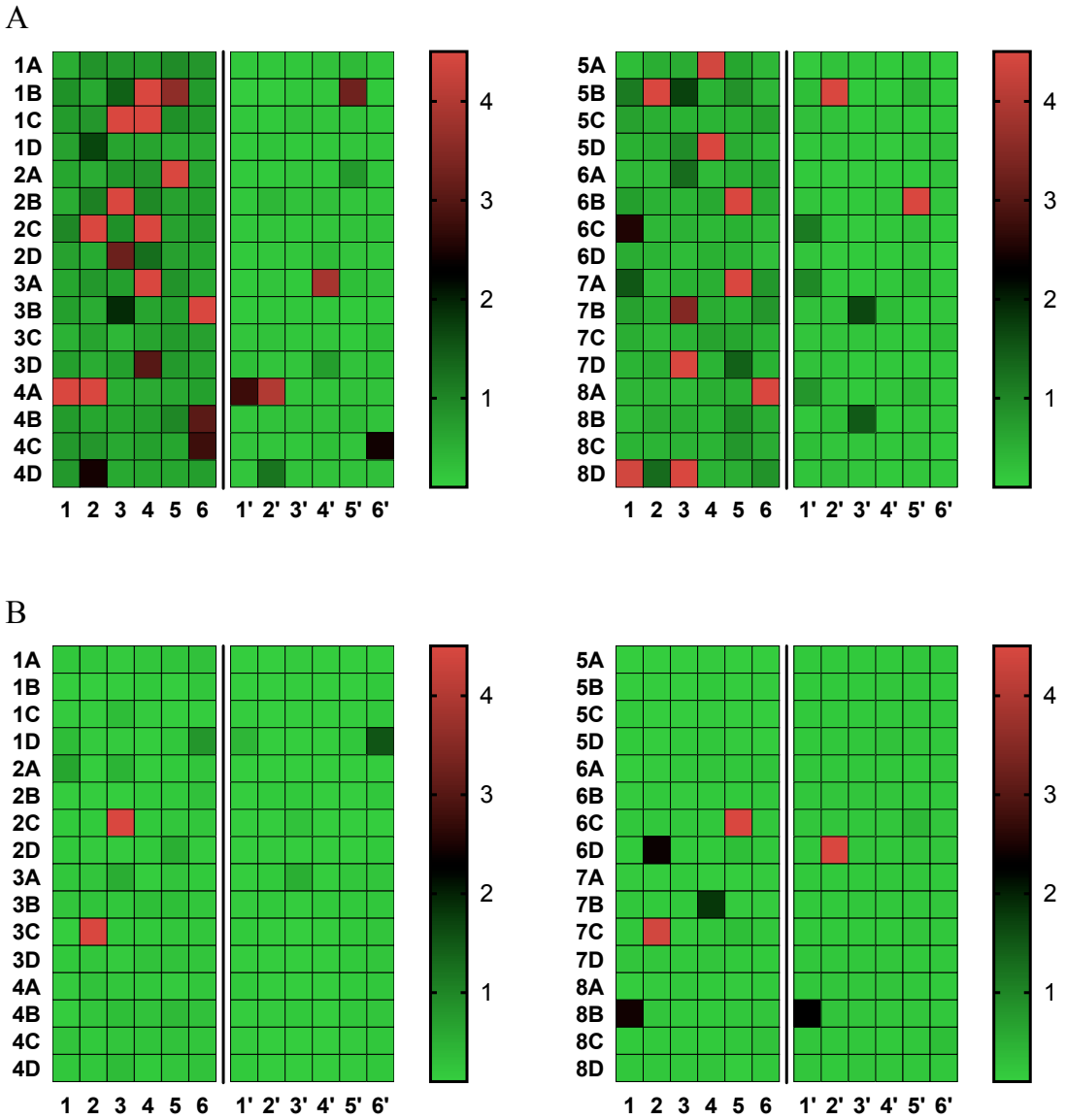

Figure 8.11 – Post-fusion screening of hybridoma cultures to identify anti-CD64 producing clones showing no cross-reactivity to ovalalbumin or linker peptide expressed as a heat map. ELISA results from first screen of hybridomas post fusion expressed as a heat map showing fusions from immunisations with peptide M311A (A) and M311B (B). Alpha numeric marking to left of heat map represents 24 well plate number and vertical well location. Numerical markings below heat-map depict horizontal well location. Hybridomas were cross-screened in parallel against non-immunising peptide depicted by N' to assess for reactivity to ovalalbumin or link peptide.

Monoclonal antibody isotyping

The ability of an antibody to recognise and bind linear peptide epitopes does not ensure its binding to native proteins due to secondary and tertiary structures present in proteins. Additionally, for the successful commercialisation of antibodies generated it is beneficial to test antibodies in multiple applications such as Western blot, IHC and flow cytometry, therefore functional assays were performed to identify suitable clones for further assessment. It must be noted that in all functional assays the source of antibody for assessment was hybridoma culture media as opposed to purified antibody and therefore the concentration of antibody is unknown and the affinities of antibodies cannot be compared. Prior to functional assays hybridomas were up-cultured and secured. A final confirmatory screen was performed which confirmed specific binding of mAbs during up-culture procedure (Fig 8.12A). Isotyping of antibodies was performed with 4 being of the IgG1 subtype, 1 IgG2A, 1 IgG2B and 2 IgM isotypes (Fig 8.12B).

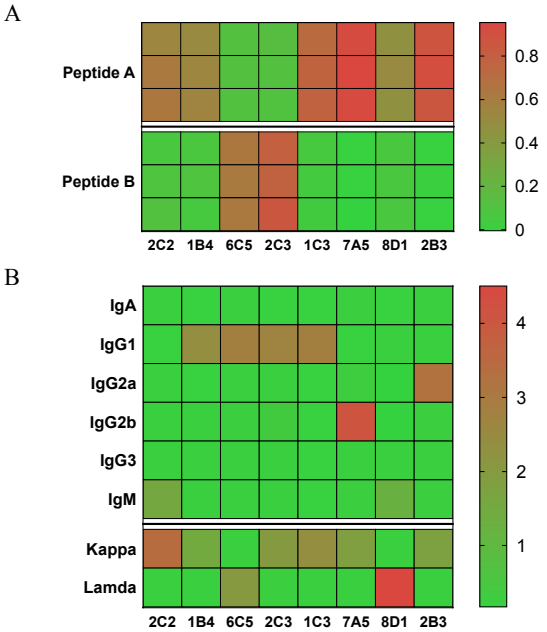

Figure 8.12 – Final ELISA screen of positive hybridomas and isotype assessment expressed as a heat maps. ELISA screen of hybridomas against immunising peptide and non-immunising peptide to assess for cross-reactivity depicted as a heat-map (A). Isotype assessment of hybridomas depicted as a heatmap (B).

Assessment of monoclonal antibodies in Western blot

Recombinant FcγR1 was loaded at 240ng per lane under reducing and non-reducing conditions followed by transfer to nitrocellulose and blotting with hybridoma media. Antibodies 6C5 and 2C3 recognised human FcγR1 under reducing conditions with a positive band observed at circa 52 kDa (Fig (8.13). The predicted molecular weight of rFcγR1is 37.5 kDa but a single band was detected at 52 kDa by the protein manufactures with the increased size predicted to be a result of glycosylation. Antibody 2B3 detected a band at the same molecular weight but only under non-reducing conditions.

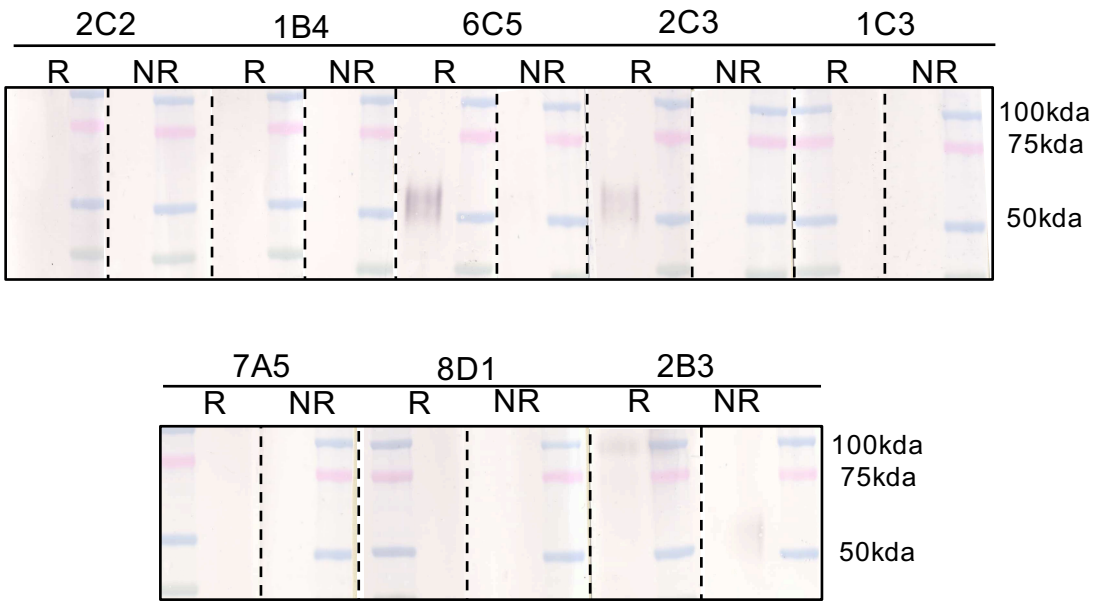

Figure 8.13 – Assessment of hybridomas using Western blot under reducing (R) and non-reducing (NR) conditions. 240ng of recombinant human CD64 was loaded per lane and incubated with undiluted hybridoma culture media.

Assessment of monoclonal antibodies in immunofluorescence cell assays

Antibodies were then tested in immunofluorescence confocal microscopy assays on human THP-1 monocytes that were differentiated to macrophages using PMA followed by differentiation towards the M1 phenotype using IFNγ to up-regulate expression of FcγR1. To assess the binding of antibodies to murine FcγR1 the J774A.2 cell line was used without stimulation as it has been shown to express FcγR1 constitutively. Immunofluorescence microscopy detected binding of antibodies 2B3 and 8D1 to human THP-1 cells, whereas 2C3 and 8D1 and to a lesser degree 2B3 bound to murine J774A2 cells (Fig 8.14A+B). The inability of 6C5 to detect murine or human native FcγR1 despite strong reactivity in Western blot under reducing conditions for human rFcγR1 is likely the result of SDS-PAGE conditions that linearise the protein and disrupt cysteine bridge structures.

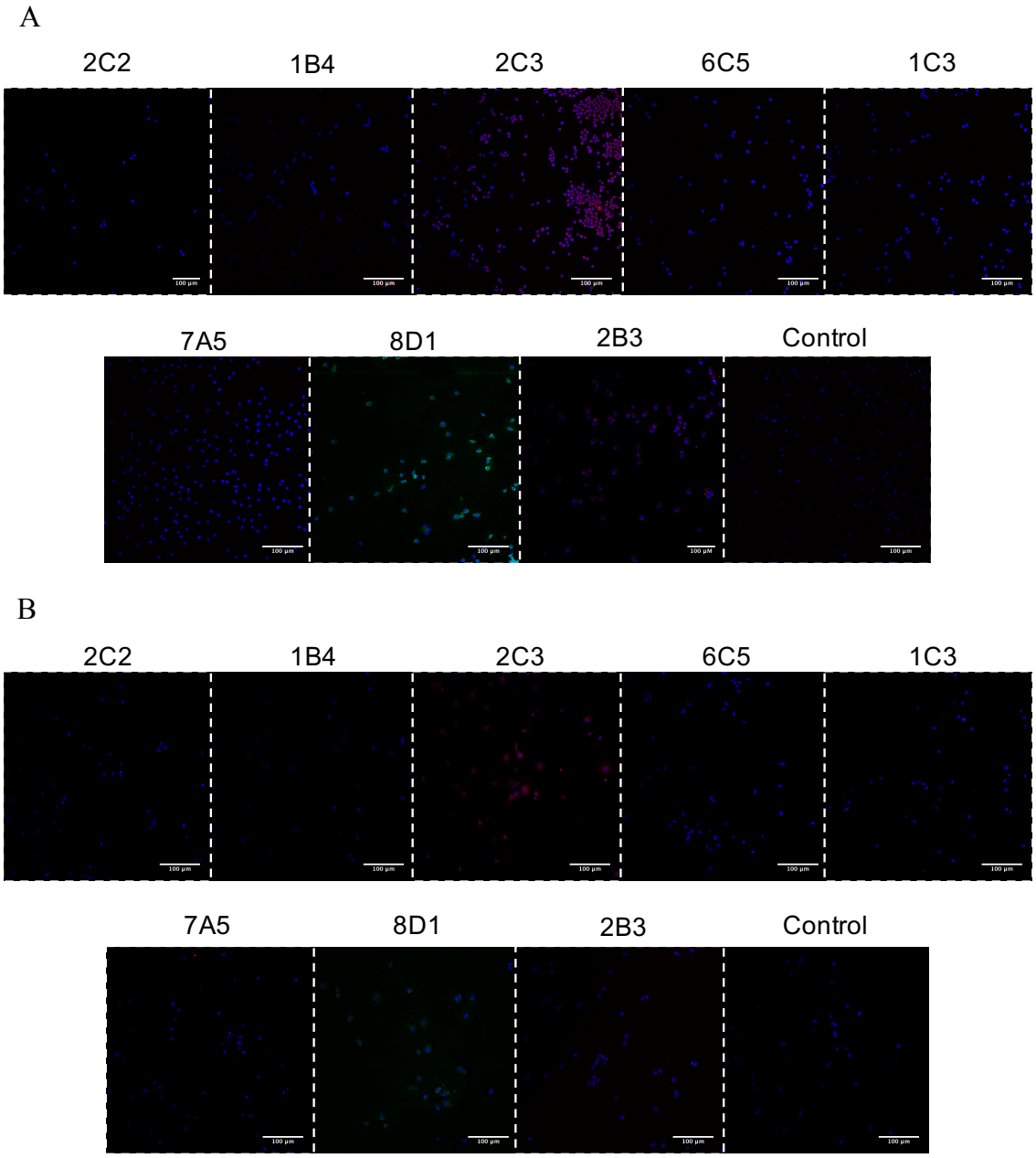

Figure 8.14 – Assessment of hybridoma clone mAbs in human THP-1 and murine J774A.2 cells. Immunofluorescence assessment using confocal microscopy of J774A.2 cells incubated with hybridoma culture media from positive clones (A). Interferon γ stimulated THP-1 cells incubated with hybridoma media from positive clones (B). Blue=DAPI nuclear stain, Red=Anti-IgG secondary and Green=Anti-IgM secondary.

Assessment of monoclonal antibody detection of CD64/FcγRI on J774A.2 cells using flow cytometry

Detection of CD64/FcγRI by hybridoma culture media was assessed by flow cytometry. Hybridomas designated 8D1, 2C2, 1C3, 2C3 and 2B3 showed increased fluorescence intensity compared to cells alone suggesting binding of mAb to murine J774A.2 CD64/FcγRI. As the concentration of antibody in hyrbidoma culture media is unknown it is not possible to compare fluorescent intensities between mAbs and data represents a binary postive or negative result only.

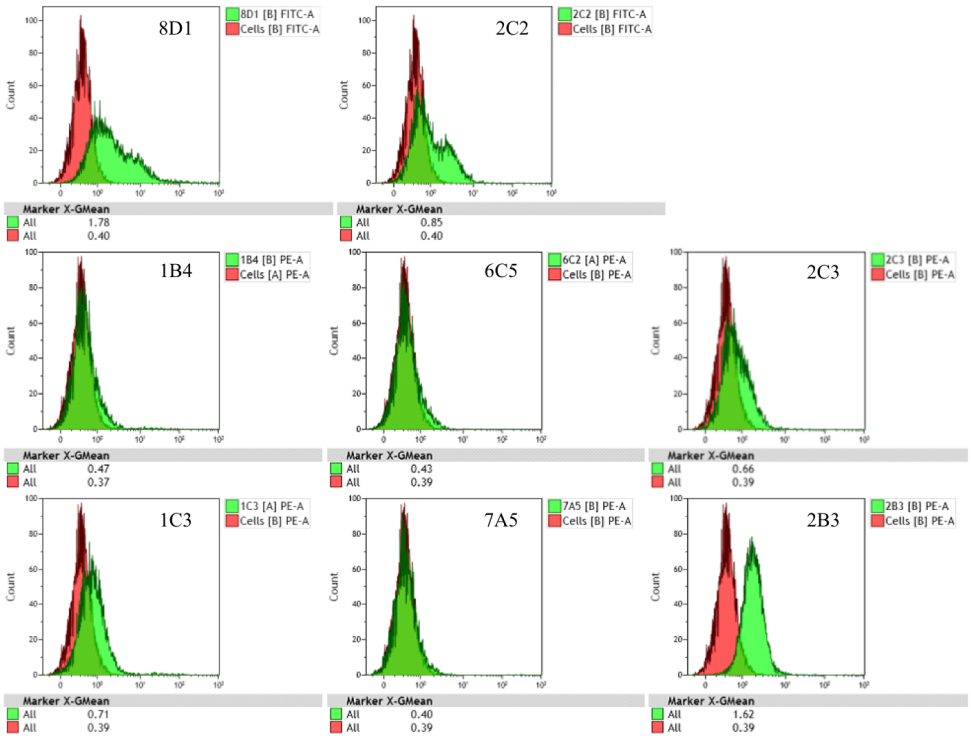

Figure 8.15 – Assessment of mAb binding to murine J774A.2 cells assessed by flow cytometry. Murine J774A.2 cells were incubated with media from hybridoma cultures prior to detection using AlexaFluor 546nm anti-mouse IgG or AlexaFluor 488nm anti-mouse IgM and detected in APC and FITC channels, respectively, using a BD bioscience FACS Canto flow cytometer. Data analysed using Beckman Coulter Kaluza software with geometric means plotted. 100,000 events recorded per analysis.

Assessment of antibody titres in serum free media preparations

Due to overall performance in WB, ELISA, flow cytometry or IF antibodies 8D1, 2C3 and 2B3 were taken forward. Additionally, these antibodies also provide an opportunity to assess antibody isotype effects on binding being of IgM, IgG1 and IgG2a isotypes. Hybridomas are traditionally cultured in 20% fetal bovine serum (FBS) and despite FBS containing much reduced concentrations of IgG compared to calf or bovine serum it still contains in excess of 300µg/ml IgG. The use of anti-mouse secondaries should eliminate any cross detection of bovine IgG bound to cell FcγRs although binding of bovine IgG may sterically hinder binding of mAbs. Additionally, the presence of bovine IgG acts as a contaminant in subsequent purification of mAbs through binding to protein A or G columns therefore the use of chemically defined serum free hybridomas was investigated. Antibody titres showed that culture media isolated from flasks seeded with equal cell numbers

cultured in SFM or CD showed no reduction in antibody production compared to FHM (Fig 8.14) so therefore all further experiments were performed using media from hybridomas cultured in chemically defined FBS free media.

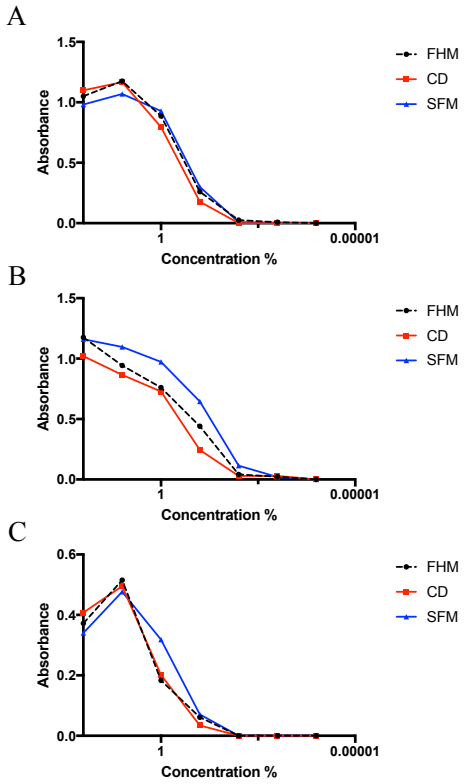

Figure 8.16 – Assessment of antibody titres post culture in chemically defined medias compared to culture in full media containing 20% FBS. Antibody titre comparisons by ELISA of hybridomas cultured in full hybridoma media with 20% FBS (FHM), chemically defined media (CD) or serum free media (SFM). Titres shown for hybridomas 2B3 (A), 2C3 (B) and 8D1 (C).

Peptide inhibition immunofluorescence assays

Peptide inhibition assays revealed isotype and species specific differences in non-specific binding of mAbs

To confirm the specificity of binding via mAb antigen recognition site and not via Fc interactions immunofluorescence experiments were repeated in THP and J774A2 cells in the presence or absence of the immunising peptide to neutralise specific binding. Interestingly, differences were observed based upon isotype tested and species of cell line. The IgG1 2C3 showed an increased binding to THP-1 cells in the presence of the immunising antigen suggesting that binding of mAb to peptide antigen increased non-specific Fc mediated binding of this mAb to human cells, whereas the IgG2A 2B3 and the IgM 8D1 showed much reduced binding in the presence of the immunising peptide suggesting binding of these mAbs was specific to FcγR1and not Fc mediated (Fig 8.18). Conversely the IgG2A mAb 2B3 showed a similar increase in binding in the presence of the immunising peptide in the murine J774A.2 cell line, whereas 2C3 and 8D1 were strongly inhibited in the presence of their respective immunising peptides (Fig 8.19). This suggests that IgG binding

to Fc receptors is increased upon antigen binding and that these effects are specific to mIgG1 in human cells but mIgG2a in murine cells.

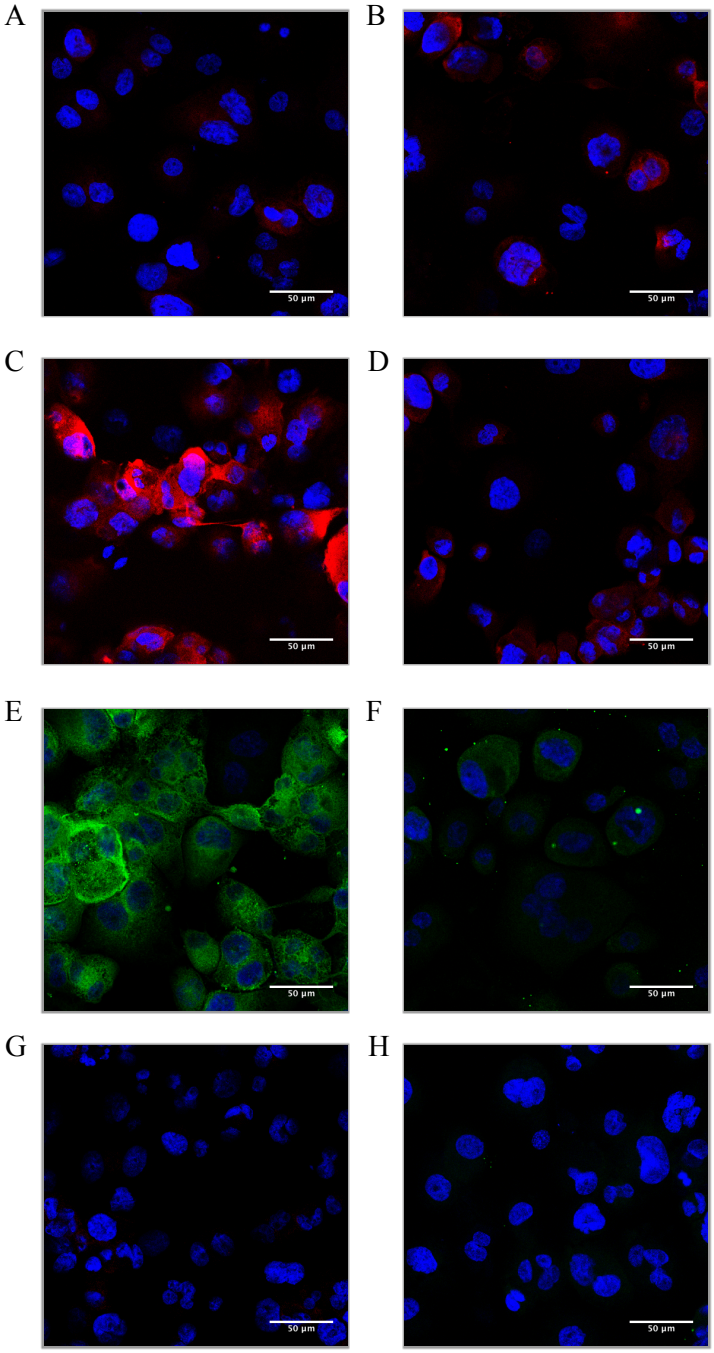

Figure 8.17 – Assessment of CD64 specific detection by mAbs using peptide inhibition assays in human THP-1 cells. Immunofluorescence assessment using confocal microscopy of IFN stimulated THP-1 cells incubated with CD culture media from 2C3 (A) and 2C3 pre-incubated with immunising peptide to neutralise binding (B). 2B3 (C), 2B3 plus peptide (D), 8D1 (E), 8D1 plus peptide (F). IgG Isotype Control (G), IgM Isotype Control (H). Blue=DAPI nuclear stain, Red=Anti-IgG secondary and Green=Anti-IgM secondary.

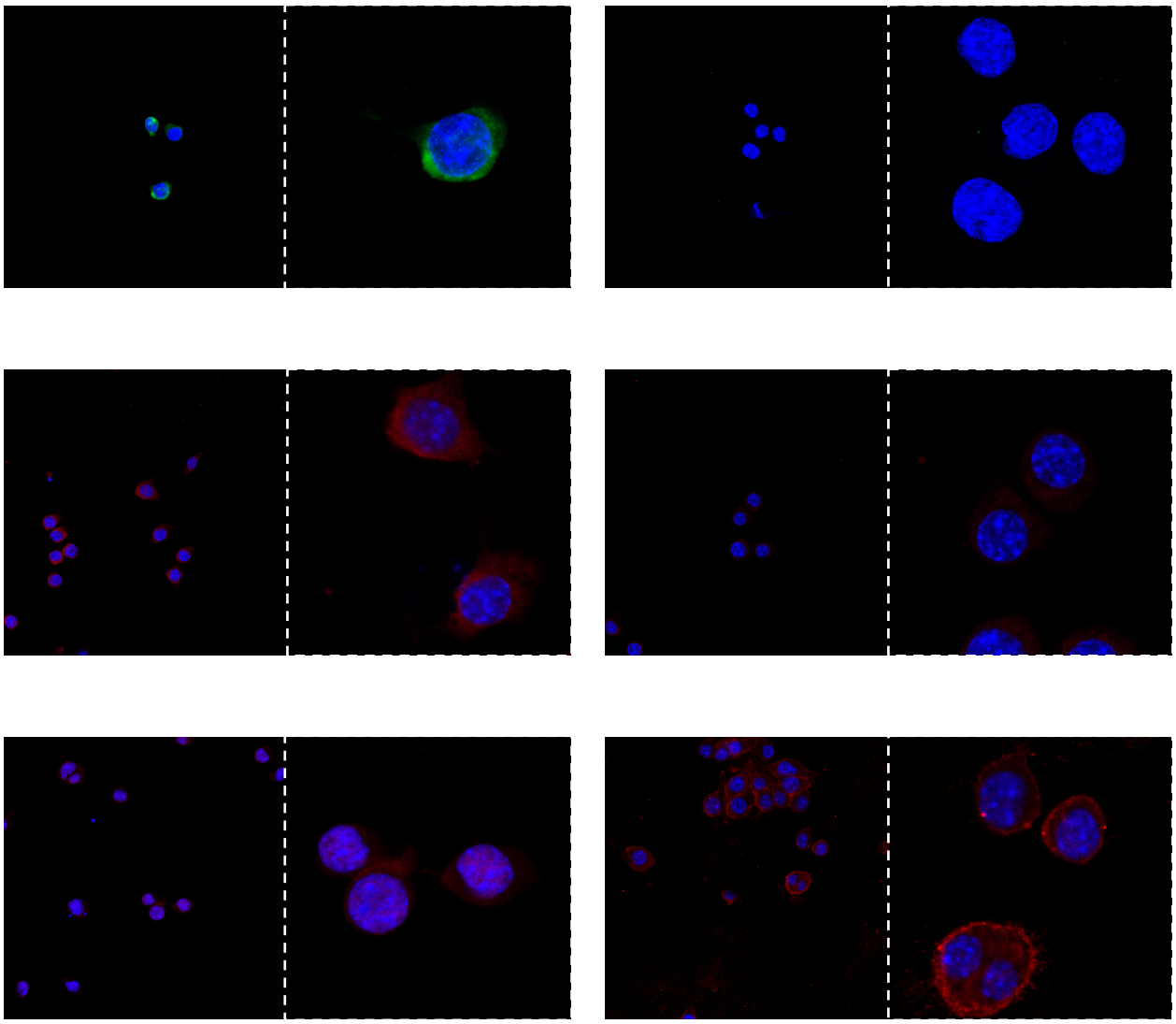

Figure 8.18 – Assessment of CD64 specific detection by mAbs using peptide inhibition assays in murine J774A.2 cells. Immunofluorescence assessment using confocal microscopy J774A.2 cells incubated with CD culture media from 8D1 (A) and 8D1 pre-incubated with immunising peptide to neutralise binding (B). 2C3 (C), 2C3 plus peptide (D), 2B3 (E), 2B3 plus peptide (F). Blue=DAPI nuclear stain, Red=Anti-IgG secondary and Green=Anti-IgM secondary.

Peptide inhibition flow cytometry assays

To further quantify binding of mAbs in presence or absence of immunising peptides, J774A.2 cells were subjected to flow cytometry after labelling with mAbs in the presence or absence of the immunising peptides. Results confirmed that observed in IF experiments with an increased signal in 2B3 labelled cells in the presence of the immunising peptide compared to 2B3 alone. A decrease in fluorescent intensity was observed for 8D1 and 2C3 labelled cells in the presence of the immunising peptides. Interestingly, a primary IgG control derived from whole mouse serum showed an increase in fluorescence suggesting non-specific binding of murine Abs in murine cells even in the absence of antigen. No increase in fluorescence was detected with an IgM isotype control confirming the lack of non-specific binding of IgM antibodies to monocytes.

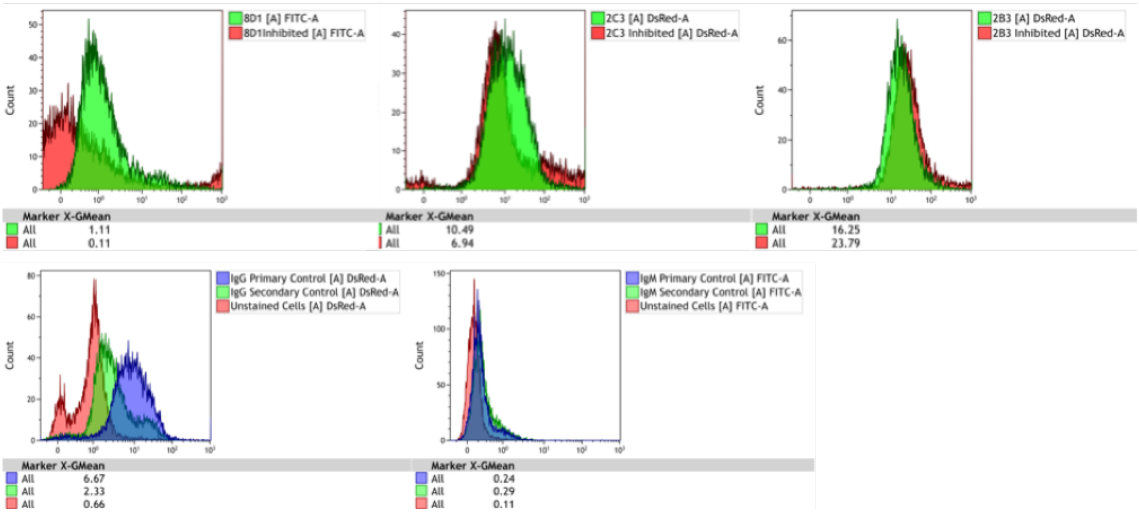

Figure 8.19 – Flow cytometry assessment of CD64 specific detection by mAbs using peptide inhibition assays in murine J774A.2 cells. Analysis by flow cytometry of mAb 8D1 (A), 2C3 (B) and 2B3 (C) binding to J774A.2 cells in the presence of absence of the neutralising immunising peptide. Isotype primary controls using murine IgG (D) or IgM (E). 100,000 events recorded per analysis.

8.4 Discussion

The overall aim of this Chapter was the elucidation of the trafficking of DDS into articular cartilage whilst validating and developing targeting moieties to articular cartilage and also to M1 macrophages of the inflamed synovium.

The work in this chapter has confirmed that trafficking into cartilage is restricted to particles smaller than NGs (~200nm) which corresponds to that observed in the literature where penetration of 38nm but not 98nm lipid particles into intact articular cartilage was shown (Rothenfluh *et al.* 2008). Smaller DDS are required if intra-cartilage targeting is to be realised, for instance the use of avidin based particles have shown some success *in vitro* due to its small (5nm) size and offers a versatile system for the conjugation of biotinylated drugs, however, retention within cartilage in this system is mediated by charge based interactions, which in the case of GAG depleted cartilage showed less than 20% retention of avidin after 24 hours (Bajpayee *et al.* 2014). Therefore, the development of active targeting to moieties at the cartilage surface was pursued in this Thesis. The work in this Chapter has validated the surface protein lubricin as a potential target for anchorage

and retention of DDS at the cartilage surface. The turn-over of lubricin is unknown but retention assays within this Chapter using 3A4 conjugated latex beads shows it is present for at least 48 hours in sufficient amounts to mediate retention. Lubricin is also present in the synovial fluid and the effects of synovial fluid lubricin on cartilage binding of 3A4 conjugated microsomes requires further investigation. Although intra-articular administration allows for a unique targeting of DDS directly to disease site that is not possible in most diseases there is a rapid clearance of molecules and particles from the synovial joint through filtration and lymphatic drainage (Evans *et al.* 2015) therefore active targeting of particles, even those of micrometre size, is likely beneficial through increased retention of DDS within the joint where degradation can maintain a slow release of therapeutics over extended time points. It must be noted, however, that most current drug delivery systems including those currently undergoing clinical trials, such as TAA loaded poly(lactic-co-glycolic acid) (PLGA) system-FX006, are unable to maintain a sustained release of therapeutics for 3 months (Kraus *et al.* 2018), the minimum time between IA injections often permitted in the clinic. The prolonged effect of a single administration of glucocorticoid therapeutics despite rapid clearance suggests that sustained release DDS are superfluous for steroidal therapeutics, however, for other therapeutics and in particular biologics, such as siRNA, an extended sustained release profile is beneficial (Sarett *et al.* 2015). Additionally, targeting of DDS to specific joint compartments could reduce systemic and local off-target effects, for example TAA is beneficial for reduction of synovial inflammation however is shown to detrimentally affect the phenotype of chondrocytes (Suntiparpluacha *et al.* 2016) therefore the ability to target immune cells in the synovium directly and in the case of FcγR1 targeting moieties, specific targeting of DDS to M1 inflammatory macrophages may be beneficial (Akinrinmade *et al.* 2017). For example, ricin toxin conjugated CD64 targeting antibodies reduced inflammation and bone damage in an adjuvant arthritis model in transgenic human CD64 rats although a comparison to total macrophage depletion would have been beneficial to assess the effects of specific CD64 expressing macrophages in this study (Vuuren *et al.* 2018).

Development of mAbs targeting the high affinity FcγR is not trivial due to the potential for non-specific interactions of IgG Fc regions with FcγR1 in addition to the low affinity FcγRs which in humans includes FcγRIIA, FcγRIIB, FcγRIIIA and FcγRIIIB that although display a low affinity for monomeric IgG have a high affinity for oligomeric and complexed antigen bound IgG (Bruhns, 2015). An additional Fc receptor is present on most cells, the neonatal Fc receptor FcRN which mediates recycling of circulating IgG rather than Fc mediated signalling events (Kuo and Aveson, 2011). There are differences in the type of FcγRs and binding affinities related to IgG subtype between human and mice with human FcγRI preferentially binding monomeric hIgG1 and showing almost no binding to hIgG2A, whereas in mice FcγRI has a strong affinity for mIgG2A and shows almost no binding of mIgG1 (Bruhns, 2015). This is consistent with the observation that murine IgG2A fulfils a role in mice similar to that of IgG1 in humans and it has been shown that monomeric murine IgG2A binds strongly to human FcγRI whereas a reduced binding was observed for murine IgG1 (mIgG1). Assessment of mAbs generated within this chapter confirmed that non-specific binding of IgG occurred in monocytes and macrophage like cell lines. The blocking of 2C3 mIgG1 with its immunising peptide resulted in increased binding to human THP-1 cells whereas in the murine J774A.2 monocyte cell line a similar effect was noted for mAb 2B3 of IgG2A isotype.

This would suggest that binding of antigen increases non-specific Fc interactions between FCγRs and IgG and that this interaction is specific to mIgG1 in human cells and mIgG2A in murine cells. The increase in non-specific interactions of 2C3 with THP-1 cells upon binding of antigen were unexpected as it is widely held that human FcγRs bind mIgG2A avidly but not mIgG1. However, there are some polymorphic variations between human FcγRIIA with FcγRIIA-R131 showing an increased binding of mIgG1 (van der Heijden *et al.* 2014). Interestingly, THP-1 express FcγRIIA-R131 and FcγRIIA-H131 (Valenzuela *et al.* 2015) therefore a potential mechanism for the increase in non-specific binding of the IgG1-2C3 is that upon antigen binding affinity is increased to FcγRIIA-R131variant. The monocytic cell line U937 expresses only the FcγRIIA-R131 (Valenzuela *et al.* 2015) and therefore future studies comparing the non-specific binding of mIgG1 between these cell lines may elucidate the effects of polymorphic variations of FcγRIIA. Oligomerisation through binding of multiple antibodies to target or by heat induced aggregation results in a greater than 400% increase in hIgG1 binding to low affinity FcγRs (Bruhns, 2015), although it is unknown whether the same conformational changes are induced by peptide antigen binding in these assays. Human FcγR1 binds monomeric mIgG2A with high affinity so from these studies it is not possible to determine the contribution of specific and non-specific Fc binding in the positive staining observed in 2B3 labelled THP-1 cells. The reduction in binding mediated by the immunising peptide would suggest that a proportion of this is indeed specific but also that mIgG2A binding to antigen does not increase the affinity of mIgG2A Fc for low affinity FcγRs as non-specific binding was not observed in peptide blocked 2B3 labelling of THP-1. Further work is required to confirm this and interactions with low affinity FcγRs could be assessed using commercially available blocking antibodies for murine FcγRII and III. Deglycosylation of IgG completely inhibits binding to FcγRs so future studies could be employed using deglycosylated mAbs to assess for non-specific versus specific binding to FcγR1. The generation of Fab or Fab'2 fragments would also remove any interference mediated by Fc regions but this was avoided as antibody conjugation strategies developed for microsomes and NGs are not compatible with mAbs lacking an Fc region.

The method used within this chapter to generate mAbs is based upon a modified method to that of Milstein and Kohler where lymphocytes are harvested from lymph nodes proximal to injection sites at just two weeks post first immunisation as opposed to several months and harvest of lymphocytes from the spleen. This method has been used successfully by the Caterson/Hughes lab to generate mAbs to highly conserved structures including glycosaminoglycan epitopes (Baker *et al.* 2015), anecdotally it has also been successful in the generation of IgM isotype antibodies, potentially due to the early harvest of lymphocytes and therefore avoidance of clonal deletion and isotype switching. This method produced two positive clones that secreted IgM isotype mAbs one of which, 8D1, was carried forward to functional testing. The use of an IgM isotype appeared to avoid issues of non-specific binding and a decrease in binding to cells was noted in the presence of the neutralising immunising peptide for both human and murine cell lines tested. There is an IgM specific Fc receptor- FcμR however its expression is limited to T and B-cells and there is no detectable FcμR present on CD14+ monocytes (Kubagawa *et al.* 2014) and macrophages (Honjo *et al.* 2013). An alternative Fc receptor that is capable of binding IgM and IgA, Fcα/μR, has been detected on murine macrophages but its expression on THP-1 and J774A2 cells is unknown. To confirm the

lack of non-specific effects of IgM isotype mAbs further work is required in primary human and murine macrophages. Conjugations are traditionally performed using IgG type mAbs and therefore conjugation protocols would require adaption for IgM, the reduction of the J-chain would result in monomeric IgM that could be conjugated in similar ways to IgG although the binding affinity of monomeric IgM would require assessment post-reduction. Therefore, in conclusion IgM subtype mAbs may prove superior to IgG subtypes in avoidance of non-specific binding, particularly in the study of macrophages that are known to express multiple Fc receptors and that expression is somewhat independent of macrophage subtype therefore non-specific binding of mAb Fc would potentially target both M1 and M2 macrophages in the synovium.

8.4.1 Summary

1. DDS of 200nm do not penetrate intact or GAG depleted cartilage therefore for targeting of NGs or microsomes to the cartilage then exposed cartilage surface targets are required.

2. Lubricin is present at the cartilage surface and its levels are not reduced by 14 days of treatment with IL-1α+OSM.

3. Conjugation of anti-lubricin mAb 3A4 to microsomes results in specific binding and retention to the cartilage surface.

4. Non-specific interactions of antigen bound antibody with FcγRs is specific to mIgG1 in human THP-1 cells and mIgG2A in murine J774A2 cells.

5. Non-specific Fc interactions can be avoided on both J774A2 and THP-1 cells using IgM isotype antibodies.

8.4.2 Conclusions

This work has confirmed that the cartilage matrix presents a formidable barrier to the trafficking of DDS and that for targeting directly to chondrocytes work is required to develop smaller DDS than the majority of systems available to date, that are often in excess of 100nm in hydrodynamic size. However, this work does present the targeting of the articular cartilage surface as a potential mechanism for retention of DDS proximal to the target chondrocytes. Further work is required to assess if this has a beneficial effect upon therapeutic diffusion to chondrocytes compared to injection of non-targeted DDS or free drug. In particular lubricin presents a suitable cartilage surface target as demonstrated by its detection at the surface 14 days post IL-1α+OSM treatment suggesting its presence may be maintained in OA states *in vivo* although this would require experimental validation.

The observation of non-specific binding of anti-CD64 mAbs in this Chapter dependant on cell species and antibody isotype has implications not only for drug delivery but standard antibody based assays where macrophages are employed as non-specific binding could potentially obscure results. Commercially available blocking antibodies are available to block FcγRII and RIII but no such antibody is available for CD64/FcγRI. Therefore, the work in this Chapter suggests that IgM subtype antibodies, that showed no non-specific binding, may in fact be preferential in antibody based assays using murine or human macrophage cells.

8.4.3 Future Work

The mAbs developed against CD64/FcγRI in this Chapter are currently being assessed by partners in the TargetCaRe consortium using a model DDS comprised of infrared dye loaded PLGA microparticles. Biodistribution and retention mediated by these targeting moieties is being assessed in mice using *in vivo* imaging. Upon successful completion of this study an assessment of the delivery of TAA to macrophages in the synovium by CD64 targeted TAA loaded PLGA microparticles will be compared to non-targeted PLGA microparticles and free drug in a CIA mouse model to assess for reductions in synovial inflammation and assessment of macrophage subtypes within the synovium mediated by targeted delivery to M1 macrophages.

References

Acharya, C., Yik, J.H.N., Kishore, A., Van Dinh, V., Di Cesare, P.E., Haudenschild, D.R., 2014. Cartilage oligomeric matrix protein and its binding partners in the cartilage extracellular matrix: Interaction, regulation and role in chondrogenesis. Matrix Biol. 37, 102–111.

Activity, A., Lark, M.W., Bayne, E.K., Flanagan, J., Harper, C.F., Hoerrner, L.A., Hutchinson, N.I., Singer, I.I., Donatelli, S.A., Weidner, J.R., Williams, H.R., Mumford, R.A., Lohmander, L.S., 1997. Aggrecan Degradation in Human Cartilage: Evidence for both Matrix Metalloproteinase and Aggrecanase Activity in Normal, Osteoarthritic, and Rheumatoid Joints. J. Clin. Invest. 100, 93–106.

Africa, S., 2017. HHS Public Access 4, 696–703. Åhrman, E., Lorenzo, P., Holmgren, K., Grodzinsky, A.J., Dahlberg, L.E., Saxne, T., Heinegård, D., Önnerfjord, P., 2014. Novel cartilage oligomeric matrix protein (COMP) neoepitopes identified in synovial fluids from patients with joint diseases using affinity chromatography and mass spectrometry. J. Biol. Chem. 289, 20908–20916.

Akasaki, Y., Hasegawa, A., Saito, M., Asahara, H., Iwamoto, Y., Lotz, M.K., 2014. Dysregulated FOXO transcription factors in articular cartilage in aging and osteoarthritis. Osteoarthr. Cartil. 22, 162–170.

Akinrinmade, O.A., Chetty, S., Daramola, A.K., Islam, M., Thepen, T., Barth, S., 2017. CD64: An Attractive Immunotherapeutic Target for M1-type Macrophage Mediated Chronic Inflammatory Diseases. Biomedicines 5, 56.

Akkiraju, H., Nohe, A., 2015. Role of Chondrocytes in Cartilage Formation, Progression of Osteoarthritis and Cartilage Regeneration. J. Dev. Biol. 3, 177–192.

Al-Sabah, A., Stadnik, P., Gilbert, S.J., Duance, V.C., Blain, E.J., 2016. Importance of reference gene selection for articular cartilage mechanobiology studies. Osteoarthr. Cartil. 24, 719–730.

Altman, D.G. and Bland, J.M. 2005. Standard deviations and standard errors. BMJ (Clinical research ed.) 331(7521), p. 903.

Antoni, C. et al. 2013. Crystallization of bi-functional ligand protein complexes. Journal of Structural Biology 182(3), pp. 246–254.

Arafat, S.N. et al. 2014. Neutrophil collagenase, gelatinase, and myeloperoxidase in tears of patients with stevens-johnson syndrome and ocular cicatricial pemphigoid. Ophthalmology 121(1), pp. 79–87. doi: 10.1016/j.ophtha.2013.06.049.

Arbab, A.S. et al. 2004. Efficient magnetic cell labeling with protamine sulfate complexed to ferumoxides for cellular MRI. Blood 104(4), p. 1217 LP-1223.

Armstrong, R.D., English, J., Gibson, T., Chakraborty, J., Marks, V., 1981. Serum methylprednisolone levels following intra-articular injection of methylprednisolone acetate. Ann. Rheum. Dis. 40, 571–4.

Arroll, B., Goodyear-Smith, F., 2004. Corticosteroid injections for osteoarthritis of the knee: meta-analysis. BMJ Br. Med. J. 328, 869.

Aweid, O., Haider, Z., Saed, A., Kalairajah, Y., 2018. Treatment modalities for hip and knee osteoarthritis: A systematic review of safety. J. Orthop. Surg. (Hong Kong) 26, 2309499018808669.

Bajpayee, A.G., Quadir, M.A., Hammond, P.T., Grodzinsky, A.J., 2016. Charge based intra-cartilage delivery of single dose dexamethasone using Avidin nano-carriers suppresses cytokine-induced catabolism long term. Osteoarthr. Cartil.

Baker, J.R., Caterson, B., Christner, J.E.B.T.-M. in E., 1982. [13] Immunological characterization of cartilage proteoglycans. In: Complex Carbohydrates Part D. Academic Press, pp. 216–235.

Barksby, H.E., Hui, W., Wappler, I., Peters, H.H., Milner, J.M., Richards, C.D., Cawston, T.E., Rowan, A.D., 2006. Interleukin-1 in combination with oncostatin M up-regulates multiple genes in chondrocytes: Implications for cartilage destruction and repair. Arthritis Rheum. 54, 540–550.

Becker, D.P. et al. 2010. Orally Active MMP-1 Sparing α-Tetrahydropyranyl and α-Piperidinyl Sulfone Matrix Metalloproteinase (MMP) Inhibitors with Efficacy in Cancer, Arthritis, and Cardiovascular Disease. Journal of Medicinal Chemistry 53(18), pp. 6653–6680.

Beekhuizen, M., Bastiaansen-Jenniskens, Y.M., Koevoet, W., Saris, D.B.F., Dhert, W.J.A., Creemers, L.B., Van Osch, G.J.V.M., 2011. Osteoarthritic synovial tissue inhibition of proteoglycan production in human osteoarthritic knee cartilage: Establishment and characterization of a long-term cartilage-synovium coculture. Arthritis Rheum. 63, 1918–1927.

Beekhuizen, M., van Osch, G.J.V.M., Bot, A.G.J., Hoekstra, M.C.L., Saris, D.B.F., Dhert, W.J.A., Creemers, L.B., 2013. Inhibition of oncostatin M in osteoarthritic synovial fluid enhances GAG production in osteoarthritic cartilage repair. Eur. Cells Mater. 26, 80–90.

Belviso, B.D. et al. 2013. Structure of matrix metalloproteinase-3 with a platinum-based inhibitor. Chemical Communications 49(48), pp. 5492–5494.

Bertini, I. et al. 2012. The catalytic domain of MMP-1 studied through tagged lanthanides. FEBS Letters 586(5), pp. 557–567.

Bishop, J.R., Schuksz, M., Esko, J.D., 2007. Heparan sulphate proteoglycans fine-tune mammalian physiology. Nature 446, 1030–1037.

Blain, E.J. et al. 2010. Boswellia frereana (frankincense) suppresses cytokine-induced matrix metalloproteinase expression and production of pro-inflammatory molecules in articular cartilage. Phytotherapy Research 24(6), pp. 905–912

Bleuel, J., Zaucke, F., Brüggemann, G., Niehoff, A., 2015. Effects of Cyclic Tensile Strain on Chondrocyte Metabolism : A Systematic Review 1–25.

Boergermann, J.H., Kopf, J., Yu, P.B., Knaus, P., 2010. Dorsomorphin and LDN-193189 inhibit BMP-mediated Smad, p38 and Akt signalling in C2C12 cells. Int. J. Biochem. Cell Biol. 42, 1802–1807.

Bondeson, J., Blom, A.B., Wainwright, S., Hughes, C., Caterson, B., Van Den Berg, W.B., 2010. The role of synovial macrophages and macrophage-produced mediators in driving inflammatory and destructive responses in osteoarthritis. Arthritis Rheum. 62, 647–657.

Bonnet, C.S., Walsh, D.A., 2005. Osteoarthritis, angiogenesis and inflammation. Rheumatology 44, 7–16.

Borra, M.T. et al. 2005. Mechanism of human SIRT1 activation by resveratrol. Journal of Biological Chemistry 280(17), pp. 17187–17195. doi: 10.1074/jbc.M501250200.

Brandt, K.D., Smith, G.N., Simon, L.S., 2000. Intraarticular injection of hyaluronan as treatment for knee osteoarthritis: What is the evidence? Arthritis Rheum. 43, 1192–1203.

Brittberg, M., Lindahl, A., Nilsson, A., Ohlsson, C., Isaksson, O., Peterson, L., 1994. Treatment of Deep Cartilage Defects in the Knee with Autologous Chondrocyte Transplantation. N. Engl. J. Med. 331, 889–895.

Butoescu, N., Seemayer, C.A., Palmer, G., Guerne, P.-A., Gabay, C., Doelker, E., Jordan, O., 2009. Magnetically retainable microparticles for drug delivery to the joint: efficacy studies in an antigen-induced arthritis model in mice. Arthritis Res. {&} Ther. 11, 1–10.

Castagnola, P., Dozin, B., Moro, G., Cancedda, R., 1988. Changes in the expression of collagen genes show two stages in chondrocyte differentiation in vitro. J. Cell Biol. 106, 461–467.

Castro-Alvarez, A., Costa, A.M., Vilarrasa, J., 2017. The Performance of several docking programs at reproducing protein-macrolide-like crystal structures. Molecules 22.

Caterson, B., Melrose, J., 2018. Keratan sulfate, a complex glycosaminoglycan with unique functional capability. Glycobiology 28, 182–206.

Chabane, N., Zayed, N., Benderdour, M., Martel-Pelletier, J., Pelletier, J.P., Duval, N., Fahmi, H., 2009. Human articular chondrocytes express 15-lipoxygenase-1 and -2: Potential role in osteoarthritis. Arthritis Res. Ther. 11, 1–12.

Champion, J.A., Walker, A., Mitragotri, S., 2008. Role of Particle Size in Phagocytosis of Polymeric Microspheres. Pharm. Res. 25, 1815–1821.

Chan, C.M., Macdonald, C.D., Litherland, G.J., Wilkinson, D.J., Skelton, A., Europe-Finner, G.N., Rowan, A.D., 2017. Cytokine-induced MMP13 expression in human chondrocytes is dependent on activating transcription Factor 3 (ATF3) Regulation. J. Biol. Chem. 292, 1625–1636.

Chan, M.M.Y., Moore, A.R., 2010. Resolution of Inflammation in Murine Autoimmune Arthritis Is Disrupted by Cyclooxygenase-2 Inhibition and Restored by Prostaglandin E2-Mediated Lipoxin A4 Production. J. Immunol. 184, 6418–6426.

Chandrasekharan, J.A., Sharma-Wali, N., 2015. Lipoxins: Nature's way to resolve inflammation. J. Inflamm. Res. 8, 181–192.

Chevalier, X., Goupille, P., Beaulieu, A.D., Burch, F.X., Bensen, W.G., Conrozier, T., Loeuille, D., Kivitz, A.J., Silver, D., Appleton, B.E., 2009. Intraarticular injection of anakinra in osteoarthritis of the knee: A multicenter, randomized, double-blind, placebo-controlled study. Arthritis Care Res. 61, 344–352.

Chia, S.L., Sawaji, Y., Burleigh, A., McLean, C., Inglis, J., Saklatvala, J., Vincent, T., 2009. Fibroblast growth factor 2 is an intrinsic chondroprotective agent that suppresses ADAMTS-5 and delays cartilage degradation in murine osteoarthritis. Arthritis Rheum. 60, 2019–2027.

Chiang, N., Serhan, C.N., Dahlen, S.-E., Drazen, J.M., Hay, D.W.P., Rovati, G.E., Shimizu, T., Yokomizo, T., Brink, C., 2006. The lipoxin receptor ALX: potent ligand-specific and stereoselective actions in vivo. Pharmacol. Rev. 58, 463–487.

Cho, H., Stuart, J.M., Magid, R., Danila, D.C., Hunsaker, T., Pinkhassik, E., Hasty, K. a., 2014. Theranostic immunoliposomes for osteoarthritis. Nanomedicine Nanotechnology, Biol. Med. 10, 619–627.

Cohen, S.B., Proudman, S., Kivitz, A.J., Burch, F.X., Donohue, J.P., Burstein, D., Sun, Y.-N., Banfield, C., Vincent, M.S., Ni, L., Zack, D.J., 2011. A randomized, double-blind study of AMG 108 (a fully human monoclonal antibody to IL-1R1) in patients with osteoarthritis of the knee. Arthritis Res. Ther. 13, R125.

Cope, P.J., Ourradi, K., Li, Y., Sharif, M., 2018. Models of osteoarthritis: the good, the bad and the promising. Osteoarthr. Cartil. 27, 230–239.

Croasdell, A., Duffney, P.F., Kim, N., Lacy, S.H., Sime, P.J., Phipps, R.P., 2015. PPAR γ and the Innate Immune System Mediate the Resolution of Inflammation. PPAR Res. 2015.

Dahms, S.O. et al. 2018. X-ray Structures of the Proprotein Convertase Furin Bound with Substrate Analogue Inhibitors Reveal Substrate Specificity Determinants beyond the S4 Pocket. Biochemistry 57(6), pp. 925–934.

Dhanaraj, V. et al. 1999. X-ray Structure of Gelatinase A Catalytic Domain Complexed with a Hydroxamate Inhibitor. Croatica Chemica Acta 72, pp575-591.

Davidson, D. et al. 2005. Fibroblast growth factor (FGF) 18 signals through FGF receptor 3 to promote chondrogenesis. Journal of Biological Chemistry 280(21), pp. 20509–20515. doi: 10.1074/jbc.M410148200.

Davidson, E.N.B., Vitters, E.L., van Lent, P.L.E.M., van de Loo, F.A.J., van den Berg, W.B., van der Kraan, P.M., 2007. Elevated extracellular matrix production and degradation upon bone morphogenetic protein-2 (BMP-2) stimulation point toward a role for BMP-2 in cartilage repair and remodeling. Arthritis Res. Ther. 9, 1–11.

de la Rica, R., Aili, D., Stevens, M.M., 2012. Enzyme-responsive nanoparticles for drug release and diagnostics. Adv. Drug Deliv. Rev. 64, 967–978.

Di Cesare, P.E., Carlson, C.S., Stolerman, E.S., Hauser, N., Tulli, H., Paulsson, M., 1996. Increased degradation and altered tissue distribution of cartilage oligomeric matrix protein in human rheumatoid and osteoarthritic cartilage. J. Orthop. Res. 14, 946–955.

Dickinson, S.C., Vankemmelbeke, M.N., Buttle, D.J., Rosenberg, K., Heinegård, D., Hollander, A.P., 2003. Cleavage of cartilage oligomeric matrix protein (thrombospondin-5) by matrix metalloproteinases and a disintegrin and metalloproteinase with thrombospondin motifs. Matrix Biol. 22, 267–278.

Divanovic, S., Dalli, J., Jorge-Nebert, L.F., Flick, L.M., Galvez-Peralta, M., Boespflug, N.D., Stankiewicz, T.E., Fitzgerald, J.M., Somarathna, M., Karp, C.L., Serhan, C.N., Nebert, D.W., 2013. Contributions of the Three CYP1 Monooxygenases to Pro-Inflammatory and Inflammation-Resolution Lipid Mediator Pathways. J. Immunol. 191, 3347–3357.

Durham, T.B. et al. 2014. Identification of potent and selective hydantoin inhibitors of aggrecanase-1 and aggrecanase-2 that are efficacious in both chemical and surgical models of osteoarthritis. Journal of Medicinal Chemistry 57(24), pp. 10476–10485.

Durigova, M., Nagase, H., Mort, J.S., Roughley, P.J., 2011. MMPs are less efficient than ADAMTS5 in cleaving aggrecan core protein. Matrix Biol. 30, 145–153.

Durigova, M., Roughley, P.J., Mort, J.S., 2008. Mechanism of proteoglycan aggregate degradation in cartilage stimulated with oncostatin M. Osteoarthr. Cartil. 16, 98–104.

Ebbesen, M.F., Whitehead, B., Ballarin-Gonzalez, B., Kingshott, P., Howard, K.A., 2013. Surface analysis of PEGylated nano-shields on nanoparticles installed by hydrophobic anchors. Pharm. Res. 30, 1758–1767.

El Mabrouk, M., Sylvester, J., Zafarullah, M., 2007. Signaling pathways implicated in oncostatin M-induced aggrecanase-1 and matrix metalloproteinase-13 expression in human articular chondrocytes. Biochim. Biophys. Acta - Mol. Cell Res. 1773, 309–320.

Ellman, M.B., Yan, D., Ahmadinia, K., Chen, D., An, H.S., Im, H.J., 2013. Fibroblast growth factor control of cartilage homeostasis. J. Cell. Biochem. 114, 735–42.

Enochson, L., Stenberg, J., Brittberg, M., Lindahl, A., 2014. GDF5 reduces MMP13 expression in human chondrocytes via DKK1 mediated canonical Wnt signaling inhibition. Osteoarthr. Cartil. 22, 566–577.

Eswaramoorthy, R., Chang, C.C., Wu, S.C., Wang, G.J., Chang, J.K., Ho, M.L., 2012. Sustained release of PTH(1-34) from PLGA microspheres suppresses osteoarthritis progression in rats. Acta Biomater. 8, 2254–2262.

Evans, C.H., Kraus, V.B., Setton, L.A., 2014. Progress in intra-articular therapy. Nat. Rev. Rheumatol. 10, 11–22. Eyre, D., 2002. Collagen of articular cartilage. Arthritis Res. 4, 30–35.

Fang, J., Nakamura, H., Maeda, H., 2011. The EPR effect: Unique features of tumor blood vessels for drug delivery, factors involved, and limitations and augmentation of the effect. Adv. Drug Deliv. Rev. 63, 136–151.

Farndale, R.W., Buttle, D.J., Barrett, A.J., 1986. Improved quantitation and discrimination of sulphated glycosaminoglycans by use of dimethylmethylene blue. Biochim. Biophys. Acta - Gen. Subj. 883, 173–177.

Fermor, H.L., 2013. Biological, biochemical and biomechanical characterisation of cartilage from the porcine, bovine and ovine hip and knee. J. Biomed. Eng. 91.

Ferreira, R.S., Simeonov, A., Jadhav, A., Eidam, O., Mott, B.T., Keiser, M.J., McKerrow, J.H., Maloney, D.J., Irwin, J.J., Shoichet, B.K., 2010. Complementarity between a docking and a high-throughput screen in discovering new cruzain inhibitors. J. Med. Chem. 53, 4891–4905.

Flannery, C.R., Little, C.B., Hughes, C.E., Curtis, C.L., Caterson, B., Jones, S.A., 2000. IL-6 and its soluble receptor augment aggrecanase-mediated proteoglycan catabolism in articular cartilage. Matrix Biol. 19, 549–553.

Flannery, C.R., Zollner, R., Corcoran, C., Jones, A.R., Root, A., Blanchet, T., Gleghorn, J.P., Bonassar, L.J., Bendele, A.M., Morris, E.A., Glasson, S.S., 2009. Prevention of Cartilage Degeneration in a Rat Model of Osteoarthritis by Intraarticular Treatment With Recombinant Lubricin 60, 840–847.

Fosang, a J., Last, K., Neame, P.J., Murphy, G., Knäuper, V., Tschesche, H., Hughes, C.E., Caterson, B., Hardingham, T.E., 1994. Neutrophil collagenase (MMP-8) cleaves at the aggrecanase site E373-A374 in the interglobular domain of cartilage aggrecan. Biochem. J. 304 (Pt 2, 347–351.

Fosang, A.J., Neame, P.J., Last, K., Hardingham, T.E., Murphy, G., Hamilton, J.A., 1992. The interglobular domain of cartilage aggrecan is cleaved by PUMP, gelatinases, and cathepsin B. J. Biol. Chem. 267, 19470–19474.

Fosang, A.J., Rogerson, F.M., East, C.J., Stanton, H., 2008. ADAMTS-5: The story so far. Eur. Cells Mater. 15, 11–26.

Frisbie, D.D., Cross, M.W., Mcilwraith, C.W., 2006. A comparative study of articular cartilage thickness in the stifle of animal species used in human pre-clinical studies compared to articular cartilage thickness in the human knee 142–146.

Fritz, G., Kaina, B., 2006. Late activation of stress kinases (SAPK/JNK) by genotoxins requires the DNA repair proteins DNA-PKcs and CSB. Mol. Biol. Cell 17, 851–861.

Frizziero, A., Giannotti, E., Oliva, F., Masiero, S., Maffulli, N., 2013. Autologous conditioned serum for the treatment of osteoarthritis and other possible applications in musculoskeletal disorders. Br. Med. Bull. 105, 169–184.

Fukuda, S., Abematsu, M., Mori, H., Yanagisawa, M., Kagawa, T., Nakashima, K., Yoshimura, A., Taga, T., 2007. Potentiation of Astrogliogenesis by STAT3-Mediated Activation of Bone Morphogenetic Protein-Smad Signaling in Neural Stem Cells. Mol. Cell. Biol. 27, 4931–4937.

Fukui, N., Zhu, Y., Maloney, W.J., Clohisy, J., Sandell, L.J., 2003. Stimulation of BMP-2 expression by pro-inflammatory cytokines IL-1 and TNF-alpha in normal and osteoarthritic chondrocytes. J. Bone Joint Surg. Am. 85–A Suppl 3, 59–66.

Fushimi, K., Troeberg, L., Nakamura, H., Lim, N.H., 2007. Functional Differences Of The Catalytic And Non- Catalytic Domains In Human Adamts-4 And Adamts-5 In Aggrecanolytic Activity . 1–25.

Ganu, V., Goldberg, R., Peppard, J., Rediske, J., Melton, R., Hu, S.I., Wang, W., Duvander, C., Heinegard, D., 1998. Inhibition of interleukin-1alpha-induced cartilage oligomeric matrix protein degradation in bovine articular cartilage by matrix metalloproteinase inhibitors: potential role for matrix metalloproteinases in the generation of cartilage oligomeric matrix pr. Arthritis Rheum. 41, 2143–2151.

Gao, G., Westling, J., Thompson, V.P., Howell, T.D., Gottschall, P.E., Sandy, J.D., 2002. Activation of the Proteolytic Activity of ADAMTS4 (Aggrecanase-1) by C-terminal Truncation. J. Biol. Chem. 277, 11034–11041.

Gelse, K., Pöschl, E., Aigner, T., 2003. Collagens - Structure, function, and biosynthesis. Adv. Drug Deliv. Rev. 55, 1531–1546.

Gendron, C., Kashiwagi, M., Ngee, H.L., Enghild, J.J., Thøgersen, I.B., Hughes, C., Caterson, B., Nagase, H., 2007. Proteolytic activities of human ADAMTS-5: Comparative studies with ADAMTS-4. J. Biol. Chem. 282, 18294–18306.

Geyer, M., Grässel, S., Straub, R.H., Schett, G., Dinser, R., Grifka, J., Gay, S., Neumann, E., Müller-Ladner, U., 2009. Differential transcriptome analysis of intraarticular lesional vs intact cartilage reveals new candidate genes in osteoarthritis pathophysiology. Osteoarthr. Cartil. 17, 328–335.

Gilbert, A.M. et al. 2007. 5-((1H-Pyrazol-4-yl)methylene)-2-thioxothiazolidin-4-one inhibitors of ADAMTS-5. Bioorganic and Medicinal Chemistry Letters 17(5), pp. 1189–1192. doi: 10.1016/j.bmcl.2006.12.020.

Gilbert, S.J., Singhrao, S.K., Khan, I.M., Gonzalez, L.G., Thomson, B.M., Burdon, D., Duance, V.C., Archer, C.W., 2009. Enhanced Tissue Integration During Cartilage Repair In Vitro Can Be Achieved by Inhibiting Chondrocyte Death at the Wound Edge. Tissue Eng. Part A 15, 1739–1749.

Gilbert, S.J. et al. 2012. Protein kinase R plays a pivotal role in oncostatin M and interleukin-1 signalling in bovine articular cartilage chondrocytes. European Cells and Materials 23(0), pp. 41–57.

Gilroy, D.W., 2005. The role of aspirin-triggered lipoxins in the mechanism of action of aspirin. Prostaglandins Leukot. Essent. Fat. Acids 73, 203–210.

Gkogkolou, P., Bohm, M., Böhm, M., 2012. Advanced glycation end products: key players in skin ageing?

Gkogkolou, Paraskevi Bohm, Markus 4, 259–270. Glasson, S.S., Askew, R., Sheppard, B., Carito, B., Blanchet, T., Ma, H.-L., Flannery, C.R., Peluso, D., Kanki, K., Yang, Z., Majumdar, M.K., Morris, E.A., 2005. Deletion of active ADAMTS5 prevents cartilage degradation in a murine model of osteoarthritis. Nature 434, 644.

Goerz, G., Ruzicka, T., Hofmann, N., Drost, H., Gruneklee, D., 1981. [Granulomatous allergic reaction of the delayed type to surfen]. Hautarzt. 32, 187–190.

Greene, M.A., Loeser, R.F., 2015. Function of the chondrocyte PI-3 kinase-Akt signaling pathway is stimulus dependent. Osteoarthr. Cartil. 23, 949–956.

Grosdidier, A., Zoete, V., Michielin, O., 2011. SwissDock, a protein-small molecule docking web service based on EADock DSS. Nucleic Acids Res. 39, 270–277. Harizi, H., Corcuff, J.B., Gualde, N., 2008. Arachidonic-acid-derived eicosanoids: roles in biology and immunopathology. Trends Mol. Med. 14, 461–469.

Hailemariam D *et al.* (2013) MicroRNA-regulated molecular mechanism underlying bovine subclinical endometritis. Reproduction, Fertility and Development 26, 898-913.

Hecht, J.T., Hayes, E., Haynes, R., Cole, W.G., 2005. COMP mutations, chondrocyte function and cartilage matrix. Matrix Biol. 23, 525–533.

Hecht, K.L.P. and J.T., 2008. The Role of Cartilage Oligomeric Matrix Protein (COMP) in Skeletal Disease. Curr. Drug Targets.

Henrotin, Y. et al. 2014. What is the current status of chondroitin sulfate and glucosamine for the treatment of knee osteoarthritis? Maturitas 78(3), pp. 184–187. doi: 10.1016/j.maturitas.2014.04.015.

Hochberg, M., Guermazi, A., Guehring, H., Aydemir, A., Wax, S., Fleuranceau-Morel, P., Reinstrup Bihlet, A., Byrjalsen, I., Ragnar Andersen, J., Eckstein, F., 2018. Efficacy and safety of intra-articular Sprifermin in symptomatic radiographic knee osteoarthritis: pre-specified analysis of 3-year data from a 5-year randomized, placebo-controlled, phase II study. Osteoarthr. Cartil. 26, S26–S27.

Hochberg, M.C., 2015. Serious joint-related adverse events in randomized controlled trials of anti-nerve growth factor monoclonal antibodies. Osteoarthr. Cartil. 23, S18–S21.

Hoekstra, R., Eskens, F.A., Verweij, J., 2001. Matrix metalloproteinase inhibitors: current developments and future perspectives. Oncologist 6, 415–27.

Honjo, K., Kubagawa, Y., Kubagawa, H., 2013. Is Toso/IgM Fc receptor (Fc R) expressed by innate immune cells? Proc. Natl. Acad. Sci. 110, E2540–E2541.

Huang, G., Chubinskaya, S., Liao, W., Loeser, R.F., 2017. Wnt5a induces catabolic signaling and matrix metalloproteinase production in human articular chondrocytes. Osteoarthr. Cartil. 25, 1505–1515.

Huegel, J., Enomoto-Iwamoto, M., Sgariglia, F., Koyama, E., Pacifici, M., 2015. Heparanase stimulates chondrogenesis and is up-regulated in human ectopic cartilage: A mechanism possibly involved in hereditary multiple exostoses. Am. J. Pathol. 185, 1676–1685.

Huegel, J., Mundy, C., Sgariglia, F., Nygren, P., Billings, P.C., Yamaguchi, Y., Koyama, E., Pacifici, M., 2013. Perichondrium phenotype and border function are regulated by Ext1 and heparan sulfate in developing long bones: A mechanism likely deranged in Hereditary Multiple Exostoses. Dev. Biol. 377, 100–112.

Hughes, C.E. et al. 1995. Monoclonal antibodies that specifically recognize neoepitope sequences generated by 'aggrecanase' and matrix metalloproteinase cleavage of aggrecan: application to catabolism in situ and in vitro. Biochemical Journal 305(Pt 3), pp. 799–804.

Hui, W., Rowan, A.D., Richards, C.D., Cawston, T.E., 2003. Oncostatin M in Combination with Tumor Necrosis Factor α Induces Cartilage Damage and Matrix Metalloproteinase Expression In Vitro and In Vivo. Arthritis Rheum. 48, 3404–3418.

Hunter, D.T.J., Hill, J.M., 1961. Surfen: a quinoline with oncogenic and heparin-neutralizing properties. Nature 191, 1378–1379.

Hunziker, E.B., Quinn, T.M., Ha, H., Mu, M.E., 2002. Quantitative structural organization of normal adult human articular cartilage d, 564–572.

Hwang, N.S. et al. 2009. NIH Public Access. 581(22), pp. 4172–4178.

Irwin, J.J., Shoichet, B.K., 2005. ZINC--a free database of commercially available compounds for virtual screening. J. Chem. Inf. Model. 45, 177–182.

Ishimaru, D., Sugiura, N., Akiyama, H., Watanabe, H., Matsumoto, K., 2014. Alterations in the chondroitin sulfate chain in human osteoarthritic cartilage of the knee. Osteoarthr. Cartil. 22, 250–258.

Ismail, H.M., Miotla-Zarebska, J., Troeberg, L., Tang, X., Stott, B., Yamamoto, K., Nagase, H., Fosang, A.J., Vincent, T.L., Saklatvala, J., 2016. Brief Report: JNK-2 Controls Aggrecan Degradation in Murine Articular Cartilage and the Development of Experimental Osteoarthritis. Arthritis Rheumatol. 68, 1165–1171.

Ismail, H.M., Yamamoto, K., Vincent, T.L., Nagase, H., Troeberg, L., Saklatvala, J., 2015. Interleukin-1 acts via the JNK-2 signaling pathway to induce aggrecan degradation by human chondrocytes. Arthritis Rheumatol. 67, 1826–1836.

Jakob, M., Demarteau, O., Schafer, D., Hintermann, B., Dick, W., Heberer, M., Martin, I., 2001. Specific growth factors during the expansion and redifferentiation of adult human articular chondrocytes enhance chondrogenesis and cartilaginous tissue formation in vitro. J. Cell. Biochem. 81, 368–377.

Jay, G.D., Waller, K.A., 2014. The biology of Lubricin: Near frictionless joint motion. Matrix Biol. 39, 17–24. Johnson, C.I., Argyle, D.J., Clements, D.N., 2016. In vitro models for the study of osteoarthritis. Vet. J. 209, 40–49.

Jones, A.R.C., Flannery, C.R., 2007. Bioregulation of lubricin expression by growth factors and cytokines. Eur. Cells Mater. 13, 40–45.

Jones, A.R.C., Gleghorn, J.P., Hughes, C.E., Fitz, L.J., Zollner, R., Wainwright, S.D., Caterson, B., Morris, E.A., Bonassar, L.J., Flannery, C.R., 2007. Binding and localization of recombinant lubricin to articular cartilage surfaces. J. Orthop. Res. 25, 283–292.

Junk, D.J., Bryson, B.L., Smigiel, J.M., Parameswaran, N., Bartel, C.A., Jackson, M.W., 2017. Oncostatin M promotes cancer cell plasticity through cooperative STAT3-SMAD3 signaling. Oncogene 36, 4001–4013.

Kaneti, L., Bronshtein, T., Malkah Dayan, N., Kovregina, I., Letko Khait, N., Lupu-Haber, Y., Fliman, M., Schoen, B.W., Kaneti, G., Machluf, M., 2016. Nanoghosts as a Novel Natural Nonviral Gene Delivery Platform Safely Targeting Multiple Cancers. Nano Lett. 16, 1574–1582.

Kanju, P., Chen, Y., Lee, W., Yeo, M., Lee, S.H., Romac, J., Shahid, R., Fan, P., Gooden, D.M., Simon, S.A., Spasojevic, I., Mook, R.A., Liddle, R.A., Guilak, F., Liedtke, W.B., 2016. Small molecule dual-inhibitors of TRPV4 and TRPA1 for attenuation of inflammation and pain. Sci. Rep. 6, 1–12.

Karsdal, M.A., Madsen, S.H., Christiansen, C., Henriksen, K., Fosang, A.J., Sondergaard, B.C., 2008. Cartilage degradation is fully reversible in the presence of aggrecanase but not matrix metalloproteinase activity. Arthritis Res. Ther. 10, 1–12.

Kasa, M., Borda, F., 1990. [Surfen allergy causing insulin depot S hypersensitivity]. Orv. Hetil. 131, 965–966,969.

Kashiwagi, M., Enghild, J.J., Gendron, C., Hughes, C., Caterson, B., Itoh, Y., Nagase, H., 2004. Altered Proteolytic Activities of ADAMTS-4 Expressed by C-terminal Processing. J. Biol. Chem. 279, 10109–10119.

Kashiwagi, M., Tortorella, M., Nagase, H., Brew, K., 2001. TIMP-3 Is a Potent Inhibitor of Aggrecanase 1 (ADAM-TS4) and Aggrecanase 2 (ADAM-TS5). J. Biol. Chem. 276, 12501–12504.

Kavanaugh, T.E., Werfel, T. a., Cho, H., Hasty, K. a., Duvall, C.L., 2015. Particle-based technologies for osteoarthritis detection and therapy. Drug Deliv. Transl. Res.

Kelwick, R., Desanlis, I., Wheeler, G.N., Edwards, D.R., 2015. The ADAMTS (A Disintegrin and Metalloproteinase with Thrombospondin motifs) family.

Kevorkian, L., Young, D.A., Darrah, C., Donell, S.T., Shepstone, L., Porter, S., Brockbank, S.M.V., Edwards, D.R., Parker, A.E., Clark, I.M., 2004. Expression Profiling of Metalloproteinases and Their Inhibitors in Cartilage. Arthritis Rheum. 50, 131–141.

Kiani, C., Chen, L., Wu, Y.J., Yee, A.J., Yang, B.B., 2002. Structure and function of aggrecan. Cell Res. 12, 19–32.

Kishimoto, T., 2006. Interleukin-6: Discovery of a pleiotropic cytokine. Arthritis Res. Ther. 8.

Klein, T., Bischoff, R., 2011. Physiology and pathophysiology of matrix metalloproteases. Amino Acids 41, 271–290.

Knudson, C.B., Knudson, W., 2001. Cartilage proteoglycans. Semin. Cell Dev. Biol. 12, 69–78.

Komori, T., Tanaka, M., Senba, E., Miyajima, A., Morikawa, Y., 2014. Deficiency of oncostatin M receptor ?? (OSMR??) exacerbates high-fat diet-induced obesity and related metabolic disorders in mice. J. Biol. Chem. 289, 13821–13837.

Koshy, P.J.T., Lundy, C.J., Rowan, A.D., Porter, S., Edwards, D.R., Hogan, A., Clark, I.M., Cawston, T.E., 2002. The modulation of matrix metalloproteinase and ADAM gene expression in human chondrocytes by interleukin-1 and oncostatin M: A time-course study using real-time quantitative reverse transcription-polymerase chain reaction. Arthritis Rheum. 46, 961–967.

Kraan, P.M. Van Der, 2018. Differential Role of Transforming Growth Factor- beta in an Osteoarthritic or a Healthy Joint 65–72.

Katz, H.R. et al. 1986. Secretory granules of heparin-containing rat serosal mast cells also posess highly sulfated chondroitin sulfate proteoglycans. Journal of Biological Chemistry 261(29), pp. 13393–13396.

Kraus, V.B., Conaghan, P.G., Aazami, H.A., Mehra, P., Kivitz, A.J., Lufkin, J., Hauben, J., Johnson, J.R., Bodick, N., 2018. Synovial and systemic pharmacokinetics (PK) of triamcinolone acetonide (TA) following intra-articular (IA) injection of an extended-release microsphere-based formulation (FX006) or standard crystalline suspension in patients with knee osteoarthritis (OA). Osteoarthr. Cartil. 26, 34–42.

Kridel, S.J. et al. 2001. Substrate Hydrolysis by Matrix Metalloproteinase-9. Journal of Biological Chemistry 276(23), pp. 20572–20578. doi: 10.1074/jbc.M100900200.

Kronke, G., Katzenbeisser, J., Uderhardt, S., Zaiss, M.M., Scholtysek, C., Schabbauer, G., Zarbock, A., Koenders, M.I., Axmann, R., Zwerina, J., Baenckler, H.W., van den Berg, W., Voll, R.E., Kuhn, H., Joosten, L.A.B., Schett, G., 2009. 12/15-Lipoxygenase Counteracts Inflammation and Tissue Damage in Arthritis. J. Immunol. 183, 3383–3389.

Krzeski, P., Buckland-Wright, C., Bálint, G., Cline, G.A., Stoner, K., Lyon, R., Beary, J., Aronstein, W.S., Spector, T.D., 2007. Development of musculoskeletal toxicity without clear benefit after administration of PG-116800, a matrix metalloproteinase inhibitor, to patients with knee osteoarthritis: A randomized, 12-month, double-blind, placebo-controlled study. Arthritis Res. Ther. 9, 1–11.

Kubagawa, H., Oka, S., Kubagawa, Y., Torii, I., Takayama, E., Kang, D.W., Jones, D., Nishida, N., Miyawaki, T., Bertoli, L.F., Sanders, S.K., Honjo, K., 2014. The long elusive IgM Fc receptor, FcμR. J. Clin. Immunol. 34, 2779–2793.

Kuo, T.T., Aveson, V.G., 2011. Neonatal Fc receptor and IgG-based therapeutics. MAbs 3, 422–430.

LaBranche, T.P., Bendele, A.M., Omura, B.C., Gropp, K.E., Hurst, S.I., Bagi, C.M., Cummings, T.R., Grantham, L.E., Shelton, D.L., Zorbas, M.A., 2017. Nerve growth factor inhibition with tanezumab influences weight-bearing and subsequent cartilage damage in the rat medial meniscal tear model. Ann. Rheum. Dis. 76, 295–302.

Lambova, S., Hermann, W., Müller- Ladner, U., 2017. Current Treatment Options for Osteoarthritis. Curr. Rheumatol. Rev. 13, 108–116.

Lang, I., Füllsack, S., Wyzgol, A., Fick, A., Trebing, J., Arana, J.A.C., Schäfer, V., Weisenberger, D., Wajant, H., 2016. Binding studies of TNF receptor superfamily (TNFRSF) receptors on intact cells. J. Biol. Chem. 291, 5022–5037.

Lanza, T.J., Durette, P.L., Rollins, T., Siciliano, S., Cianciarulo, D.N., Kobayashi, S. V, Caldwell, C.G., Springer, M.S., Hagmann, W.K., 1992. Substituted 4,6-diaminoquinolines as inhibitors of C5a receptor binding. J. Med. Chem. 35, 252–258.

Lees, S., Golub, S.B., Last, K., Zeng, W., Jackson, D.C., Sutton, P., Fosang, A.J., 2015. Bioactivity in an Aggrecan 32-mer Fragment Is Mediated via Toll-like Receptor 2. Arthritis Rheumatol. 67, 1240–1249.

Lin, H.-C., Lin, T.-H., Wu, M.-Y., Chiu, Y.-C., Tang, C.-H., Hour, M.-J., Liou, H.-C., Tu, H.-J., Yang, R.-S., Fu, W.-M., 2014. 5-Lipoxygenase Inhibitors Attenuate TNF-α-Induced Inflammation in Human Synovial Fibroblasts. PLoS One 9, e107890.

Ling, T.-Y. et al. 2003. Fatty acids modulate transforming growth factor-β activity and plasma clearance. The FASEB Journal 17(11), pp. 1559–1561. doi: 10.1096/fj.02-1063fje.

Little, C.B. et al. 2009. Matrix metalloproteinase 13–deficient mice are resistant to osteoarthritic cartilage erosion but not chondrocyte hypertrophy or osteophyte development. Arthritis & Rheumatism 60(12), pp. 3723–3733. doi: 10.1002/art.25002.

Little, C.B., Meeker, C.T., Golub, S.B., Lawlor, K.E., Farmer, P.J., Smith, S.M., Fosang, A.J., 2007. Blocking aggrecanase cleavage in the aggrecan interglobular domain abrogates cartilage erosion and promotes cartilage repair. J. Clin. Invest. 117, 1627–1636.

Liu, C.J., Kong, W., Ilalov, K., Yu, S., Xu, K., Prazak, L., Fajardo, M., Sehgal, B., Di Cesare, P.E., 2006. ADAMTS-7: a metalloproteinase that directly binds to and degrades cartilage oligomeric matrix protein. FASEB J. 20, 988–990.

Livak, K.J., Schmittgen, T.D., 2001. Analysis of Relative Gene Expression Data Using Real-Time Quantitative PCR and the $2-\Delta\Delta CT$ Method. Methods 25, 402–408.

Livshits, G., Zhai, G., Hart, D.J., Kato, B.S., Wang, H., Williams, F.M.K., Spector, T.D., 2009. Interleukin-6 is a significant predictor of radiographic knee osteoarthritis: The Chingford Study. Arthritis Rheum. 60, 2037–2045.

Loffredo, F.S., Pancoast, J.R., Cai, L., Vannelli, T., Dong, J.Z., Lee, R.T., Patwari, P., 2014. Targeted delivery to cartilage is critical for in vivo efficacy of insulin-like growth factor 1 in a rat model of osteoarthritis. Arthritis Rheumatol. (Hoboken, N.J.) 66, 1247–55.

Lohmander, L.S., Hellot, S., Dreher, D., Krantz, E.F.W., Kruger, D.S., Guermazi, A., Eckstein, F., 2014. Intraarticular sprifermin (recombinant human fibroblast growth factor 18) in knee osteoarthritis: A randomized, double-blind, placebo-controlled trial. Arthritis Rheumatol. 66, 1820–1831.

Loughlin, J., Dowling, B., Chapman, K., Marcelline, L., Mustafa, Z., Southam, L., Ferreira, A., Ciesielski, C., Carson, D.A., Corr, M., 2004. Functional variants within the secreted frizzled-related protein 3 gene are associated with hip osteoarthritis in females. Proc. Natl. Acad. Sci. 101, 9757–9762.

Luan, Y., Kong, L., Howell, D.R., Ilalov, K., Fajardo, M., Bai, X.H., Di Cesare, P.E., Goldring, M.B., Abramson, S.B., Liu, C.J., 2008. Inhibition of ADAMTS-7 and ADAMTS-12 degradation of cartilage oligomeric matrix protein by alpha-2-macroglobulin. Osteoarthr. Cartil. 16, 1413–1420.

Manka, S.W. et al. 2012. Structural insights into triple-helical collagen cleavage by matrix metalloproteinase 1. Proceedings of the National Academy of Sciences 109(31), p. 12461 LP-12466.

Matsuzaki, T., Alvarez-Garcia, O., Mokuda, S., Nagira, K., Olmer, M., Gamini, R., Miyata, K., Akasaki, Y., Su, A.I., Asahara, H., Lotz, M.K., 2018. FoxO transcription factors modulate autophagy and proteoglycan 4 in cartilage homeostasis and osteoarthritis. Sci. Transl. Med. 10.

McCance, K.L., *et al.* 2010. Collagen Structure and Stability. PLoS One 78, 929–958.

McCoy, A.M., 2015. Animal Models of Osteoarthritis: Comparisons and Key Considerations. Vet. Pathol. 52, 803–818.

McNulty, A.L., Rothfusz, N.E., Leddy, H.A., Guilak, F., 2013. Synovial fluid concentrations and relative potency of interleukin-1 alpha and beta in cartilage and meniscus degradation. J. Orthop. Res. 31, 1039–1045.

Miller, R.E., Ishihara, S., Tran, P.B., Golub, S.B., Last, K., Miller, R.J., Fosang, A.J., Malfait, A.-M., 2018. An aggrecan fragment drives osteoarthritis pain through Toll-like receptor 2. JCI Insight 3, 1–9.

Milner, J.M. et al. 2003. Inhibition of furin-like enzymes blocks interleukin-1α/oncostatin M-stimulated cartilage degradation. Arthritis and Rheumatism 48(4), pp. 1057–1066. doi: 10.1002/art.10873.

Miyamoto, Y., Mabuchi, A., Shi, D., Kubo, T., Takatori, Y., Saito, S., Fujioka, M., Sudo, A., Uchida, A., Yamamoto, S., Ozaki, K., Takigawa, M., Tanaka, T., Nakamura, Y., Jiang, Q., Ikegawa, S., 2007. A functional polymorphism in the 5´ UTR of GDF5 is associated with susceptibility to osteoarthritis. Nat. Genet. 39, 529.

Miyaoka, Y., Tanaka, M., Naiki, T., Miyajima, A., 2006. Oncostatin M inhibits adipogenesis through the RAS/ERK and STAT5 signaling pathways. J. Biol. Chem. 281, 37913–37920.

Monk, P.N., Scola, A.M., Madala, P., Fairlie, D.P., 2007. Function, structure and therapeutic potential of complement C5a receptors. Br. J. Pharmacol. 152, 429–448.

Moulharat, N., Lesur, C., Thomas, M., Pastoureau, P., Anract, P., Ceuninck, F. De, Sabatini, M., 2004. Effects of transforming growth factor- on aggrecanase production and proteoglycan degradation by human chondrocytes in vitro 296–305.

Mundy, C., Yang, E., Takano, H., Billings, P.C., Pacifici, M., 2018. Heparan sulfate antagonism alters bone morphogenetic protein signaling and receptor dynamics, suggesting a mechanism in Hereditary Multiple Exostoses. J. Biol. Chem. jbc.RA117.000264.

Nagase, H., Visse, R., Murphy, G., 2006. Structure and function of matrix metalloproteinases and TIMPs. Cardiovasc. Res. 69, 562–573.

Natoli, R.M. et al. 2008. Temporal effects of impact on articular cartilage cell death, gene expression, matrix biochemistry, and biomechanics. Annals of Biomedical Engineering 36(5), pp. 780–792.

Naini, S.M.A., Yanicostas, C., Hassan-Abdi, R., Blondeel, S., Bennis, M., Weiss, R.J., Tor, Y., Esko, J.D., Soussi-Yanicostas, N., 2018. Surfen and oxalyl surfen decrease tau hyperphosphorylation and mitigate neuron deficits in vivo in a zebrafish model of tauopathy. Transl. Neurodegener. 7, 1–9.

Nasi, S., Ea, H.K., So, A., Busso, N., 2017. Revisiting the role of interleukin-1 pathway in osteoarthritis: Interleukin-1α and -1β, and NLRP3 inflammasome are not involved in the pathological features of the murine menisectomy model of osteoarthritis. Front. Pharmacol. 8, 1–12.

Necas, J., Bartosikova, L., Brauner, P., Kolar, J., 2008. Hyaluronic acid (hyaluronan): A review. Vet. Med. (Praha). 53, 397–411.

Neu, C.P., Reddi, A.H., Komvopoulos, K., Schmid, T.M., Cesare, P.E. Di, 2010. Friction coefficient and superficial zone protein are increased in patients with advanced OA. Arthritis {&} Rheumatol. 62, 2680–2687.

Ni, J., Yuan, X.M., Yao, Q., Peng, L.B., 2015. OSM is overexpressed in knee osteoarthritis and Notch signaling is involved in the effects of OSM on MC3T3-E1 cell proliferation and differentiation. Int. J. Mol. Med. 35, 1755–1760.

Nieminen, H.J., Salmi, A., Karppinen, P., Hæggström, E., Hacking, S.A., 2014. The potential utility of high-intensity ultrasound to treat osteoarthritis. Osteoarthr. Cartil. 22, 1784–1799.

Oh, C. Do, Chang, S.H., Yoon, Y.M., Lee, S.J., Lee, Y.S., Kang, S.S., Chun, J.S., 2000. Opposing role of mitogen-activated protein kinase subtypes, Erk-1/2 and p38, in the regulation of chondrogenesis of mesenchymes. J. Biol. Chem. 275, 5613–5619.

Olivotto, E., Otero, M., Marcu, K.B., Goldring, M.B., 2015. Pathophysiology of osteoarthritis: Canonical NF-ϰB/IKKβ-dependent and kinase-independent effects of IKKα in cartilage degradation and chondrocyte differentiation. RMD Open 1, 1–6.

Olson, D.E., Sleiman, S.F., Bourassa, M.W., Wagner, F.F., Gale, J.P., Zhang, Y.-L., Ratan, R.R., Holson, E.B., 2015. Hydroxamate-based histone deacetylase inhibitors can protect neurons from oxidative stress via a histone deacetylase-independent catalase-like mechanism. Chem. Biol. 22, 439–445.

Pagadala, N.S., Syed, K., Tuszynski, J., 2017. Software for molecular docking: a review. Biophys. Rev. 9, 91–102.

Pan, J., Chang, Q., Wang, X., Son, Y., Zhang, Z., Chen, G., Luo, J., Bi, Y., Chen, F., Shi, X., 2010. Reactive oxygen species-activated Akt/ASK1/p38 signaling pathway in nickel compound-induced apoptosis in BEAS 2B cells. Chem. Res. Toxicol. 23, 568–577.

Park, H.I., Jin, Y., Hurst, D.R., Monroe, C.A., Lee, S., Schwartz, M.A., Sang, Q.-X.A., 2003. The Intermediate S 1 ´ Pocket of the Endometase/Matrilysin-2 Active Site Revealed by Enzyme Inhibition Kinetic Studies, Protein Sequence Analyses, and Homology Modeling. J. Biol. Chem. 278, 51646–51653.

Park, Y. et al. 2005. BMP-2 induces the expression of chondrocyte-specific genes in bovine synovium-derived progenitor cells cultured in three-dimensional alginate hydrogel. Osteoarthritis and Cartilage 13(6), pp. 527–536.

Parmar, P. a., Chow, L.W., St-Pierre, J.-P., Horejs, C.-M., Peng, Y.Y., Werkmeister, J. a., Ramshaw, J. a. M., Stevens, M.M., 2015. Collagen-mimetic peptide-modifiable hydrogels for articular cartilage regeneration. Biomaterials 54, 213–225.

Parrish, W.R., Byers, B.A., Su, D., Geesin, J., Herzberg, U., Wadsworth, S., Bendele, A., Story, B., 2017. Intra-articular therapy with recombinant human GDF5 arrests disease progression and stimulates cartilage repair in the rat medial meniscus transection (MMT) model of osteoarthritis. Osteoarthr. Cartil. 25, 554–560.

Pasternak, B. and Aspenberg, P. 2009. Metalloproteinases and their inhibitorsdiagnostic and therapeutic opportunities in orthopedics. Acta Orthopaedica 80(6), pp. 693–703. doi: 10.3109/17453670903448257.

Patwari, P., Gao, G., Lee, J.H., Grodzinsky, A.J., Sandy, J.D., 2005. Analysis of ADAMTS4 and MT4-MMP indicates that both are involved in aggrecanolysis in interleukin-1-treated bovine cartilage. Osteoarthr. Cartil. 13, 269–277.

Peeler, J., Ripat, J., 2018. The effect of low-load exercise on joint pain, function, and activities of daily living in patients with knee osteoarthritis. Knee 25, 135–145.

Perni, S., Prokopovich, P., 2017. Poly-beta-amino-esters nano-vehicles based drug delivery system for cartilage. Nanomedicine Nanotechnology, Biol. Med. 13, 539–548.

Pickarski, M., Hayami, T., Zhuo, Y., Duong, L.T., 2011. Molecular changes in articular cartilage and subchondral bone in the rat anterior cruciate ligament transection and meniscectomized models of osteoarthritis. BMC Musculoskelet. Disord. 12.

Plaas, A.H.K., Wong-Palms, S., Roughley, P.J., Midura, R.J., Hascall, V.C., 1997. Chemical and immunological assay of the nonreducing terminal residues of chondroitin sulfate from human aggrecan. J. Biol. Chem. 272, 20603–20610.

Posey, K.L., Hayes, E., Haynes, R., Hecht, J.T., 2004. Role of TSP-5/COMP in Pseudoachondroplasia. Int. J. Biochem. Cell Biol. 36, 1005–1012.

Prasadam, I., Mao, X., Wang, Y., Shi, W., Crawford, R., Xiao, Y., 2012. Inhibition of p38 pathway leads to OA-like changes in a rat animal model. Rheumatology 51, 813–823.

Pratta, M.A., Yao, W., Decicco, C., Tortorella, M.D., Liu, R.Q., Copeland, R.A., Magolda, R., Newton, R.C., Trzaskos, J.M., Arner, E.C., 2003. Aggrecan Protects Cartilage Collagen from Proteolytic Cleavage. J. Biol. Chem. 278, 45539–45545.

Q, A.J.F., Neamell, P.J., Last, K., Hardinghamll, T.E., Murphy, G., Hamilton, J.A., 2001. J. Biol. Chem.-1992-Fosang-19470-4 267, 1–5.

Rasmussen, H.S., McCann, P.P., 1997. Matrix metalloproteinase inhibition as a novel anticancer strategy: A review with special focus on Batimastat and Marimastat. Pharmacol. Ther. 75, 69–75.

Recchiuti, A., 2014. Immunoresolving Lipid Mediators and Resolution of Inflammation in Aging. J. Gerontol. Geriatr. Res. 03.

Reesink, H.L., Watts, A.E., Mohammed, H.O., Jay, G.D., Nixon, A.J., 2017. Lubricin/proteoglycan 4 increases in both experimental and naturally occurring equine osteoarthritis. Osteoarthr. Cartil. 25, 128–137.

Reis, M.B., Pereira, P.A.T., Caetano, G.F., Leite, M.N., Galvão, A.F., Paula-Silva, F.W.G., Frade, M.A.C., Faccioli, L.H., 2017. Lipoxin A4 encapsulated in PLGA microparticles accelerates wound healing of skin ulcers. PLoS One 12, e0182381.

Richards, C.D., 2013. 512103 2013.

Rivas-Ramirez, P., Gadotti, V.M., Zamponi, G.W., Weiss, N., 2017. Surfen is a broad-spectrum calcium channel inhibitor with analgesic properties in mouse models of acute and chronic inflammatory pain. Pflügers Arch. - Eur. J. Physiol. 1325–1334.

Rose, B.J., Kooyman, D.L., 2016. A Tale of Two Joints: The Role of Matrix Metalloproteases in Cartilage Biology. Dis. Markers 2016.

Rothenfluh, D. a, Bermudez, H., O'Neil, C.P., Hubbell, J. a, 2008. Biofunctional polymer nanoparticles for intra-articular targeting and retention in cartilage. Nat. Mater. 7, 248–254.

Roughley, P.J., Mort, J.S., 2014. The role of aggrecan in normal and osteoarthritic cartilage. J. Exp. Orthop. 1, 8.

Roughley, P.J., White, R.J., 1980. Age-related changes in the structure of the proteoglycan subunits from human articular cartilage. J. Biol. Chem. 255, 217–224.

Rowan, A., Hui, W., Cawston, T.E., Richards, C.D., 2003. Adenoviral gene transfer of interleukin-1 in combination with oncostatin M induces significant joint damage in a murine model. Am. J. Pathol. 162, 1975–1984.

Rowan, A.D., Koshy, P.J.T., Shingleton, W.D., Degnan, B.A., Heath, J.K., Vernallis, A.B., Spaull, J.R., Life, P.F., Hudson, K., Cawston, T.E., 2001. Synergistic effects of glycoprotein 130 binding cytokines in combination with interleukin-1 on cartilage collagen breakdown. Arthritis Rheum. 44, 1620–1632.

Ryan, R.E., Martin, B., Mellor, L., Jacob, R.B., Tawara, K., McDougal, O.M., Oxford, J.T., Jorcyk, C.L., 2015. Oncostatin M binds to extracellular matrix in a bioactive conformation: implications for inflammation and metastasis. Cytokine 72, 71–85.

Salmaso, S., Caliceti, P., 2013. Stealth Properties to Improve Therapeutic Efficacy of Drug Nanocarriers. J. Drug Deliv. 2013, 1–19.

Sandy, J.D. et al. 1992. The structure of aggrecan fragments in human synovial fluid. Evidence for the involvement in osteoarthritis of a novel proteinase which cleaves the Glu 373-Ala 374 bond of the interglobular domain. Journal of Clinical Investigation 89(5), pp. 1512–1516.

Saravanakumar, G., Kim, J., Kim, W.J., 2016. Reactive-Oxygen-Species-Responsive Drug Delivery Systems: Promises and Challenges. Adv. Sci. 1600124.

Sarett, S.M., Nelson, C.E., Duvall, C.L., 2015. Technologies for controlled, local delivery of siRNA. J. Control. Release 218, 94–113.

Sato, T., Konomi, K., Yamasaki, S., Aratani, S., Tsuchimochi, K., Yokouchi, M., Masuko-Hongo, K., Yagishita, N., Nakamura, H., Komiya, S., Beppu, M., Aoki, H., Nishioka, K., Nakajima, T., 2006. Comparative analysis of gene expression profiles in intact and damaged regions of human osteoarthritic cartilage. Arthritis Rheum. 54, 808–817.

Schechter, I. and Berger, A. 1967. On the size of the active site in proteases. I. Papain. Biochemical and Biophysical Research Communications 27(2), pp. 157–162. doi: https://doi.org/10.1016/S0006-291X(67)80055-X.

Schepetkin, I.A., Kirpotina, L.N., Hammaker, D., Kochetkova, I., Khlebnikov, A.I., Lyakhov, S.A., Firestein, G.S., Quinn, M.T., 2015. Anti-Inflammatory Effects and Joint Protection in Collagen-Induced Arthritis after Treatment with IQ-1S, a Selective c-Jun N-Terminal Kinase Inhibitor. J. Pharmacol. Exp. Ther. 353, 505–516.

Schmidt, T.A., Gastelum, N.S., Han, E.H., Nugent-Derfus, G.E., Schumacher, B.L., Sah, R.L., 2008. Differential regulation of proteoglycan 4 metabolism in cartilage by IL-1α, IGF-I, and TGF-β1. Osteoarthr. Cartil. 16, 90–97.

Schmidt, T.A., Gastelum, N.S., Nguyen, Q.T., Schumacher, B.L., Sah, R.L., 2007. Boundary lubrication of articular cartilage: Role of synovial fluid constituents. Arthritis Rheum. 56, 882–891.

Schnitzer, T.J., Marks, J.A., 2015. A systematic review of the efficacy and general safety of antibodies to NGF in the treatment of OA of the hip or knee. Osteoarthr. Cartil. 23, S8–S17.

Schuksz, M., Fuster, M.M., Brown, J.R., Crawford, B.E., Ditto, D.P., Lawrence, R., Glass, C. a, Wang, L., Tor, Y., Esko, J.D., 2008. Surfen, a small molecule antagonist of heparan sulfate. Proc. Natl. Acad. Sci. U. S. A. 105, 13075–13080.

Schulze-Tanzil, G., de Souza, P., Villegas Castrejon, H., John, T., Merker, H.-J., Scheid, A., Shakibaei, M., 2002. Redifferentiation of dedifferentiated human chondrocytes in high-density cultures. Cell Tissue Res. 308, 371–379.

Schumacher, B.L., Schmidt, T.A., Voegtline, M.S., Chen, A.C., Sah, R.L., 2005. Proteoglycan 4 (PRG4) synthesis and immunolocalization in bovine meniscus. J. Orthop. Res. 23, 562–568.

Shapovalov, M. V, Dunbrack, R.L.J., 2011. A smoothed backbone-dependent rotamer library for proteins derived from adaptive kernel density estimates and regressions. Structure 19, 844–858.

Shieh, H.S., Tomasselli, A.G., Mathis, K.J., Schnute, M.E., Woodard, S.S., Caspers, N., Williams, J.M., Kiefer, J.R., Munie, G., Wittwer, A., Malfait, A.M., Tortorella, M.D., 2011. Structure analysis reveals the flexibility of the ADAMTS-5 active site. Protein Sci. 20, 735–744.

Shkhyan, R., Van Handel, B., Bogdanov, J., Lee, S., Yu, Y., Scheinberg, M., Banks, N.W., Limfat, S., Chernostrik, A., Franciozi, C.E., Alam, M.P., John, V., Wu, L., Ferguson, G.B., Nsair, A., Petrigliano, F.A., Vangsness, C.T., Vadivel, K., Bajaj, P., Wang, L., Liu, N.Q., Evseenko, D., 2018. Drug-induced modulation of gp130 signalling prevents articular cartilage degeneration and promotes repair. Ann. Rheum. Dis. annrheumdis-2017-212037.

Shoulders, M.D., Raines, R.T., 2009. Collagen Structure and Stability. Annu. Rev. Biochem. 78, 929–958.

Simpson, R.J., Jensen, S.S., Lim, J.W.E., 2008. Proteomic profiling of exosomes: current perspectives. Proteomics 8, 4083–99.

Smith, R.J., Rohloff, N.A., Sam, L.M., Justen, J.M., Deibel, M.R., Cornette, J.C., 1989. Recombinant Human Interleukin-lc~ And Recombinant Human Interleukin-1/3 Stimulate Cartilage Matrix Degradation And Inhibit Glycosaminoglycan Synthesis. Inflammation 13.

Sodin-Semrl, S., Taddeo, B., Tseng, D., Varga, J., Fiore, S., 2000. Lipoxin A4 Inhibits IL-1 -Induced IL-6, IL-8, and Matrix Metalloproteinase-3 Production in Human Synovial Fibroblasts and Enhances Synthesis of Tissue Inhibitors of Metalloproteinases. J. Immunol. 164, 2660–2666.

Sokolove, J., Lepus, C.M., 2013. Role of inflammation in the pathogenesis of osteoarthritis: latest findings and interpretations. Ther. Adv. Musculoskelet. Dis. 5, 77–94.

Song, R.-H., D. Tortorella, M., Malfait, A.-M., Alston, J.T., Yang, Z., Arner, E.C., Griggs, D.W., 2007. Aggrecan degradation in human articular cartilage explants is mediated by both ADAMTS-4 and ADAMTS-5. Arthritis Rheum. 56, 575–585.

Song, R.H., Tortorella, M.D., Malfait, A.M., Alston, J.T., Yang, Z., Arner, E.C., Griggs, D.W., 2007. Aggrecan degradation in human articular cartilage explants is mediated by both ADAMTS-4 and ADAMTS-5. Arthritis Rheum. 56, 575–585.

Sophia Fox, A.J., Bedi, A., Rodeo, S.A., 2009. The basic science of articular cartilage: Structure, composition, and function. Sports Health 1, 461–468.

Steenvoorden, M.M.C., Huizinga, T.W.J., Verzijl, N., Bank, R.A., Ronday, H.K., Luning, H.A.F., Lafeber, F.P.J.G., Toes, R.E.M., DeGroot, J., 2006. Activation of receptor for advanced glycation end products in osteoarthritis leads to increased stimulation of chondrocytes and synoviocytes. Arthritis Rheum. 54, 253–263.

Stracke, J.O., Fosang, A.J., Last, K., Mercuri, F.A., Pendás, A.M., Llano, E., Perris, R., Di Cesare, P.E., Murphy, G., Knäuper, V., 2000. Matrix metalloproteinases 19 and 20 cleave aggrecan and cartilage oligomeric matrix protein (COMP). FEBS Lett. 478, 52–56.

Struglics, A., Larsson, S., Pratta, M.A., Kumar, S., Lark, M.W., Lohmander, L.S., 2006. Human osteoarthritis synovial fluid and joint cartilage contain both aggrecanase- and matrix metalloproteinase-generated aggrecan fragments. Osteoarthr. Cartil. 14, 101–113.

Su, Y.-P., Chen, C.-N., Huang, K.-C., Chang, H.-I., Lee, K.-C., Lo, C.-M., Chang, S.-F., 2018. Leptin induces MMP1/13 and ADAMTS 4 expressions through bone morphogenetic protein-2 autocrine effect in human chondrocytes. J. Cell. Biochem. 119, 3716–3724.

Sun, X.-H., Liu, Y., Han, Y., Wang, J., 2016. Expression and Significance of High-Mobility Group Protein B1 (HMGB1) and the Receptor for Advanced Glycation End-Product (RAGE) in Knee Osteoarthritis. Med. Sci. Monit. 22, 2105–2112.

Suntiparpluacha, M., Tammachote, N., Tammachote, R., 2016. induces oxidative stress , and alters gene expressions of human chondrocytes 4985–4992.

Surve, C.R., Lehmann, D., Smrcka, A. V., 2014. A chemical biology approach demonstrates G protein subunits are sufficient to mediate directional neutrophil chemotaxis. J. Biol. Chem. 289, 17791–17801.

Surve, C.R., To, J.Y., Malik, S., Kim, M., Smrcka, A. V., 2016. Dynamic regulation of neutrophil polarity and migration by the heterotrimeric G protein subunits G i-GTP and G . Sci. Signal. 9, ra22-ra22.

Suzuki, K., Takahashi, S., Watanabe, K., Fujioka, D., Nakamura, T., Obata, J., Kawabata, K., Katoh, R., Matsumoto, M., Kugiyama, K., 2014. The expression of groups IIE and V phospholipase A2 is associated with an increased expression of osteogenic molecules in human calcified aortic valves. J. Atheroscler. Thromb. 21, 1308–1325.

Takahashi, N., Knudson, C.B., Thankamony, S., Ariyoshi, W., Im, H., Knudson, W., 2010. NIH Public Access 62, 1338–1348. Tamer, T.M., 2013. Hyaluronan and synovial joint: Function, distribution and healing. Interdiscip. Toxicol. 6, 111–125.

Tammachote, N., Kanitnate, S., Yakumpor, T., Panichkul, P., 2016. Intra-Articular, Single-Shot Hylan G-F 20 Hyaluronic Acid Injection Compared with Corticosteroid in Knee Osteoarthritis. J Bone Jt. Surg Am 98, 885–892.

Tchetverikov, I., Lohmander, L.S., Verzijl, N., Huizinga, T.W.J., TeKoppele, J.M., Hanemaaijer, R., DeGroot, J., 2005. MMP protein and activity levels in synovial fluid from patients with joint injury, inflammatory arthritis, and osteoarthritis. Ann. Rheum. Dis. 64, 694–698.

Tetsunaga, T., Nishida, K., Furumatsu, T., Naruse, K., Hirohata, S., Yoshida, A., Saito, T., Ozaki, T., 2011. Regulation of mechanical stress-induced MMP-13 and ADAMTS-5 expression by RUNX-2 transcriptional factor in SW1353 chondrocyte-like cells. Osteoarthr. Cartil. 19, 222–232.

Thorne, N., Auld, D.S., Inglese, J., 2010. Apparent activity in high-throughput screening: origins of compound-dependent assay interference. Curr. Opin. Chem. Biol. 14, 315–324.

Tobiume, K., Matsuzawa, A., Takahashi, T., Nishitoh, H., Morita, K.I., Takeda, K., Minowa, O., Miyazono, K., Noda, T., Ichijo, H., 2001. ASK1 is required for sustained activations of JNK/p38 MAP kinases and apoptosis. EMBO Rep. 2, 222–228.

Toh, W.S., Brittberg, M., Farr, J., Foldager, C.B., Gomoll, A.H., Hui, J.H.P., Richardson, J.B., Roberts, S., Spector, M., 2016. Cellular senescence in aging and osteoarthritis: Implications for cartilage repair. Acta Orthop. 87, 6–14.

Tomida, T., Takekawa, M., Saito, H., 2015. Oscillation of p38 activity controls efficient pro-inflammatory gene expression. Nat. Commun. 6, 1–9.

Tortorella, M., Pratta, M., Liu, R.Q., Abbaszade, I., Ross, H., Burn, T., Arner, E., 2000. The thrombospondin motif of Aggrecanase-1 (ADAMTS-4) is critical for aggrecan substrate recognition and cleavage. J. Biol. Chem. 275, 25791–25797.

Tortorella, M.D. et al. 2009. Structural and inhibition analysis reveals the mechanism of selectivity of a series of aggrecanase inhibitors. J.Biol.Chem. 284, pp. 24185–24191

Treble, N.J., Jensen, F.O., Bankier, A., Rogers, J.G., Cole, W.G., 1990. Development of the hip in multiple epiphyseal dysplasia. Natural history and susceptibility to premature osteoarthritis. J. Bone Joint Surg. Br. 72, 1061–1064.

Trowbridge, J.M., Gallo, R.L., 2002. Dermatan sulfate: new functions from an old glycosaminoglycan. Glycobiology 12, 117R–125R.

Tsolis, K.C., Bei, E.S., Papathanasiou, I., Kostopoulou, F., Gkretsi, V., Kalantzaki, K., Malizos, K., Zervakis, M., Tsezou, A., Economou, A., 2015. Comparative proteomic analysis of hypertrophic chondrocytes in osteoarthritis. Clin. Proteomics 12, 1–16.

Tsuchida, A.I., Beekhuizen, M., Hart, M.C., Radstake, T.R.D.J., Dhert, W.J. a, Saris, D.B.F., Osch, G.J.V.M. Van, Creemers, L.B., 2014. Cytokine profiles in the joint depend on pathology , but are different between synovial fluid , cartilage tissue and cultured chondrocytes. Arthritis Res. Ther. 1–15.

Tsuchiya, K., Maloney, W.J., Vu, T., Hoffman, A.R., Huie, P., Sibley, R., Schurman, D.J., Smith, R.L., 1997. Osteoarthritis: Differential expression of matrix metalloproteinase-9 mRNA in nonfibrillated and fibrillated cartilage. J. Orthop. Res. 15, 94–100.

Umber, F., Störring, F.K., Föllmer, W., 1938. Erfolge mit Einem Neuartigen Depotinsulin Ohne Protaminzusatz (Surfen-Insulin). Klin. Wochenschr. 17, 443–446.

V Gordon, G., Villanueva, T., R Schumacher, H., Gohel, V., 1984. Autopsy study correlating degree of osteoarthritis, synovitis and evidence of articular calcification, The Journal of rheumatology.

Valenzuela, N.M., Trinh, K.R., Mulder, A., Morrison, S.L., Reed, E.F., 2015. Monocyte recruitment by HLA IgG-activated endothelium: the relationship between IgG subclass and FcgammaRIIa polymorphisms. Am. J. Transplant 15, 1502–1518.

van der Heijden, J., Nagelkerke, S., Zhao, X., Geissler, J., Rispens, T., van den Berg, T.K., Kuijpers, T.W., 2014. Haplotypes of FcγRIIa and FcγRIIIb Polymorphic Variants Influence IgG-Mediated Responses in Neutrophils. J. Immunol. 192, 2715 LP-2721.

Van der Kraan, P.M., Van den Berg, W.B., 2012. Chondrocyte hypertrophy and osteoarthritis: Role in initiation and progression of cartilage degeneration? Osteoarthr. Cartil. 20, 223–232.

Vincent, T., Hermansson, M., Bolton, M., Wait, R., Saklatvala, J., 2002. Basic FGF mediates an immediate response of articular cartilage to mechanical injury. Proc. Natl. Acad. Sci. U. S. A. 99, 8259–8264.

von der Mark, K., Gauss, V., von der Mark, H., Muller, P., 1977. Relationship between cell shape and type of collagen synthesised as chondrocytes lose their cartilage phenotype in culture. Nature 267, 531–532.

Vuuren, A.J. Van, Roon, J.A.G. Van, Stuij, I., Harmsen, M.C., Pamela, M.J., Winkel, J.G.J. Van De, Thepen, T., 2018. CD64-Directed Immunotoxin Inhibits Arthritis in a Novel CD64 Transgenic Rat Model.

Vyver, A. Van De, Clockaerts, S., Lest, C.H.A. Van De, Wei, W., Verhaar, J., Osch, G.J.V.M. Van, Bastiaansen-jenniskens, Y.M., 2018. Synovial Fluid Fatty Acid Profiles Differ between Osteoarthritis and Healthy Patients.

Wainwright, S.D., Bondeson, J., Caterson, B., Hughes, C.E., 2013. ADAMTS-4-v1 Is a splice variant of ADAMTS-4 that is expressed as a protein in human synovium and cleaves aggrecan at the interglobular domain. Arthritis Rheum. 65, 2866–2875.

Wainwright, S.D., Bondeson, J., Hughes, C.E., 2006. An alternative spliced transcript of ADAMTS4 is present in human synovium from OA patients. Matrix Biol. 25, 317–320.

Wang, M., Sampson, E.R., Jin, H., Li, J., Ke, Q.H., Im, H.J., Chen, D., 2013. MMP13 is a critical target gene during the progression of osteoarthritis. Arthritis Res. Ther. 15, R5.

Wang, P., Mao, Z., Pan, Q., Lu, R., Huang, X., Shang, X., Zhang, R., You, H., 2018. Histone deacetylase-4 and histone deacetylase-8 regulate interleukin-1β-induced cartilage catabolic degradation through MAPK/JNK and ERK pathways. Int. J. Mol. Med. 41, 2117–2127.

Wang, P., Tortorella, M., England, K., Malfait, A.M., Thomas, G., Arner, E.C., Pei, D., 2004. Proprotein Convertase Furin Interacts with and Cleaves Pro-ADAMTS4 (Aggrecanase-1) in the trans-Golgi Network. J. Biol. Chem. 279, 15434–15440.

Wang, Q., Rozelle, A.L., Lepus, C.M., Scanzello, C.R., Song, J.J., Larsen, D.M., Crish, J.F., Bebek, G., Ritter, S.Y., Lindstrom, T.M., Hwang, I., Wong, H.H., Punzi, L., Encarnacion, A., Shamloo, M., Goodman, S.B., Wyss-Coray, T., Goldring, S.R., Banda, N.K., Thurman, J.M., Gobezie, R., Crow, M.K., Holers, V.M., Lee, D.M., Robinson, W.H., 2011. Identification of a central role for complement in osteoarthritis. Nat. Med. 17, 1674–1679.

Wang, X., Monteagudo, S., Lories, R., 2018. EXT1 and EXT2 regulate chondrogenesis by modulation of WNT signaling. Osteoarthr. Cartil. 26, S97.

Warford, J., Doucette, C.D., Hoskin, D.W., Easton, A.S., 2014. Murine T cell activation is regulated by surfen (bis-2-methyl-4-amino-quinolyl-6-carbamide). Biochem. Biophys. Res. Commun. 443, 524–530.

Warford, J.R., Lamport, A.-C., Clements, D.R., Malone, A., Kennedy, B.E., Kim, Y., Gujar, S.A., Hoskin, D.W., Easton, A.S., 2018. Surfen, a proteoglycan binding agent, reduces inflammation but inhibits remyelination in murine models of Multiple Sclerosis. Acta Neuropathol. Commun. 6, 4.

Wei, J.-L., Fu, W., Hettinghouse, A., He, W.-J., Lipson, K.E., Liu, C.-J., 2018. Role of ADAMTS-12 in Protecting Against Inflammatory Arthritis in Mice By Interacting With and Inactivating Proinflammatory Connective Tissue Growth Factor.

Weiss, R.J., Gordts, P.L.S.M., Le, D., Xu, D., Esko, J.D., Tor, Y., 2015. Small molecule antagonists of cell-surface heparan sulfate and heparin–protein interactions. Chem. Sci. 6, 5984–5993.

Williams, J.D., Khan, A.R., Cardinale, S.C., Butler, M.M., Bowlin, T.L., Peet, N.P., 2014. Small molecule inhibitors of anthrax lethal factor toxin. Bioorg. Med. Chem. 22, 419–434.

Willis, E.L. et al. 2017. Progesterone Receptor and Prostaglandins Mediate Luteinizing Hormone-Induced Changes in Messenger RNAs for ADAMTS Proteases in Theca Cells of Bovine Periovulatory Follicles. Molecular reproduction and development 84(1), pp. 55–66.

Wojdasiewicz, P., Poniatowski, L.A., Szukiewicz, D., 2014. The role of inflammatory and anti-inflammatory cytokines in the pathogenesis of osteoarthritis. Mediators Inflamm. 2014, 561459.

Wuyts, W., Van Hul, W., De Boulle, K., Hendrickx, J., Bakker, E., Vanhoenacker, F., Mollica, F., Lüdecke, H.J., Sayli, B.S., Pazzaglia, U.E., Mortier, G., Hamel, B., Conrad, E.U., Matsushita, M., Raskind, W.H., Willems, P.J., 1998. Mutations in the EXT1 and EXT2 genes in hereditary multiple exostoses. Am. J. Hum. Genet. 62, 346–354.

Xu, D., Young, J., Song, D., Esko, J.D., 2011. Heparan sulfate is essential for high mobility group protein 1 (HMGB1) signaling by the receptor for advanced glycation end products (RAGE). J. Biol. Chem. 286, 41736–41744.

Yamamoto, K., Owen, K., Parker, A.E., Scilabra, S.D., Dudhia, J., Strickland, D.K., Troeberg, L., Nagase, H., 2014. Low Density Lipoprotein Receptor-related Protein 1 (LRP1)-mediated Endocytic Clearance of a Disintegrin and Metalloproteinase with Thrombospondin Motifs-4 (ADAMTS-4): Functional Differences Of Non-catalytic Domains Of Adamts-4 And Adamts-5 In Lrp1 Binding. J. Biol. Chem. 289, 6462–6474.

Yamamoto, K., Troeberg, L., Scilabra, S.D., Pelosi, M., Murphy, C.L., Strickland, D.K., Nagase, H., 2013. LRP-1-mediated endocytosis regulates extracellular activity of ADAMTS-5 in articular cartilage. FASEB J. 27, 511–521.

Yamauchi, J., Nagao, M., Kaziro, Y., Itoh, H., 1997. Activation of p38 Mitogen-activated Protein Kinase by Signaling through G Protein-coupled Receptors. J. Biol. Chem. 272, 27771–27777.

Yazici, Y., McAlindon, T.E., Fleischmann, R., Gibofsky, A., Lane, N.E., Kivitz, A.J., Skrepnik, N., Armas, E., Swearingen, C.J., DiFrancesco, A., Tambiah, J.R.S., Hood, J., Hochberg, M.C., 2017. A novel Wnt pathway inhibitor, SM04690, for the treatment of moderate to severe osteoarthritis of the knee: results of a 24-week, randomized, controlled, phase 1 study. Osteoarthr. Cartil. 25, 1598–1606.

Zhang, Q.-S., Eaton, G.J., Diallo, C., Freeman, T.A., 2016. Stress-Induced Activation of Apoptosis Signal-Regulating Kinase 1 Promotes Osteoarthritis. J. Cell. Physiol. 231, 944–953.

Zhen, E.Y., Brittain, I.J., Laska, D.A., Mitchell, P.G., Sumer, E.U., Karsdal, M.A., Duffin, K.L., 2008. Characterization of metalloprotease cleavage products of human articular cartilage. Arthritis Rheum. 58, 2420–2431.

Zien, A., Aigner, T., Zimmer, R., 2001. Centralization : a new method for the normalization of gene expression data 17, 323–331.